THE ROLE OF THE CRH/CRHR1 SYSTEM IN GLIAL CELLS FOLLOWING ACUTE BRAIN INJURY

Clemens Ries

Graduate School of
Systemic Neurosciences

LMU Munich

Dissertation at the

Graduate School of Systemic Neurosciences

Ludwig-Maximilians-Universität München

November 2023

Supervisor
PD Dr. Jan M. Deussing
Neurogenetics
Max Planck Institute of Psychiatry

First Reviewer:	PD Dr. Jan M. Deussing
Second Reviewer:	Professor Dr. Silvia Cappello
External Reviewer:	Professor Dr. Klaus-Armin Nave

Date of Submission:	13.11.2023
Date of Defense:	16.05.2024

Table of contents

Abbreviation list

ACTH	*Adenocorticotropic hormone*
ALS	*Amyotrophic lateral sclerosis*
BAC	*Bacterial artificial chromosome*
BBB	*Blood brain barrier*
BCAS1	*Breast carcinoma amplified sequence 1*
Ca^{2+}	*Calcium*
CNPase	*2',3'-Cyclic-nucleotide 3'-phosphodiesterase*
CNS	*Central nervous system*
Cre	*Cyclisation recombinase*
CRE	*Cyclic AMP response element*
CREB	*cAMP response element binding protein*
CRHR	*Corticotropin-releasing hormone receptor*
CSF	*Cerebrospinal fluid*
CSPG4	*Chondroitin proteoglycan 4*
CX_3CR_1	*C-X3-C motif chemokine receptor 1*
ENPP6	*Extracellular enzymes ectonucleotide pyrophosphatase/phosphodiesterase 6*
ER	*Endoplasmatic reticulum*
GalR1	*Galanin receptor*
GFAP	*Glial fibrillary acidic protein*
GPCR	*G-protein coupled receptor*
GPR17	*G-protein coupled receptor 17*
GRE	*Glucocorticoid response element*
HPA axis	*Hypothalamic-pituitary-adrenal axis*
IBA1	*Ionized calcium-binding adapter molecule 1*
IFN-γ	*Interferon γ*

IL-1 β	*Interleukin 1 β*
IL-6	*Interleukin 6*
iOPCs	*Inflammatory OPCs*
KO	*Knockout*
KOR	*Kappa opioid receptor*
LDCV	*Large dense core vesicles*
LGE	*Lateral ganglionic eminence*
LIF-1	*Leukemia-inhibitory factor 1*
loxP	*Locus of cross over X of P1*
MAG	*Myelin-associated glycoprotein*
MAPK	*Mitogen-activated protein kinase*
MBP	*Myelin basic protein*
MDD	*Major depressive disorder*
MGE	*Medial ganglionic eminence*
MHC1	*Major histocompatibility complex 1*
MOR	*μ opioid receptor*
MS	*Multiple sclerosis*
NG2	*Neural/glial antigen 2*
NGR1	*Neuregulin 1*
O-2A	*Oligodendrocyte-type-2 astrocyte*
OE	*Overexpression*
OL	*Oligodendrocytes*
OLCs	*Oligodendrocyte lineage cells*
OLIG2	*Oligodendrocyte transcription factor 2*
OPC	*Oligodendrocyte progenitor cells*
pCREB	*Phosphorylated cAMP response element binding protein*

PDGF	*Platelet derived growth factor*
PDGFRα	*Platelet derived growth factor receptor α*
PFC	*Prefrontal cortex*
PKA	*Protein kinase A*
PLP	*Proteolipid protein*
PVN	*Nucleus paraventricularis*
RE-1/NRSE	*Neuron-restrictive silencing element*
REST	*RE-1 silencing transcription factor*
Shh	*Sonic Hedgehog*
SSRs	*Site-specific recombinases*
TAZ	*PDZ-binding motif*
TBI	*Traumatic brain injury*
TGFβ2	*Transforming growth factor β2*
TGFβR2	*Transforming growth factor β receptor type II*
TLR4	*Toll-like receptor 4*
TNFα	*Tumor necrosis factor alpha*
TORC	*Transducer of regulated CREB-activity*
VEGF	*Vascular endothelial growth factor*
YAP	*Yes-associated protein 1*

Abstract

This cumulative-style doctoral thesis consists of two studies revolving around the corticotropin-releasing hormone (CRH), its role in oligodendrogenic processes following injury as well as the in-depth characterization of mouse models for its analysis. We identified a subpopulation of oligodendrocyte progenitor cells (OPCs) in which CRH expression is triggered upon acute injury by using different CRH reporter models, direct anti-CRH staining and *Crh* mRNA visualization. This CRH-expressing subpopulation of OPCs showed an OPC-like injury response with inward migration, strong proliferation and later differentiation. Although the general injury reaction of CRH^+ OPCs was comparable to the whole population of OPCs, their dynamics differed, supposedly caused by their high maturation rate of 80%. CRH expression was further found to happen at very early stages, starting within the first 12h following injury, therefore, preceding proliferation. Subsequently, expression of CRH persisted only within the first 3 days post injury (dpi). Furthermore, CRHR1, the high affinity receptor of CRH, was identified on OPCs and astrocytes surrounding the injury site, serving as potential targets of injury-triggered CRH expression and release. Using different gain- and loss-of-function approaches we demonstrated that CRH modulates astrocytic activation stages in a CRHR1-dependent manner, as elevated GFAP levels were only observed following CRH injection when CRHR1 was present. Furthermore, CRH system downregulation by global CRHR1 or OPC-specific CRH inactivation led to a reduced number of OPCs at 7 dpi and an increased number of OLs, that was later explained by an increased generation of new OLs using a label retaining experiment. Therefore, CRH released from OPCs apparently triggers a stalling mechanism of OPC differentiation which is mediated by CRHR1-expressing OPCs and astrocytes. In sum this study presents a novel neuropeptide system modulating OPC differentiation processes, which could serve as therapeutic target to enhance OL regeneration following acute injury.

This study was complemented by a much-needed characterization of a newly available *CRH-FlpO* reporter line. In this study, the *CRH-FlpO* line was compared to the widely used *CRH-Cre* line, which is considered as the gold standard for transgenic CRH reporting. By using 9 different reporter lines we were able to show that FlpO-dependent reporting in *CRH-FlpO::Ai65F* mice, although replicating endogenous CRH expression patterns, is inferior in its capacity to report the whole population of CRH-expressing cells. By using Cre and FlpO in combination with different reporters, we demonstrated that overall recombination efficacy of FlpO is lower than that of Cre. Additionally, we determined that an elevation in CRH expression by applying an acute stress model increases the number of reported cells. Therefore, FlpO dependent recombination and reporting is highly dependent on the overall strength but also context-dependent activity of the driving promoter. This has consequences for all studies using mouse lines harboring FlpO for genetic recombination: i) When comparing Cre- and FlpO-driven reporting the strength of the driving promoter has to be taken into account, ii) when using intersectional approaches to label specific subpopulations the efficacy of reporting is determined by the recombination

efficiency of FlpO and iii) when using FlpO for overexpression or knock-out of a certain marker an in-depth validation of their efficacy in the specific population is necessary. In sum, our results show that a careful and comprehensive analysis of FlpO-driven mouse lines is mandatory and should pay particular attention to the expression strength of the driving promoter.

Results connected to the characterization of FlpO were essential when interpreting the data related to the identification of CRH expression in OPCs. Because of the limited accessibility of CRH and its receptor CRHR1 by antibody-mediated approaches, the study relied heavily on transgenic mouse models, using both Cre and FlpO. Especially, differences in the number of reported cells between different mouse lines could be explained by these results which made a reasonable evaluation of gathered data possible.

In sum, this thesis presents a thorough evaluation study of FlpO driven recombination efficacy whose results laid the ground for the identification and characterization of a novel OPC-derived neuropeptide system contributing to OLC differentiation processes.

1 Introduction

1.1 Cellular composition of the brain

Already in the late 19th century, it was acknowledged by leading scientists Rudolph Virchow, Santiago Ramon y Cajal and Pio del Rio-Hortega, that neurons were not the only cell type present in the brain. Starting with the discovery of astrocytes and microglia, soon also oligodendrocytes (OLs) and later oligodendrocyte progenitor cells (OPCs) were discovered (y Cajal 1913; Penfield 1924; Virchow 1846; del Rio-Hortega, Iglesias-Rozas, and Garrosa 2012; Hortega 1918; Rio-Hortega 1939; Raff, Miller, and Noble 1983) (Fig. 1). Starting from their identification, these cells were considered as cell types acting as so called "Nervenkit" (German for nerve glue) mainly giving structural support to the surrounding neurons. Therefore, they were put together under the phrase neuroglia (Greek: glia = glue). Now, after decades of research, we can say with certainty that glial cells are an indispensable part of the mammalian brain and that their significance lays far beyond structural support (Colonna and Butovsky 2017; Eugenín-von Bernhardi and Dimou 2016; Dimou and Gallo 2015; Verkhratsky et al. 2021). In many cases, glial cells lay the basis for a functional central nervous system (CNS) and take important roles under physiological, but also pathological conditions. In the following I will give a short overview over the main glial cell types and their role in the mammalian brain, specifically focusing on OL lineage cells (OLCs).

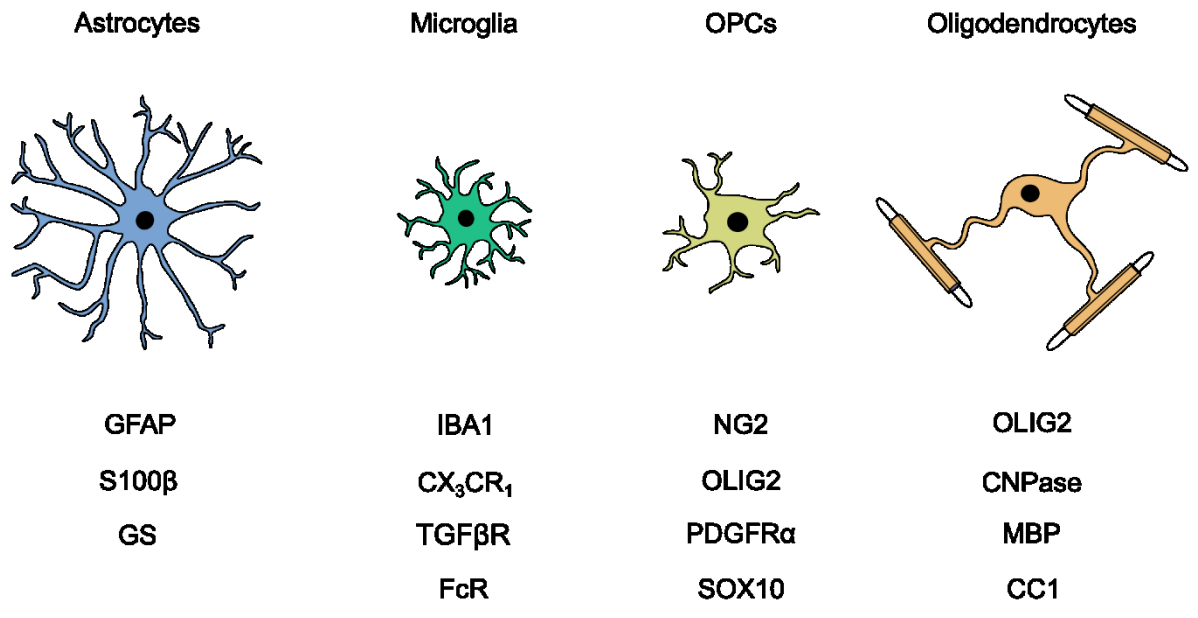

Figure 1: The four glial cell types of the CNS with specific markers for their identification. Abbreviations: GFAP, Glial fibrillary acidic protein. S100β, S100 calcium-binding protein β. GS, Glutamine Synthetase. IBA1, Ionized calcium-binding adapter molecule 1. CX_3CR_1, C-X3-C motif chemokine receptor 1. TGFβR, Transforming growth factor receptor β. FcR, Fc receptor. NG2, Neural/glial antigen 2. OLIG2, Oligodendrocyte transcription factor 2. PDGFRα,

Platelet derived growth factor receptor α. SOX10, SRY-box transcription factor 10. CNPase, 2′,3′-Cyclic-nucleotide 3'-phosphodiesterase. MBP, Myelin basic protein. CC1, Anti-adenomatous polyposis coli clone *CC1*.

1.2 Astrocytes

Astrocytes, the first glial cell type identified, are present in all brain regions and have been thoroughly investigated. In the spinal cord, these stellate cells originate from the progenitor motor neuron domain and are generated by progenitors that also give rise to motor neurons and cells of the OL lineage (Bergles and Richardson 2016). In the brain they are generated by radial glia cells (Lundgaard et al. 2014). Their functions are very diverse including the maintenance of brain homeostasis and the blood brain barrier (BBB), participation in the tripartite synapse and reaction to injury (Verkhratsky et al. 2021). Typically, astrocytes express several intermediate filament proteins like vimentin and glial fibrillary acidic protein (GFAP) as well as Calcium (Ca^{2+}) binding protein S100β (Lundgaard et al. 2014) (Fig. 1). Despite their rather homogeneous distribution within the CNS, astrocytes resemble a heterogenous population of cells. Shortly after their first identification, it was acknowledged that, depending on the brain region, two main morphologies could be segregated: fibrous and protoplasmic astrocytes (Andriezen 1893; Koelliker 1889). Protoplasmic astrocytes are mainly found in the grey matter where they contact neurons and blood vessels with their fine and complex processes (Hawkins and Davis 2005). Neurovascular coupling, a process in which local cerebral blood flow is increased in locations of enhanced synaptic activity, is dependent on astrocytic Ca^{2+} signaling (Anderson and Nedergaard 2003; Filosa, Bonev, and Nelson 2004). Protoplasmic astrocytes are organized in non-overlapping domains. While contacting up to 100,000 synapses, they facilitate synaptic function by, e.g., glutamate reuptake and processing or supply of energy (Allen and Eroglu 2017). Fibrous astrocytes, on the other hand, are located mainly in the white matter. Their processes, up to 300 µm long, are aligned with myelinating fibers and interact with the axons at nodes of Ranvier (Lundgaard et al. 2014; Butt, Duncan, and Berry 1994). Recent studies have implicated these astrocytes in the modulation of white matter structure by release of thrombin protease inhibitors (Dutta et al. 2018). Their morphological diversity is also evident on the transcriptional level, with brain region-specific and context-dependent transcriptional subtypes (Tsai et al. 2012; Hasel et al. 2021). Adult astrocytes retain some of the original patterning information from their radial glial ancestors and, thus, are a promising target for reprogramming. In recent years, astrocytes have been successfully reprogrammed into different neuronal subtypes, thereby promoting neuronal regeneration after brain injury (Mattugini et al. 2019). Besides their influence on cerebral blood flow, myelination and their potential in neuronal reprogramming, astrocytes have been shown to be critical in many physiological processes like the regulation of the sleep-wake cycle as well as learning and memory (Peng et al. 2023; Gibbs, Hutchinson, and Hertz 2008; Kol et al. 2020). Moreover, they are connected to many disease pathologies and have become a promising target for therapeutic intervention (Lee, Wheeler, and Quintana 2022).

1.3 Microglia

Microglia are the resident immune cells of the CNS and the first responders when it comes to inflammatory processes caused by, e.g., brain injury. They are, other than the astrocytes and OLCs, not derived from the neuroectoderm, but from the mesodermal yolk-sac and populate the brain during early development (Ginhoux et al. 2010). During development, microglia have been shown to modulate synapse formation and clear the brain from neuronal debris (Paolicelli et al. 2011). In the adult CNS, microglia can be identified by the expression of ionized calcium-binding adapter molecule 1 (IBA1) or C-X3-C motif chemokine receptor 1 (CX_3CR_1) (Fig. 1). They surveille their environment, search for potential threats or debris to be phagocytosed and potentially take part in synaptic modulation (Schafer, Lehrman, and Stevens 2013). In their role as orchestrators of CNS inflammation, microglia have also been implicated to be majorly involved in neuropsychiatric diseases like Alzheimer's disease or major depressive disorder (MDD) (Bachiller et al. 2018; von Muecke-Heim et al. 2021; Lewcock et al. 2020).

1.4 Oligodendrocyte lineage cells

1.4.1 Oligodendrocytes and their progenitors

OLs were discovered during the early 20th century and termed oligodendroglia, *glia with very few processes* (Del Rio-Hortega 2012). The myelinating property of these cells was not clearly shown until electron microscopy studies in the late 20th century proved them to wrap around nearby axons (Bunge, Bunge, and Pappas 1962). Since then, OLs are acknowledged as the myelinating cells of the CNS. With their processes they tightly wrap around nearby axons, increasing conduction velocity and providing trophic support (Nave and Werner 2014; Bergles and Richardson 2016). Oligodendrogenesis, the process of OL generation is a life-long process, in which new OLs are formed depending on the need for myelin in a specific brain region. Investigation by Tripathi and colleagues showed that >90% of OLs survive longer than 20 months *in vivo* (Tripathi et al. 2017). Thus, once formed OLs seem to be a highly stable population. Although myelin is present in almost all regions of the brain, it is not distributed homogeneously (de Faria et al. 2021). The majority of OLs and myelin can be found in fiber tracts as the corpus callosum, anterior commissure, capsule or optic tract. In other regions, like the cortex but especially in the cerebellum, OLs resemble the minority of all cells (Tripathi et al. 2017). For a long time, it was not known how OLs were generated, until in 1983 Raff and colleagues identified a new cell type, that generated type-2 astrocytes or oligodendrocytes depending on the culture conditions (Raff, Miller, and Noble 1983). Also *in vivo*, these oligodendrocyte-type-2 astrocyte (O-2A) progenitors were shown to be present and to generate mature OLs (Nishiyama et al. 1996a). Nowadays they are commonly known as NG2 glia and oligodendrocyte precursor or progenitor cells (OPCs). In the following, I will give an overview of these only recently discovered cells, their developmental origin and the diverse properties attributed to them.

1.4.2 Oligodendrocyte progenitor cells

OPCs are the fourth glial cell type of the central nervous system (Peters 2004; Nishiyama et al. 2009). Since their discovery, OPCs have been given many different names, e.g., O-2A cells, polydendrocytes, NG2 cells, NG2 glia, oligodendrocyte precursor or progenitor cells. Referring to the cells' properties of proliferation and OL generation they will be termed OPCs throughout this thesis.

1.4.3 Defining properties of OPCs

OPCs make up 5% of all cells in the murine brain (Dawson et al. 2003). They are homogeneously distributed within the CNS and are organized in a grid-like structure. While each of them takes up a non-overlapping domain, which separates them from other OPCs in close proximity, their filopodia are highly dynamic structures which extend and retract constantly (Hughes et al. 2013) (Fig. 2). They can be clearly defined by the expression of typical OLC-specific markers OLIG2 and SOX10 as well as by the OPC-specific markers platelet derived growth factor receptor α (PDGFRα) and chondroitin proteoglycan 4 (CSPG4) , also known as neural/glial antigen 2 (NG2) (Fig. 3). One important and unique property of OPCs is their ability to continuously proliferate in the brain parenchyma, generating new OPCs upon loss of a neighboring cell or need for new OLs. Whether proliferation is a prerequisite for differentiation is a highly debated matter within the field and seems to be dependent on the context (Xiao et al. 2016; Kamen et al. 2022; Bonetto, Belin, and Karadottir 2021).

1.4.4 Developmental origin of OPCs

In the developing brain, OPCs emerge from neural progenitors in three distinct brain regions (Fig. 2). The initial wave of OPCs is derived from Nkx2.1-expressing progenitors located in the medial ganglionic eminence (MGE) and the anterior entopeduncular area at embryonic day 12.5 (E12.5). Subsequently, a second wave of OPCs is generated around E15.5 in the lateral ganglionic eminence (LGE), originating from Gsh2-positive progenitors. These OPCs then migrate gradually into the cortex. The proper development of ventrally-derived OPCs and its timing depend on sonic hedgehog (Shh) signaling (Tekki-Kessaris et al. 2001; Orentas et al. 1999; Cai et al. 2005; Hashimoto et al. 2018). Following birth, MGE-derived OPCs are gradually eliminated and replaced by a third wave of dorsally derived OPCs. These third-wave OPCs are generated from endogenous Emx1-positive precursors located in the dorsal ventricular zone (Kessaris et al. 2006; Crawford et al. 2016). The distribution of the different populations of OPCs is only known for specific brain regions including motor cortex, anterior commissure or corpus callosum (Kessaris et al. 2006; Tripathi et al. 2011). In cortical regions and the corpus callosum, Emx1-derived OPCs resemble the majority of cells, whereas, the anterior commissure is mainly populated by Gsh2-derived OPCs. Nkx2.1-derived cells are largely eliminated from the brain and only represent a small minority of OPCs, e.g., in the anterior commissure. Our current knowledge about the distribution of the different populations is mainly based on the two, previously

mentioned, studies (Kessaris et al. 2006; Tripathi et al. 2011; Cristobal and Lee 2022). A systematic analysis of other brain regions, including mid- and hindbrain, appears necessary to better understand the distribution of adult OPCs.

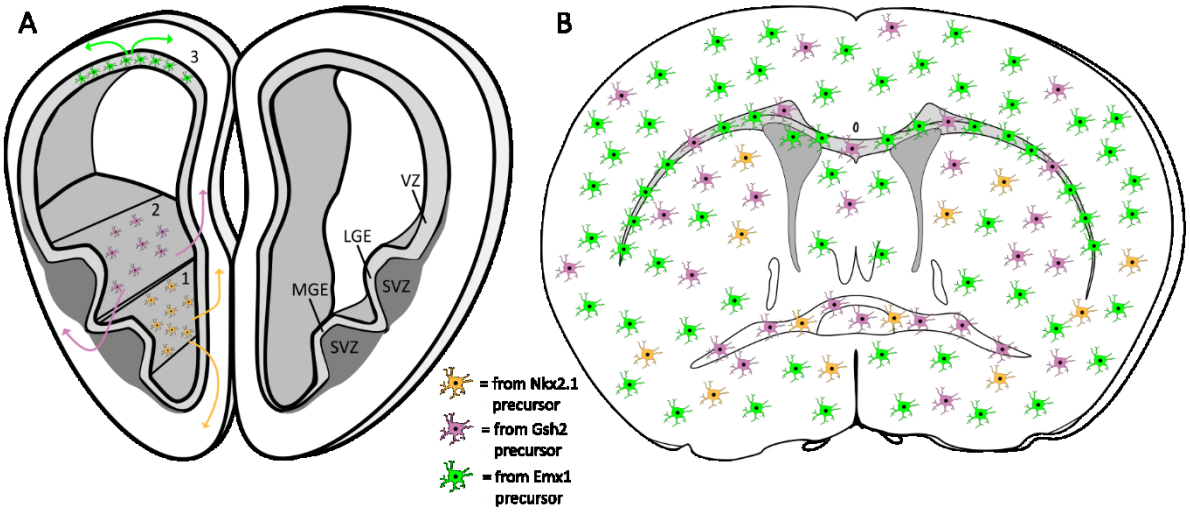

Figure 2: Developmental waves of OPCs. A, Three developmental waves originating in the median (MGE) (1) and lateral (LGE) (2) ganglionic eminence and the dorsal ventricular zone (3) from Nkx2.1, Gsh2 and Emx1 precursor cells, respectively. B, Grid-like organization of OPCs in the adult murine brain with origin-dependent distribution [based on (Ries 2018)].

1.4.5 OPCs of different origin: Functional redundancy or plasticity?

1.4.5.1 Regional heterogeneity of OPCs

Due to their different origins, the question regarding possible functional differences came to the forefront. Multiple ablation studies indicated that OPCs of different waves seem to be functionally redundant, as their elimination is compensated for by the others and no striking functional differences could be found (Jakel and Dimou 2017; Vigano and Dimou 2016). On the other hand, this seeming redundancy in functionality could also be caused by a high degree of plasticity (Kamen et al. 2022). Despite the fact that dorsally and ventrally derived OPCs populate preferential brain regions in the adult brain, their electrical properties were found to be indistinguishable in corpus callosum and the spinal cord (Tripathi et al. 2011). Still, distinct physiological properties like expression of certain ion channels and the capability to generate premature action potentials were only found in white matter OPCs (Chittajallu, Aguirre, and Gallo 2004). Also, their capability to generate OLs has been shown to be dependent on their developmental origin and their localization in the adult mouse brain, with dorsally derived OPCs showing a higher capacity for remyelination following demyelination and white matter OPCs having a generally higher tendency to generate OLs (Crawford et al. 2016; Dimou et al. 2008). A conclusive determination of whether adult OPC function is primarily driven by their developmental origin or by environmental factors has not been reached, yet. Nevertheless, the capability of OPCs to

generate OLs has been extensively investigated, analyzed and confirmed by many independent groups. Although oligodendrogenesis and myelination have been shown to be highly dynamic processes, even in the adult brain, their high stability and, therefore, relatively low demand for new OLs raises the question regarding additional functionalities. Driven by this question, researchers have analyzed the OPCs population extensively and identified many different physiological processes in which they are involved. As described above, OPCs show region-specific properties. But even within the same region, OPCs are a diverse population of cells showing a plethora of different characteristics, implying also functional diversity within the population and/or under certain conditions.

1.4.5.2 OPCs and the BBB

In recent years, OPCs have been described to be influenced by and interact with the vasculature of the CNS (Pfeiffer 2022). Vascular endothelial growth factor (VEGF), a potent stimulator of angiogenesis, has been shown to induce OPC migration *in vitro* (Hayakawa et al. 2011). The loss of its subtype C (VEGF-C) lead to a reduced number of OPCs in the optic nerve of mouse embryos and the *in vitro* stimulation with VEGF-C increased OPC proliferation (Le Bras et al. 2006). VEGF also influences OPC proliferation in other brain regions (Hiratsuka et al. 2019). In the adult mouse brain, OPC protrusions were not only shown to contact blood vessels (Pfeiffer, Sherafat, and Nishiyama 2021), but also influence BBB integrity under certain disease conditions, by a failure of detachment following migration along the vasculature (Niu et al. 2019).

1.4.5.3 OPCs as modulators of the immune response

Lately, OPCs have also been implicated in immune modulatory processes in the CNS. OPCs can inhibit microglial activation via transforming growth factor β2 (TGFβ2) and its type II receptor (TGFβR2). Following OPC ablation, microglial activation was elevated upon immune stimulation, implicating OPC-mediated TGFβ2/TGFβR2 signaling as key regulator of CX_3R_1 mediated activation (Zhang et al. 2019) . Besides, *in vitro* and *in vivo* studies show that astrocyte-derived Interferon γ (IFN-γ) reduces OPC numbers and induces major histocompatibility complex 1 (MHC1)-expression and antigen presentation by OPCs (Kirby et al. 2019). *In vitro*, cross presentation to cytotoxic CD8 T-cells leads to OPC death. A comparable disease specific phenotype was already identified in single cell analysis from multiple sclerosis (MS) tissue and later termed inflammatory OPCs (iOPCs) (Falcao et al. 2019; Kirby and Castelo-Branco 2021).

1.4.5.4 Secretory function of OPCs

As already highlighted by the two previous examples, OPCs do not only receive signals from their environment, but also influence the surrounding tissue by secreting substances. Already early on, data suggested that OPC-derived factors influence physiological processes, as OPC-conditioned medium or co-culturing with OPCs increased neuronal survival, had proangiogenic effects on endothelial cells and

increased pericyte proliferation. Though, the signals mediating these effects were unknown (Wilkins, Chandran, and Compston 2001; Wilkins et al. 2003; Seo et al. 2014; Yuen et al. 2014). Today, many different types of signals have been identified in *in vitro* studies, e.g., growth factors, neurotrophins, neuromodulatory factors, morphogens and cytokines (Parolisi and Boda 2018). Whether comparable processes also play a role *in vivo* remains unclear. Therefore, OPCs' capacity for secretion needs further investigation and confirmation (Birey et al. 2015; Zhang et al. 2019; Shen, Larm, and Gundlach 2003). As described in the previous part, OPCs show a variety of characteristics and are implicated in different processes within the CNS. This diversity has also been shown on the transcriptional level in recent sequencing studies (Beiter et al. 2022). Whether this heterogeneous nature is caused by the presence of endogenously different OPC subpopulations or is induced by context and environmental factors remains unclear. Also, whether all the described processes can be separated from OPCs' role as oligodendrogenic cells or just contribute to this process remains incompletely understood. Oligodendrogenesis itself and possible modulatory processes will be further described in the following part.

1.4.6 Oligodendrogenesis: A postnatal process with different stages

As described previously, OPCs are a diverse population of cells, with the capacity to generate OLs and therefore drive myelination during development but also throughout life (Rivers et al. 2008; Zhu et al. 2011). Early studies in human post mortem tissue but also in rats and other mammals showed that myelin formation starts within the spinal cord at early postnatal stages (Jacobson 1963; Banik and Smith 1977; Flechsig Of Leipsic 1901; Flechsig 1927). From there, myelination progresses to less archaic brain regions through the brain stem towards the telencephalon with its cortical hemispheres in a caudo-rostral manner (Jacobson 1963; Banik and Smith 1977; Flechsig Of Leipsic 1901; Flechsig 1927). The maximum of myelin deposition within the rat spinal cord and the brain lays between P15-20 and P20-30, respectively (Cohen and Guarnieri 1976). The process of myelination is preceded by OPC differentiation, which can be separated into three loose stages: i) OPC, ii) premyelinating OL ii) and myelinating OL stage (Fig. 3). These stages should not be seen as separate entities, but as terms describing the current progress within the differentiation/maturation process. Whereas, OPCs and OLs have been clearly defined by specific markers like NG2 and PDGFRα or CC1, myelin basic protein (MBP) and Proteolipid protein (PLP), respectively, for preOLs such markers weren't available (Kamen et al. 2022) (Fig. 3). Only the recently identified markers like breast carcinoma amplified sequence 1 (BCAS1) and extracellular enzymes ectonucleotide pyrophosphatase/phosphodiesterase 6 (ENPP6) enable a clear identification of this transient stage, significantly improving its analysis (Fard et al. 2017; Xiao et al. 2016) (Fig. 3). In development but also during regeneration oligodendrogenesis is an inefficient process characterized by an overproduction of premyelinating OLs (Trapp et al. 1997; Nishiyama et al. 1996b; Hughes et al. 2018). Followed by strong OPC proliferation, premyelinating OLs are generated. During this process, PDGFRα and CSPG4 are downregulated. The downregulation of PDGFRα makes this cell stage less sensitive for platelet derived growth factor (PDGF), which promotes

cell survival and proliferation (Barres et al. 1992; Nishiyama et al. 1996b; Barres and Raff 1994). The high metabolic demand due to their constant increase in total membrane surface and the limited access to growth factors, presumably, lead to the death of the majority of preOLs (up to 80%) (Hughes et al. 2018; Trapp et al. 1997; Sun et al. 2018). The apoptosis of these cells has been shown to be mediated by the Bax/Bak system (Kawai et al. 2009; Sun et al. 2018) . Firstly, *Bak* and *Bax* mRNA were identified in OLs during maturation *in vitro (Kawai et al. 2009)*. $Bak^{-/-}/Bax^{-/-}$ cells were shown to be resistant to apoptosis *in vitro* and their *in vivo* knockout (KO) lead to increased ectopic presence of myelinating OLs (Sun et al. 2018). Therefore, it seems, as if the premature death of premyelinating OLs resembles the default mode and their survival an exception, which is initiated by finding a stable connection with a nearby axon. The exact reason for this extensive overproduction and the consequential high energy demand and waste, is not fully clear. Certainly, comparable processes are known and well described in many other cell types, like neurons, during development in which their survival is also dependent on the supply of neurotrophic factors (Raff et al. 1993).

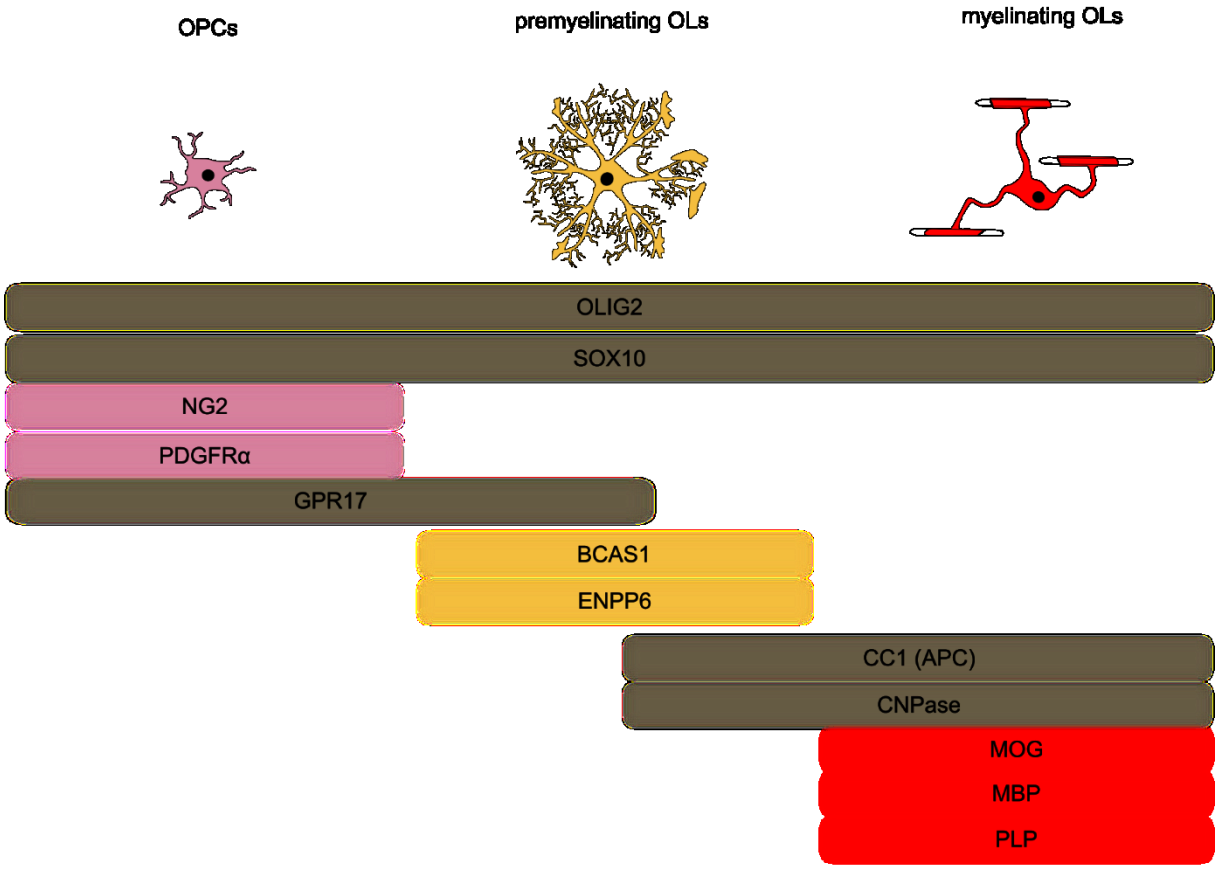

Figure 3: Stage-dependent markers expressed in the OL lineage. Lineage markers OLIG2 and SOX10. OPC-specific markers NG2 and PDGFRα. Premyelinating OL markers BCAS1 and ENPP6. Markers defining mature OLs like MOG, MBP and PLP. Other markers like GPR17 are expressed in a subpopulation and by more than one stage. Markers CC1 and CNPase are expressed during terminal differentiation and early maturation.

1.4.7 Myelination: Wrapping of an axon

Once the connection is built, the OL tightly wraps its lamellipodia around the axon with its growing end sliding below the already formed upper layers creating a so-called internode between two nodes on Ranvier (Snaidero et al. 2014). During this process, the internode grows in radial and in longitudinal direction simultaneously. While new membrane is added at the inner tongue for radial growth, the inner most layer also expands laterally, squeezing itself under the already existing sheets, thereby, creating the paranode. The myelin sheet is not compacted yet and open cytoplasmic channels connect the inner tongue with the cell body through so called Schmitt-Lantermann incisures. The intracellular compaction is mediated by MBP, in a zipper-like manner (Aggarwal et al. 2013). MBP pulls together the two membranes, creating the major dense line in compacted myelin sheets. In this process, 2′,3′-Cyclic-nucleotide 3'-phosphodiesterase (CNPase), one of the most abundant myelin proteins, seems to act as an inhibitor. It has been shown to organize the cytoskeleton, thereby, counteracting MBP-mediated membrane compaction (Snaidero et al. 2017). The extracellular compaction, on the other hand, is less well understood in the CNS. Although proteins like PLP and apolipoprotein D have been implicated in the process, the exact mechanism remains elusive (Nave and Werner 2014; García-Mateo et al. 2018). At the compacted stage, the inner tongue and cell body are only connected by the still uncompacted paranodal loops (Michalski and Kothary 2015). During postnatal development the growth of one OL can be 5.000 μm^2/ day and the complete myelin sheet can consist of up to 160 membrane layers with an internodal length of up to 1.7 mm (Nave and Werner 2014). Membrane expansion has been shown to be mediated by vesicular SNARE proteins VAMP2/3-dependent exocytosis (Lam et al. 2022). Despite the previously described understanding about the myelination process, not all components are already fully understood, e.g., it is still elusive why a specific axon is myelinated and at what level this decision is encoded. Also, the exact mechanisms needed for the recently and extensively characterized plasticity of myelination within the adult murine brain are incompletely understood (Xin and Chan 2020; Foster, Bujalka, and Emery 2019; Mount and Monje 2017; de Faria et al. 2021). In the following we will describe our current understanding of the initiation process of oligodendrogenesis and myelination.

1.4.8 Initiation and modulation of OPC differentiation

Myelin is a crucial part within the CNS. As OLs wrap around nearby axons insulating them to increase their conduction velocity and providing them with essential nutritional support, the reasons why not all axons in the CNS are myelinated remains unclear. In culture, the myelinating properties of OPCs were studied and myelination was found to be mainly dependent on substrate diameter and did not even dependent on cellular material for myelination (Voyvodic 1989; Friede 1972; Lee et al. 2012). In the peripheral nervous system expression of neuregulin 1 type III (NGR1) above a certain threshold leads to the initiation of myelination by Schwann cells (Taveggia et al. 2005). NRG1 in turn is dependent on the axon caliber (0.4 – 1.2 μm), wherefore, axonal diameter seems to be the main driver of peripheral

myelination. In the CNS, also smaller sized axons (0.2 µm) can be myelinated. Central myelination seems to be influenced by more than axonal diameter, as NGR1 levels do not trigger oligodendroglial myelination (Lee et al. 2012).

1.4.8.1 Neuron-OPC synapses as modulators of OPC physiology

Interestingly, neurons form glutamatergic synapses with AMPA receptor-expressing OPCs, potentially enabling them to directly react to neuronal activity. These synapses closely resemble those formed between neurons with all properties defining them (Bergles et al. 2000). Soon after this discovery, OPCs and OLs were shown to also express functional NMDA receptors, making them especially sensitive to signaling from glutamatergic neurons further raising the question whether neuronal activity might influence their physiology (Karadottir et al. 2005). As $GABA_A$ receptor-expressing OPCs are also contacted by GABAergic interneurons OPC physiology seems to be influenced by different neuronal populations and stimuli (Lin and Bergles 2004). These neurotransmitter-mediated neuron-OPC interactions were shown to influence proliferation, migration, differentiation and maturation of OPCs *in vitro* and *in vivo* (Gautier et al. 2015; Lundgaard et al. 2013). The so-called, activity-dependent myelination is today a widely accepted model for CNS myelination and is influenced by these synaptic contacts (Gibson et al. 2014; Hughes et al. 2018; Osso, Rankin, and Chan 2021; Eugenin von Bernhardi and Dimou 2022; Wake, Lee, and Fields 2011; Monje 2015). But, oligodendrogenesis is also modulated by neurotransmitter-independent processes. It can be influenced by hormones, the interaction with other glial cells or with extracellular matrix (ECM) components and G-protein coupled receptor (GPCR)-mediated signaling.

1.4.8.2 Hormonal influence on OPCs

Already early on it was acknowledged that thyroid hormones, triiodothyronine (T3) and thyroxin (T4), produced in the thyroid gland positively influence OPC differentiation and OL generation (Barres, Lazar, and Raff 1994; Almazan, Honegger, and Matthieu 1985). Still, thyroid hormones promote terminal differentiation by inducing cell-cycle arrest and increased pro-differentiation gene transcription (Lee and Petratos 2016). Although these hormones have profound effects on oligodendrogenesis, their relevance seems to lay in the coordination of developmental differentiation processes as OPCs also differentiate in their absence (Barres, Lazar, and Raff 1994). Neuropeptides, like dynorphin or galanin, but also other hormones, like steroids and estrogens, have also been connected to OLC differentiation (Long et al. 2021a).

1.4.8.3 Glia-glia interactions contributing to OPC differentiation

The interaction with other glial cell types, like astrocytes, has long been implicated in the modulation of OPCs and oligodendrogenesis. Firstly, astrocytes are a major source of PDGF inside the CNS and can modulate OPCs' capacity to proliferate and differentiate (Pringle et al. 1989; Richardson et al. 1988).

Secondly, they are connected to OLs via gap junctions, forming a glial syncytium by which fast communication and molecule transfer is enabled (Hughes and Stockton 2021; Orthmann-Murphy et al. 2007; Stephan, Eitelmann, and Zhou 2021; Vana et al. 2007). Astrocytic contribution to remyelination in MS has recently been shown in a study by Molina-Gonzales an colleagues (Molina-Gonzalez et al. 2023) but their role in developmental and adult oligodendrogenesis, especially *in vivo*, is less well understood (Tognatta et al. 2020). As most of the studies showing microglia or astrocytes modulating OPC proliferation or differentiation have been performed *in vitro*, further experiments need to clarify their functional significance in the *in vivo* situation.

1.4.8.4 ECM components and stiffness

The same is true for OPC-ECM interactions. While ECM density and certain ECM components like hyaluronan or CSPG have been shown to influence OPC differentiation and OL generation, their role *in vivo* is not clear (Kuboyama et al. 2017; Back et al. 2005). Hyaluronan was found to be upregulated in MS lesions and to inhibit remyelination via TLR2 signaling, but its role under physiological conditions is less well understood (Back et al. 2005; Sloane et al. 2010). Certain transcription factors like Yes-associated protein 1 (YAP) and its paralog transcriptional coactivator with PDZ-binding motif (TAZ), which are regulated by ECM-dependent signaling, are already known to play a role in Schwann cell myelination (Feltri et al. 2021). Very recently, YAP and TAZ have also been identified to be involved in OL remyelination *in vivo,* without any major influence on physiological myelination processes *(Hong et al. 2023)*. More research is needed to elucidate the functional role of ECM-OPC interaction under physiological conditions, e.g., during development.

In sum, oligodendrogenesis is a process, which, even in the adult brain, is highly plastic and influenced by many different environmental factors. An additional potential contributor is GPCR signaling, which has already been shown to influence OLCs physiology and differentiation. One of the GPCRs already implicated in modulation of OPC stage transition will be further described in the following part.

1.4.9 GPR17: A GPCR influencing oligodendrogenesis

One of the GPCRs already connected to OPC differentiation is the G-protein coupled receptor 17 (GPR17). This receptor is expressed in a subpopulation of OPCs and functions as a gate keeper for oligodendrogenesis by inhibiting OPC differentiation (Chen et al. 2009; Fumagalli et al. 2015). Once OPCs exit mitosis, GPR17 is upregulated and distributed from the Golgi apparatus to the cellular processes. The cells stop dividing and progressively lose their NG2 expression. Subsequent downregulation of GPR17 is a necessity for OL maturation as blocking GPR17 downregulation leads to its impairment (Fumagalli et al. 2015). Interestingly, their differentiation rate under physiological conditions is low and is only increased following mechanical injury in the cortex, but not after ischemia (Bonfanti et al. 2017; Vigano et al. 2016). Therefore, the question whether $GPR17^+$ OPCs serve as a reserve pool following pathological conditions, as proposed by Vigano and colleagues, is still debated

(Vigano et al. 2016). In a recent study by Miralles and colleagues, the long-term fate (up to 1 year) and density of GPR17-expressing OPCs was analyzed following repeated tamoxifen induction in *GPR17-CreERT2::GFP* mice (Miralles et al. 2023). It was shown that $GPR17^{+}$ cells are a stable and distinct subpopulation of OPCs. Also, this study confirmed that $GPR17^{+}$ OPCs do not contribute to the generation of OLs under physiological conditions (Miralles et al. 2023). The contribution of GPR17 under pathological conditions was recently investigated in the $SOD1^{G93A}$ amyotrophic lateral sclerosis (ALS) mouse model (Bonfanti et al. 2020). ALS is characterized by progressive loss of motor neurons and also linked to impaired oligodendrogenesis. GPR17 protein was increased in spinal cord during early and late stages of disease progression. Isolated OPCs showed impaired differentiation, which was rescued by inhibition of GPR17 (Bonfanti et al. 2020). Further, GPR17 has been connected to demyelinating disease pathology following analysis of human MS tissue (Angelini et al. 2021). Although cellular mechanisms of GPR17 seem to be well understood and might resemble an example of context-dependent modulation of OPC differentiation by a GPCR, the exact role of this subpopulation of OPCs, especially under physiological conditions, remains unclear.

1.5 Brain injury, neuroinflammation and regeneration

Traumatic brain injury (TBI) can be separated into two different categories: i) the non-penetrating TBI, characterized by an external force to the skull, strong enough to damage the brain by its own movement within the skull and ii) the penetrating TBI, in which local damage is caused by an external object which directly penetrates the brain (NINDS 2023). In both cases the brain can be massively injured, leading to cellular death and BBB breakdown. The injury itself can be separated in two parts. The primary injury which is caused by the mechanical disruption and the subsequent secondary damage (Huntemer-Silveira et al. 2021). Both injury stages are accompanied by major neuronal, but also OL death. The following axonal degeneration, caused by loss of OL support, induces more demyelination and OL degeneration and subsequently leads to more axonal damage (Huntemer-Silveira et al. 2021). Therefore, secondary injury can also affect parts distant from the actual injury site. The brains' endogenous reaction to damage is mainly mediated by the previously described glial cell types: (i) microglia, (ii) astrocytes and (iii) OPCs (Fig. 4). All of these three contribute to the reaction to injury in the brain, but not all of them are triggered by the same stimuli. Microglia, the resident immune cells of the brain, react to all types of injuries, whereas OPCs and astrocytes only react when the tissue or the BBB is disrupted (Dimou and Gotz 2014). Microglia can react within hours after an insult (Nimmerjahn, Kirchhoff, and Helmchen 2005). As tissue resident macrophages, they quickly start to phagocytose surrounding debris from dead cells. They also start to proliferate, become hypertrophic and release pro-inflammatory cytokines, like tumor necrosis factor alpha (TNFα), as well as toxic substances like nitric oxide (Loane and Kumar 2016) (Fig. 4). Within the first 24-48 h OPCs start their reaction which is characterized by three stages. Initially, and unlike the other glial cell types, they are able to actively move towards the injury site (Fig. 4, B). Subsequently, they proliferate with up to 100-fold of their baseline rate (Dimou and Gotz 2014).

This steep increase in cell numbers is followed by the differentiation of cells into myelinating OLs, which is accompanied by the previously described reduction in total cell numbers also observed during developmental and adult myelination (Fig. 4 C, D). Next to this oligodendrogenic reaction, the role of OPCs following injury is less well understood. As described above, TGFβ2-mediated communication with microglia might influence the injury environment following mechanical injury (Zhang et al. 2019). The so-called astrogliosis by reactive astrocytes also starts within the first 24 h after insult by upregulation of structural proteins and activation markers like glial fibrillary acidic protein (GFAP) and vimentin (Robel, Berninger, and Gotz 2011) (Fig. 4, B, C). Accompanied by an increase in cell body size, these hypertrophic astrocytes also release other proinflammatory substances like Interleukin-6 (IL-6), IL-1 β and TNFα. This astrocytic cytokine-release has been shown to be mediated by toll-like receptor 4 (TLR4)-dependent signalling (Jiang et al. 2018). Besides, astrocytes have been shown to increase their PDGFA production upon inflammatory stimulation by TNFα and TGFβ, possibly influencing OPC proliferation following injury (Silberstein et al. 1996). The palisading astrocytes develop processes towards the injury site without active migration towards it. Astrogliosis is also connected to a proliferative response of juxtavascular astrocytes, starting around 3 days after injury (Bardehle et al. 2013). The proliferative reaction reaches its peak after 5-7 days but is limited to one division in only 10-20% of the cells (Dimou and Gotz 2014). In spinal cord injury, genetic ablation of astrocytes causes an increase in inflammatory processes, increased numbers of infiltrating leukocytes, a larger injury site and a delayed closure of the BBB (Faulkner et al. 2004). Nevertheless, the exact role of astrocytes and OPCs following TBI, either being beneficial or detrimental, is not fully clear. For example, axonal regeneration has been shown to be inhibited by myelin-associated proteins like myelin-associated glycoprotein (MAG), Nogo or semaphorin3 (Nave and Werner 2014; Filbin 2003; McKerracher and Rosen 2015).

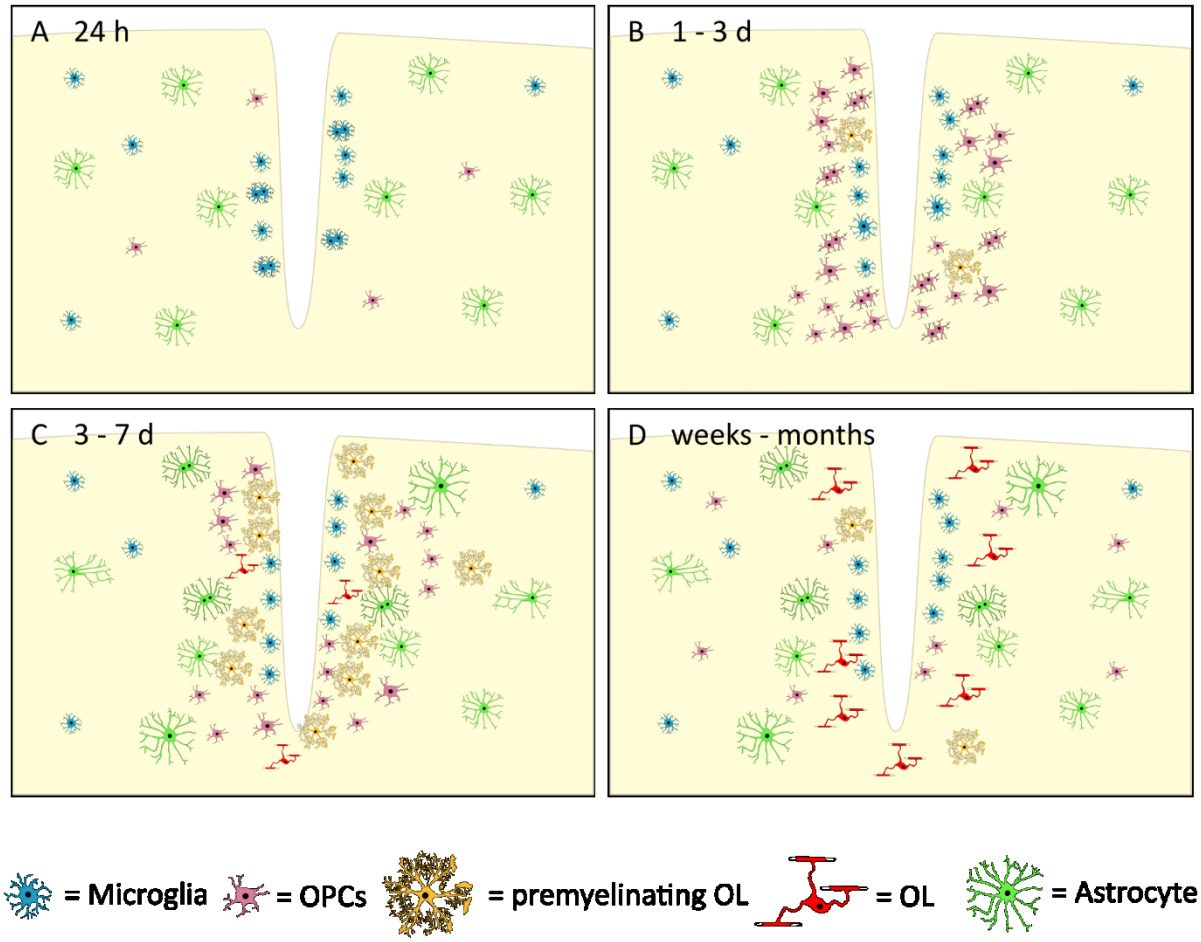

Figure 4: Glial cells and their time-dependent reaction to injury. A, Following injury, microglia react by proliferation within the first 24h. B, OPC proliferation and early differentiation into premyelinating OLs within first 1-3 dpi. C, Between 3 and 7 dpi astrocytic proliferation, hypertrophy and process elongation towards injury site, ongoing OPC proliferation, differentiation and overproduction of premyelinating OLs and first generation of mature OLs. D, Weeks and months following injury OPC numbers decrease, regeneration of the OL pool and remyelination take place [based on (Ries 2018)].

1.6 Neuropeptides

Neuropeptides are one of the most heterogeneous type of signalling molecules with a great diversity concerning their target structures, but also their biological functions. They have been shown to play a major role in a wide range of physiological processes (Burbach 2011). Nevertheless, due to their structural diversity, the number of isoforms and their relatively low expression level under physiological conditions their investigation has proven to be challenging (DeLaney et al. 2018). In the following, I will give an overview of their discovery, structure and the physiological hallmarks defining them. Additionally, I will describe their relevance for CNS function in neuronal, but also non-neuronal cells of the central nervous system with a special focus on the stress-related neuropeptide corticotropin-releasing hormone (CRH).

1.6.1 What are neuropeptides?

Neuropeptides are a special type of peptide hormones, which were first found to be produced and secreted by neurons (Bohus and De Wied 1966; De Wied 1971). Therefore, most of what we know about them has been investigated in neurons or neurosecretory cells. As we will see in one of the following chapters, neuropeptides have also been identified in many non-neuronal cell types.

1.6.1.1 Structure and intracellular processing

One common feature of neuropeptides in neurons is their release via the regulated secretory pathway. Therefore, neuropeptides share a common structure, which enables them to be processed and released via this route. Neuropeptides are expressed as pre-pro peptides, which carry an N-terminal 20-25 amino acid long signal peptide, which facilitates their entrance into the secretory route (Larhammar 2009; Burbach 2011). This extension is directly removed upon entering the endoplasmatic reticulum (ER). The pro-neuropeptide leaves the ER and enters the Golgi apparatus for further processing. A common feature of neuropeptides is that from the same pro-hormone different cell-specific neuropeptides can be generated. Therefore, the pro-neuropeptide is cleaved by a specific subtype of subtilisin proteases, the pro-hormone convertases (Apletalina et al. 1998). These convertases, with cell-specific expression patterns, lead to the differences in mature neuropeptides originating from the same pro-hormone, described above. Further modifications of the neuropeptide include C-terminal amidation, N- and O-glycosylation, sulfation, glycosylation and acetylation. In most cases, C-terminal amidation is required for biological activity of the peptide and is performed by peptidyl-aminotransferases. During the amidation process a C-terminal glycine acts as donor for the preceding amino acid (Burbach 2011).

1.6.1.2 Storage and release initiation

When leaving the Golgi apparatus neuropeptides are stored in large dense-core vesicles (LDCVs) in which many of the above-mentioned modifications can still take place. These vesicles with a diameter of > 70 nm (neurotransmitter vesicles diameter 40 – 50 nm) are found not only in neurons but also in other secretory cells like endocrine, chromaffin, neuroendocrine and immune cells (Thureson-Klein and Klein 1990). In these non-neuronal cell types their size (300 – 1000 nm) exceeds that of neuronal LDCVs (Merighi 2018). Depending on the cell type, LDCVs can store hormones, cytokines, biogenic amines, neurotransmitters or ATP.

The release from LDCVs in the neurohypophysis has been shown to increase with spike frequency, which is dependent on cytosolic Ca^{2+} changes and has to be initiated by a strong stimulus, as they are not docked, but have to be transported to the site of their release (Dreifuss et al. 1971; Bondy, Gainer, and Russell 1987; Gainer et al. 1986; Jackson, Konnerth, and Augustine 1991; Muschol and Salzberg 2000; Lang et al. 1997; Tooze, Martens, and Huttner 2001). Therefore, their Ca^{2+}-dependent secretion has to be initiated by prolonged stimuli and is relatively slow compared to fast-acting neurotransmitters (Tawfik et al. 2021; Hökfelt et al. 1980). Release can occur by full fusion, "kiss and run" or "cavicapture" exocytosis and might require a unique set of proteins regulating their transport and release (Tsuboi, McMahon, and Rutter 2004; Sieburth et al. 2005; Sieburth, Madison, and Kaplan 2007). One has to keep in mind, that most of these processes have been studies in the neurohypophysis in which not only LDCV size (180-200 nm) but also their number greatly differs from that in other neurons. Because neuropeptides are synthesized and packed at the Golgi, they have to be transported along the axon and cannot simply be taken up like neurotransmitters. The underlying release mechanisms have to be seen in the light of limited capacity and slow replenishment of filled vesicles (van den Pol 2012).

1.6.1.3 Neuropeptide expression patterns

The expression and release pattern of neuropeptides can be separated into three different categories. Some are expressed at high levels under physiological conditions and, therefore, are always readily available. Others, like substance P in the trigeminal ganglion, are lowly expressed and specifically upregulated when needed, e.g., following nerve injury (Abd El-Aleem and Morales-Aza 2019; Fu et al. 2013). The last type, e.g., galanin in primary sensory neurons, is only expressed during development, but can be upregulated in adulthood under certain conditions. It has to be considered that one neuropeptide can fall into all three categories, depending on the neuronal subtype expressing it (Hökfelt et al. 2000).

1.6.1.4 Cellular release sites and volume transmission

Another distinctive property of neuropeptides lies in the distance over which they can exert their effects. Neurotransmitters are typically released predominantly at the presynaptic zone and diffuse and interact with their receptors within a few tens of nanometers, before undergoing rapid degradation and reuptake. Their membrane interaction is mainly mediated by ionotropic receptors causing direct and rapidly reversed changes in membrane polarization (Ludwig and Leng 2006).

In the case of neuropeptides, it is known that their release is not confined to the synapse but can also occur at extra-synaptic locations, like the axon, soma, and dendrites (Ludwig and Stern 2015). It is, therefore, at least in part spatially independent of synaptic wiring. Furthermore, their interaction with target receptors can be effective over long distances, also due to their relatively long half-lives (Ludwig and Leng 2006; Jan and Jan 1982; Mens, Witter, and van Wimersma Greidanus 1983). Therefore, neuropeptides seemingly are less spatially and temporally restricted, then neurotransmitters (Ludwig and Leng 2006).

Inside the brain, this kind if long-range signaling, which is conducted through the extracellular space or the cerebrospinal fluid (CSF), is commonly called “volume transmission”. The term originates from the observed mismatch of ß-endorphin and Met-/Leu-enkephalin terminals and their receptors, μ and δ opioid receptors, proposing long range, synapse-independent signal transduction as a possible mechanism (Agnati et al. 1986). On the other hand, long-distance diffusion would hinder a specific effect of a neuropeptide released by a distinct neuronal population. Furthermore, neuropeptides are actively degraded in the extra cellular space by membrane anchored peptidases like neprilysin also known as endopeptidase-24.11 (Grady et al. 1997; Wagner et al. 2015), decreasing their diffusion distance and limiting their long-range biological effect. Therefore, diffusion may be more relevant in a locally restricted manner, acting within the micrometer range around the secretion site, as proposed by Van den Pol in a “local diffusion hypothesis” (van den Pol 2012). Nonetheless, in selected instances, neuropeptides may be released in substantial quantities and exert their effects over long distances. Still, this phenomenon seems to be the exception rather than the rule (van den Pol 2012). In sum, neuropeptides have the potential to act over longer distances and greater time-windows than neurotransmitters because of the characteristics described above.

1.6.2 Neuropeptides and their receptors

Another contributing factor is that neuropeptides predominantly target GPCRs. These receptors can amplify signals enabling them to detect the low nanomolar concentrations of peptide, whereas ionotropic neurotransmitter receptors respond in the micromolar range (van den Pol 2012).

GPCRs are the largest group of membrane proteins and are commonly divided into 5 families: rhodopsin (family A), secretin (family B), glutamate (family C), adhesion and Frizzled/Taste2. All of these share their seven transmembrane α-helical segments and influence different intracellular pathways, mediated

by their interaction with G-proteins (Rosenbaum, Rasmussen, and Kobilka 2009). Neuropeptides can bind to different receptors expressed by target neurons (e.g. CRH, NPY). They commonly interact with members of family A and B_1 (Burcin Duan and Necla Birgul 2018). A detailed description of the interaction of the neuropeptide CRH with its receptor corticotropin-releasing hormone receptor type 1 (CRHR1), belonging to the class B, and its downstream effects can be found elsewhere (Ries and Deussing 2020). Still, it has to be mentioned, that GPCR signaling and its effects are highly dependent on the expressing cell type and the specific neuropeptide-GPCR interaction that is analyzed, as can be shown by the biological function a single peptide can exert in different contexts. Differential receptor binding is further promoted by degradation or truncation of neuropeptides by various peptidases following release (Hökfelt et al. 2000; Wagner et al. 2015).

1.7 Neuropeptides in glia

Neuropeptides, as their name already suggests, have mainly been studied in neurons. Therefore, most of what we know about them, e.g., their release mechanisms or their biological functions, we have learned from studies concentrating on neuronal communication. Nevertheless, neuropeptides can also be expressed and secreted from other cell types, including glial cells (Ubink, Calza, and Hökfelt 2003). Although, at least in astrocytes, neuropeptide release has been shown to be associated with vesicular release, glial cells were mainly believed to solely have a constitutive secretory pathway in which substances cannot be stored and directly released upon stimulation, not comparable to the neuronal regulated release (Ubink et al. 1994; Krzan et al. 2003). In astrocytes, this view has been revised, because astrocytes possess some of the hallmarks of regulated exocytosis, like SNARE proteins and exert Ca^{2+} changes upon stimulation (Vardjan et al. 2019; Hur et al. 2010). Compared to astrocytes, which have been shown to also form LDCVs, OLs have been mainly connected to micro vesicular or exosome release (Reiter and Bongarzone 2020). In OPCs this issue has not been properly addressed, yet. In the following part I will give an overview about what is known about neuropeptide-glia interaction, prerequisites for glial release and possible functions concentrating on astrocytes and the OL lineage.

1.7.1 Neuropeptide expression in glial cells: The pioneering role of astrocytes

Neuropeptide expression by glial cells was first shown in the late 1990s by Shinoda and colleagues (Shinoda et al. 1989). In their study, they showed that astrocytes cultured from different brain regions express a specific set of neuropeptides. Somatostatin was shown to be mainly expressed in cerebellar astrocytes, whereas enkephalin and proenkephalin were mainly found in cortex, cerebellum and striatum. Since then, especially astrocytes were shown to express different neuropeptides under distinct conditions, e.g., during development or following injury (Low, Allen, and Melner 1992; Bunnemann et al. 1992; Vilijn et al. 1988; Shinoda, Marini, and Schwartz 1992; Fu et al. 2013; Buzas 2002). Still, these experiments were predominantly performed *in vitro* and showed either mRNA or protein presence, only.

Therefore, the function of neuropeptides and astrocytes *in vivo*, remains unclear. Recent studies suggest, that neuropeptides are not only expressed by astrocytes but can also regulate physiological processes, like proliferation of neuronal stem cells, by modulating astrocytic function (Asrican et al. 2020).

1.7.2 Dynorphin and galanin: Neuropeptides and their role in oligodendrogenesis

1.7.2.1 Dynorphin

One of the best studied neuropeptides in the context of glial cells and especially the OL lineage is dynorphin. Dynorphin A, derived from prodynorphin, is the main variant in the brain and spinal cord under physiological conditions. Its preferential receptor is the κ opioid receptor (KOR). Dynorphin A, a neuropeptide closely connected to pain, was also found to be elevated following traumatic CNS injuries like spinal cord injury as early as 4 hpi (Faden et al. 1985; Przewłocki et al. 1988; Yakovlev and Faden 1994). Dynorphin A can exert deleterious effects under supraphysiological conditions, supposedly by interacting with glutamate receptors and its KO leads to a decrease in caspase positive cells following spinal cord injury (Adjan et al. 2007). The finding that the inhibition of μ opioid receptor (MOR)) and KOR in pregnant rats by buprenorphine lead to a concentration-dependent effect on MBP levels and that opioid receptor expression in the severely hypomyelinated JIMPY mice is reduced, connected opioid receptors to OL pathologies (Sanchez et al. 2008; Eschenroeder et al. 2012; Knapp, Adjan, and Hauser 2009). Furthermore, KOR activation alleviates disease score in the experimental autoimmune encephalomyelitis (EAE) model and a KOR agonist was shown to enhance OL maturation (Du et al. 2016; Mei et al. 2016). Just recently, dynorphins KOR-dependent role in stress connected oligodendrogenesis was shown by Osso and colleagues (Osso, Rankin, and Chan 2021). Their experiments showed that dynorphin A, released by non-myelinated axons in the striatum, drives oligodendrogenesis and myelination of surrounding neurons. Furthermore, they imply dynorphin A with a role in developmental oligodendrogenesis.

1.7.2.2 Galanin

Another neuropeptide that has been connected to the OL lineage is galanin. In an early experiment investigating the influence of KCl-induced cortical spreading depression on galanin expression in the murine brain, *galanin* mRNA upregulation was identified in OPCs (Shen, Larm, and Gundlach 2003). Besides, an increase of the galanin receptor (GalR1) mRNA was identified in cortical neurons. Furthermore, galanin positive OPCs were also identified under physiological conditions in different brain regions (Shen, Larm, and Gundlach 2003). This physiological expression was shown to start between P2 and P5 and persist up to P40 in the corpus callosum (Shen et al. 2005). Because galanin overexpression was shown to increase endogenous MBP levels (Lyubetska et al. 2015), galanin's role in demyelinating disease was analyzed. Galanin expression was shown to modulate EAE severity with its overexpression (OE) leading to an attenuation of symptoms and its inhibition or KO increasing

disease severity without a clear functional explanation (Wraith et al. 2009). The attenuation of demyelination by galanin OE and its worsening following galanin KO was also shown in the cuprizone model (Zhang et al. 2012; Gresle et al. 2015). Furthermore, leukemia-inhibitory factor 1 (LIF-1) was shown to be the main driver of galanin-dependent OL survival *in vitro* and *in vivo*. LIF-dependent upregulation of galanin in OLs following cuprizone treatment was shown by comparison of LIF KO and WT mice (Gresle et al. 2015).

In sum, dynorphin A and galanin can be seen as examples for how neuropeptides can influence or even drive physiological processes in non-neuronal cells upon neuronal or non-neuronal release. In the following we will take a closer look at an extensively investigated neuropeptide which has, at least so far, not been implicated in the modulation of glial processes.

1.8 Corticotropin-releasing hormone

1.8.1 CRH and its receptors

Mature CRH, also known as corticotropin-releasing factor (CRF), is a 41 amino acid neuropeptide. It belongs to a family with urocortin 1-3, urotensin-1 and sauvagine (Spiess, Villarreal, and Vale 1981; Donaldson et al. 1996). It is directly connected to the reaction to stress and expressed widely throughout the brain. Its two receptors, corticotropin-releasing hormone receptors 1 and 2 (CRHR1 and CRHR2) are also found in many different tissues throughout the body, including the brain. As GPCRs, CRH receptors consist of seven α-helical transmembrane domains and signal through heterotrimeric G-proteins (Perrin and Vale 1999; Hillhouse and Grammatopoulos 2006). The receptors are encoded by 2 different genes and differ in their ability to bind CRH and their other ligands but share almost 70 % sequence homology. CRHR1 is the high affinity receptor for CRH and binds to it with a 15 times higher affinity than to CRHR2 (Hauger et al. 2003; Perrin and Vale 1999). Urocortin 1 binds with a comparable affinity to both receptors and urocortins 2 and 3 are exclusive ligands of CRHR2 (Hauger et al. 2003).

1.8.2 CRH and its connection to stress

The CRH/CRHR1 system is a crucial element of the bodies stress response via the hypothalamic-pituitary-adrenal (HPA) axis. Upon activation of parvocellular neurosecretory cells of the nucleus paraventricularis of the hypothalamus (PVN) by psychosocial stress, CRH is produced and released into the portal vasculature. Upon binding of CRH to its receptor CRHR1 in the anterior pituitary, adrenocorticotropic hormone (ACTH) is secreted into the blood stream. After sensing this hormone, cells of the adrenal cortex produce and secrete corticosterone into the blood. This steroid has three general effects: i) It causes the upregulation of the catabolic metabolism, ii) inhibits the immune system to increase the amount of energy that can be used for coping with the stressful situation and iii) inhibits the production and release of CRH and ACTH to prevent an excessive reaction via a negative feed-back loop (Neil A. Campbell 2009; Mark F. Bear 2009) (Fig. 5). Besides in the PVN, CRH production and

secretion is also present in other, extrahypothalamic regions, like the extended amygdala, including the bed nucleus of the stria terminalis, the central amygdala and the lateral part of the interstitial nucleus of the anterior commissure, the hippocampus, as well as the piriform and prefrontal cortex (PFC) (Cummings et al. 1983; Swanson et al. 1983; Waters et al. 2015; Chang et al. 2022). Despite the fact that CRH has been implicated in behaviors relevant for coping with salient environmental stimuli including arousal, anxiety- and fear-related behaviors involving extrahypothalamic CRH/CRHR1 neurocircuits, many aspects of its function remain elusive (Heinrichs and Koob 2004; Lowry and Moore 2006; Refojo et al. 2011; Fuzesi et al. 2016; Sanford et al. 2017; Dedic et al. 2018; McCall et al. 2015; Chang et al. 2022). Nevertheless, some general mechanisms have been proposed. CRH is stored in LDCVs and, therefore, always readily available. Upon the arrival of a stimulus, CRH is released instantaneously and the expression of *Crh* starts with the transcription of the primary mRNA within minutes after the stimulation. Already one hour after the stimulus the level of mature *Crh* mRNA starts to increase and the reservoir of the neuropeptide is restored (Aguilera and Liu 2012). It is worth mentioning that these results were gathered exclusively in the PVN and, therefore, might not translate to other neuronal populations or even other cell types. Neither the stimuli nor the exact release mechanism and location, either synaptically or via some way of volume transmission, are fully understood (van den Pol 2012).

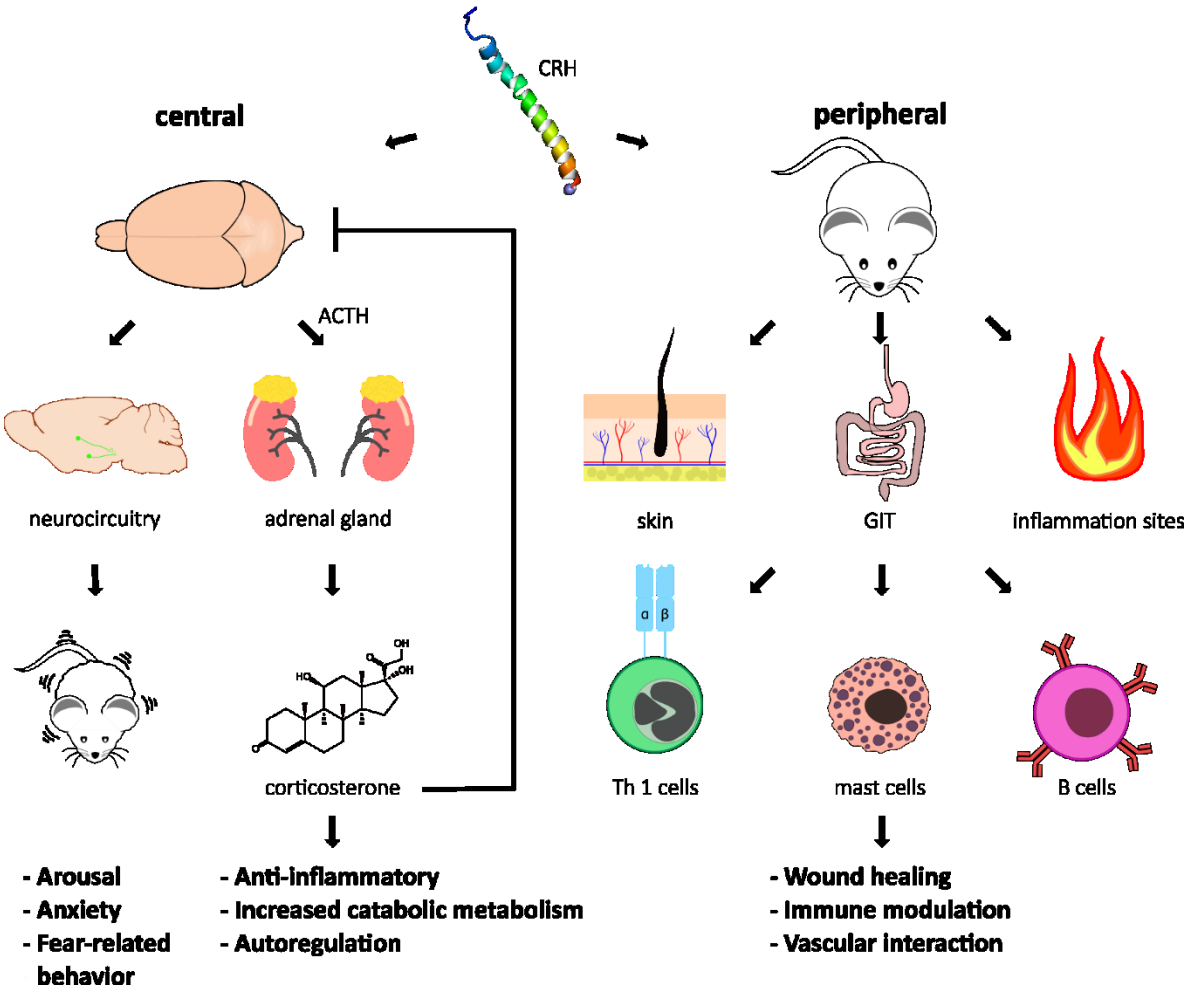

Figure 5: Central and peripheral actions of CRH. Direct involvement in the stress neurocircuitry with role in arousal, anxiety and fear-related behavior. HPA axis activation with subsequent corticosterone release from adrenal gland leading to anti-inflammatory action, increased catabolic metabolism and autoregulation via negative feedback-loop by downregulation of CRH release in the PVN. Peripheral CRH, its expression sites and target cells. Involvement in wound healing, immune modulation and interaction with vasculature in the periphery by local release [based on (Ries 2018)].

1.8.3 CRH coding region

The *Crh* gene comprises two exons separated by one intron dividing the 5' untranslated region (5'-UTR) (Fig. 5). The proximal 5' sequence contains a glucocorticoid response element (GRE), an estrogen responsive element and a cyclic adenosine monophosphate (cAMP) response element (CRE) (Seasholtz, Thompson, and Douglass 1988; Malkoski and Dorin 1999; Vamvakopoulos and Chrousos 1993). A neuron-restrictive silencing element (RE-1/NRSE), potentially represses *Crh* transcription in non-neuronal tissue and is located in the intron of the *Crh* gene (Seth and Majzoub 2001a).

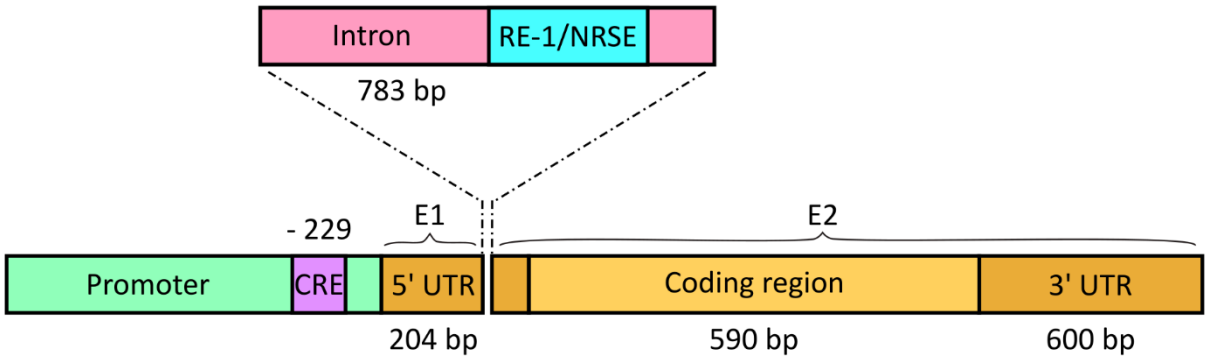

Figure 6: The rat *Crh* gene with promoter and flanking UTRs. Abbreviations, CRE, cyclic AMP response element. UTR, untranslated region. RE-1/NRSE, neuron restrictive silencing element. Bp, base pairs. E1,2: exon 1, 2 [(Ries 2018) based on (Aguilera and Liu 2012)].

1.8.4 Upstream signalling

Following stress CRH-expressing neurons are activated, which is accompanied by the expression of immediate early genes like c-fos and the phosphorylation and nuclear translocation of transcription factors like cAMP response element binding protein (CREB) or mitogen-activated protein kinases (MAPKs) like ERK1/2 (Khan et al. 2007; Kovacs and Sawchenko 1996; Weinberg, Girotti, and Spencer 2007) (Fig. 6). *Crh* transcription is thought to depend on a cAMP/protein kinase A (PKA)-connected signalling pathway that leads to the recruitment of phosphorylated CREB (pCREB) to the CRE (Seasholtz, Thompson, and Douglass 1988) (Fig. 6). *Crh*-expression is regulated by an interaction of pCREB with the cAMP-dependent transducer of regulated CREB-activity (TORC), wherefore it also depends on the presence of cAMP. pCREB activity is potentiated by this co-activator. cAMP-increase inside the cell activates PKA, thereby, inhibiting the phosphorylation of TORC and leading to the release of TORC from scaffolding protein 14-3-3, by which it is bound under physiological conditions. Following nuclear translocation, TORC interacts with pCREB and promotes the expression of *Crh*. TORC2 is the most abundant TORC-subtype in the brain and has already been shown to co-localize with CRH^+ neurons in the PVN (Liu et al. 2011; Itoi et al. 1996; Aguilera and Liu 2012).

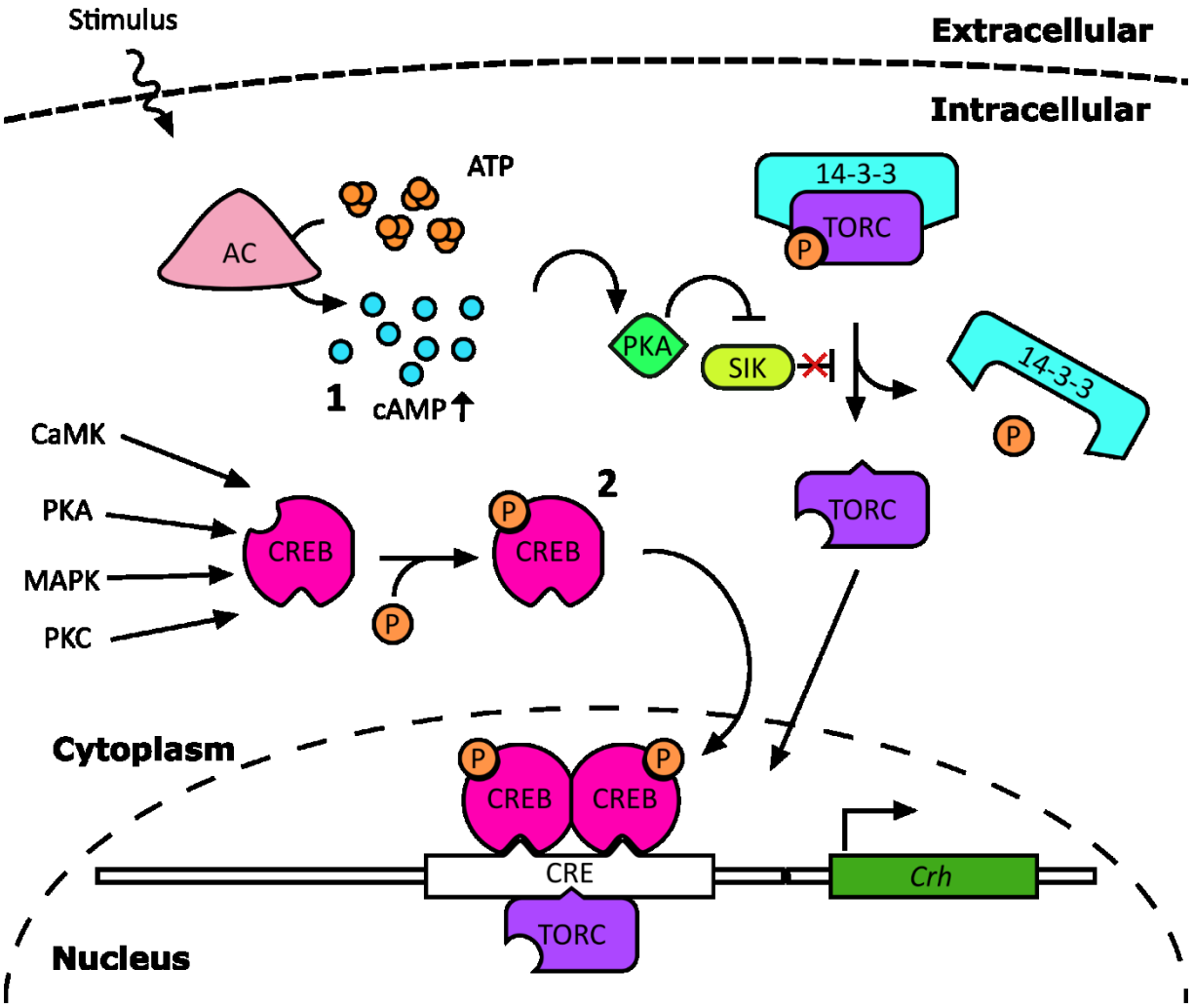

Figure 7: Upstream signaling pathways controlling *Crh* expression in PVN neurons. Intracellular increase of cAMP level (1) in combination with the phosphorylation of CREB (2) is essential for *Crh* expression. Abbreviations, AC, Adenylyl cyclase. ATP, Adenosine triphosphate. cAMP, cyclic adenosine monophosphate. PKA, Protein kinase A. SIK, Salt inducible kinase. TORC, Transducer of regulated CREB activity. CREB, cAMP response element binding protein. P, Monophosphate. CRE, cAMP response element. CaMK, Ca^{2+}/calmodulin-dependent protein kinase. MAPK, Mitogen-activated protein kinase. PKC, Protein kinase C [(Ries 2018) based on (Aguilera and Liu 2012)].

1.8.5 Peripheral CRH

Despite its main function in the HPA axis, CRH, released from parvocellular cells in the hypothalamus, has been proposed to act on peripheral structures because CRHR1 and CRHR2 can be found in different tissues in the periphery. Since the evidence for central CRH's ability to cross the BBB is rather weak, (Martins, Banks, and Kastin 1997), peripheral CRHRs are more likely to be targeted by CRH expressed in the periphery (Fig. 5).

Indeed, CRH is expressed and released directly in peripheral tissues like the skin, adrenal glands, heart, spleen, thymus, gastrointestinal tract and other organs (Baigent and Lowry 2000; Dave, Eiden, and Eskay 1985; Slominski et al. 2001; Webster, Battaglia, and De Souza 1989). Its receptors, were also identified in these tissues and on different immune cells like granulocytes, macrophages/monocytes, T-

cells, mast cells and on other cycling or resident immune cells (Mousa et al. 2003; Singh and Fudenberg 1988; Webster et al. 1990). CRHR2 expressed in B cells induces the activation of different signalling pathways and a decrease in cell viability following CRH administration, *in vitro* (Harle et al. 2018) (Fig. 5). Peripheral CRH has been implicated in severe skin disease like psoriasis, which is also connected to mast cell activation (Tagen et al. 2007). $CRHR1^+$ mast cells are activated and start to produce and release VEGF which increases the vascular permeability, following CRH administration (Theoharides et al. 1998). Whether CRH-mediated activation also leads to degranulation, release of tryptase, histamine, IL-6, IL-3, TNFα or other mast cell activation markers remains unclear. Interestingly, mast cells, in addition to their CRHR1-expression can also express CRH (Cao et al. 2005; Kempuraj et al. 2004). Recent research concentrated on CRH's role in the skin, in which it is assumed to be released by local cells, but also neuronal nerve endings. Since the identity of tissue resident CRH-expressing cells *in vivo*, has not been shown conclusively, this issue remains unresolved (Rassouli, Liapakis, and Venihaki 2018; Rassouli et al. 2011).

1.8.5.1 CRH, CRHR1 and their influence on brain injury/recovery

Although CRH and its' receptors have not been studied extensively in the context of brain injuries, there is evidence that the system might contribute to the brains reaction to certain pathologies. Just recently, CRH was connected to the brains' reaction to physical stress as CRH was shown to be upregulated in the hippocampus following thoracic trauma (Cursano et al. 2021). Moreover, synaptic loss and memory deficits in this trauma-induced delirium-like syndrome model is prevented by CRHR1 antagonism (Cursano et al. 2021). CRH has also been connected to the general pathogenesis of ischemic injury (Lyons, Anderson, and Meyer 1991; Strijbos, Relton, and Rothwell 1994) because *Crh* mRNA has been shown to be upregulated directly after stroke (Choi et al. 2001; Wong et al. 1995). Additionally, ischemic brain injury was shown to be reduced following the administration of CRHR antagonists (Loddick, Turnbull, and Rothwell 1998; Lyons, Anderson, and Meyer 1991; Mackay et al. 2001; Strijbos, Relton, and Rothwell 1994). Besides, CRH can influence glial cells, which are a major factor in the brain's reaction to injury. Microglia, for example, were found to express CRHR1 and CRHR2. Microglial activation lead to an upregulation of CRHR1 *in vitro* (Stevens et al. 2003). The *in vitro* administration of CRH led to the proliferation of microglia and the release of TNFα (Wang, Ji, and Dow 2003). But not only microglia, but also astrocytes were found to react to changes in CRH/CRHR-signaling. Reduced cerebral injury was shown in CRHR1 deficient mice after focal ischemia and a connection to a possible expression by astrocytes as well as microglia has been drawn (Stevens et al. 2003). In a more recent study, the effect of the CRHR1-specific antagonist antalarmin on neuroplasticity, inflammation, neuroprotection and behavioral recovery following global cerebral ischemia was tested. Results indicate, that CRHR1 blockade has beneficial effects on behavioral as well as cellular recovery and decreases GFAP, IBA1 and TNFα levels (de la Tremblaye et al. 2017a). In general, the involvement of CRH in

the reaction to brain injury and its expression by glial cell types, in particular *in vivo*, has not been deeply studied in the past and, therefore, the involved processes and mechanisms are largely unknown.

1.8.6 CRH and its connection to the OL lineage

The interaction between the immune system and the HPA axis, mainly driven by CRH, is commonly known (Gaillard 1994). Therefore, CRH-mediated activity of the HPA axis was investigated in the EAE model in Lewis rats (Calza et al. 1997). It was shown that *Crh* mRNA was reduced in the PVN prior to the peak of symptoms. No clear conclusion about its effect on EAE pathology was drawn. Later on, CRH was shown to induce increased cAMP levels in OLs in mixed glial cultures and to promote axonal outgrowth in primary neurons (Wiemelt, Lehtinen, and McMorris 2001; Yuan et al. 2010). Although a connection to microglia and OLs is drawn, no direct effect of CRH on these cells is described. In sum, it is not known, whether CRH is directly involved in processes connected to the OL lineage (Long et al. 2021b).

1.9 How to target CRH and CRHR1 *in vivo*

Targeting CRH or its receptor CRHR1, has proven to be difficult. CRH is, as typical for a neuropeptide, packed in LDCVs and transported along the cellular processes, which makes soma staining difficult. CRHR1 is a GPCR, which has already been shown to have a relatively low expression *in vivo* (Chang et al. 2022). Additionally, the limited availability to or the total lack of properly working antisera contributes to their low accessibility. The best performing antiserum against CRH, raised in the 1980s in the Vale lab, is limited in its accessible amount and can only be used for certain applications, but not for brain wide screens (Bloom et al. 1982; Itoi et al. 2014). A suitable antibody against CRHR1 is not available (Refojo et al. 2011) and, although methods like RNA-scope are an alternative, whole brain analysis are not possible for the majority of research groups. The cheaper alternative *in-situ* hybridization limits or even prevents the combination with other immune stainings. Therefore, research in the field has turned towards using transgenic mouse models to study the CRH/CRHR1 system. In the following I will give a short overview over the most commonly used models.

1.9.1 Site-specific recombinases (SSRs)

The accessibility of DNA modulatory systems has increased massively in the past decades. Already in the 1980s, researchers found and characterized a protein derived from a P1 bacteriophage that would change science forever. This protein was the cyclisation recombinase (Cre). This 38.5 kDa protein is able to recognize specific sites within its own genome called locus of cross over X of P1 (loxP) sites and recombine them with each other (Sternberg and Hamilton 1981; Hoess, Ziese, and Sternberg 1982). Following its identification and characterization it was first transferred and implemented into mammalian cells and later used to alter the murine genome (Sauer and Henderson 1988). The integration

of loxP sites around a gene/region of interest, and the subsequent recombination causes the excision and KO of the enclosed region or gene. This scientific milestone improved genetic manipulation and enabled the cell type-specific delivery of genetic alterations, by driving Cre with a cell type-specific promoter. In combinations with the plethora of different reporter proteins discovered later on, the staining-free labeling of cell populations within the living organism is nowadays a common approach. The later implementation of other recombinases like FLP, with its FRT sites for recombination, and its combinatorial use with the Cre/lox system increased the specificity even further (Dymecki and Kim 2007; Broach, Guarascio, and Jayaram 1982; Pan, Clary, and Sadowski 1991; Rodríguez et al. 2000). Today, these systems are used for cell type-specific gene KO or the insertion of transgenes encoding reporters, sensors or effector molecules enabling the manipulation and visualization of molecules, cells and circuits (Deussing 2013). To use different SSRs in a combinatorial fashion, their exact spatial and temporal expression patterns need to be known and, thus, have to be characterized in detail (Zhao et al. 2023).

1.9.2 CRH reporter models

Due to the previously described difficulties in visualizing CRH *in vivo*, extensive efforts have been undertaken to access this population of cells by developing CRH reporter lines. First models were generated by random insertion into the mouse genome using classical (Keegan et al. 1994) or large bacterial artificial chromosomes (BAC)-based constructs to insert the complete 8.7 (Alon et al. 2009; Sarkar et al. 2011) or a shortened 3 kb promoter region (Martin et al. 2010). These reporter lines did not fully recapitulate the endogenous expression pattern of CRH and also showed ectopic expression in regions where CRH endogenously was not present (Keegan et al. 1994; Alon et al. 2009; Martin et al. 2010). Therefore, currently used models are mainly based on Knock-in of Cre into the *Crh* locus (Taniguchi et al. 2011; Itoi et al. 2014; Kono et al. 2017). This approach has been proven to be superior in its capacity to generate reliable and reproducible reporter and Cre expression. As the expression of CRH within the CNS is rather heterogeneous, including different neuronal subpopulations, the use of additional recombinases, like FLP, to precisely target these different populations seems beneficial. The currently used *CRH-FlpO* line (Salimando et al. 2020), also a knock-in line, was deeply characterized only recently (Zhao et al. 2023). These SSR-driven models are supplemented with direct insertions of reporters into the CRH locus, which enable the direct visualization of up and downregulation of the *Crh* gene under different circumstances (Kono et al. 2017).

2 Manuscripts

2.1 Brain injury-induced expression of neuropeptide CRH in oligodendrocyte progenitor cells influences early oligodendroglial differentiation

Authors:

Clemens Ries[1,2,3*], Antonio Miralles Infante[4], Julia von Poblotzki[1], Alessandro Ulivi[5], Iven-Alex von Mücke-Heim[1,3], Simon Chang[1,6], Kenji Sakimura[7], Keiichi Itoi[8], Alessio Attardo[5], Leda Dimou[4], Jan M. Deussing[1,2,3*]

Affiliations:

[1] Max Planck Institute of Psychiatry, Molecular Neurogenetics, Munich, Germany.

[2]Graduate School of Systemic Neuroscience, Ludwig Maximilians University, Munich, Germany

[3] International Max Planck Research School of Translational Psychiatry, Munich, Germany

[4] Molecular and Translational Neuroscience, Department of Neurology, Ulm University, Ulm, Germany.

[5] Leibniz Institute for Neurobiology, Department of Cellular Neuroscience, Magdeburg, Germany.

[6] Translational Genetics, Helmholtz Pioneer Campus, Helmholtz Zentrum München, Munich, Germany.

[7] Department of Animal Model Development, Brain Research Institute, Niigata University, Niigata 951-8585, Japan.

[8] Super-Network Brain Physiology, Graduate School of Life Sciences, Tohoku University, Sendai 980-8577, Japan.

[*]Corresponding Authors:

Clemens Ries

Email: clemens_ries@psych.mpg.de

Jan M. Deussing

Email: deussing@psych.mpg.de

Tel: +49 (0)89 30622 8111

Fax: +49 (0)89 30622 1936

Max Planck Institute of Psychiatry, Molecular Neurogenetics

Kraepelinstr. 2-10, 80804 Munich, Germany

Author Contributions

C.R. designed, led and performed all experiments, analyzed and interpreted data and wrote the manuscript. T.M.I. performed GPR17 staining and analysis, provided scientific input and subedited the manuscript. J.P. performed the quantification of CRHR1-expressing astrocytes after reporter virus injection, analyzed data and subedited the manuscript. A. U. helped with cannula implantations for *in vivo* imaging, gave scientific expertise, helped with image acquisition at the 2-photon setup and subedited the manuscript. S. C. aided methodological and scientific expertise. I.M.H. aided methodological expertise in cranial window implantation, provided scientific input and subedited the manuscript. K.S. and K.I. created and provided the CRH-Venus mouse line and reviewed the manuscript. A.A. provided scientific input concerning 2-photon imaging, reviewed and subedited the manuscript. L.D. provided constant scientific input, helped with planning label retaining experiments, reviewed and subedited the manuscript. J. M. D. provided essential scientific advice and support, supervised all experiments and analysis, reviewed and edited the manuscript.

Abstract

The function of neuropeptides and their receptors in oligodendrocyte progenitor cells (OPCs) has largely been overlooked so far. Here, we describe a novel neuropeptide system in OPCs, formed by the corticotropin-releasing hormone (CRH) and its type 1 receptor (CRHR1). First, we discovered CRH expression in a subpopulation of OPCs, which possess a high capacity for differentiation into oligodendrocytes. Immediate *de novo* expression of this stress-related peptide is among the earliest reactions to injury reported so far. Furthermore, we identified CRHR1-expressing astrocytes and OPCs as CRH targets. Functionally, we show that excessive CRH elevates the activation state of astrocytes after acute injury in a CRHR1-dependent manner and that the inhibition of CRH/CRHR1 signaling in both OPCs and astrocytes amplifies the generation of oligodendrocytes. Altogether, our findings delineate a novel CRH/CRHR1 system involving OPCs and astrocytes regulating oligodendrocyte generation, implying that neuropeptides play a vital role in regenerative processes following acute brain injury.

Introduction

In recent years, oligodendrocyte progenitor cells (OPCs), also known as NG2-glia, have attracted increasing attention in connection to the brain's reaction to damage and subsequent regenerative processes. OPCs are the main source of myelinating oligodendrocytes (OLs) and have been widely accepted as the fourth major glial cell type of the central nervous system (CNS)[1, 2, 3]. Upon acute injury, OPCs proliferate and migrate towards the injury core[4, 5, 6]. OPCs' potential for OL regeneration after cortical injury has been shown to be diverse and their function in regeneration beyond oligodendrogenesis remains elusive[6, 7, 8]. In regeneration, but also in development and adulthood, oligodendrogenesis is an inefficient process characterized by an overproduction of premyelinating OLs, of which only a fraction reaches the mature stage[9, 10, 11]. Although the exact mechanisms are still under investigation, oligodendrogenesis and myelination have already been shown to be dependent on neuronal activity but are also influenced by G protein-coupled receptor signaling and by the interaction with other cell types or extracellular matrix components[10, 12, 13, 14].

The corticotropin-releasing hormone (CRH) is a 41 amino acid neuropeptide expressed in neurons throughout the brain, where it is stored in large dense core vesicles. Together with its high affinity G protein-coupled receptor CRH receptor type 1 (CRHR1), CRH orchestrates the neuroendocrine, autonomic and behavioral stress response[15, 16]. In the paraventricular nucleus of the hypothalamus, CRH acts as gatekeeper, controlling the activity of the hypothalamic-pituitary-adrenal (HPA) axis regulating the release of glucocorticoids as prime effectors of the stress response[17]. In addition to its role in HPA axis regulation, CRH has been implicated in behaviors relevant for coping with salient environmental stimuli including arousal, anxiety- and fear-related behaviors involving extrahypothalamic CRH/CRHR1 neurocircuits[18, 19, 20, 21, 22, 23, 24, 25]. Beyond its extensively studied role in modulating the response to psychosocial stressors, the CRH/CRHR1 system has anecdotally been reported to affect the brain's reaction to physical damage. Previous studies reported that genetic inactivation of CRHR1 or administration of specific antagonists alleviated ischemic brain injury. However, the underlying processes and involved cell types remained unclear[26, 27].

In this study, we discovered the presence of a CRH/CRHR1 system in OPCs. We show that CRH is expressed by a subpopulation of OPCs following acute injury and subsequently acts in a CRHR1-dependent manner as a modulator of astrocyte activation and OL generation.

Results

De novo expression of CRH in a subpopulation of OPCs in response to acute brain injury

To investigate the distribution and connectivity of CRH-expressing neurons in the murine brain, stereotaxic injections of fluorescent retro-beads were performed in the ventral tegmental area (VTA) of *CRH-Cre::Ai9* reporter mice, in which CRH expression is reported via tdTomato (**Fig. 1a, Supplementary Table 1**). Analyzing injected brains, we consistently observed an aggregation of tdTomato$^+$ cells with non-neuronal morphology in close proximity to the injection site (**Fig. 1b**). Since the involvement of CRH in the reaction to brain damage was largely unknown, this intriguing observation demanded further investigation. First, we assessed whether *de novo* CRH expression upon acute injury represents a global phenomenon that can be triggered by acute stab wound injury without substance injection. To this end, stab wounds, using a Hamilton cannula, were inflicted on three different brain regions of *CRH-Cre::Ai9* mice: i) prefrontal cortex, ii) striatum, and iii) midbrain (MB). In all regions, the appearance of tdTomato$^+$ cells was observed 3 days post injury (dpi) (**Fig. 1c**). To specify the identity of the newly appearing tdTomato$^+$ cells, immuno stainings for different glial (GFAP, Iba1 and NG2) and neuronal (NeuN) markers were performed (**Fig. 1d, Supplementary Fig. 1a-c**). Non-neuronal tdTomato$^+$ cells around the injury site only showed co-localization with the oligodendrocyte progenitor cell (OPC) marker NG2, specifying these cells as OPCs (**Fig. 1d**). Using the intersectional reporter mouse line *CRH-FlpO::NG2-CreERT2::Ai65* in which co-expression of CRH and NG2 triggers the expression of tdTomato in a FlpO- and Cre-dependent manner, CRH expression in OPCs was confirmed (**Fig. 1e,f, Supplementary Table 1**). However, tdTomato is continuously expressed after the excision of the floxed transcriptional terminator. Thus, the Cre/lox system reports CRH expression only indirectly and in a fate mapping manner. To have a direct measure of CRH expression upon acute injury, we used combined immunostaining against CRH and the OPC specific marker PDGFRα showing clear co-localization in several cells surrounding the injury site (**Fig. 1g,g'**). Characteristic for a neuropeptide, CRH was localized in vesicular structures throughout the PDGFRα$^+$ cells. Lastly, we demonstrate CRH expression also on the mRNA level by double *in-situ* hybridization using riboprobes against *Crh* and *Pdgfrα* (**Fig. 1h**). Intriguingly, CRH-expressing OPCs could only be identified under injury conditions but not in naive mice. In summary, we demonstrate that CRH is indeed expressed by OPCs in the brain as a reaction to acute injury.

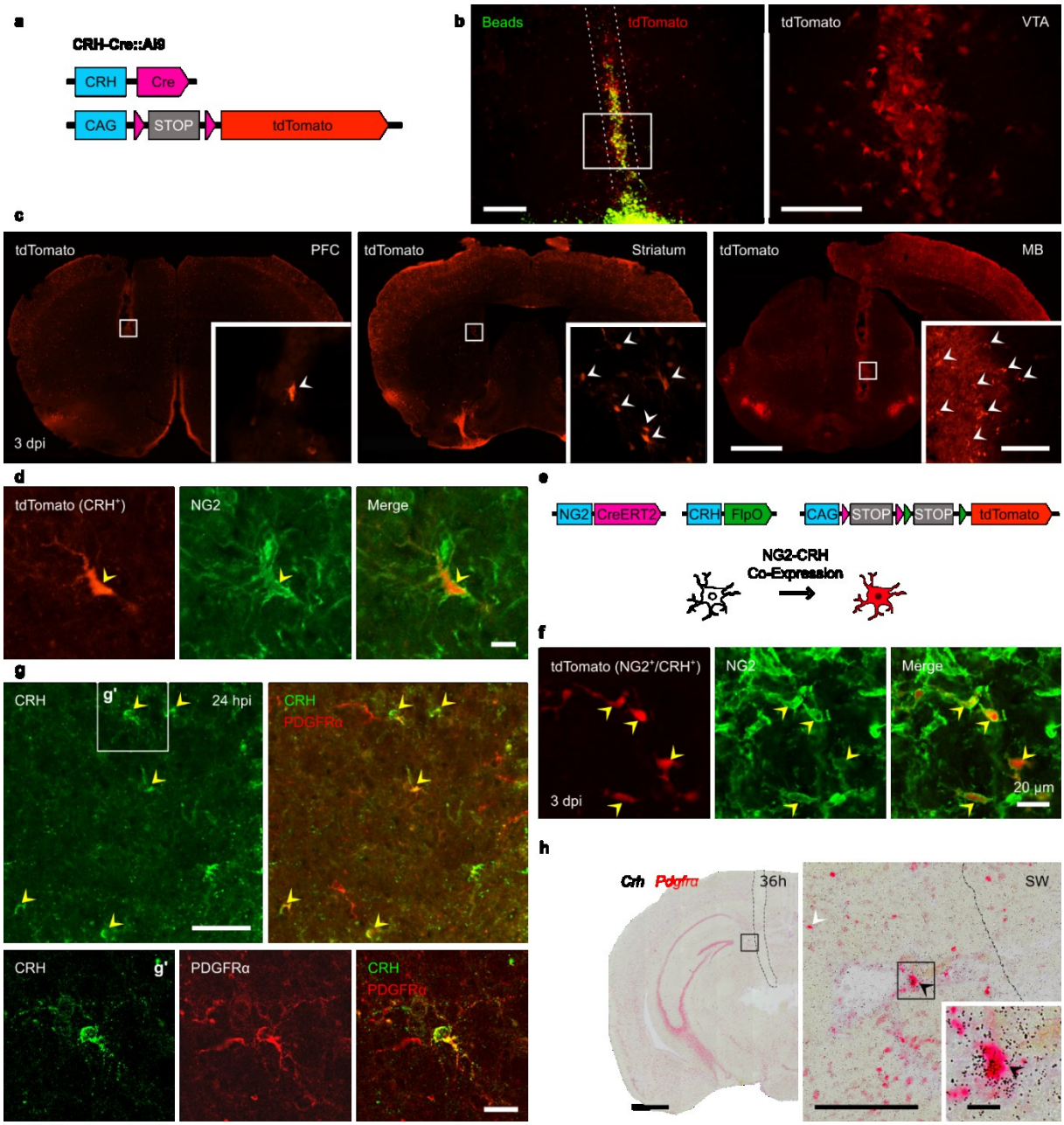

Fig. 1: Identification of CRH-expressing OPC subpopulation. a, Graphical illustration of the *CRH-Cre::Ai9* reporter mouse model. **b**, Injection site of fluorescent beads and needle tract (framed by white dotted lines) with aggregation of tdTomato$^+$ cells around the injury site. Scale bars, 100 µm. **c**, Aggregation of CRH-expressing (tdTomato$^+$) cells around injury sites in prefrontal cortex (PFC), striatum and midbrain (MB) in *CRH-Cre::Ai9* mice. Scale bars, 1000 µm (overview), 50 µm (close up). **d**, Immuno staining for NG2 at the injury site in *CRH-Cre::Ai9* mice, showing co-localization with tdTomato. Scale bar, 10 µm. **e**, Graphical illustration of intersectional reporter mouse line *CRH-FlpO::NG2-CreERT2::Ai65* for monitoring CRH/NG2 co-expression. **f**, Confocal images of CRH-expressing (tdTomato$^+$) cells at injury site at 3 dpi stained for NG2. Scale bar, 50 µm. **g**, Confocal image of combined CRH/PDGFRα staining showing co-expressing cells around the injury site at 24 hpi. Scale bar, 50 µm. **g'**, Magnification of CRH/PDGFRα co-expressing cell. Scale bar, 20 µm. **h**, Double *in situ* hybridization at 36 hpi in *CRH-Cre::Ai9* mice against *Crh* and *Pdgfra*. White arrowhead, *Crh*$^-$/*Pdgfra*$^+$ cell. Black arrowhead,

Crh^{+}/*Pdgfra*$^{+}$. Scale bars, 100 µm (overview), 200 µm (close up), 20 µm (smaller inset). For images a-f: White arrowheads indicate cells or structures. Yellow arrowheads indicate co-localization of two markers.

Dynamics of CRH-expressing OLCs are distinct from the whole population of OLCs

To interrogate the population dynamics of CRH-expressing oligodendrocyte lineage cells (OLCs), we first focused on their proliferative capacity and analyzed changes in their cell number after injury. *CRH-Cre::Ai9* mice were subjected to stab wound injury in the midbrain and sacrificed at 1, 2, 3, 7, 14, 23, 69 or 128 dpi (**Fig. 2a**). tdTomato^{+}/Olig2^{+} cells were quantified in a 300 µm radius around the wound center with 50-100 µm medio-lateral resolution (**Fig. 2a, Supplementary Method 1a-c**). The quantification in the whole area revealed a considerable increase of tdTomato^{+}/Olig2^{+} cells between 2 (14 ± 8.13/ mm^2) and 7 dpi (168 ± 27.85/ mm^2) followed by a significant decrease until 128 dpi (55 ± 6.56 cells/ mm^2) (**Fig. 2b**). Also, when restricting the analysis to the first 50 µm around the wound center, dynamics were comparable. The density of tdTomato^{+}/Olig2^{+} cells, however, was considerably higher (614 ± 87.62 cells/mm^2). The medio-lateral distribution of CRH-expressing OLCs over time, depicted in the heatmap, shows their initial appearance within the entire area of analysis (0-300 µm distance) (**Fig. 2c**). Gradually, the majority of cells aggregated at the inner parts of the wound and the number of tdTomato^{+}/Olig2^{+} cells at more distant sites decreased (**Fig. 2c**). These findings raised the question whether the increase in tdTomato^{+}/Olig2^{+} cells was caused by *de novo* expression of CRH in an increasing number of independent cells or by proliferation of a starter population of CRH-expressing OPCs passing tdTomato expression to their progeny. Indeed, tdTomato^{+}/Olig2^{+} cells did not only show *de novo* expression of CRH but also co-expression of the proliferation marker Ki67 (**Fig. 2d**). Quantification revealed that, while at 2 dpi the vast majority of Olig2^{+}/tdTomato^{+} cells were Ki67^{+} (98 ± 1.75%), the proportion of co-expressing cells dropped significantly until 7 dpi (18 ± 2.31%) (**Fig. 2e, Supplementary Fig. 1d**). To assess the size and dynamics of the CRH-expressing OLC subpopulation in relation to the entire OLC population, we first determined the total number of Olig2^{+} cells around the injury site. We detected a strong increase between 1 (1310 ± 71.20 cells/ mm^2) and 7 dpi (2564 ± 94.86 cells/ mm^2), which slowed down but persisted until 128 dpi (3195 ± 165.6 cells/ mm^2) (**Fig. 2f).** Next, we investigated the proportion of tdTomato^{+}/Olig2^{+} cells of all Olig2^{+} cells, detecting a steady increase until 7 dpi in the whole area (6 ± 0.58%) as well as in the first 50 µm (15.67 ± 0.67%) (**Fig. 2g,h**). Unlike the whole population of Olig2^{+} cells, we observed a decline of tdTomato^{+}/Olig2^{+} cells until 128 dpi in the whole area (2.33 ± 0.67%) and in the first 50 µm (6.67 ± 2.40%) (**Fig. 2g,h**). The number of cells on the contralateral side remained stable over the whole course of the experiment (**Fig. 2i**). In sum, these results demonstrate that the increase in CRH-expressing OPCs' cell number is caused by the *de novo* appearance of CRH-expressing OPCs and by a typical OPC-like proliferative response to acute injury. It further confirms that their dynamics are distinct from the whole OLC population with regards to their subsequent maintenance, potentially caused by their high maturation rate.

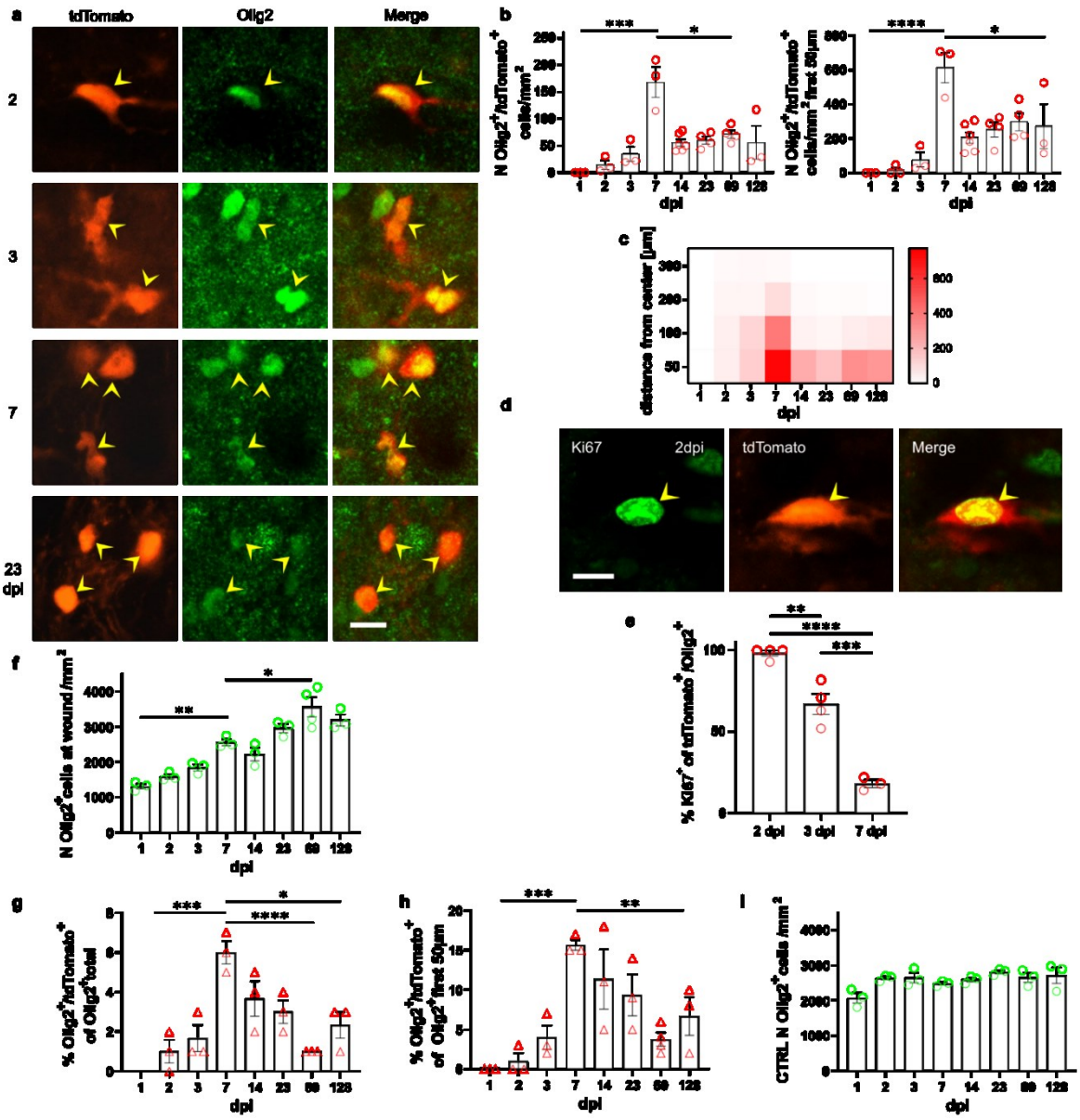

Fig. 2: CRH$^+$ OLCs dynamics differ from the general OLC population. a, Representative confocal images of *CRH-Cre::Ai9* mice at 2, 3, 7 and 23 dpi stained for Olig2, showing co-localization of tdTomato and Olig2. Scale bar, 10 µm. **b**, Left: Quantification of Olig2$^+$/tdTomato$^+$ cells at ± 300 µm around the injury site. Significant changes in cell numbers over time were observed (One-way ANOVA: $F_{(7, 21)}$= 11.37, $p < 0.0001$) with a significant increase between 1 and 7 dpi ($p < 0.001$, 95% C.I. = -239,7, -96,35) followed by a decrease between 7 and 128 dpi ($p = 0.007$, 95% C.I. = 40.55 , 183.9). Right: Quantification of Olig2$^+$/tdTomato$^+$ cells at ± 50 µm around the injury site. Significant changes could be observed in cell numbers over time (One-way ANOVA: $F_{(7, 21)}$= 10.27, $p < 0.0001$) with an increase between 1 and 7 dpi ($p < 0.0001$, 95% C.I. = -909.2 , -318.7) followed by a decrease between 7 and 128 dpi ($p = 0.0158$, 95% C.I. = 47.3 , 637.8). **c**, Heat map showing the number of Olig2$^+$/tdTomato$^+$ cells in spatio-temporal resolution. **d**, Confocal image of Ki67 staining at 2 dpi. Scale bar, 10 µm. **e**, Quantification of Ki67$^+$/tdTomato$^+$/Olig2$^+$ of all tdTomato$^+$/Olig2$^+$ cells shows a significant decrease between 2 and 7 dpi (One-way-ANOVA: $F_{(2, 8)} = 81.16$, $p < 0.0001$). **f**, Total number of Olig2$^+$ cells at ± 300 µm

around injury site. Significant increase over time (One-way-ANOVA: $F_{(4, 11)} = 7.169$, $p = 0.0043$). **g**, Significant change in percentage of Olig2$^+$/tdTomato$^+$ cells of all Olig2$^+$ cells at ± 300 µm (One-way-ANOVA: $F_{(6, 14)} = 8.264$, $p = 0.0006$) and **h**, at ± 50 µm (One-way-ANOVA: $F_{(7, 17)} = 7.769$, $p = 0.0003$). **i**, Quantification of Olig2$^+$ cells in CTRL region on the contralateral side. N_{TP} = 3-6 mice for all experiments. For all images: Yellow arrowheads indicate co-localization of two markers. TP, timepoint.

CRH-expressing OPCs mature into myelinating oligodendrocytes

One function of OPCs in the context of brain injury is the regeneration of the OL population[8]. Therefore, we investigated the fate of CRH-expressing cells in more detail by evaluating their differentiation capacity using NG2/Olig2 and CC1/Olig2 double stainings. At the time of their first appearance between 2 and 3 dpi, all (100 ± 0%) of tdTomato$^+$/Olig2$^+$ cells were also NG2$^+$ (**Fig. 3a**) and appeared between 50 and 300 µm from the wound center. No co-localization with the OL marker CC1 was found. Subsequently, the proportion of NG2$^+$ cells of the tdTomato$^+$/Olig2$^+$ population steadily decreased, reaching a minimum at 128 dpi (7.67 ± 4.10%), while the percentage of CC1$^+$ cells among tdTomato$^+$/Olig2$^+$ cells continuously increased until 128 dpi (76.33 ± 3.67%) (**Fig. 3b,c**). CRH$^+$ OLCs possessed oligodendrocyte-like morphologies and were present in the midbrain as well as in the white matter (WM) (**Fig. 3d**). The myelinating character of these cells was confirmed by co-localization with the myelin proteins CNPase and MBP at 4 months post injury (**Fig. 3e**). These results indicate that CRH-expressing OPCs predominantly mature into myelinating oligodendrocytes after acute injury and are highly stable once integrated (**Supplementary Fig. 2**). To further substantiate these findings on a single cell level, we used *CRH-Cre::Ai9* and *CRH-FlpO::NG2-CreERT2::Ai65* mice for repeated *in vivo* two-photon imaging. For cortical imaging, a cranial window in combination with an acute stab wound injury was used. To image WM processes, a cannula was implanted into the cortex, resembling an injury itself. Using these methods, single cells were identified and followed over several weeks confirming proliferation (**Fig. 3f**), movement towards the injury site (**Fig. 3g**) and the subsequent maturation, as can be inferred from the morphological changes leading to the characteristic appearance of a myelinating oligodendrocyte (**Fig. 3h**). On top of that, long-term imaging in the WM of *CRH-FlpO::NG2-CreERT2::Ai65* mice (cannula implantation) revealed that immature OLs not functionally integrated at 31 dpi predominantly disappeared, whereas mature oligodendrocytes persisted over the entire imaging period (**Supplementary Fig. 3a-d'', e-h**). Immature premyelinating OLs were discriminated from OPCs by their round, highly ramified morphology (**Supplementary Fig. 3d''**), the high motility of their processes and the growth cone-like structures along those processes (**Supplementary Movie 1,2**)[28]. OPCs were identified by their typical elongated cell body and the rather slow movement of processes (**Supplementary Movie 3**). Taken together, these results show that CRH-expressing OPCs appear under different injury conditions, proliferate, move towards the injury site and mature into myelinating oligodendrocytes.

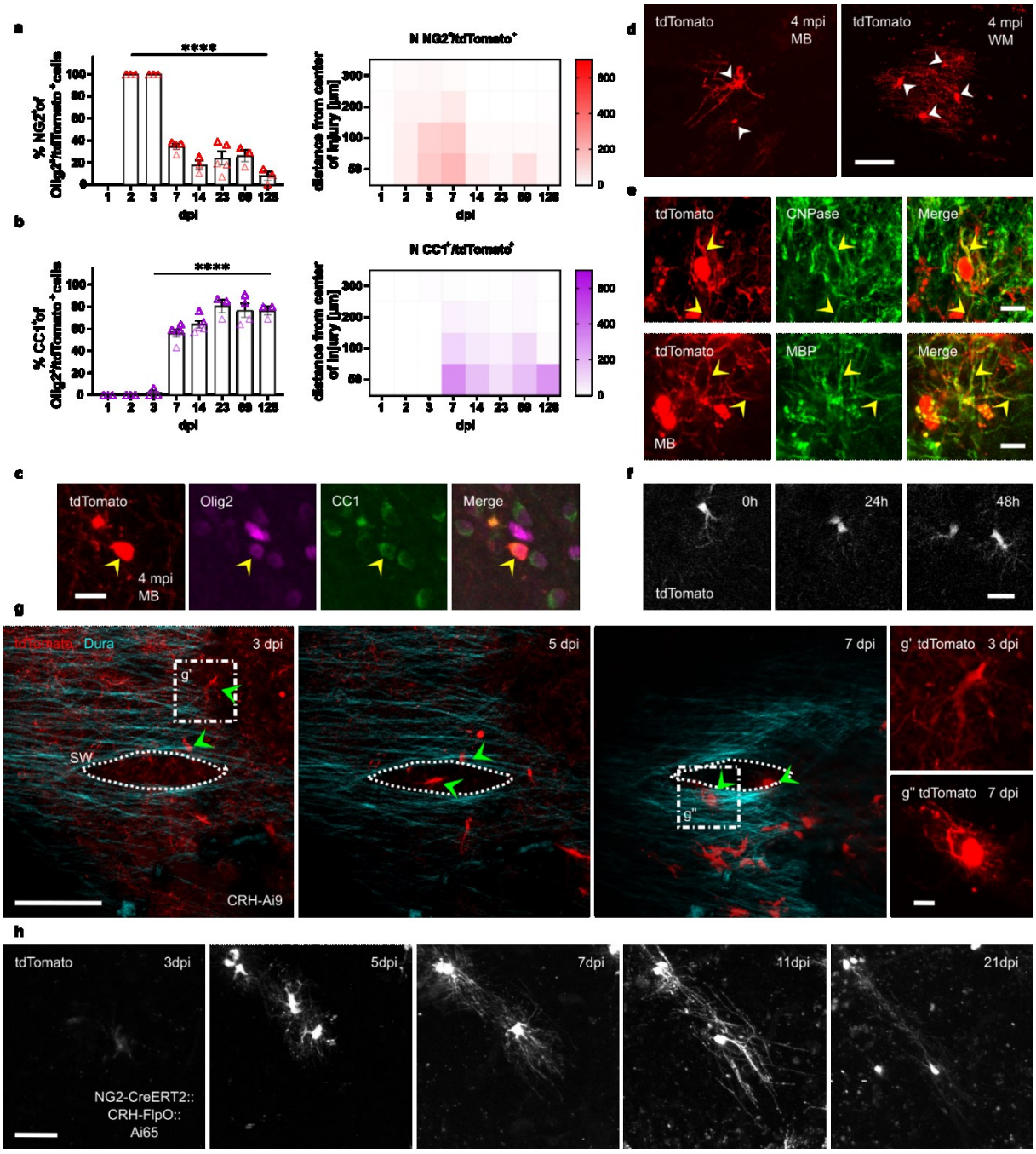

Fig. 3: CRH$^+$ OPCs mature into myelinating OLs. a, Left, percentage of NG2$^+$/Olig2$^+$/tdTomato$^+$ cells out of all Olig2$^+$/tdTomato$^+$ cells showing a significant decrease starting between 3 and 7 dpi (One-way ANOVA: $F_{(6, 17)}$= 68.5, $p < 0.0001$). Right, Number of NG2$^+$/tdTomato$^+$ cells in spatio-temporal resolution. N_{TP} = 3-6 mice. **b**, Left, percentage of CC1$^+$/Olig2$^+$/tdTomato$^+$ cells of all Olig2$^+$/tdTomato$^+$ cells showing an increase starting between 3 and 7 dpi (One-way ANOVA: $F_{(6, 17)}$= 68.5, $p < 0.0001$). Right, Number of CC1$^+$/tdTomato$^+$ cells in spatio-temporal resolution. N_{TP} = 3-6 mice. **c**, Confocal image of Olig2 and CC1 staining at 4 months post injury in MB. Scale bar, 10 µm. **d**, Diverse morphology of tdTomato$^+$ cells at 4 mpi in MB (left) and WM (right). Scale bar, 50 µm. **e**, Confocal images of anti-CNPase and anti-MBP staining showing co-localization with tdTomato$^+$ cells. Scale bar, 10 µm. **f**, 2-photon image of a proliferating tdTomato$^+$ OPC in WM over the course of 48 h. Scale bar, 20µm. **g**, Representative 2-photon images of a cortical injury (white lining: injury site in dura) between 3 and

7 dpi. Arrowheads (green) indicate cells moving towards wound center. Scale bar, 100 µm. g' and g'', morphological change of single cell between 3 and 7 dpi. Scale bar, 10 µm. **h**, Representative 2-photon images of tdTomato$^+$ OPCs in one ROI after implantation of hippocampal cannula between 3 and 21 dpi maturing into oligodendrocytes. Scale bar, 50 µm. For all images, White arrowheads indicate cells or structures. Yellow arrowheads indicate co-localization of two markers.

Induction of CRH expression in OPCs is an early response to brain injury

After defining the key properties of CRH-expressing OPCs with regards to proliferation and maturation, we focused on the injury-induced expression of the neuropeptide CRH itself. To this end, we took advantage of the *CRH-Venus* mouse line[29]. In this mouse line, Venus was inserted in the *Crh* locus, which facilitates direct monitoring of CRH expression via the reporter (**Fig. 4a, Supplementary Table 1**). This enabled us to visualize the distribution of CRH$^+$ cells and provided a proxy to assess CRH expression kinetics as these are directly correlated with the Venus expression driven by the endogenous *Crh* promoter. *CRH-Venus* mice were subjected to stab wound injury and Venus$^+$/NG2$^+$ cells were identified around the injury site (**Fig. 4a**). Furthermore, CRH immune staining showed clear co-localization of Venus and CRH, validating Venus as a proxy for CRH expression (**Fig. 4b**). To assess the expression kinetics Venus$^+$/Olig2$^+$ OPCs (at early timepoints $N_{CRH^+Olig2^+} = N_{CRH^+NG2^+}$, **Fig. 3a**) were quantified around the injury site at different timepoints between 12 and 168 hours post injury (hpi) (**Fig. 4c**). The first Venus$^+$ OPCs were detected as early as 12 hpi, indicating that CRH is expressed as an immediate reaction to the injury (**Fig. 4c**). Between 12 (12 ± 2.08 cells) and 48 hpi (80.33 ± 12.39 cells), the number of Venus-expressing OPCs increased. After 96 (6.67 ± 0.88 cells) and 168 hpi (4.67 ± 1.20 cells) only few cells were traceable, suggesting that Venus and, thus, CRH expression predominantly occurs within the first 3 to 4 dpi. Of note, at 12 and 24hpi all cells were present as individual single cells, whereas at 36 (46.25 ± 0.94%) and 60 hpi (76.74 ± 3.22%), a high proportion of cells were part of a multiplet, likely emerging from proliferation (**Fig. 4d**). Indeed, immuno staining revealed that a large proportion of Venus$^+$ cells were also Ki67$^+$ but only starting from 36 hpi (39.73 ± 2.83%) onwards (**Fig. 4e**). These results, in combination with the observation that the vast majority of Olig2$^+$/tdTomato$^+$ cells was Ki67$^+$ at 2 dpi (98 ± 1.75%) in the *CRH-Cre::Ai9* model (**Fig. 2e**), indicate that in the sequence of reactions to injury CRH expression precedes proliferation.

CRHR1-expressing OPCs and astrocytes are potential targets of OPC-derived CRH

The expression and likely release of CRH from OPCs as an early response to injury raises the question of potential target cells. The canonical high-affinity receptor of CRH is the CRHR1. Since CRH is expressed and released at the injury site, we investigated whether CRHR1-expressing glial cells also occurred in vicinity of the wound. Therefore, we used the *CRHR1-Cre::Tau-LSL-FlpO::Ai9* mouse model, in which tdTomato expression is activated in all CRHR1$^+$ cells, but selectively deleted from CRHR1$^+$ neurons. Removal of tdTomato from neurons is achieved by CRHR1-Cre-induced FlpO

expression, which is driven by the *Mapt* (Tau) promoter. This system allows to reduce the background caused by neuronal CRHR1-Cre expression significantly and thereby facilitates the visualization of CRHR1-expressing non-neuronal cells (**Fig. 4f, Supplementary Table 1**). When analyzing stab wounds at 3 dpi, we found CRHR1-expressing cells aggregating around the injury site that were identified as OPCs by NG2 staining (**Fig. 4g**). To our surprise, $CRHR1^+/NG2^+$ cells were also present on the non-injured contralateral site but also throughout the brain under physiological conditions (**Fig. 4h**). Some $CRHR1^+$ cells around the injury site did not co-localize with NG2 but were identified as reactive astrocytes by GFAP staining (**Fig. 4i**). Similar to $CRHR1^+$ OPCs, a smaller number of $CRHR1^+$ astrocytes were also detectable throughout the brain under physiological conditions (**Fig. 4j**). To better understand this potential interaction between OPC derived CRH and CRHR1 on astrocytes and OPCs we first wanted to test whether the CRHR1 expression shown in Cre-driver-based reporter lines still persisted in adulthood. Since we are still lacking reliable CRHR1-specific antibodies, we had to choose other approaches for detection of CRHR1 expression [20]. To test for the presences of CRHR1 in astrocytes, we used an adeno-associated virus (AAV) which harbors a floxed expression cassette consisting of a tdTomato linked to a GFP in reverse orientation (**Fig. 4k**) under the control of the human *GFAP* promoter. Injected into the brain of CRHR1-Cre mice, the virus caused tdTomato expression in $GFAP^+$ cells, which was switched to the expression of GFP upon Cre-mediated inversion of the expression cassette in $GFAP^+/CRHR1^+$ cells (**Fig. 4l,l'**). Around the injection site, the majority of cells was $tdTomato^+$ at 14 dpi, but GFP^+ cells (202.6 ± 26.98 GFP^+) were also present (**Fig. 4l,l',m**) demonstrating CRHR1 expression in astrocytes. Because of the lack of OPC-specific promoters we used two different approaches to validate the expression of CRHR1 in OLCs: i) AAV-mediated reporting of CRHR1 expression and ii) direct visualization of CRHR1 expression in $CRHR1^{\Delta EGFP}$ mice. For AAV mediated reporting we used an AAV harboring a floxed expression cassette consisting of a reverse GFP, which was injected in *CRHR1-Cre* mice (**Fig. 4n**). Upon Cre-mediated recombination the GFP was expressed under the control of the ubiquitously active *cytomegalovirus* (*CMV*) promoter in all CRHR1 expressing cells around the injection site. CRHR1-expressing OLCs were identified by co-staining with Olig2 (**Fig. 4o,o'**). To assess CRHR1 expression in OPCs under physiological conditions we took advantage of the $CRHR1^{\Delta EGFP}$ mouse line which is characterized by a knock-in of GFP into the *Crhr1* locus, which serves as valid proxy for CRHR1 expression **(Supplementary Fig. 4a, Supplementary Table 1)** [20]. Co-staining with PDGFRα showed clear co-localization with GFP-expressing cells of the WM, identifying these cells as OPCs (**Supplementary Fig. 4b,b'**).

Taken together, these observations clearly show CRHR1 expression in OPCs and astrocytes, qualifying them as potential targets of CRH following injury.

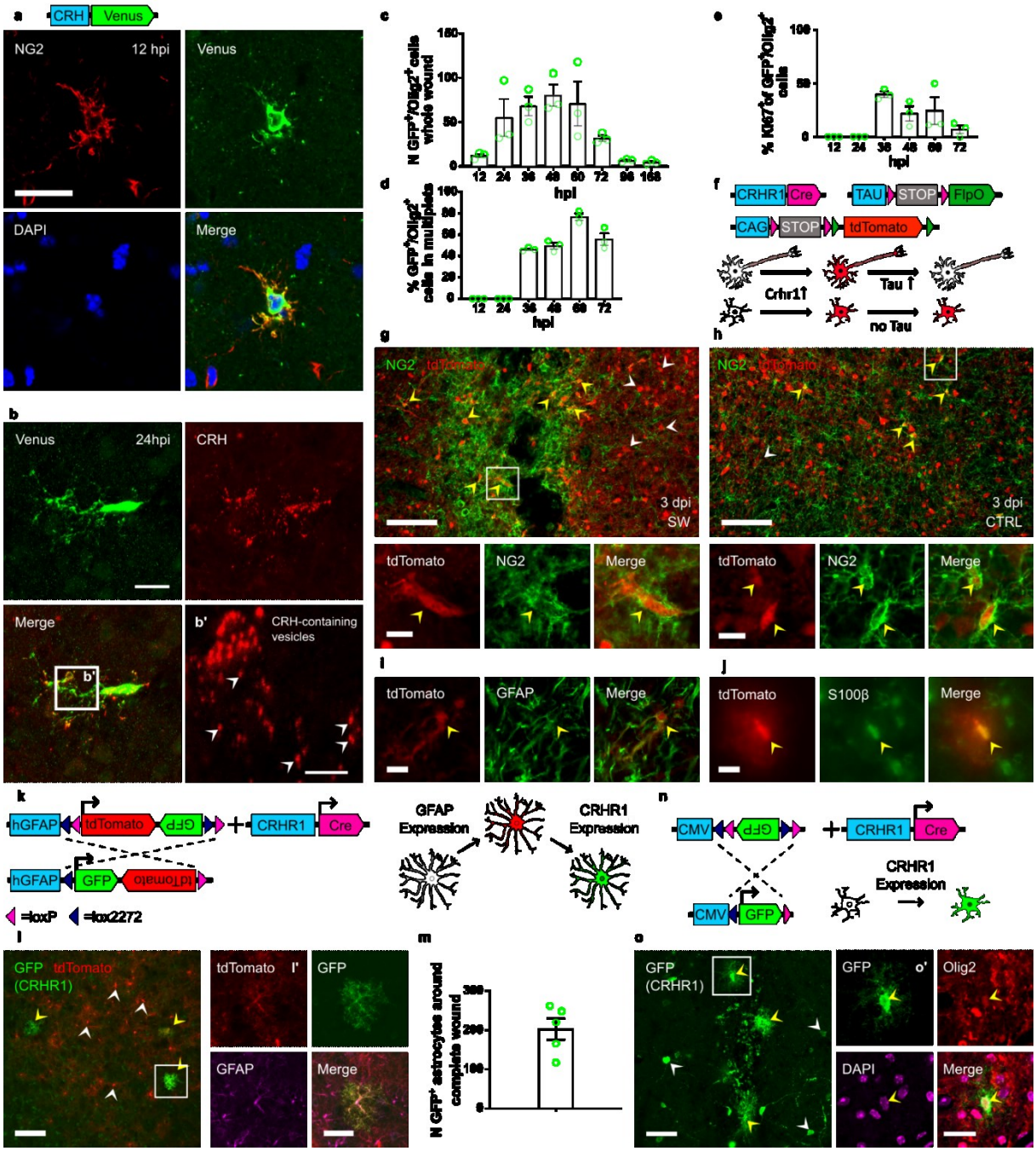

Fig. 4: OPC-derived CRH targets CRHR1$^+$ OPCs and astrocytes. a, Graphical illustration of *CRH-Venus* reporter mouse model. Representative confocal images of NG2/GFP co-localization at 12 hpi. Scale bar, 20 µm. **b**, Confocal image of GFP-expressing cell at injury site in *CRH-Venus* mice stained for CRH protein. Scale bars, 20 µm (overview), 5 µm (close up). **c**, Quantification of GFP$^+$/Olig2$^+$ cells around the injury site between 12 and 168 hpi indicate a significant increase between 12 and 48 hpi followed by a significant decrease until 168 hpi (One-way ANOVA: $F_{(7, 16)}$= 5.765, p = 0.0018). N_{TP} = 3 mice. **d**, Percentage of NG2$^+$/GFP$^+$ in a multiplet of cells. N_{TP} = 3 mice. **e**, Quantification of Ki67$^+$ cells of all GFP$^+$/Olig2$^+$ cells. N_{TP} = 3 mice. **f**, Graphical illustration of *CRHR1-Cre::Tau-LSL-FlpO::Ai9* mouse model. **g**, Confocal image of NG2 staining around the wound and **h**, at the uninjured contralateral side at 3 dpi identifying cells as CRHR1-expressing OPCs. Insets, co-localization of tdTomato and NG2. Scale bars: 100 µm (overviews), 10 µm (insets). **i**, Confocal image of GFAP staining of

tdTomato$^+$ astrocyte at injury site. Scale bar, 10 µm. **j**, Confocal image of S100β staining of tdTomato$^+$ cells under physiological conditions. Scale bar, 10 µm. **k**, Graphical illustration of injected AAV construct and *CRHR1-Cre* mouse line for the confirmation of CRHR1 expression in astrocytes. **l**, Overview of AAV injection site. Yellow arrow heads: GFP- (CRHR1$^+$) expressing cells. White arrow heads: tdTomato- (CRHR1$^-$) expressing astrocytes. Scale bar, 100 µm. **l'**, Confocal image of tdTomato$^+$/GFP$^+$/GFAP$^+$ astrocyte at injury site confirming co-localization of markers. Scale bar, 50 µm. **m**, Quantification of total number of GFP$^+$/tdTomato$^+$, GFP$^+$/tdTomato$^-$ and all GFP$^+$ astrocytes around the injury site. N = 6 animals. **n**, Graphical illustration of injected AAV construct and *CRHR1-Cre* mouse line for the confirmation of CRHR1 expression in OPCs. **o**, Overview of AAV injection site. Yellow arrow heads: GFP- (CRHR1$^+$) expressing non-neuronal cells. White arrow heads: GFP- (CRHR1$^+$) expressing neuronal cells. Scale bar, 50 µm. **o'**, Confocal image of GFP$^+$/Olig2$^+$ OLC at injury site confirming co-localization of markers. Scale bar, 20 µm. White arrowheads indicate cells or structures. Yellow arrowheads indicate co-localization of two markers.

CRHR1$^+$ OLCs are distinct from CRH$^+$ OLCs and increase their population with age

The identification of CRHR1-expressing OPCs surrounding the injury site raised the question whether the CRH/CRHR1 system identified in OPCs is of autocrine or paracrine nature, i.e., whether ligand and receptor are co-localized or exist in distinct OPC populations. To address this question, we used intersectional *CRH-FlpO::CRHR1-Cre::Ai65* reporter mice in which CRH-CRHR1 co-expression is visualized via tdTomato (**Fig. 5a, Supplementary Table 1**). Indeed, tdTomato$^+$ cells were found to surround the injury site at different timepoints (**Fig. 5b**), suggesting that CRH- and CRHR1-expressing OPCs overlap. To quantify the overlap, we took advantage of a mouse model enabling the parallel visualization of CRH and CRHR1 expression by separate reporters. To this end we used the *CRH-FlpO::CRHR1-Cre::Ai65F::Sun1-GFP* mouse line in which CRH expression is reported by tdTomato and CRHR1 expression by GFP fused to the nuclear membrane localization marker Sun1 (**Fig. 5c, Supplementary Table 1**). TdTomato$^+$ (CRH)/GFP$^+$ (CRHR1) cells were identified around the injury site, but little overlap of reporter gene expression was observed. The quantification of tdTomato$^+$ cells co-expressing GFP revealed an overlap of 4.9 ± 0.49% (**Fig. 5d,e**), thereby clearly separating the CRH and CRHR1-expressing populations of OPCs. To further assess the potential role of CRHR1-expressing OLCs under physiological conditions we quantified their number at different postnatal timepoints (P8, 1.5, 3 and 5 months) in *CRHR1-Cre::Tau-LSL-FlpO::Ai9* mice. CRHR1-expressing OLCs were found at all ages (**Fig. 5g-j**). Firstly, the total number of CRHR1-expressing OPCs was quantified at all timepoints in the cortex (CX), WM including corpus callosum, capsule and anterior commissure as well as in the MB. The number of CRHR1-expressing OPCs increased over time, showing a significant gain between 3 and 5 months in the CX (2.61 ± 0.96 to 19.67 ± 3.54 cells/ mm^2) and MB (9.78 ± 2.13 to 28.44 ± 8.30 cells/ mm^2) (**Fig. 5k,l**). This resulted in a significant increase in the percentage of tdTomato$^+$ OPCs of all OPCs in the CX (1.88 ± 0.35 to 7.07 ± 1.44%) and MB (4.36 ± 0.87 to 10.42 ± 2.64%) but not in the WM (2.09 ± 0.89% to 4.81 ± 0.39 %) between 1.5 and 5 months (**Fig. 5m**). In addition, we quantified the total number of tdTomato$^+$/Olig2$^+$ cells, which differed between distinct

brain regions and ages. In the CX, the cell numbers were lowest at all timepoints, while the numbers in WM and MB were comparable at 1.5 and 3 months. Generally, the number of tdTomato$^+$/Olig2$^+$ cells significantly increased towards 5 months of age, which was more pronounced in the WM (100.70 ± 37.35 to 362.78 ± 95.95 cells/mm^2) than in the MB (124.06 ± 19.62 to 217.5 ± 33.17 cells/mm^2) (**Fig. 5k,n**). Since the number of OLs increases with age, we examined whether the increase in CRHR1$^+$ OLCs was comparable to the whole population of OLs[30]. We quantified the total number of Olig2$^+$ cells (**Supplementary Fig. 4c**) and calculated the percentage of CRHR1$^+$/Olig2$^+$ cells, which indeed significantly increased in WM and MB over time (**Fig. 5o**). This increase in the proportion of CRHR1$^+$/Olig2$^+$ cells suggested that CRHR1$^+$ OLCs increased their number at a higher rate than the population of CRHR1$^-$ OLCs, implicating that the CRHR1$^+$ OPC subpopulation may play an important role in adult OL maturation and potentially also myelination.

Therefore, we analyzed whether the CRHR1$^+$ OPC population showed co-expression of GPR17, a marker closely connected to maturation processes in OPCs[8, 31, 32, 33]. The quantification of CRHR1$^+$/GPR17$^+$ cells was performed in *CRHR1-Cre::Sun1-GFP* mice, in which CRHR1 expression is again reflected by nuclear GFP expression. It revealed that 42.73 ± 5.41% of GPR17$^+$ cells with a strong GPR17 expression in the MB were also CRHR1$^+$ (**Supplementary Fig. 4d**). The majority of CRHR1$^+$/GPR17$^+$ cells with a highly ramified morphology was PDGFRα$^-$ (89.30 ± 1.32%), classifying these cells as later stages in OPC development (**Supplementary Fig. 4e,g**). These findings are in line with previous results showing that high expression of GPR17 is present in immature or premyelinating, PDGFRα$^-$, OLs[34]. The fraction of CRHR1-expressing cells among PDGFRα$^+$ cells was comparable (9.73 ± 1.18%) to the percentage of CRHR1$^+$ cells previously found within the NG2$^+$ population in *CRHR1-Cre::Tau-LSL-FlpO::Ai9* mice (10.42 ± 2.64%) (**Fig. 5l,m**), independently confirming these results. Whether CRHR1$^+$ cells represent a subpopulation of GPR17$^+$ cells or the co-expression of these markers occurs only under certain conditions, remains to be examined.

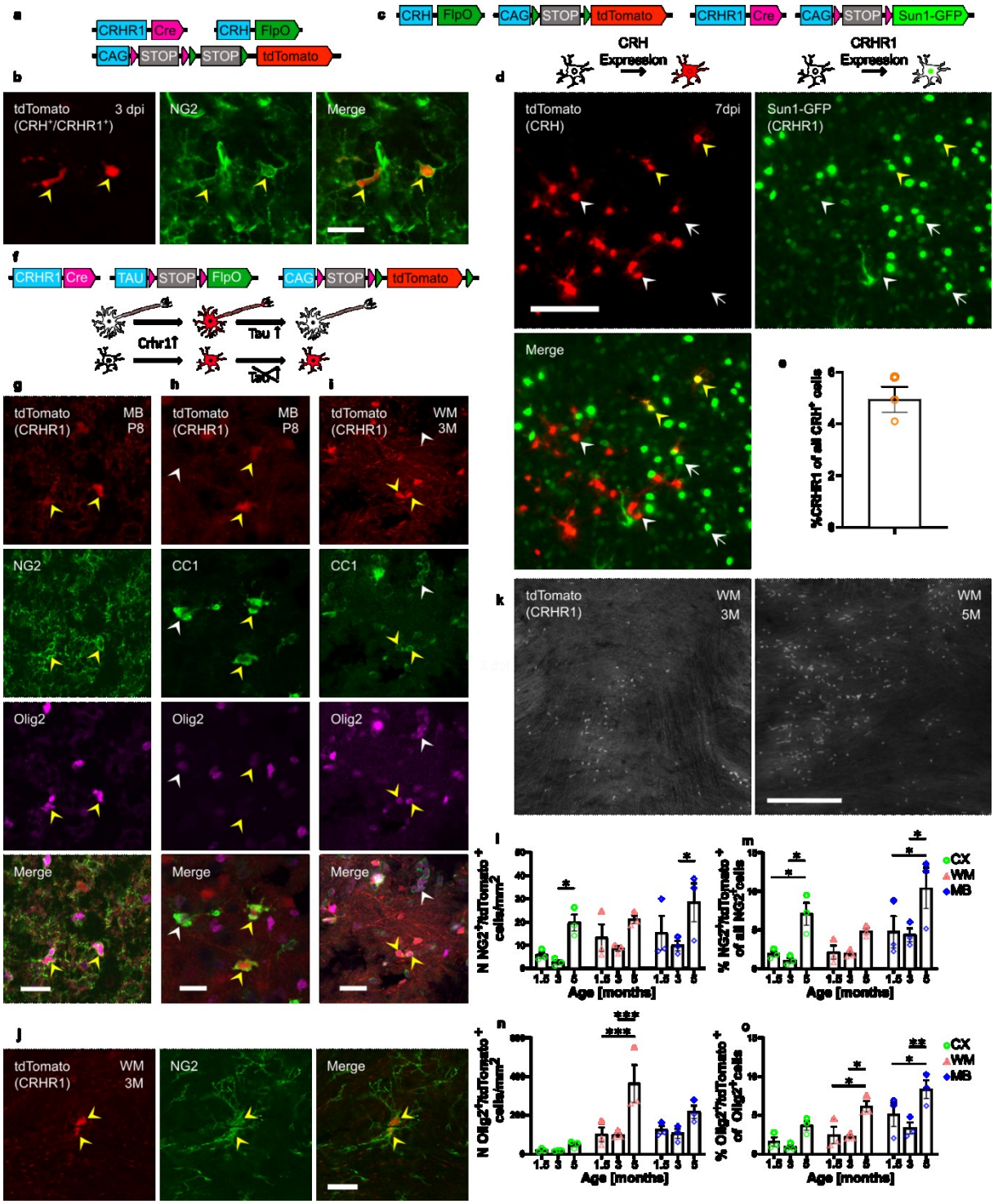

Fig. 5: Quantification and characterization of CRHR1$^+$ OLC population. a, Graphical depiction of *CRH-FlpO::CRHR1-Cre::Ai65* reporter mouse model. **b**, tdTomato$^+$/NG2$^+$ cells at injury site at 3 dpi demonstrating co-expression of CRH and CRHR1. Scale bar, 20 µm. **c**, Graphical illustration of *CRH-FlpO::CRHR1-Cre::Ai65F::Sun1-GFP* reporter mouse model to study the percentage of overlap between the CRH- and CRHR1-expressing populations of OLCs. **d**, Confocal images of injury site in *CRH-FlpO::CRHR1-Cre::Ai65F::Sun1-GFP* mice at 7 dpi showing expression and co-expression of tdTomato (CRH) and SUN1-GFP (CRHR1). Scale bar, 100 µm. Arrowheads show tdTomato$^+$/Sun1-GFP$^-$ (white) and tdTomato$^+$/Sun1-GFP$^+$ (yellow) cells. Arrows show Sun1-GFP$^+$/tdTomato$^-$ cells. **e**, Quantification of CRHR1$^+$/CRH$^+$ of all CRH$^+$ cells. N = 3 animals. **f,**

Graphical illustration of *CRHR1::Tau-LSL-FlpO::Ai9* reporter mouse model. **g-j**, Confocal images showing co-localization of tdTomato (CRHR1) with NG2 and CC1 at P8 and at 3 months. Scale bar, 20 µm. **k**, Maximum intensity projections of confocal images of WM at 3 and 5 months of age showing an increase in tdTomato$^+$ cells. Scale bar, 200 µm. **l**, Quantification of NG2$^+$/tdTomato$^+$ cells at 1.5, 3 and 5 months of age in CX, WM and MB showing significant increase in CX and MB (Two-way ANOVA: time, $F_{(2, 18)}$= 10.34, p = 0.001, N_{TP} = 3 mice). **m**, Percentage of NG2$^+$/tdTomato$^+$ of all NG2$^+$ cells showing significant increase over time (Two-way ANOVA: time, $F_{(2, 18)}$= 13.46, p = 0.003, N_{TP} = 3 mice). **n**, Quantification of NG2$^+$/tdTomato$^+$ cells at 1.5, 3 and 5 months of age in CX, WM and MB showing a significant increase in WM (Two-way ANOVA: Interaction, $F_{(4, 18)}$= 3.323, p = 0.0333; time, $F_{(2, 18)}$= 12.19, p = 0.0005; region, $F_{(2, 18)}$= 14.69, p = 0.002, N_{TP} = 3 mice). **o**, % Olig2$^+$/tdTomato$^+$ of all Olig2$^+$ cells showing significant increase over time in WM and MB (Two-way ANOVA: time, $F_{(2, 18)}$= 16.65, p < 0.0001; region, $F_{(2, 18)}$= 12.54, p = 0.0004, N_{TP} = 3 mice). For all images, White arrowheads indicate cells or structures. Yellow arrowheads indicate co-localization of two markers. For all Two-way ANOVAs, Sidak's post hoc test, *p < 0.05, ****p < 0.0001.

CRH-induced activation of astrocytes requires CRHR1

After the identification of CRHR1-expressing cells around the injury site as potential targets of OPC-derived CRH, we investigated the functional impact of the CRH/CRHR1 system on these cell types. Hence, we first conducted a series of stab wound experiments using gain-of-function (GOF) approaches involving: i) mice with a conditional brain-wide (*CRH-COE^{CNS}*) or, (ii) NG2-restricted (*CRH-COE^{NG2}*) overexpression (OE) and iii) local injection of CRH. To analyze potential OLC changes we quantified the number of OLs (CC1$^+$/Olig2$^+$), OPCs (CC1$^-$/Olig2$^+$), total number of OLCs (Olig2$^+$) and the amount of OLs of all OLCs (CC1$^+$/Olig2$^+$ of Olig2$^+$). No significant differences were observed between CRH-injected or OE animals in comparison to respective controls neither at the injury site nor at non-injured regions (**Supplementary Fig. 5, 6**). To evaluate the astrocytic response to the injury under conditions of CRH excess, we quantified the intensity of the GFAP staining as a marker reflecting the activation state of astrocytes (**Supplementary Method 2**). *CRH-COE^{CNS}* or *CRH-COE^{NG2}* mice did not show any significant differences with regards to GFAP staining intensity following injury compared to respective littermate controls (**Supplementary Fig. 7a,b**). A significant increase in the GFAP intensity was only found in CRH-injected compared to vehicle-treated mice at 3 but not at 7 dpi (**Fig. 6a,b**). Accordingly, the number of GFAP$^+$ cells in a radius of 300 µm around the injury site at 3 dpi was also found to be increased (**Fig. 6c**). To further disentangle whether this upsurge was indeed based on an actual increase in astrocyte numbers or caused by an enhanced fluorescent signal per individual cell, we measured the intensity of random cells around the injury site. This analysis revealed an increased GFAP intensity per cell at 3 and 7 dpi, suggesting that CRH directly augmented astrocyte activation (**Fig. 6d**). The effect of the injection itself on GFAP compared to a sham injury was negligible (**Supplementary Fig. 7c,d**). To further characterize the astrocytic reaction to CRH we also quantified astrocytic proliferation by Ki67/GFAP co-staining, vascular survival/regeneration by CD31 staining and neuronal survival by NeuN staining. These assessments did not reveal any differences between the conditions

(**Supplementary Fig. 7e-g**). The discrepancy in GFAP levels between CRH OE and injection of CRH is likely caused by a desensitization effect due to long-term exposure before injury and by the rather moderate overexpression, which in these mouse lines is driven by the *Rosa26* promoter. Nevertheless, these findings raised the intriguing possibility that the previously identified small population of CRHR1^{+} astrocytes around the injury site (**Fig. 4i,l,l'**) might mediate the CRH-dependent effects on astrocyte activation. Next, we investigated whether the differences in astrocytic activation caused by CRH-injection were indeed CRHR1-dependent. Therefore, we injected CRH in *CRHR1*$^{\Delta EGFP}$ mice lacking a functional CRHR1 (**Fig. 6e,f, Supplementary Table 1**). At 3 dpi, the intensity of the GFAP staining in WT animals was comparable to the previous experiment, but knockout (KO) animals displayed reduced astrocyte activation as indicated by attenuated GFAP staining intensity (**Fig. 6g,h**). Using vimentin as another activation marker, we confirmed that astrocytes in KO mice were indeed less activated following CRH application at 3 dpi (**Fig. 6i**). The further analysis of genotype-dependent differences in the astrocyte activation state by TNFα/Vimentin staining did only show a non-significant decrease in KO animals and no change in the proliferative response (**Fig. 6j,k, Supplementary Fig. 7h**).

In summary, these results demonstrate that excessive CRH has a direct and CRHR1-dependent impact on the activation state of astrocytes but not on the number or maturation of OLCs.

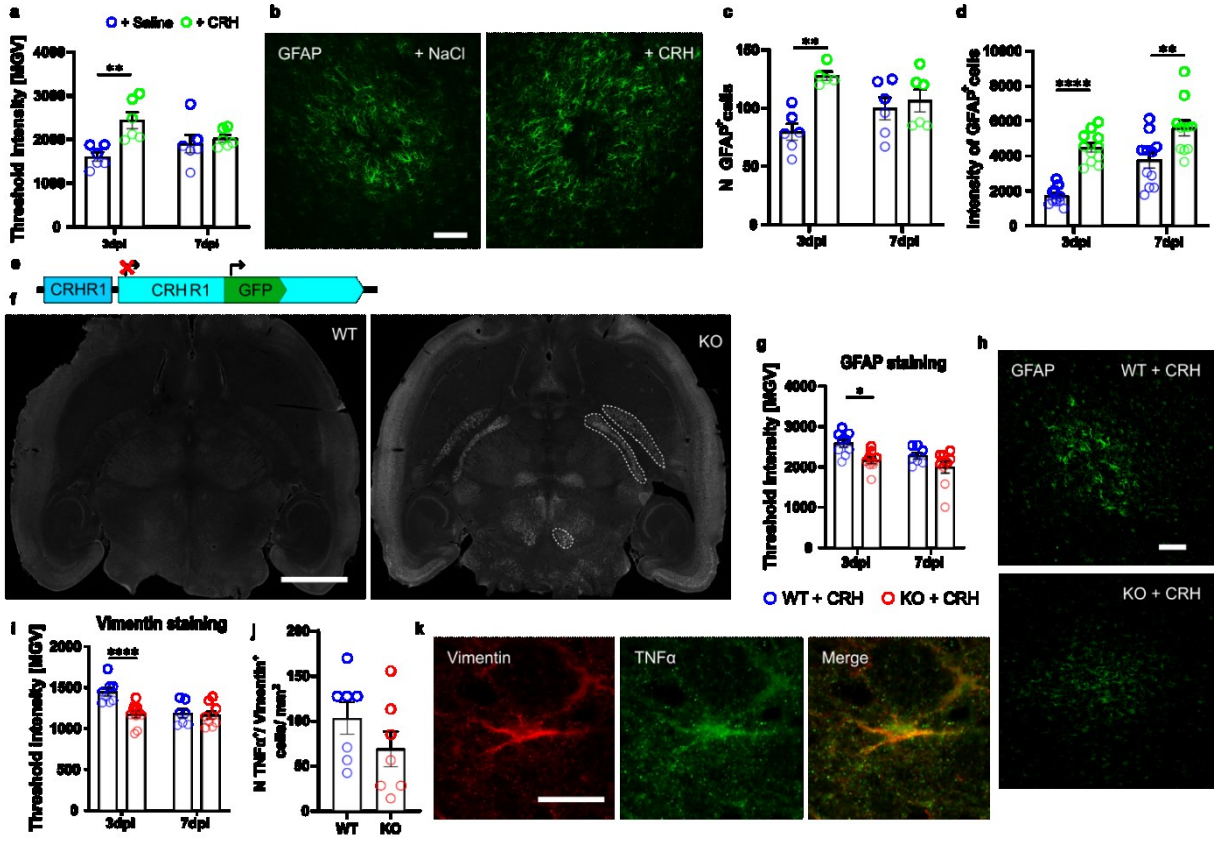

Fig. 6: CRHR1-dependent modulation of astrocyte activation state following injury. a, Quantification of GFAP intensity (mean gray value, MGV) around injury after CRH or saline injection in *CRHR1 Cre::Tau LSL-FlpO::Ai9* mice showing a significant increase after CRH injection at 3 dpi (Two-way ANOVA: interaction,

$F_{(1,20)}$= 5.262, p = 0.0328; condition, $F_{(1,20)}$= 9.331, p = 0.0063, $N_{+saline/TP}$ = 6, $N_{+CRH/TP}$ = 6). **b**, Representative image of GFAP intensity differences around injection site at 3 dpi after saline or CRH injection. Scale bar, 100 µm. **c**, Number of $GFAP^+$ cells around the injury site is significantly increased after CRH injection (Two-way ANOVA: interaction, $F_{(1,20)}$= 5.262, p = 0.0328; condition, $F_{(1,20)}$= 11.29, p = 0.0033, $N_{+saline/TP}$ = 6, $N_{+CRH/TP}$ = 6). **d**, Intensity of random single cells around the injection site at 3 and 7 dpi after saline or CRH injection showing a significant increase in single cell intensity after CRH injection (Two-way ANOVA: time, $F_{(1,40)}$= 20.83, p < 0.0001; condition, $F_{(1,40)}$= 44.67, p < 0.0001, $N_{+saline/TP}$ = 6, $N_{+CRH/TP}$ = 6). **e**, Graphical illustration of CRHR1 KO by GFP Knock-in into *Crhr1* locus in $CRHR1^{\Delta EGFP}$ mice. **f**, Overview of horizontal sections of CRHR1 WT (up) and KO (bottom) mice. White encirclement highlights examples of GFP expression in CRHR1 KO animals which is not present in WT animals. Scale bar, 1000 µm. **g**, CRHR1-dependency of CRH-effect is shown by significantly reduced MGV of GFAP intensity around injury site after CRH injection in CRHR1 KO compared to WT animals at 3 dpi (Two-way ANOVA: time, $F_{(1,30)}$= 4.811, p = 0.0362; genotype, $F_{(1,30)}$= 10.87, p < 0.0025, 3 dpi: n_{WT+CRH} = 9, N_{KO+CRH} = 9, 7 dpi: N_{WT+CRH} = 7, N_{KO+CRH} = 9). **h**, Representative image of GFAP intensity around injection site at 3 dpi after CRH injection in WT or CRHR1 KO animals. Scale bar, 100 µm. **i,** The effect on the general activation status of the astrocytes is shown by additionally significantly reduced MGV of Vimentin intensity around injury site after CRH injection in CRHR1 KO compared to WT animals at 3 dpi (Two-way ANOVA: time, $F_{(1,30)}$= 8.437, p = 0.0068; genotype, $F_{(1,30)}$= 9.639, p < 0.0025, interaction, $F_{(1,30)}$= 7.144, p = 0.012, 3 dpi: n_{WT+CRH} = 9, N_{KO+CRH} = 9, 7 dpi: N_{WT+CRH} = 7, N_{KO+CRH} = 9). **j**, Quantification of $TNF\alpha^+/Vimentin^+/mm^2$ around injury site in CRHR1 KO vs WT animals at 3 dpi showing non-significant reduction in KO animals. N = 7 animals/genotype. **k**, Confocal images of Vimentin-TNFα co-staining showing co-expression of both markers. Scale bar, 20 µm. For all Two-way ANOVAs, Sidak's post hoc test, *p < 0.05, ****p < 0.0001.

Disruption of the CRH/CRHR1 system decreases the OPC population around the injury site

To study the potential consequences of inhibiting the CRH/CRHR1 system following brain injury, we pursued different loss-of-function (LOF) approaches using the following genetic mouse models: i) conditional tamoxifen-inducible NG2-specific CRH KO ($CRH^{NG2\text{-}cKO}$), ii) global constitutive CRHR1 KO ($CRHR1^{\Delta EGFP}$) and iii) conditional tamoxifen-inducible NG2-specific CRHR1 KO ($CRHR1^{NG2\text{-}cKO}$) mice (Supplementary Table 1). Before assessing the effect of global and NG2-specific KOs, the recombination efficiency following tamoxifen treatment was assessed and shown to be at 66.3 ± 1.6 % (Supplementary Fig. 8a,b). The analysis of astrocyte activation via GFAP staining revealed that total GFAP levels were comparable between all different experimental conditions without any significant differences between KO and CTRL animals (**Supplementary Fig. 8c-e**).

In $CRH^{NG2\text{-}cKO}$ mice, the number of OLs at 3 dpi was comparable between cKO and CTRL mice. Compared to 3 dpi, the number of OLs increased at 7 dpi and cKO mice showed a trend towards a higher, yet not statistically significant, number of OLs compared to CTRL animals (**Fig. 7a**). The number of OPCs around the injury site was significantly reduced in cKO animals at 7 dpi **(Fig. 7b,e,f**). Therefore, the proportion of OLs of all OLCs was significantly increased in cKO animals at 7 dpi (**Fig. 7c-f**).

Similar to *CRH*$^{NG2\text{-}cKO}$ mice, the global loss of CRHR1 expression in *CRHR1*$^{\Delta EGFP}$ led to a significant reduction in OPCs and also to a higher proportion of OLs of all OLCs at 7 dpi (**Fig. 7h,j,k,l**), while the total number of OLs and OLCs was unchanged (**Fig. 7g,i**). Finally, the selective deletion of CRHR1 from OPCs was insufficient to reproduce previously observed changes, as no genotype-dependent differences were observed in CRHR1$^{NG2\text{-}cKO}$ mice (**Supplementary Fig. 8f-i**). The numbers of OLs, OPCs and OLCs in non-injured regions were similar between all experimental conditions and did not show significant differences between KO and CTRL animals (**Supplementary Fig. 9a-f**). These results suggest an involvement of both CRHR1-expressing OPCs and astrocytes in the OLC-specific changes observed in CRH/CRHR1-dependent LOF conditions at 7 dpi.

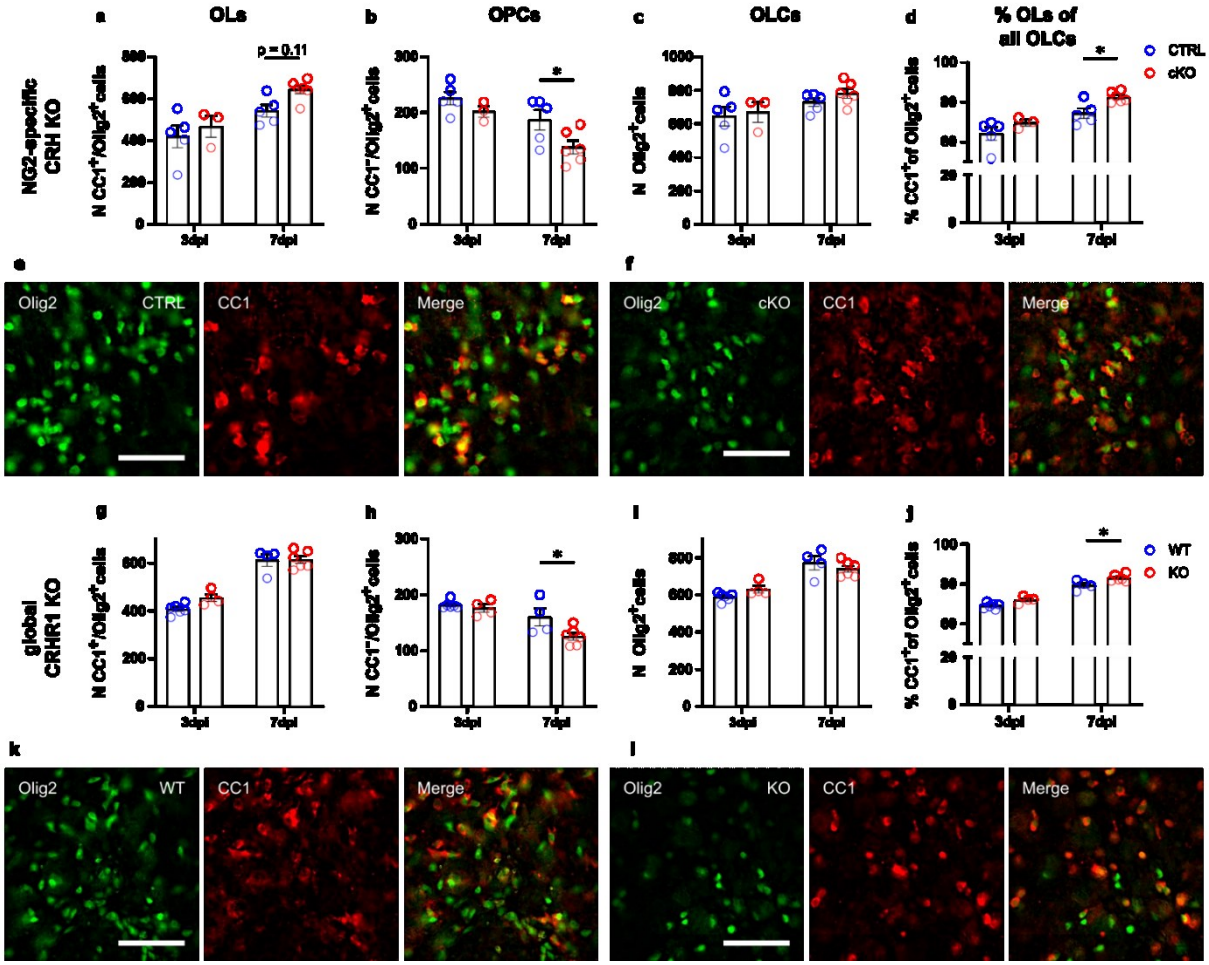

Fig. 7: CRH/CRHR1 system LOF influences OLC population dynamics after acute injury. a, Number of CC1$^+$/Olig2$^+$ cells at 3 and 7 dpi in NG2-specific CRH cKO vs CTRL animals showing a non-significant increase of CC1$^+$ cells at 7 dpi in NG2-specific CRH cKO animals (Two-way ANOVA: time, $F_{(1,15)}$= 15.14, p = 0.0014; genotype, $F_{(1,15)}$= 3.76, p = 0.0714, $N_{CTRL\ 3dpi}$ = 5, $N_{cKO\ 3dpi}$ = 5, $N_{CTRL\ 7dpi}$ = 5, $N_{KO\ 7dpi}$ = 6). **b**, Significant reduction in the number of CC1$^-$/Olig1$^+$ cells in NG2-specific CRH cKO compared to WT animals (Two-way ANOVA: time, $F_{(1,15)}$= 12.45, p = 0.003; genotype, $F_{(1,15)}$= 6.3, p = 0.024). **c**, The total number of Olig2$^+$ cells significantly increased over time (Two-way ANOVA: time, $F_{(1,15)}$= 5.254, p = 0.0368;) but not between conditions. **d**,

Percentage of $CC1^+$ of all $Olig2^+$ cells showing a significant increase in NG2-specific CRH cKO compared to CTRL animals and a general increase over time (Two-way ANOVA: time, $F_{(1,15)}= 23.07$, $p = 0.0002$; genotype, $F_{(1,15)}= 8.078$, $p = 0.0124$). **e and f,** Representative images of Olig2 CC1 staining in CTRL (e) and cKO (f) animals showing increased number of $Olig2^+/CC1^-$ cells in CTRL animals. Scale bars, 50 µm. **g**, Number of $CC1^+/Olig2^+$ showing no significant difference between conditions (Two-way ANOVA: time, $F_{(1,16)}= 130.5$, $p < 0.0001$; $n_{WT\ 3dpi} = 6$, $N_{KO\ 3dpi} = 4$, $N_{WT\ 7dpi} = 4$, $N_{KO\ 7dpi} = 6$). **h**, Significant decrease in the number of $CC1^-/Olig2^+$ cells at 7 dpi in global CRHR1 KO animals (Two-way ANOVA: time, $F_{(1,16)}= 19.84$, $p = 0.0004$; genotype, $F_{(1,16)}= 6.244$, $p = 0.0237$). **i**, Increase of $Olig2^+$ cells between 3 and 7 dpi but no significant difference between conditions (Two-way ANOVA: time, $F_{(1,16)}= 50.61$, $p < 0.0001$). **j**, Significant increase of the % of $CC1^+$ cells of $Olig2^+$ cells at 7 dpi in global CRHR1 KO animals (Two-way ANOVA: time, $F_{(1,16)}= 163.3$, $p < 0.0001$; genotype, $F_{(1,16)}= 16.08$, $p = 0.001$). **k and l**, Representative images of CC1/Olig2 staining in WT (e) and KO (f) animals showing decreased number of $CC1^-/Olig2^+$ cells in animals. Scale bars, 50 µm. For all Two-way ANOVAs, Sidak's post hoc test, $*p < 0.05$, $****p < 0.0001$.

CRH/CRHR1 system inhibition increases the number of newly formed OLs following injury

Next, we examined whether the reduction of OPCs following CRH/CRHR1 system blockade is caused by reduced proliferation of OPCs between 3 and 7 dpi or by a faster differentiation rate of OPCs. To this end, we performed a label retaining experiment using *CRHR1*$^{\Delta EGFP}$ KO mice which were treated with the intercalating substance 5-Bromo-2'-deoxyuridine (BrdU) within the first week post injury to label proliferating cells (OPCs). Animals were either sacrificed at 3 or 7 dpi or after a retaining phase at 6 weeks post injury (wpi) (**Fig. 8a**). No significant differences in the total number of $BrdU^+$ or $BrdU^+/Olig2^+$ cells were found at any of the timepoints analyzed in WT and KO mice (**Supplementary Fig. 9g,h**). The quantification of $BrdU^+/CC1^-/Olig2^+$ cells showed no significant difference between WT and KO animals, suggesting equal proliferative activation of OPCs (**Fig. 8c**). We then quantified the number of $BrdU^+/CC1^+/Olig2^+$ cells around the injury site and found a significant increase in these newly generated OLs at 7 dpi which was absent at 6 wpi (**Fig. 8d**). The analysis of the whole population of $CC1^+/Olig2^+$ cells within 300 µm around the injury site revealed a slight increase in KO animals at 7dpi (**Fig. 8e**), which reached statistical significance when restricting the evaluation to the inner 150 µm of the wound. Within this area, the number of $CC1^+/Olig2^+$ cells was significantly increased in KO animals (**Fig. 8f**). The mean difference was twice as high as the difference in $BrdU^+/CC1^+/Olig2^+$ cells suggesting that direct differentiation from OPCs without proliferation and concomitant BrdU integration contributed to these differences. To further substantiate the observed differences in the total number of OLs around the injury site we went back to the data gathered in NG2-specific CRH$^{NG2\text{-}cKO}$ and CRHR1$^{NG2\text{-}cKO}$ mice at 7 dpi and restricted our analysis to the inner 150 µm around the injury site. In both cases an increase in the number of $CC1^+/Olig2^+$ cells in KO animals compared to respective CTRLs/WTs was visible (**Fig. 8g,h**). Although these differences were not statistically significant they are in line with our current model that inhibition of the CRH/CRHR1 system positively influences OL generation following injury. Especially, because this effect was not visible in any of the GOF

experiments (data not shown). To further investigate the influence of the CRHR1 KO on the general recovery process of the injury, myelination, vascular regeneration and neuronal survival/regeneration were assessed by MBP, CD31 and NeuN staining. The MBP coverage and intensity was unchanged between genotypes at 6 wpi (**Supplementary Fig. 9i**). The total length of $CD31^+$ vasculature increased between 7 dpi and 6 wpi, but did not show any genotype specific difference (**Supplementary Fig. 9j,k**). In contrast, the number of $NeuN^+$ cells was significantly higher in KO animals compared to WT at 7 dpi, but not at 6 wpi (**Supplementary Fig. 9l,m**). This result hints in the direction that the reduced CRH/CRHR1 system signaling not only lead to a significant increase in newly formed OLs, but also to an improved short-term survival of neurons. Subsequently, we investigated the influence of the CRH/CRHR1 system on the generation of newly formed OLs under physiological conditions in the WM. *CRHR1*$^{\Delta EGFP}$ mice were treated with BrdU for 2 weeks, followed by a 3 week-period without BrdU before sacrifice (**Fig. 8i**). None of the analyzed $BrdU^+$ OLC populations showed a significant difference between WT and KO mice under physiological conditions (**Fig. 8j,k**). Thus, the CRH/CRHR1 system seems to influence rather the speed of OPC differentiation, impairing a fast differentiation at early timepoints post injury. Accordingly, OPC maturation is faster when this inhibitory drive is released by blocking the CRH/CRHR1 system.

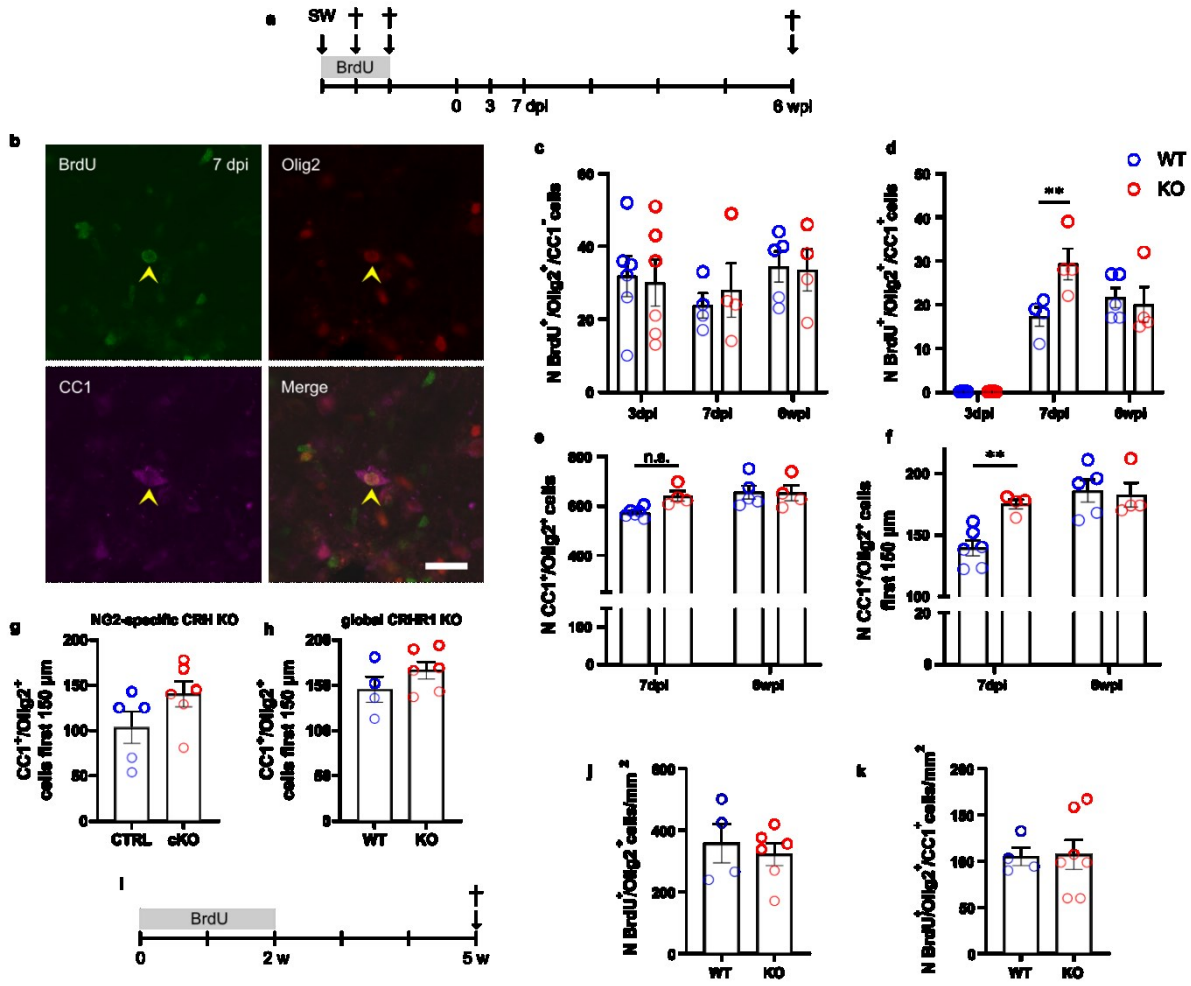

Fig. 8: CRH/CRHR1 system regulates early differentiation after injury. a, Experimental scheme of BrdU label retaining experiment after acute injury. **b**, Confocal image of BrdU/Olig2/CC1 staining at 7 dpi showing co-localization. **c**, Quantification of $BrdU^+/Olig2^+/CC1^-$ cells in 300 µm radius around injury site at 3 dpi, 7 dpi and 6 wpi in WT and KO animals showing no significant differences between conditions. **d**, Quantification of $BrdU^+/Olig2^+/CC1^+$ cells around injury site showing significantly increased number of newly generated OLs in KO animals at 7 dpi (Two-way ANOVA: time, $F_{(2,23)}= 77.67$, $p < 0.003$; genotype, $F_{(2,23)}= 3.841$, $p = 0.0622$, Sidak's post hoc test, *$p < 0.05$, ****$p < 0.0001$, $N_{WT\ 3dpi} = 6$, $N_{KO\ 3dpi} = 6$, $N_{WT\ 7dpi} = 4$, $N_{KO\ 7dpi} = 4$, $N_{WT\ 6wpi} = 5$, $N_{KO\ 6wpi} = 4$). **e-f,** Quantification of $CC1^+/Olig2^+$ cells in whole wound area (e) and within 150 µm (f) showing significant increase of OLs at 7 dpi within 150 µm (Two-way ANOVA: time, $F_{1,15)}= 12$, $p = 0.0035$; genotype, $F_{(1,15)}= 4.316$, $p = 0.0553$, Sidak's post hoc test, *$p < 0.05$, ****$p < 0.0001$,, $N_{WT\ 7dpi} = 6$, $N_{KO\ 7dpi} = 4$, $N_{WT\ 6wpi} = 5$, $N_{KO\ 6wpi} = 4$). **g and h**, Quantification of $CC1^+/Olig2^+$ cells in the first 150 µm around the injury site in NG2-specific CRH KO (g) and global CRHR1 KO (h) **i**, Experimental scheme of BrdU label retaining experiment in naive animals. **j**, Quantification of $BrdU^+/ Olig2^+$ cells. **k**, Quantification of $BrdU^+/ Olig2^+/ CC1^+$ cells showing no significant differences between WT and KO animals ($n_{WT}= 4$, $N_{KO}= 6$). Yellow arrowheads indicate co-localization of markers.

Discussion

Neuropeptides represent a large and diverse group of molecules commonly considered as neuromodulators, which have been implicated in a wide variety of processes in the CNS. So far, they have been investigated predominantly in the context of neuronal development and as modulators of synaptic transmission[35, 36, 37]. In our study we identified and characterized a novel CRH/CRHR1 system in glial cells, in which OPC-derived CRH targets CRHR1-expressing astrocytes and OPCs and modulates early oligodendrogenesis and neuronal survival. The discovery of CRH expression in OPCs starting within 12 hpi, thus, preceding proliferation, is to the best of our knowledge, the first in-depth description of neuropeptide expression in OPCs but also among the earliest reaction of OPCs towards acute injury described so far.

The injury response of CRH-expressing OPCs in the MB investigated here is in line with those reported for OPCs in development and adult remyelination with a strong proliferative response between 2 and 7 dpi, a subsequent decrease in population size and increased differentiation[7, 9, 10]. Their high maturation rate of 80%, however, distinguishes them from cortical OPCs, which have been reported to possess a rather low oligodendrogenic potential following acute injury[7]. When comparing CRH-expressing OPCs to all OLCs in close proximity to the injury site a slight difference in their population dynamics is visible, which could also be explained by their high maturation rate. Enhanced OPC differentiation would translate into a higher number of premyelinating OLs which do not find a stable connection and therefore degenerate. This would explain the observed stronger decrease of CRH-expressing OLCs. Whether this is the only cause for the identified differences or other factors are involved, needs to be clarified in future experiments. Nevertheless, the presence of OLs generated from CRH-expressing OPCs up to four months following acute injury highlights their high endurance upon stable integration[30]. Interestingly, CRH-expressing OPCs or thereof derived OLs are not present in the mouse brain under non-injury conditions. This sparks the question for potential physiological stimuli inducing CRH expression in OPCs. In this context it is noteworthy that experimental mice in their artificial habitat and social environment are largely deprived of natural environmental stimuli such as food deprivation, exposure to predators or activation of the immune system in the context of infections - challenges which might have an impact on CRH expression in OPCs, independent of brain injury.

Nevertheless, we clearly show that CRH expression is induced by acute injury. The biological effect of a peptide ligand is mediated and amplified by its respective receptor and activation of downstream signaling pathways. Accordingly, the number of ligand-expressing cells does not allow to extrapolate a system´s physiological relevance as is well known from the neuronal CRH/CRHR1 system in context of the stress response[16]. Therefore, although CRH-expressing OPCs represent only 7 - 15% of the entire OLCs population around the injury site, the identification of CRHR1-expressing OPCs and astrocytes in close proximity to the injury site highlights the potential of the system to influence the brains reaction to injury.

We identified CRHR1$^+$ OPCs as a separate entity showing only minor overlap with the CRH$^+$ OPC population indicating that CRH/CRHR1 system-related OPCs interact with each other in a previously unprecedented manner, as no other peptidergic system has been described in OPCs so far. The implications of this potential interaction were investigated by different LOF and GOF experiments showing that decreased CRH/CRHR1 signaling lead to a significant decrease in OPCs at 7 dpi, which was later explained by an increase in the number of BrdU$^+$ newly generated OLs. The observation that also the number of BrdU$^-$ OLs in close proximity was increased following CRHR1 KO suggests that the system affects also direct differentiation. The fact that all LOF experiments, except the NG2-specific CRHR1 KO, showed comparable effects concerning the number of CC1$^+$/Olig2$^+$ cells, underscores the significance of the results. Since the number of newly generated OLs, but also the total number of OLs was comparable at 6 wpi it is highly likely that the CRH/CRHR1 system influences OPC differentiation speed rather than OL maturation. Although the remyelination potential might have been higher at 7 dpi, the number of stably integrated OLs at 6 wpi did not differ because the demand for remyelination determined by the extension of the injury site and collateral loss of OLs were also comparable between genotypes. In contrast to the role of CRHR1-expressing OPCs, the influence of CRHR1-expressing astrocytes in this context is more complex. CRH injection leads to a CRHR1-dependent increase in GFAP as well as vimentin expression as shown by injection in WT mice and KO studies, but has neither a direct effect on astrocytic proliferation, vascular or neuronal survival nor on the OLC population. Nevertheless, CRHR1 inactivation leads to OLC changes in global but not in NG2-specific CRHR1 KO mice, implying that CRHR1$^+$ astrocytes play an essential role. Therefore, our data suggest that CRH has an impact on astrocytic GFAP signaling but only influences the OLC population when CRH/CRHR1 signaling is decreased. This hypothesis is further supported by the finding that the decrease in the number of TNFα$^+$ astrocytes and the parallel increase in short term neuronal survival, detected in CRHR1 KO compared to WT mice, was not observed in the comparison of CRH and saline injected WT mice. Therefore, the observed TNFα differences in astrocytes of KO mice rather resemble a reduction than a missing increase compared to astrocytes of WT mice, which is caused by the absence of the receptor. Otherwise a comparable decrease of TNFα$^+$ astrocytes should also have been observable in saline injected WT mice. These results are in line with previous reports demonstrating that reduced astrocytic activation which entails decreased IFN-gamma release is beneficial for OL maturation and neuronal survival [38, 39, 40]. Therefore, CRH/CRHR1-dependent astrocyte signaling seems to promote a beneficial environment rather than directly impacting OPC differentiation.

CRHR1-expressing OPCs and astrocytes are also present under non-injury conditions raising the question for their role in brain physiology. Quantification of CRHR1$^+$ OLCs revealed that their number increased more dramatically than the rest of the OLC population. The growth in the number of CRHR1-expressing OLCs exceeds the increase in CRHR1-expressing OPCs, suggesting that newly generated OLs are the source of this increase. Thus, CRHR1$^+$ OPCs contribute strongly to the generation of OLs in the adult mouse brain. The co-localization with the stage-dependent marker and so-called “gate keeper

of differentiation" GPR17 tightens the connection of this population to adult OL generation. Although, this appears contradictory to the previous data showing that the CRH/CRHR1 system represents a stalling mechanism for OPC differentiation, it is not. First of all, the differentiation and generation of OLs by the CRHR1-expressing population of OPCs is influenced by more factors than just the CRHR1. The high maturation tendency of CRHR1$^+$ OPCs in the adult brain may necessitate the CRHR1 system to stall premature differentiation only under certain circumstances. Secondly, the comparison of newly generated OLs in WT vs CRHR1 KO animals under physiological conditions showed that the overall number of OLs is unchanged under these conditions. We can only hypothesize about potential conditions, other than acute injury, in which premature differentiation might be stalled in CRHR1$^+$ OPCs. One possible condition could be stress, leading to elevated CRH release from neurons of stress-related neurocircuitries[25, 41]. Accordingly, recent studies have shown that myelination or the number of OLs can be altered in stress-related disorders[42, 43, 44]. Considering that CRH is well-known as a stress peptide and for its implication in stress-related pathologies the investigation of the influence of stress on the CRH/CRHR1 system in OPCs is an obvious line of future research [3].

Together with recent findings that dynorphin released by unmyelinated neurons is essential for OPC differentiation and myelination[14], our results strengthen the hypothesis that neuropeptides play an important role in OPC differentiation, potentially involving other glial cell types like astrocytes. Besides, and in opposition to fast acting neurotransmitters, neuropeptides possess slow release kinetics and predominantly act via G protein-coupled receptors, making them ideally suited to modulate long-lasting myelination changes[36].

Ultimately, our data not only unravel the CRH/CRHR1 system as an important player in OL maturation but also point towards the system´s potential as a promising pharmacological target to increase the remyelination capacity after conditions of demyelination occurring in many neuropsychiatric and demyelinating diseases but also after traumatic brain injury.

Online Methods

Animals

All animal experiments and protocols were legally approved by the Ethics Committee for the Care and Use of Laboratory Animals of the Government of Upper Bavaria, Germany. 2-6 month old mice were group housed under standard lab conditions (22 ± 1°C, 55 ± 5% humidity) with ad libitum access to food and water on a 12:12 h light:dark schedule with weekly cage changes. Regular genotyping was performed by polymerase chain reaction (PCR) analysis of tail DNA. Global and conditional knockouts and global and conditional overexpressing mice were assigned to experimental groups based on their genotype. Age matched littermates were used as controls in all experiments. Mice with incorrect injury or injection were excluded from the experiment. The following mouse lines were used:

CRH-Cre (*Crh*$^{tm1(cre)Zjh}$, Jackson Laboratory stock no. 012704)[45], *CRH-FlpO* (*Crh*$^{tm1.1(flpo)Bsab}$, Jackson Laboratory stock no. 031559)[46], *CRHR1-Cre* (*Crhr1*$^{tm4.1(cre)Jde}$)[23], *CRH-Venus* (*Crh*$^{tm1.1Ksak}$)[29]; *Tau-LSL-FlpO*[47], *NG2-CreERT2* (*Tg(Cspg4-cre/Esr1*)BAkik*, Jackson Laboratory stock no. 008538)[48], , *Nestin-Cre* (*Tg(Nes-cre)1Kln*, Jackson Laboratory stock no. 003771)[49], *Ai9* (*Gt(ROSA)26Sor*$^{tm9(CAG-tdTomato)Hze}$, Jackson Laboratory stock no. 007909)[50], *Sun1-GFP* (*Gt(ROSA)26Sor*$^{tm5(CAG-Sun1/sfGFP)Nat}$, Jackson Laboratory stock no. 021039)[51], *Ai65* (*Gt(ROSA)26Sor*$^{tm65.1(CAG-tdTomato)Hze}$, Jackson Laboratory stock no. 021875)[50], *Ai65F* (*Gt(ROSA)*$^{26Sortm65.2(CAG-tdTomato)Hze/J}$, Jackson Laboratory stock no. 032864*)*, *CRH*^{loxP} (*Crh*$^{tm1.1Jde}$)[23], *CRHR1*^{loxP} (*Crhr1*$^{tm2.2Jde}$)[52], *CRH-OE* (*Gt(ROSA)26Sor*$^{tm1(Crh)Jde}$)[53], *CRHR1*$^{\Delta EGFP}$ (*Crhr1*^{tm1Jde})[20].

The following double and triple transgenic lines were generated in this study by cross-breeding of single transgenic lines (detailed description included in Supplementary Table 1): *CRH-Cre::Ai9*, *NG2-CreERT2::Ai9*, *CRH-FlpO::NG2-CreERT2::Ai65*, *CRH-FlpO::CRHR1-Cre::Ai65*, *CRH*$^{NG2\text{-}cKO}$ *(CRH*^{loxP}*::NG2-CreERT2:: Ai9*), *CRHR1*$^{NG2\text{-}cKO}$ *(CRHR1*^{loxP}*::NG2-CreERT2)*, *CRH-COE*^{NG2} *(CRH-COE::NG2-CreERT2)*, *CRH-COE*^{CNS} (*CRH-COE::Nestin-Cre)*, *CRHR1-Cre:Tau-LSL-FlpO::Ai9*, *CRHR1-Cre::Sun1-GFP*, *CRH-FlpO::Ai65F::CRHR1-Cre::Sun1-GFP.*

Stereotaxic surgeries

For all experiments requiring stereotaxic surgeries, mice received analgesic treatment prior, during and after surgery. Animals were anesthetized using isoflurane (CP-Pharma) and placed in a stereotaxic frame. Acute injury, fluorescent bead, CRH, saline and virus injections, cranial window or hippocampal cannula implantation was performed as described in the sections below.

Acute injury for CRH$^+$ OLC quantification and modulation experiments

After opening of the skin and removal of a bone flap using a dental drill, the syringe was slowly inserted and removed from the tissue. The following coordinates were used: PFC: AP 2.2, ML 1.0, DV -3.2; Striatum: AP 1.2, ML 1.5, DV -3.3; MB: AP -3, ML 1.0, DV -4. Injuries were inflicted using a 24-gauge Hamilton syringe. Injuries for label retaining experiments were performed using a 33-gauge Hamilton syringe to reduce background for BrdU staining.

Fluorescent bead-, CRH-, saline-, hGFAP-virus and CMV-GFP-virus injection

For injections, head skin was opened. A bone hole was drilled using a dental drill. The syringe was inserted. Then, Fluorencent beads (Green Retrobeads™ IX, Lumafluor, 500 nl), CRH (C3042, Sigma, 200 nM in 1 % acetic acid in saline, 200 nl) saline (1 %acetic acid, 200 nl),hGFAP-virus (ssAAV-5/2-hGFAP-hHBbI/E-dlox-dTomato-EGFP(rev)-dlox-WPRE-bGHp(A); Viral Vector Facility ETH Zurich, v421, 500 nl) or CMV-eGFP-virus (AAV1/2-CMV-DIO-eGFP, Vector Biolabs, 500 nl) were injected at a speed of 100 nl/ min with a 33 gauge syringe (Hamilton). After injection was finished, the syringe was pulled out 1 mm and, after a waiting time of 2 minutes, slowly and finally removed from the tissue. The following coordinates were used: AP -3, ML 1.0, DV -3.7.

Cranial window implantation with injury infliction

After stereotaxic fixation, a round piece of skin, ~8 mm in diameter, was removed. Under repeated application of cold saline to prevent overheating, a round piece of cranial bone was drilled out (approx. 5 mm diameter). A double-edged knife was moved in (DV: -0.8 mm) and out of the brain parenchyma three times. A drop of sterile saline was applied to the open brain tissue and a 5 mm cover slip was placed over the opening and subsequently fixed using quick adhesive cement (Parkell C&B Metabond clear powder L, Quick Base B, Universal Catalyst C). The custom-made head plate was positioned on top of the head and fixed using Kallocryl (Speiko, liquid component 1609 and powder 1615).

Implantation of subcortical imaging cannula

Preparation and implantation of the subcortical imaging cannula were performed as described before [54]. The cannula consisted of a cylindrical metal tube, 1.6 mm height and 3.5 mm diameter, sealed at the bottom with a glass coverslip. After stereotaxic fixation of the animals, the head skin was removed. Under repeated application of cold saline to prevent overheating, a round piece of cranial bone (approx.

3.5 mm diameter) was gently removed using a trephine. After removal of the bone flap, the cortex was slowly aspirated using a vacuum pump until the corpus callosum, identified as white matter horizontal fibers, was exposed. The imaging cannula was gently inserted into the cavity and immediately fixed using a quick adhesive cement (Parkell C&B Metabond, clear powder L, Quick base B, Universal Catalyst C). Finally, a custom-made head plate was fixed as described above.

In-vivo 2-photon imaging

2-photon imaging experiments were done using an Ultima IV microscope from Bruker, equipped with an InSight DS+Dual laser system. We tuned the laser to 1040 nm to excite tdTomato, while 920 nm laser wavelength was used to image the dura. During imaging, the average power at the tissue did not exceed 40mW. Animals were anesthetized using isoflurane and fixed under the microscope using a custom-made head plate holder. We kept the animals' temperature constant by means of a heating pad set to 37 °C. Z-stacks were acquired with 2-5 µm step size using an Olympus XLPlan N 25×/1.00 SVMP objective at magnification zoom 1x and 2.38x. We acquired images averaged over 4-16 repetitions per each imaging plane. For time-lapse imaging, images were acquired every 60 s for 20-30 min.

Experimental setup modulation of CRH/CRHR1 system in glial cells

For experiments with inducible Cre recombinase lines, recombination was induced by i.p. injection of TAM two times within the 7 days before injury infliction. For modulation experiments, animals were injured or injected as described above. Mice were sacrificed at 3 or 7 dpi and analyzed for GFAP staining intensity, number of $GFAP^+$ cells, number of OLs ($CC1^+$/ $Olig2^+$), OPCs ($CC1^-$/ $Olig2^+$), all OLCs ($Olig2^+$) cells and the percentage of OLs of all OLCs ($CC1^+$ of all $Olig2^+$ cells).

Label retaining experiment

BrdU 1 mg/ kg was added to the drinking water (1 % w/w sucrose). In case of injury experiments, treatment started at the day of injury infliction and was sustained for a maximum of 7 days (7 dpi and 6 wpi mice) or until sacrifice (3 dpi). For naive labeling of CRHR1 KO mice, treatment was applied for two consecutive weeks followed by a retaining time of three weeks.

Cryosectioning

Animals were sacrificed using isoflurane and subsequently perfused with ice cold 1xPBS and 4 % PFA. After recovery of the brain, it was post fixed in 4 % PFA on ice for 6 h, transferred to 30 % sucrose in 1xPBS. and incubated at 4 °C for 48 h. Brains were frozen on dry ice and cut either coronally or horizontally in 40 µm sections using a cryostat (Leica). Sections were collected in cryoprotection solution (25 % Ethylene glycol, 25 % glycerol, 50% dH2O in 1xPBS) and stored at -20 °C until further use. For DISH mice were killed by cervical dislocation. After fast recovery the brain was frozen on dry

ice and stored at -80 °C until further use.Coronal sections (20 µm) were generated using a cryostat (Leica). After thaw-mounting onto SuperFrost slides, sections were dried and kept at -80 °C.

Immuno fluorescence staining

Immuno fluorescence staining was conducted using different protocols depending on the combination of antigens of interest. For NG2/ Olig2 and NG2/Ki67 staining, a two-day protocol was performed. In brief, slices were washed 3x in 1x PBS, followed by blocking in 2 % normal goat serum in 0.05 % Triton-X100 and 1x PBS. Sections were incubated in primary anti-NG2 antibody at 4 °C under shaking overnight. After washing, sections were incubated in secondary antibodies for 2 h at room temperature (RT). After washing, antigen retrieval (AR) was performed in citrate buffer (75 °C, 1 h). After washing, primary anti-Olig2 or anti-Ki67 antibody was incubated as described before. After washing, secondary antibody was applied as described before and sections were washed and mounted using Fluoromount-G™ mounting medium (+/- DAPI, Invitrogen, 15586276).

For CC1/ Olig2, Ki67/ Olig2 and Ki67/ Olig2/ GFP staining, washing was performed followed by AR as described before. After washing, sections were blocked. Primary and secondary antibody incubation were also conducted as described before.

For anti-GFP, anti-GFAP, anti-Vimentin, anti-S100β, anti-IBA1, anti-NeuN, anti-MBP, anti-CNPase and anti-CD31 staining sections were washed and blocked as described above. Primary and secondary antibody treatment were performed as mentioned above.

For CRH, staining sections were washed and blocked as described before. Primary antibody was added and sections were incubated for 5 days under shaking at 4 °C. Secondary antibody treatment was performed as described above.

For BrdU staining, two different protocols were used. Sections were washed and AR was achieved either with citrate buffer (2.94 g/l, pH 6, 1 h, 75 °C) for injury sites or with HCl (2 M, 10 min, 37 °C) followed by borate buffer (10 min, RT) for naive brains. After washing sections were blocked and primary and secondary antibody staining was performed as described above.

For GPR17 staining sections were quenched with H_2O_2 (1 % in dH_2O) for 15-30 min. Sections were blocked and incubated with anti-GPR17 Ab as described above. Secondary antibody staining was performed using a biotinylated goat-anti-rabbit (rb) Ab for 2 h at RT. After washing horse-radish-peroxidase (HRP) was applied for 30 min at RT. Samples were incubated in Tyramine solution (stock 1:20 in 1x amplification dilution) for 3-10 min. After washing samples were mounted and covered as described above.

The following primary antibodies and dilutions were used: rb NG2 (1:200, Merck, AB5320), rb Olig2 (1:200, Merck, AB9610), mouse (ms) Olig2 (1:200, Merck, MABN50), ms APC (CC1) (1:200, Merck, OP80), rb GPR17 (1:500, Sigma, SAB4501250), ms CNPase (1:1000, Abcam, ab6319), rb MBP (1:500, obtained from Klaus-Armin Nave, MPI exp. Medicine, Goettingen)[55], rb Ki67 (1:500 - 1:1000, Abcam, Ab15580), rat BrdU (1:500 – 1:1000, Abcam, 6326), rb Iba1 (1:500 – 1:1000, Synaptic Systems,

234013), ms NeuN (1:500, Abcam, Ab13970), rb GFAP (1:500 – 1:3000, Abcam, ab7260), ms S100β (1:500, Sigma, AMAB91038), chicken (ck) Vimentin (1:1000, Merck, AB5733), rb CRH (1:20000, obtained from Paul E. Sawchenko, Salk Institute, CA.), ck GFP (1:500 – 1:1000, Aves, GFP-1020), rb RFP (1:500, Rockland, 600-401-379), rat CD31 (1:200, BD Pharmingen™, 550274).
The following secondary antibodies were used: goat anti rb Alexa 488, Alexa 568, Alexa 594 or Alexa 647, goat anti ms Alexa 488, Alexa 568, Alexa 594 or Alexa 647, goat anti rat Alexa 488 or Alexa 568 and goat anti ck Alexa 488.

Double in situ hybridization

DISH was performed as previously described [20, 23]. The following riboprobes were used: *Crh (5' UTR to Exon 2): 70 to 469 bp of* NM_205769.2, *Pdgfrα*: 1583 to 2434 bp of NM_011058.1.

Image acquisition

Images for quantification of cell numbers and intensity measurements were acquired using an Olympus VS120 Slide Scanner. For overview and close up acquisition, the 4x or 20x objective was used, respectively. Exposure times were chosen to yield the best signal to noise ratio and minimal photodamage. Images were extracted and saved as .tif files.
Qualitative images of cells of interest were taken with a Laser scanning confocal microscope (Carl Zeiss). 20x water-, 40x and 63x oil-immersion objectives were used. Laser settings were adjusted to yield the best signal to noise ratio. Images were acquired with 1024x1024 pixel size and a scan speed between 3 and 7.

Quantification of CRH-expressing OPCs in *CRH-Cre::Ai9* mice

A 28 µm z-stack with a step size of 3 µm was acquired around the injury site. The counting matrix was generated with a custom Fiji macro. Cells in the different areas between +/-300 µm were counted using Fiji's manual counting tool. To generate comparable counts, consistent contrast settings were used for each quantification.
Quantification of CRHR1-expressing OLCs at 1.5, 3 and 5 months in *CRHR1-Cre::LSL-FlpO::Ai9* mice
After CC1/ Olig2 or NG2/ Olig2 staining was performed, z-stacks (28 µm depth, 3 µm step size, 1 mm^2 ROI) were acquired in CX, CC, AC, OT and MB. CC1 and NG2/ tdTomato co-expressing cells were quantified in the whole ROI. The number of all $Olig2^+$ cells was counted in a consistent subregion (64000 μm^2) and upscaled to cells/ mm^2.

Quantification of cells in CRH/ CRHR1 system modulation experiments

Horizontal sections were imaged as described above. After setting the wound center, the circular counting matrix with a radius of 300 µm and medio-lateral resolution of 50 µm was generated using a custom macro in Fiji (**Supplementary Method 1**). Cells were counted with the manual Fiji counting tool. Consistent contrast settings were used for each quantification.

GFAP and Vimentin intensity measurements

For intensity measurements, a custom macro in Fiji was used. In brief, the GFAP/ Vimentin channel was extracted from the multi-channel picture, and maximum intensity z-projection was performed. After thresholding, the average intensity in the area above the chosen threshold (between 100 and 1000 MGV) was measured (**Supplementary Method 2a,b**).

Quantification of $CD31^+$ vascularization

For preprocessing of images custom Fiji macros complemented with segmentation by the machine learning assisted image anaylsis tool Ilastik was used. In brief, the preprocessed and z-projected image was segmented using Ilastik. The segmented binary picture was skeletonized and analyzed using Fijis built-in Skeletonize (2D/3D) and Analyze-Skeleton (2D/3D) functions. Total length of vasculature was analyzed from the extracted data (**Supplementary Method 2c-f**).

Movie annotation

Movies were created based on 2-photon time-lapse imaging using Fiji. Arrows were added using a freely accessible plugin[56].

Statistical analysis

For statistical analysis, GraphPad Prism 8 was used. One-way ANOVA followed by Bonferroni's and two-way ANOVA followed by Sidak's post hoc test were performed. Values are reported as means ± standard error of mean (s.e.m.). Statistical significance was defined as $P < 0.05$. No statistical methods were used to predetermine sample sizes, but it was based on those previously reported in other publications[7, 14]. During analysis, experimenters were blinded to experimental conditions.

Data availability

Additional data, supporting the findings of this study are available from the corresponding author upon reasonable request.

Code availability

All macros used in this study are available from the corresponding author upon reasonable request.

Acknowledgments

The authors thank Sabrina Bauer and Steffanie Unkmeir for their assistance with genotyping and Andrea Parl for her constant assistance in the lab and Elfi Fesl for proofreading the manuscript. We thank Klaus-Armin Nave and Sandra Goebbels for their scientific input and for sharing different antibodies with us. Additionally, we thank Mathias Schmidt for providing AAV1/2-CMV-DIO-eGFP virus.

Author Contributions

C.R. designed, led and performed all experiments, analyzed and interpreted data and wrote the manuscript. T.M.I. performed GPR17 staining and analysis, provided scientific input and subedited the manuscript. J.P. performed the quantification of CRHR1-expressing astrocytes after reporter virus injection, analyzed data and subedited the manuscript. A. U. helped with cannula implantations for *in vivo* imaging, gave scientific expertise, helped with image acquisition at the 2-photon setup and subedited the manuscript. S. C. aided methodological and scientific expertise. I.M.H. aided methodological expertise in cranial window implantation, provided scientific input and subedited the manuscript. K.S. and K.I. created and provided the CRH-Venus mouse line and reviewed the manuscript. A.A. provided scientific input concerning 2-photon imaging, reviewed and subedited the manuscript. L.D. provided constant scientific input, helped with planning label retaining experiments, reviewed and subedited the manuscript. J. M. D. provided essential scientific advice and support, supervised all experiments and analysis, reviewed and edited the manuscript.

Conflict of Interest

The authors declare no competing interests.

References

1. Raff MC, Miller RH, Noble M. A glial progenitor cell that develops in vitro into an astrocyte or an oligodendrocyte depending on culture medium. *Nature* **303**, 390-396 (1983).
2. Jakel S, Dimou L. Glial Cells and Their Function in the Adult Brain: A Journey through the History of Their Ablation. *Frontiers in Cellular Neuroscience* **11**, (2017).
3. Nishiyama A, Serwanski DR, Pfeiffer F. Many roles for oligodendrocyte precursor cells in physiology and pathology. *Neuropathology* **41**, 161-173 (2021).
4. Hughes EG, Kang SH, Fukaya M, Bergles DE. Oligodendrocyte progenitors balance growth with self-repulsion to achieve homeostasis in the adult brain. *Nature Neuroscience* **16**, 668-+ (2013).
5. Simon C, Gotz M, Dimou L. Progenitors in the adult cerebral cortex: cell cycle properties and regulation by physiological stimuli and injury. *Glia* **59**, 869-881 (2011).
6. von Streitberg A*, et al.* NG2-Glia Transiently Overcome Their Homeostatic Network and Contribute to Wound Closure After Brain Injury. *Front Cell Dev Biol* **9**, 662056 (2021).
7. Dimou L, Simon C, Kirchhoff F, Takebayashi H, Gotz M. Progeny of Olig2-expressing progenitors in the gray and white matter of the adult mouse cerebral cortex. *J Neurosci* **28**, 10434-10442 (2008).
8. Vigano F*, et al.* GPR17 expressing NG2-Glia: Oligodendrocyte progenitors serving as a reserve pool after injury. *Glia* **64**, 287-299 (2016).
9. Trapp BD, Nishiyama A, Cheng D, Macklin W. Differentiation and Death of Premyelinating Oligodendrocytes in Developing Rodent Brain. *Journal of Cell Biology* **137**, 459-468 (1997).
10. Hughes EG, Orthmann-Murphy JL, Langseth AJ, Bergles DE. Myelin remodeling through experience-dependent oligodendrogenesis in the adult somatosensory cortex. *Nature Neuroscience* **21**, 696-+ (2018).
11. Barres BA*, et al.* Cell-Death and Control of Cell-Survival in the Oligodendrocyte Lineage. *Cell* **70**, 31-46 (1992).
12. Hughes EG, Stockton ME. Premyelinating Oligodendrocytes: Mechanisms Underlying Cell Survival and Integration. *Frontiers in Cell and Developmental Biology* **9**, (2021).
13. Gibson EM*, et al.* Neuronal Activity Promotes Oligodendrogenesis and Adaptive Myelination in the Mammalian Brain. *Science* **344**, 487-+ (2014).
14. Osso L, Rankin K, Chan J. Experience-dependent myelination following stress is mediated by the neuropeptide dynorphin. *Glia* **69**, E401-E401 (2021).
15. Joels M, Baram TZ. OPINION The neuro-symphony of stress. *Nat Rev Neurosci* **10**, 459-U484 (2009).
16. Deussing JM, Chen A. The Corticotropin-Releasing Factor Family: Physiology of the Stress Response. *Physiol Rev* **98**, 2225-2286 (2018).
17. Ulrich-Lai YM, Herman JP. Neural regulation of endocrine and autonomic stress responses. *Nat Rev Neurosci* **10**, 397-409 (2009).
18. Heinrichs SC, Koob GF. Corticotropin-releasing factor in brain: A role in activation, arousal, and affect regulation. *J Pharmacol Exp Ther* **311**, 427-440 (2004).
19. Lowry CA, Moore FL. Regulation of behavioral responses by corticotropin-releasing factor. *Gen Comp Endocr* **146**, 19-27 (2006).
20. Refojo D*, et al.* Glutamatergic and Dopaminergic Neurons Mediate Anxiogenic and Anxiolytic Effects of CRHR1. *Science* **333**, 1903-1907 (2011).
21. Fuzesi T, Daviu N, Cusulin JIW, Bonin RP, Bains JS. Hypothalamic CRH neurons orchestrate complex behaviours after stress. *Nature Communications* **7**, (2016).
22. Sanford CA*, et al.* A Central Amygdala CRF Circuit Facilitates Learning about Weak Threats. *Neuron* **93**, 164-178 (2017).
23. Dedic N*, et al.* Chronic CRH depletion from GABAergic, long-range projection neurons in the extended amygdala reduces dopamine release and increases anxiety. *Nature Neuroscience* **21**, 803-+ (2018).

24. McCall JG*, et al.* CRH Engagement of the Locus Coeruleus Noradrenergic System Mediates Stress-Induced Anxiety. *Neuron* **87**, 605-620 (2015).
25. Chang S*, et al.* Tripartite extended amygdala - basal ganglia CRH circuit drives arousal and avoidance behaviour. *bioRxiv*, 2022.2003.2015.484057 (2022).
26. Stevens SL*, et al.* Reduced cerebral injury in CRH-R1 deficient mice after focal ischemia: a potential link to microglia and atrocytes that express CRH-R1. *J Cereb Blood Flow Metab* **23**, 1151-1159 (2003).
27. de la Tremblaye PB, Benoit SM, Schock S, Plamondon H. CRHR1 exacerbates the glial inflammatory response and alters BDNF/TrkB/pCREB signaling in a rat model of global cerebral ischemia: implications for neuroprotection and cognitive recovery. *Prog Neuropsychopharmacol Biol Psychiatry* **79**, 234-248 (2017).
28. Michalski J-P, Kothary R. Oligodendrocytes in a Nutshell. *Frontiers in Cellular Neuroscience* **9**, (2015).
29. Kono J*, et al.* Distribution of corticotropin-releasing factor neurons in the mouse brain: a study using corticotropin-releasing factor-modified yellow fluorescent protein knock-in mouse. *Brain Struct Funct* **222**, 1705-1732 (2017).
30. Tripathi RB, Jackiewicz M, McKenzie IA, Kougioumtzidou E, Grist M, Richardson WD. Remarkable Stability of Myelinating Oligodendrocytes in Mice. *Cell Rep* **21**, 316-323 (2017).
31. Ciana P*, et al.* The orphan receptor GPR17 identified as a new dual uracil nucleotides/cysteinyl-leukotrienes receptor. *EMBO J* **25**, 4615-4627 (2006).
32. Lecca D*, et al.* The recently identified P2Y-like receptor GPR17 is a sensor of brain damage and a new target for brain repair. *PLoS One* **3**, e3579 (2008).
33. Chen Y*, et al.* The oligodendrocyte-specific G protein-coupled receptor GPR17 is a cell-intrinsic timer of myelination. *Nat Neurosci* **12**, 1398-1406 (2009).
34. Fumagalli M*, et al.* The Ubiquitin Ligase Mdm2 Controls Oligodendrocyte Maturation by Intertwining mTOR with G Protein-Coupled Receptor Kinase 2 in the Regulation of GPR17 Receptor Desensitization. *Glia* **63**, 2327-2339 (2015).
35. Russo AF. Overview of Neuropeptides: Awakening the Senses? *Headache* **57 Suppl 2**, 37-46 (2017).
36. van den Pol AN. Neuropeptide transmission in brain circuits. *Neuron* **76**, 98-115 (2012).
37. Guillaumin MCC, Burdakov D. Neuropeptides as Primary Mediators of Brain Circuit Connectivity. *Front Neurosci* **15**, 644313 (2021).
38. Lin WS, Kemper A, Dupree JL, Harding HP, Ron D, Popko B. Interferon-gamma inhibits central nervous system remyelination through a process modulated by endoplasmic reticulum stress. *Brain* **129**, 1306-1318 (2006).
39. Kiray H, Lindsay SL, Hosseinzadeh S, Barnett SC. The multifaceted role of astrocytes in regulating myelination. *Experimental Neurology* **283**, 541-549 (2016).
40. Goldshmit Y*, et al.* Rapamycin increases neuronal survival, reduces inflammation and astrocyte proliferation after spinal cord injury. *Molecular and Cellular Neuroscience* **68**, 82-91 (2015).
41. Peng J*, et al.* A Quantitative Analysis of the Distribution of CRH Neurons in Whole Mouse Brain. *Front Neuroanat* **11**, 63 (2017).
42. Bonnefil V*, et al.* Region-specific myelin differences define behavioral consequences of chronic social defeat stress in mice. *Elife* **8**, (2019).
43. Breton JM, Barraza M, Hu KY, Frias SJ, Long KLP, Kaufer D. Juvenile exposure to acute traumatic stress leads to long-lasting alterations in grey matter myelination in adult female but not male rats. *Neurobiol Stress* **14**, 100319 (2021).
44. Raabe FJ*, et al.* Oligodendrocytes as A New Therapeutic Target in Schizophrenia: From Histopathological Findings to Neuron-Oligodendrocyte Interaction. *Cells* **8**, (2019).
45. Taniguchi H*, et al.* A Resource of Cre Driver Lines for Genetic Targeting of GABAergic Neurons in Cerebral Cortex (vol 71, pg 995, 2011). *Neuron* **72**, 1091-1091 (2011).
46. Salimando GJ, Hyun M, Boyt KM, Winder DG. BNST GluN2D-Containing NMDA Receptors Influence Anxiety- and Depressive-like Behaviors and Modulate Cell-

Specific Excitatory/Inhibitory Synaptic Balance. *Journal of Neuroscience* **40**, 3949-3968 (2020).
47. Pivetta C, Esposito MS, Sigrist M, Arber S. Motor-Circuit Communication Matrix from Spinal Cord to Brainstem Neurons Revealed by Developmental Origin. *Cell* **156**, 537-548 (2014).
48. Zhu XQ, Hill RA, Dietrich D, Komitova M, Suzuki R, Nishiyama A. Age-dependent fate and lineage restriction of single NG2 cells. *Development* **138**, 745-753 (2011).
49. Tronche F*, et al.* Disruption of the glucocorticoid receptor gene in the nervous system results in reduced anxiety. *Nat Genet* **23**, 99-103 (1999).
50. Madisen L*, et al.* A robust and high-throughput Cre reporting and characterization system for the whole mouse brain. *Nature Neuroscience* **13**, 133-U311 (2010).
51. Mo A*, et al.* Epigenomic Signatures of Neuronal Diversity in the Mammalian Brain. *Neuron* **86**, 1369-1384 (2015).
52. Kuhne C*, et al.* Visualizing Corticotropin-Releasing Hormone Receptor Type 1 Expression and Neuronal Connectivities in the Mouse Using a Novel Multifunctional Allele. *J Comp Neurol* **520**, 3150-3180 (2012).
53. Lu A*, et al.* Conditional mouse mutants highlight mechanisms of corticotropin-releasing hormone effects on stress-coping behavior. *Mol Psychiatr* **13**, 1028-1042 (2008).
54. Ulivi AF*, et al.* Longitudinal Two-Photon Imaging of Dorsal Hippocampal CA1 in Live Mice. *Jove-J Vis Exp*, (2019).
55. Meschkat M*, et al.* White matter integrity in mice requires continuous myelin synthesis at the inner tongue. *Nature Communications* **13**, (2022).
56. Daetwyler S, Modes CD, Fiolka R. Fiji plugin for annotating movies with custom arrows. *Biol Open* **9**, (2020).

Supplementary files

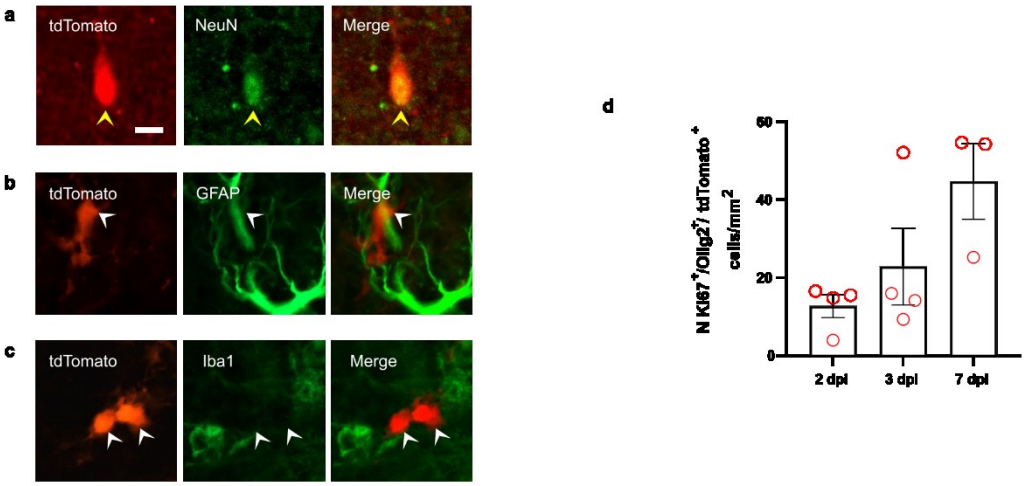

Supplementary Fig. 1: Identification of CRH-expressing cells at injury site and density of Ki67$^+$ fraction. a-c, Immuno stainings for NeuN, GFAP and Iba1 at the injury site in *CRH-Cre::Ai9* mice, showing only co-localization of tdTomato with NeuN. **d**, Quantification of Ki67$^+$/Olig2$^+$/tdTomato$^+$ cells/mm^2 at ± 300 µm around the injury site showing non-significant increase in the number of CRH-expressing Ki67$^+$ cells. N_{TP} = 3 - 4 mice. For all images, White arrowheads indicate cells or structures. Yellow arrowheads indicate co-localization of two markers.

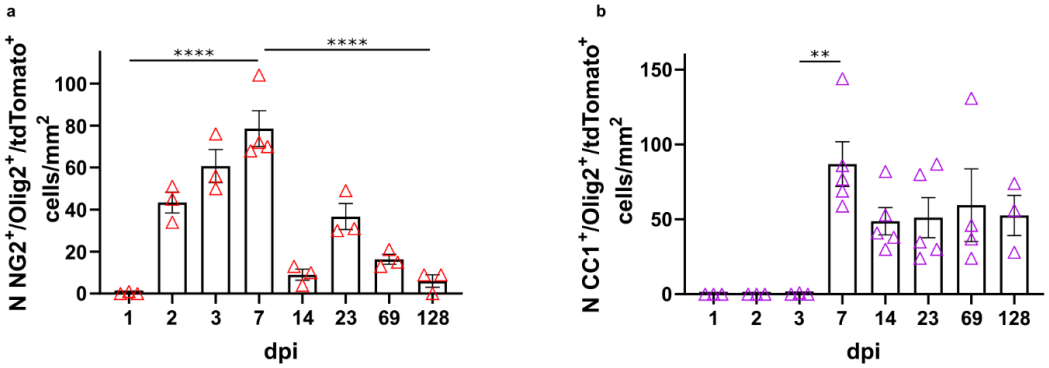

Supplementary Fig. 2: Population dynamics of NG2$^+$/Olig2$^+$/tdTomato$^+$ and CC1$^+$/Olig2$^+$/tdTomato$^+$ cells following acute injury. a, Quantification of NG2$^+$/tdTomato$^+$ cells/mm^2 at ± 300 µm around the injury site. Significant changes in cell numbers over time could be observed (One-way ANOVA: $F_{(7, 17)}$= 26.14, $p < 0.0001$) with a significant increase between 1 and 7 dpi ($p < 0.001$, 95% C.I. = -106.9, -49.48) followed by a decrease between 7 and 128 dpi ($p < 0.0001$, 95% C.I. = 43.81, 101.2). **b**, Quantification of CC1$^+$/tdTomato$^+$ cells/mm^2 at ± 300 µm around the injury site. Significant changes in cell numbers over time could be observed (One-way ANOVA: $F_{(7,23)}$= 5.186, p =0.0012 with a significant increase between 3 and 7 dpi (p = 0.0081, 95% C.I. = -158.4, -14.90) followed by a non-significant decrease. Between 14 and 128 dpi cell numbers were constant, N_{TP} = 3 - 5 mice.

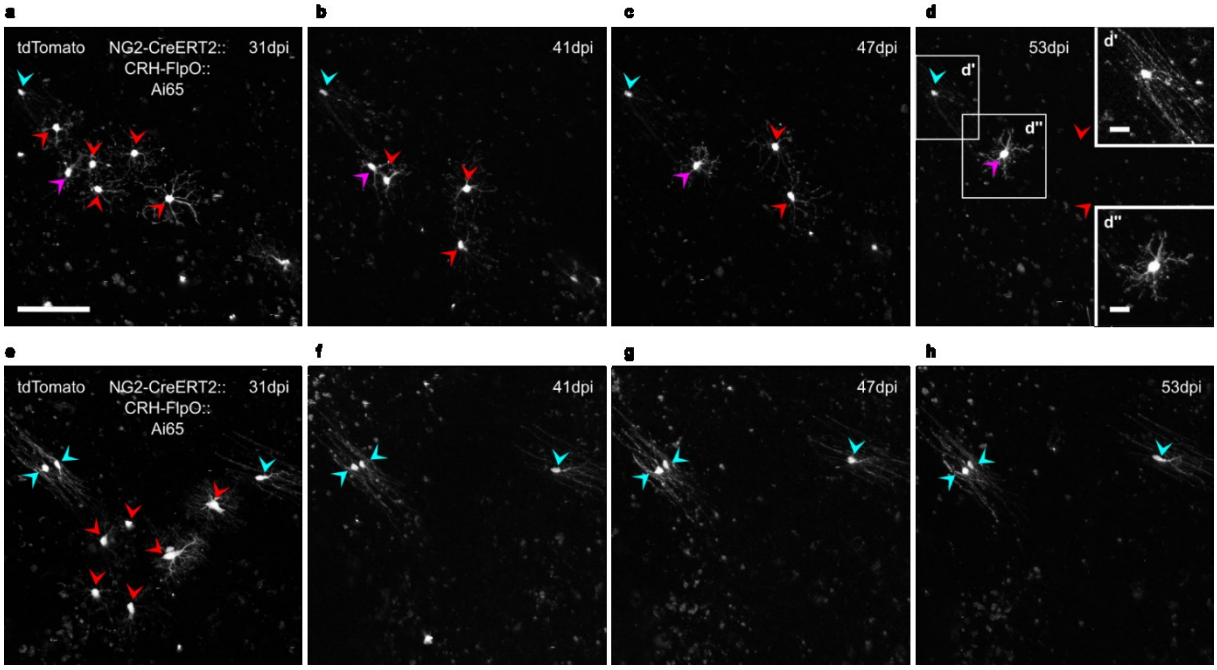

Supplementary Fig. 3: Not all CRH-expressing OLCs are stable integration. a-d, 2-photon *in vivo* images of CRH-expressing OPCs after hippocampal cannula implantation at 31 (**a, e**), 41 (**b, f**), 47 (**c, g**) and 53 dpi (**d, h**) showing disappearance of immature premyelinating OLs with highly motile processes and growth cone like structures and long-lasting stability of mature OLs. For all images: red arrowheads indicate disappearing cells. Purple arrowhead indicates persisting cells. Cyan arrowheads indicate stable, myelinating OLs (as judged by morphology). Scale bars, 100 µm (overview), 20 µm (close up **d' and d''**).

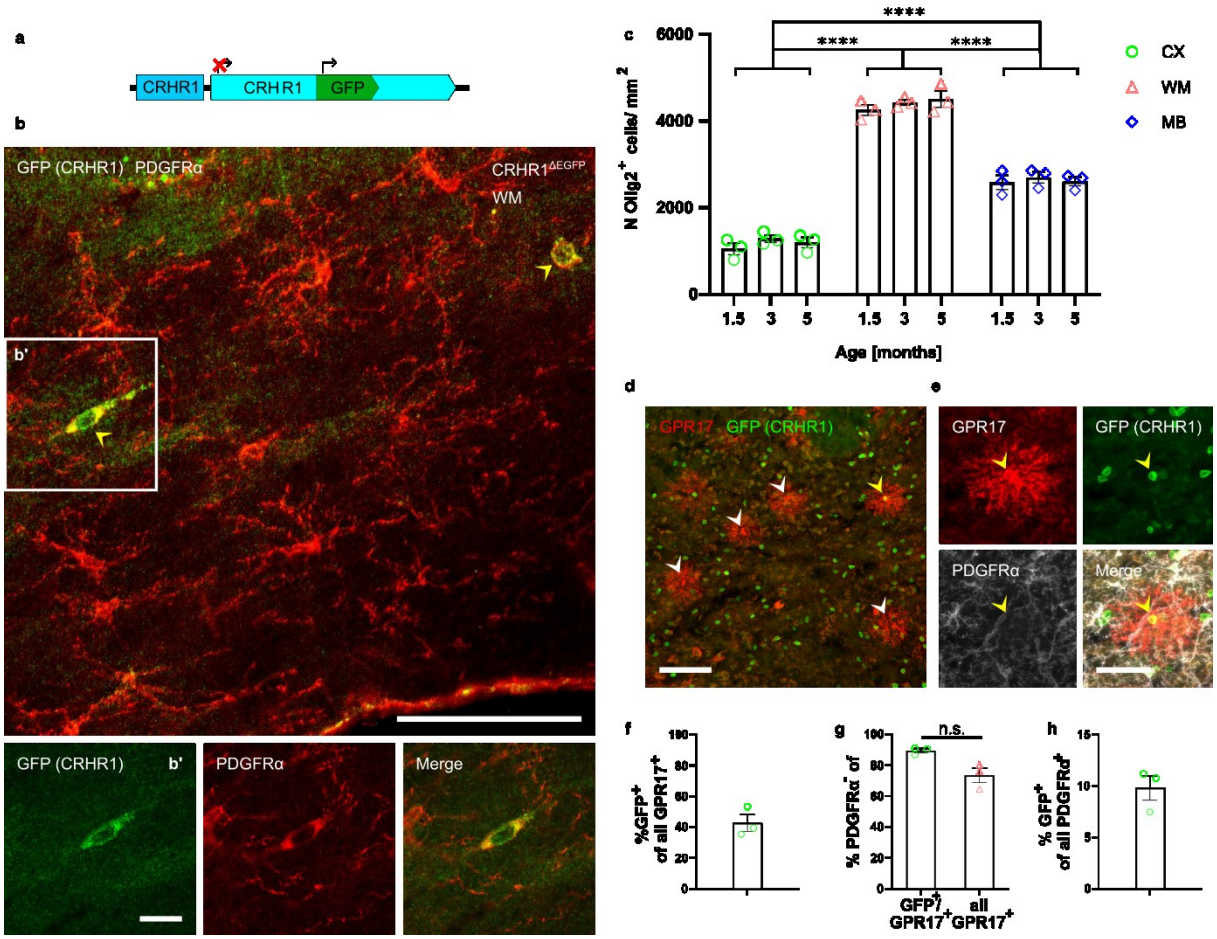

Supplementary Fig. 4: Characterization and quantification of CRHR1-expressing OLCs. a, Graphical illustration of CRHR1$^{\Delta EGFP}$ mouse model. **b,** GFP-PDGFRα staining in WM of CRHR1$^{\Delta EGFP}$ mice showing CRHR1^{+}/PDGFRα^{+} cells. Scale bar, 100 µm (overview). 20 µm (close up **b'**). **c,** Quantification of Olig2^{+} cells in CX, WM and MB at 1.5, 3 and 5 months of age shows no increase in the total number of Olig2^{+} cells. The number of Olig2^{+} cells are significantly different between regions and highest in WM followed by MB and CX (Two-way ANOVA: region, $F_{(2,18)}$= 480.2, $p < 0.0001$, $N_{TP} = 3$ mice). **d,** Maximum intensity projection of confocal image of GPR17 staining in CRHR1-Cre::Sun1-GFP mice. Scale bar, 100 µm. **e,** Confocal image of GPR17^{+}/GFP^{+}/PDGFRα^{-} cell, Scale bar, 50 µm. **f,** Quantification of percentage of GFP^{+} of all GPR17^{+} cells. **g,** Quantification of percentage of PDGFRα^{-} of GFP^{+}/GPR17^{+} and of all GPR17^{+} cells. **h,** Quantification of percentage of GFP^{+} of all PDGFRα^{+} cells. For all images, White arrowheads indicate cells or structures. Yellow arrowheads indicate co-localization of two markers.

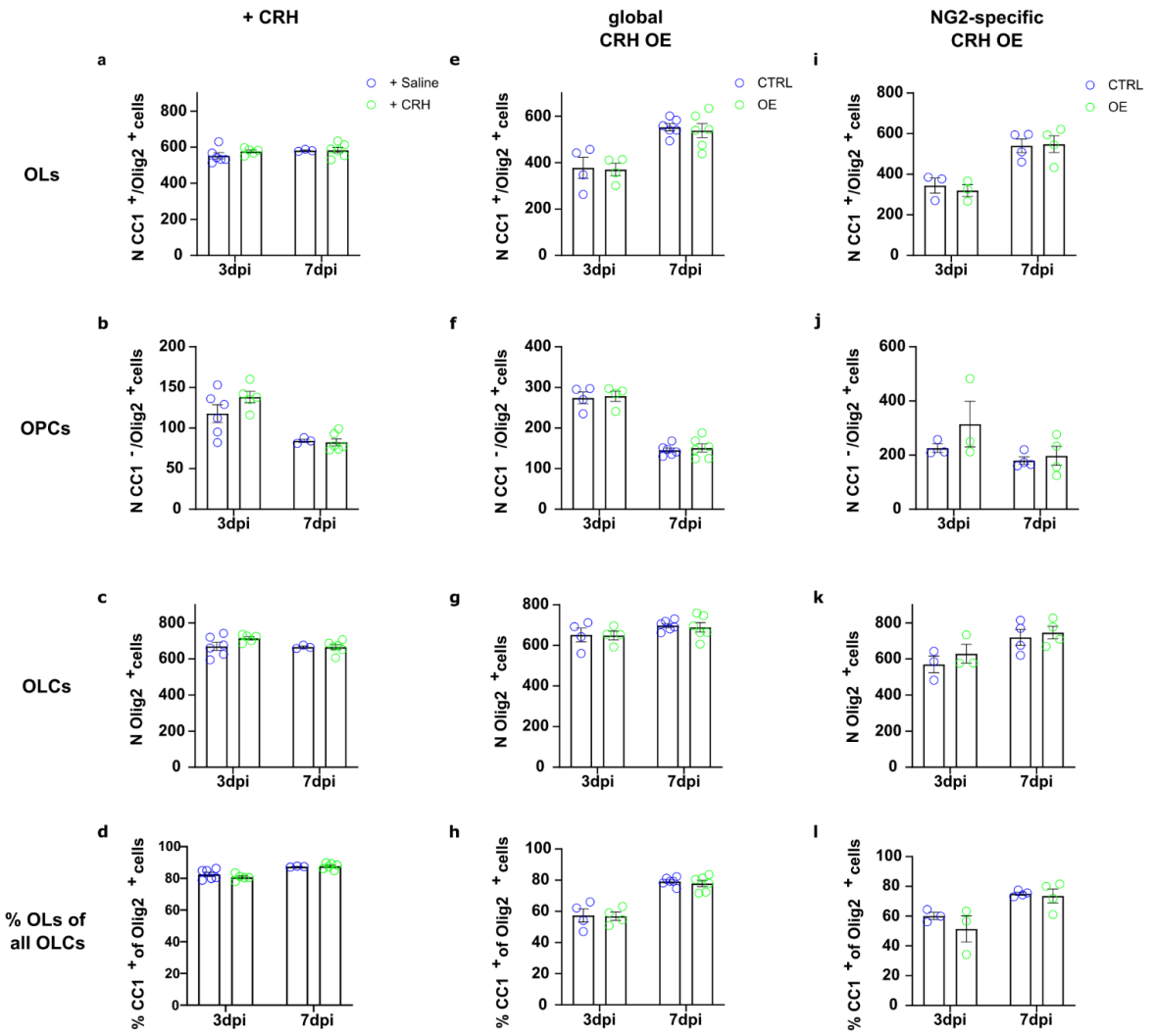

Supplementary Fig. 5: GOF approaches do not influence OLC population dynamics. a-d, Quantification of $CC1^+/Olig2^+$ (**a**), $CC1^-/Olig2^+$ (**b**), $Olig2^+$ (**c**) and percentage of $CC1^+$ of all $Olig2^+$ cells (**d**) after CRH or saline injections, (**e-h**) in brain-wide CRH OE or CTRL animals (CRH-COE^{CNS}), and, (**i-l**), in NG2-specific CRH OE or CTRL animals (CRH COE::NG2 CreERT2) show no significant differences between conditions, $N_{TP/Group}$ = 3 - 7 mice.

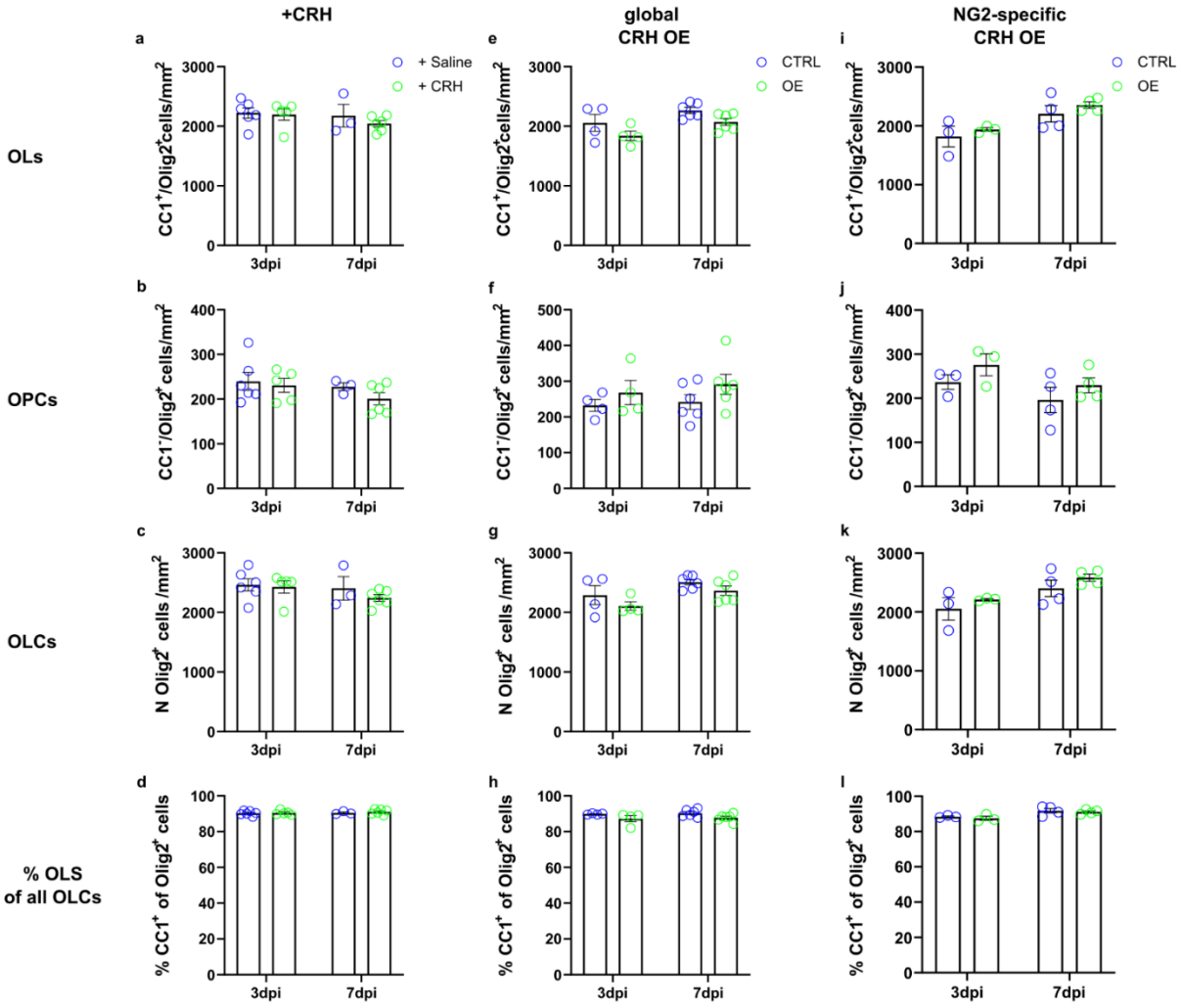

Supplementary Fig. 6: Quantification of OLC populations in non-injured region of GOF experiments. a-d, Quantification of $CC1^+/Olig2^+$ (**a**), $CC1^-/Olig2^+$ (**b**), $Olig2^+$ (**c**) and percentage of $CC1^+$ of all $Olig2^+$ cells (**d**) in non-injured region of CRH injection, brain-wide CRH OE mice *(*CRH-COE^{CNS}*)* (**e-h**), and NG2-specific CRH OE mice (**i-l**). Absolute numbers for all populations are comparable between lines, $N_{TP/Group}$ = 3 - 7 mice.

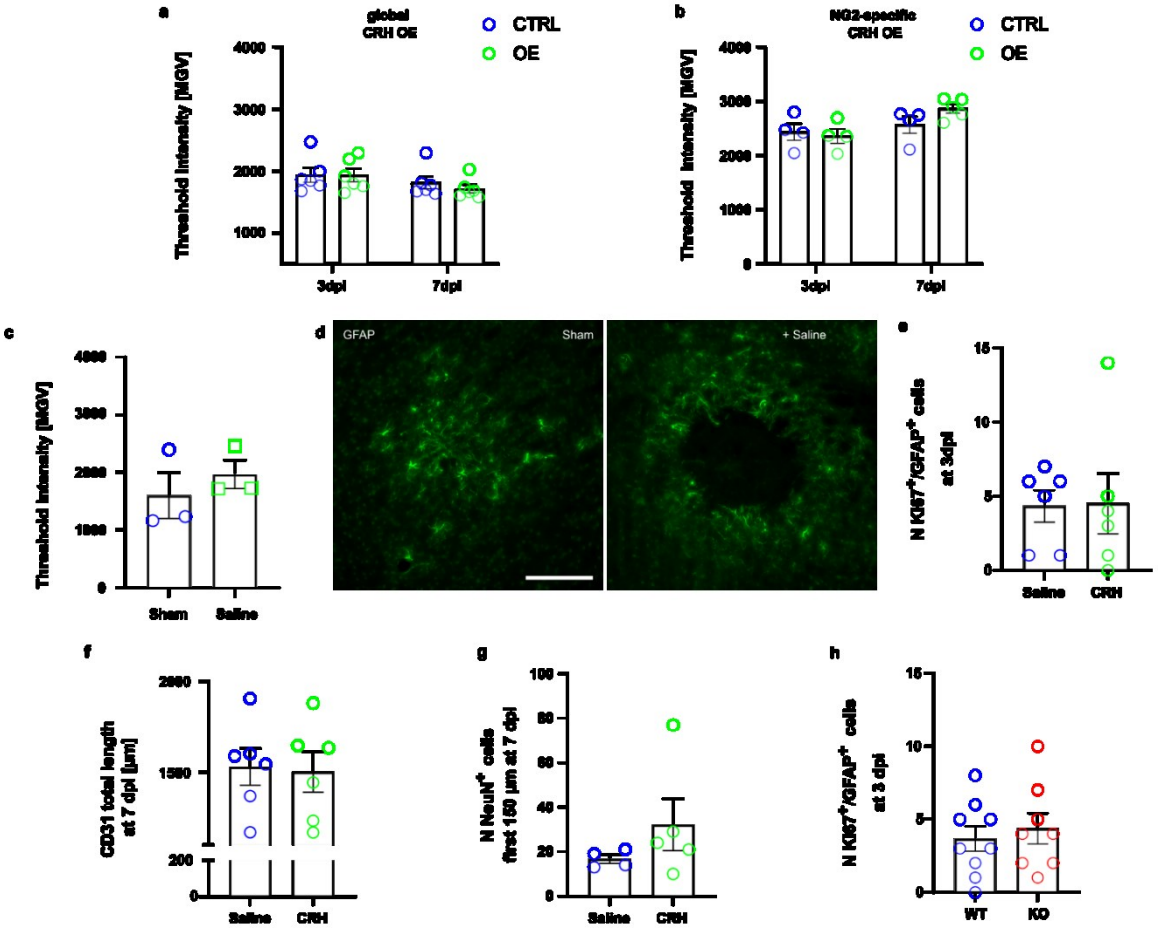

Supplementary Fig. 7: Characterization of injury site in GOF experiments. **a,** Mean gray values (MGVs) of threshold intensity measurements of GFAP staining in brain-wide CRH OE (**a**) and NG2-specific CRH OE mice (**b**), $N_{TP/Group}$ = 4 - 6 mice. **c**, Mean gray values (MGVs) of threshold intensity measurements of GFAP staining in sham or saline injected WT animals, N_{TP} = 3 mice. **d**, Representative images of GFAP staining around sham and saline injection sites. **e,** Quantification of $Ki67^+/GFAP^+$ cells at 3 dpi in *CRHR1-Cre::Tau-LSL-FlpO::Ai9* mice at 3 dpi after saline or CRH injection, N = 6 mice/condition. **f**, Quantification of length of $CD31^+$ vasculature around injury site of saline vs CRH injected *CRHR1-Cre::Tau-LSL-FlpO::Ai9* animals at 7 dpi, N = 6 mice/condition. **g**, Quantification of $NeuN^+$ cells in the first 150 µm around injury site at 7 dpi in saline vs CRH injected animals, N = 4-5 mice/condition. **h**, Quantification of $Ki67^+/GFAP^+$ cells at 3 dpi in CRHR1 WT or KO mice at 3 dpi after CRH injection, N = 8-9 mice/condition.

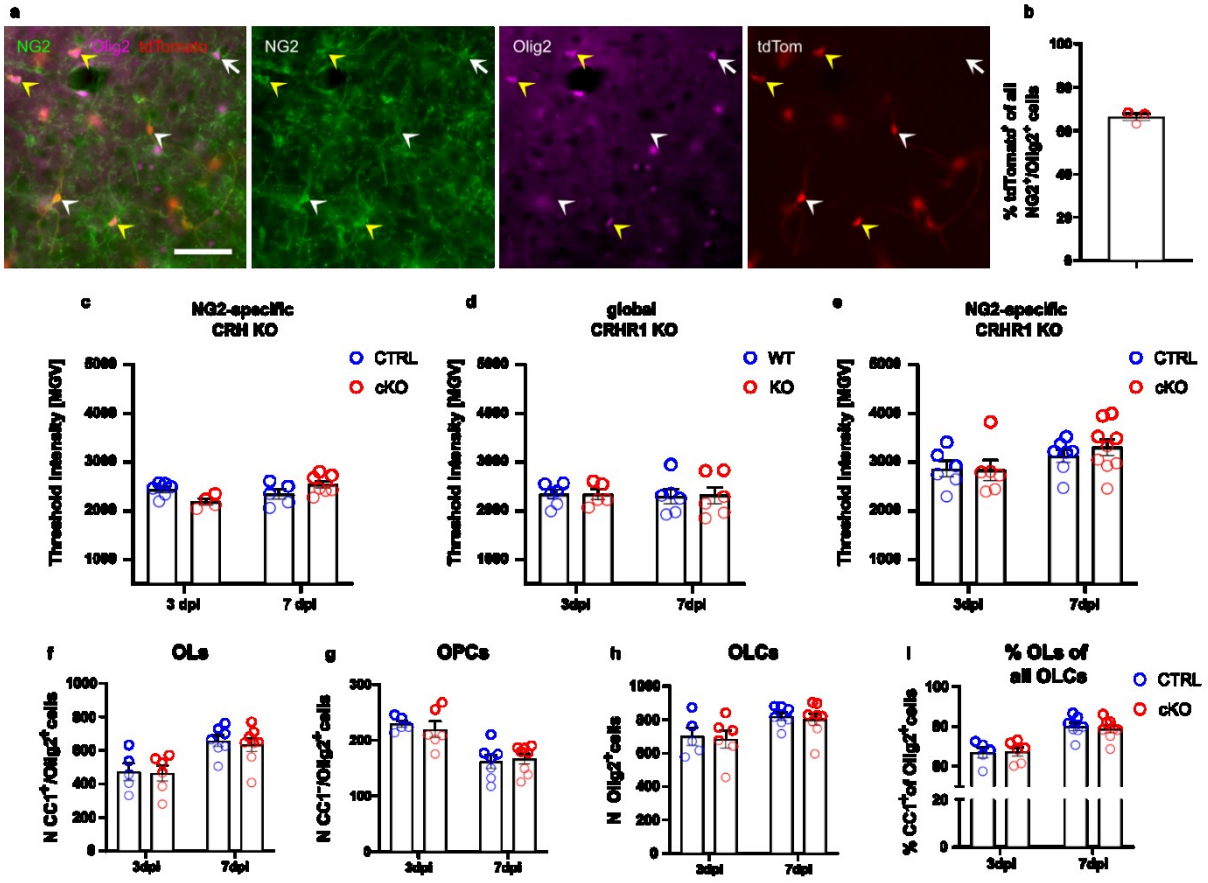

Supplementary Fig. 8: Validation of NG2-specific CRH KO, OLC quantification and GFAP intensity measurements in LOF experiments. a, Representative image of tdTomato expression in $NG2^+/Olig2^+$ cells following TAM induction in NG2-specific CRH KO ($CRH^{NG2\text{-}cKO}$) animals showing effective Cre induction and consequent CRH KO. Scale bar, 50 µm. Arrowheads indicate recombined OPCs ($tdTomato^+/NG2^+/Olig2^+$) (yellow) and recombined pericytes ($tdTomato^+/NG2^+/Olig2^-$) (white), arrows indicate not-recombined OPCs ($tdTomato^-/NG2^+/Olig2^+$). **b,** Quantification $tdTomato^+$ cells of all $NG2^+/Olig2^+$ cells showing a recombination efficiency of 66.3 ± 1.6 %. **c-e**, Mean gray values (MGVs) of threshold intensity measurements of GFAP staining in NG2-specific CRH KO, global CRHR1 KO (**b**) and NG2-specific CRHR1 KO (**c**), $N_{TP/Group}$ = 4 - 9 mice. **f-i**, No significant differences between conditions in NG2-specific CRHR1-cKO vs WT animals in number of $CC1^+/Olig2^+$ cells (Two-way ANOVA: time, $F_{(1,22)}$= 17.77, p = 0.0004, $N_{CTRL\ 3dpi}$ = 5, $N_{cKO\ 3dpi}$ = 6, $N_{CTRL\ 7dpi}$ = 7, $N_{KO\ 7dpi}$ = 8). $CC1^-/Olig2^+$ cells (Two-way ANOVA: time, $F_{(1,22)}$= 29.79, p < 0.0001), $Olig2^+$ cells (Two-way ANOVA: time, $F_{(1,22)}$= 8.402, p = 0.0083) and percentage of $CC1^+$ of all $Olig2^+$ cells (Two-way ANOVA: time, $F_{(1,22)}$= 32.99, p < 0.0001).

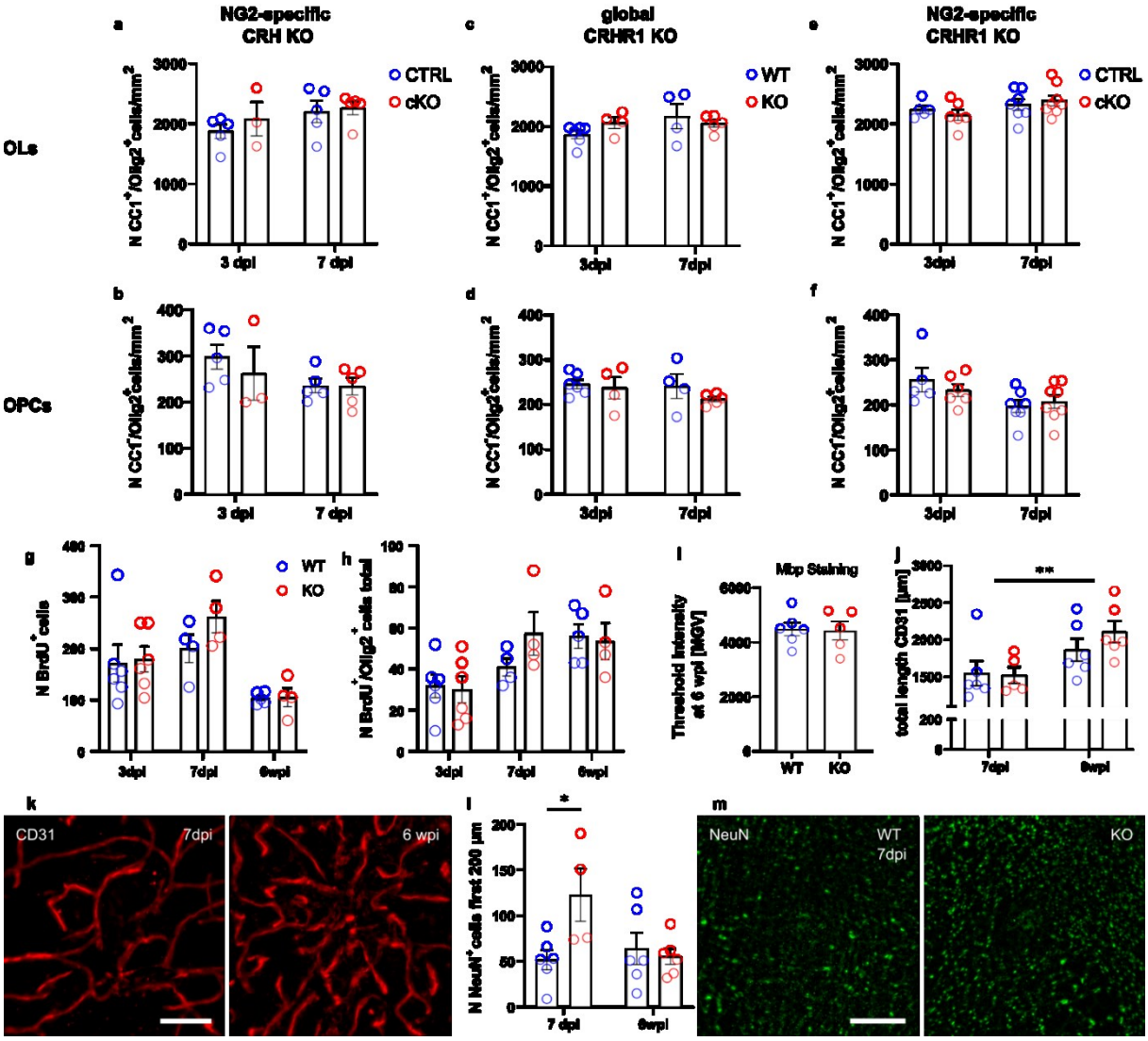

Supplementary Fig. 9: Quantification of OLC population in non-injured regions and characterization of injury in LOF experiments. a-d, Quantification of $CC1^+/Olig2^+$ (**a**), $CC1^-/Olig2^+$ (**b**) and in non-injured region of NG2-specific CRH KO, global CRHR1 KO (**c-d)** and NG2-specific CRHR1 KO (**e-f**). Numbers for all populations are comparable between lines, $N_{TP/Group}$ = 3 - 8 mice. **g-h**, Quantification of $BrdU^+$ and $BrdU^+/Olig2^+$ cells in a 300 µm radius around injury site at 3 dpi, 7 dpi and 6 wpi in WT and KO animals showing no significant differences between conditions. **i**, Mean grey value (MGV) of threshold analysis of MBP staining at injury site at 6 wpi, N = 5-6. **j**, Quantification of total length of $CD31^+$ vasculature around injury site at 7 dpi and 6 wpi showing significant increase over time without genotype effect (Two-way ANOVA: time, $F_{(1,19)}$= 9.346, p = 0.0065; genotype, $F_{(1,19)}$= 0.5439, p = 0.4699, $N_{WT\ 7dpi}$ = 6, $N_{KO\ 7dpi}$ = 5, $N_{WT\ 6wpi}$ = 6, $N_{KO\ 6wpi}$ = 6). **k**, Representative Confocal image of CD31 staining around injury site at 7 dpi and 6 wpi. Scale bar, 50 µm. **l**, Quantification of $NeuN^+$ cells within the first 150 µm around the injury site at 7 dpi and 6 wpi showing significant increase in CRHR1 KO animals at 7 dpi (Two-way ANOVA: time, $F_{(1,18)}$= 2.920, p = 0.1047; genotype, $F_{(1,18)}$= 3.795, p = 0.0672, $N_{WT\ 7dpi}$ = 6, $N_{KO\ 7dpi}$ = 4, $N_{WT\ 6wpi}$ = 6, $N_{KO\ 6wpi}$ = 6). **m**, Representative images of NeuN staining in WT and CRHR1 KO animals at 7 dpi. Scale bar, 200 µm. For all Two-way ANOVAs: Sidak's post hoc test, *p < 0.05, ****p < 0.0001.

Supplementary Table 1: Details of used mouse lines

Mouse line	Individual Mouse Lines	MGI Allele	MGI Identifier	Description/ Reporting
CRH-Cre::Ai9	*CRH-Cre* *Ai9*	*Crh$^{tm1(cre)Zjh}$* *Gt(ROSA)26Sor$^{tm9(CAG-tdTomato)Hze}$*	MGI:4452089 MGI:3809523	tdTomato expression in CRH-expressing cells
NG2-CreERT2::Ai9	*NG2-CreERT2* *Ai9*	*Tg(Cspg4-cre/Esr1*)BAkik* *Gt(ROSA)26Sor$^{tm9(CAG-tdTomato)Hze}$*	MGI:4819178 MGI:3809523	tdTomato expression in NG2-expressing cells after induction by tamoxifen
CRH-Venus	*CRH-Venus*	*Crh$^{tm1.1Ksak}$*	MGI:6144041	Venus knock-in into *Crh* locus
CRH-FlpO::NG2-CreERT2::Ai65	*CRH-FlpO* *NG2-CreERT2* *Ai65*	*Crh$^{tm1.1(flpo)Bsab}$* *Tg(Cspg4-cre/Esr1*)BAkik* *Gt(ROSA)26Sor$^{tm65.1(CAG-tdTomato)Hze}$*	MGI:6116854 MGI:4819178 MGI:5478743	tdTomato expression in CRH and NG2 co-expressing cells after induction by tamoxifen
CRH-FlpO::CRHR1-Cre::Ai65	*CRH-FlpO* *CRHR1-Cre* Ai65	*Crh$^{tm1.1(flpo)Bsab}$* *Crhr1$^{tm4.1(cre)Jde}$* *Gt(ROSA)26Sor$^{tm65.1(CAG-tdTomato)Hze}$*	MGI:6116854 MGI:6201420 MGI:5478743	tdTomato expression in CRH and CRHR1 co-expressing cells
CRH$^{NG2\text{-}cKO}$ (*CRH^{loxP}:: NG2-CreERT2::Ai9*)	*CRH^{loxP}* *NG2-CreERT2* *Ai9*	*Crh$^{tm1.1Jde}$* *Tg(Cspg4-cre/Esr1*)BAkik* *Gt(ROSA)26Sor$^{tm9(CAG-tdTomato)Hze}$*	MGI:6201415 MGI:4819178 MGI:3809523	CRH knockout and tdTomato expression in NG2-expressing cells after induction by tamoxifen; tdTomato allowed quantification of recombination efficiency
CRHR1$^{NG2\text{-}cKO}$ (*CRHR1^{loxP}::NG2-CreERT2*)	*CRHR1^{loxP}* *NG2-CreERT2*	*Crhr1$^{tm2.2Jde}$* *Tg(Cspg4-cre/Esr1*)BAkik*	MGI:5440013 MGI:4819178	CRHR1 knockout in NG2-expressing cells after induction by tamoxifen
CRH-COE^{NG2} (*CRH-COE::NG2-CreERT2*)	*CRH-COE* *NG2-CreERT2*	*Gt(ROSA)26Sor$^{tm1(Crh)Jde}$* *Tg(Cspg4-cre/Esr1*)BAkik*	MGI:3815322 MGI:4819178	CRH overexpression in NG2-expressing cells after induction by tamoxifen
CRH-COE^{CNS} (*CRH-COE::Nestin-Cre*)	*CRH-COE* *Nestin-Cre*	*Gt(ROSA)26Sor$^{tm1(Crh)Jde}$* *Tg(Nes-cre)1Kln*	MGI:3815322 MGI:2176173	CRH overexpression in the entire central nervous system
CRHR1$^{\Delta EGFP}$	*CRHR1$^{\Delta EGFP}$*	*Crhr1^{tm1Jde}*	MGI:5294436	EGFP knock-in into *Crhr1* locus Global/constitutive CRHR1 knockout

CRHR1-Cre::Tau-LSL-FlpO::Ai9	*CRHR1-Cre* *Tau-LSL-FlpO* *Ai9*	*Crhr1*$^{tm4.1(cre)Jde}$ *pending* *Gt(ROSA)26Sor*$^{tm9(CAG-tdTomato)Hze}$	MGI:6201420 pending MGI:3809523	tdTomato expression in CRHR1-expressing cells; deletion of tdTomato expression in cells with high MAPT expression, enrichment of tdTomato expression in glial CRHR1-expressing cells
CRHR1-Cre::Sun1-GFP	*CRHR1-Cre* *Sun1-GFP*	*Crhr1*$^{tm4.1(cre)Jde}$ *Gt(ROSA)26Sor*$^{tm5(CAG-Sun1/sfGFP)Nat}$	MGI:6201420 MGI:5443817	GFP expression in nuclear membrane of CRHR1-expressing cells
CRH-FlpO::Ai65F::CRHR1-Cre::Sun1-GFP	*CRH-FlpO* *Ai65F* *CRHR1-Cre* *Sun1-GFP*	*Crh*$^{tm1.1(flpo)Bsab}$ *Gt(ROSA)26Sor*$^{tm65.2(CAG-tdTomato)Hze/J}$ *Crhr1*$^{tm4.1(cre)Jde}$ *Gt(ROSA)26Sor*$^{tm5(CAG-Sun1/sfGFP)Nat}$	MGI:6116854 MGI:6260212 MGI:6201420 MGI:5443817	tdTomato expression in CRH-expressing cells and GFP expression in in nuclear membrane of CRHR1-expressing cells

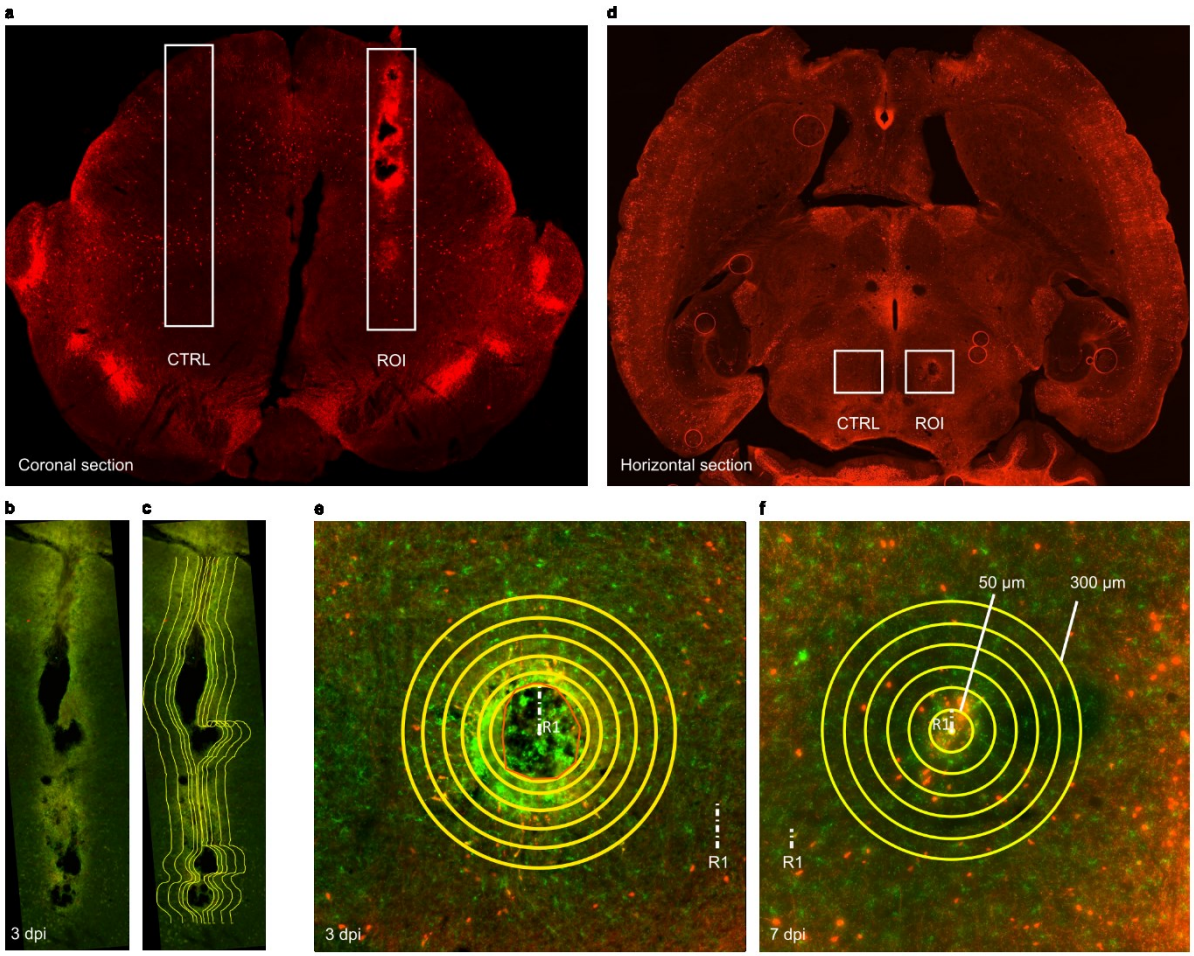

Supplementary Method 1: Quantification matrices used for wound analysis. a, Coronal overview of acute injury in MB of *CRH-Cre::Ai9* mice. White squares: CTRL region and ROI around injury site. **b**, ROI around injury site. **c**, counting matrix generated automatically around center of wound. Subareas from 50 to 300 µm around injury site. **d**, Horizontal overview of acute injury in MB of *CRH-Cre::Ai9* mice. White squares: CTRL region and ROI around injury site. **e, f**, Quantification matrix at 3 dpi (**e**) and 7 dpi (**f**). Matrix consist of 6 circles with radii from 50 to 300 µm.

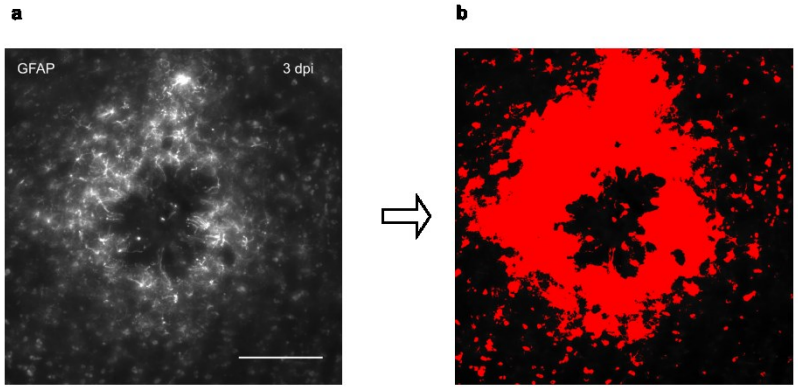

Supplementary Method 2: Workflow of threshold intensity measurement. a, Maximum intensity z-projection of GFAP staining around injury site. Scale bar, 200 µm. **b**, Thresholded image. Red = area with intensity above threshold (e.g. 1500 mean gray value (MGV)). Staining intensity was only measured in area above threshold.

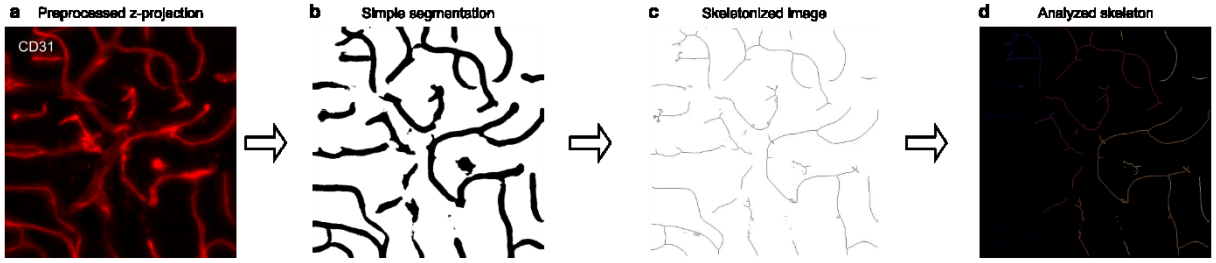

Supplementary Method 3: Workflow of CD31$^+$ vasculature quantification. a, Preprocessed image for analysis. **b,** Segmented image after processing by Ilastik**. c,** Skeletonized image processed with "Skeletonize (2D/3D)" function of Fiji. **d**, Analyzed skeleton application of Fiji built-in function "Analyze-Skeleton (2D/3D)".

2.2 Differential CRH expression level determines efficiency of Cre- and Flp-dependent recombination

Front. Neurosci., 03 August 2023
DOI: 10.3389/fnins.2023.1163462

Chen Zhao[1†], Clemens Ries[1†], Ying Du[1†], Jingwei Zhang[1], Kenji Sakimura[2], Keiichi Itoi[3], Jan M. Deussing[1*]

[†]Contributed equally

[1] Molecular Neurogenetics, Max Planck Institute of Psychiatry, Munich, Germany
[2] Department of Animal Model Development, Brain Research Institute, Niigata University, Niigata, Japan
[3] Super-Network Brain Physiology, Graduate School of Life Sciences, Tohoku University, Sendai, Japan
[†] These authors contributed equally to this work.

*** Correspondence:**
Jan M. Deussing
deussing@psych.mpg.de

Keywords: Corticotropin-releasing hormone, CRH, CRF, Cre, Flp, reporter

Author Contributions

CZ, CR, and YD designed and performed all experiments, analyzed and interpreted data, drafted figures, and wrote the manuscript. JZ performed a subset of experiments and reviewed the manuscript. KS and KI provided materials, edited the manuscript and contributed scientific advice. JD designed the project, supervised all experiments and analyses, edited the manuscript, and provided scientific advice, guidance and support. All authors contributed to the article and approved the submitted version.

My contribution to this publication in detail:

For this publication, I sacrificed, cut and mounted *CRH-FlpO::CRH-Cre::Ai65* animals. I imaged the analyzed regions in all mouse lines and drafted all figures, but Fig. 6. Additionally, I was critically involved in the interpretation of data. Besides, I drafted the discussion and subedited the manuscript.

Abstract

Corticotropin-releasing hormone-expressing (CRH^+) neurons are distributed throughout the brain and play a crucial role in shaping the stress responses. Mouse models expressing site-specific recombinases (SSRs) or reporter genes are important tools providing genetic access to defined cell types and have been widely used to address CRH^+ neurons and connected brain circuits. Here, we investigated a recently generated *CRH-FlpO* driver line expanding the CRH system-related tool box. We directly compared it to a previously established and widely used *CRH-Cre* line with respect to the *FlpO* expression pattern and recombination efficiency. In the brain, *FlpO* mRNA distribution fully recapitulates the expression pattern of endogenous *Crh*. Combining both *Crh* locus driven SSRs driver lines with appropriate reporters revealed an overall coherence of respective spatial patterns of reporter gene activation validating *CRH-FlpO* mice as a valuable tool complementing existing *CRH-Cre* and reporter lines. However, a substantially lower number of reporter-expressing neurons was discerned in *CRH-FlpO* mice. Using an additional CRH reporter mouse line (*CRH-Venus*) and a mouse line allowing for conversion of Cre into FlpO activity (*CAG-LSL-FlpO*) in combination with intersectional and subtractive mouse genetic approaches, we were able to demonstrate that the reduced number of tdTomato reporter-expressing CRH^+ neurons can be ascribed to the lower recombination efficiency of FlpO compared to Cre recombinase. This discrepancy particularly manifests under conditions of low CRH expression and can be overcome by utilizing homozygous *CRH-FlpO* mice. These findings have direct experimental implications which have to be carefully considered when targeting CRH^+ neurons using *CRH-FlpO* mice. However, the lower FlpO-dependent recombination efficiency also entails advantages as it provides a broader dynamic range of expression allowing for the visualization of cells showing stress-induced CRH expression which is not detectable in highly sensitive *CRH-Cre* mice as Cre-mediated recombination has largely been completed in all cells generally possessing the capacity to express CRH. These findings underscore the importance of a comprehensive evaluation of novel SSR driver lines prior to their application.

1 Introduction

Genetically engineered mouse models (GEMMs) are potent tools used in neuroscience research and crucial for understanding mechanisms underlying neurological and psychiatric disorders. *Cre-loxP* and *Flp-FRT* are site-specific recombinase (SSR) systems widely used in GEMMs. The combination of *Cre-/Flp*-expressing mouse strains with recombinase-dependent reporters or effectors has proven as a versatile and efficient approach offering a myriad of options ranging from manipulation of gene expression and cell activity to visualization of molecules, cells and circuits (Deussing, 2013; Luo et al., 2018; Arias et al., 2022).

Corticotropin-releasing hormone (CRH; also known as corticotropin-releasing factor, CRF) is a neuropeptide playing a critical role in different aspects of the body´s stress response. CRH in the paraventricular nucleus of the hypothalamus (PVN) controls the neuroendocrine response by activating the hypothalamic-pituitary-adrenal (HPA) axis and regulating adrenocorticotropic hormone (ACTH) secretion from the pituitary which, in turn, triggers the synthesis and release of glucocorticoids from the adrenal glands as ultimate effectors of the stress response (Ulrich-Lai and Herman, 2009). Parvocellular CRH neurons in the PVN are localized at the apex of the HPA axis and represent a specialized subpopulation of excitatory CRH neurons co-expressing the vesicular glutamate transporter 2 (VGLUT2) (Dabrowska et al., 2013; Romanov et al., 2017; Dedic et al., 2018b).

Beyond the PVN, CRH is widely expressed throughout the brain (Peng et al., 2017). Here, in contrast to the PVN, CRH is predominantly found in inhibitory neurons expressing GABAergic markers, such as glutamic acid decarboxylase (also known as glutamate decarboxylase) 65 and 67 (GAD65/GAD67) (Romanov et al., 2017; Dedic et al., 2018b; Dedic et al., 2019). Inhibitory CRH neurons show a high degree of morphological and physiological diversity (Wang et al., 2021). For instance, in the cortex, CRH neurons co-express markers of different subpopulations of GABAergic neurons, such as vasoactive intestinal peptide (VIP), calretinin (CR), cholecystokinin (CCK) and somatostatin (SOM), but not parvalbumin (PV) or neuropeptide Y (NPY) (Kubota et al., 2011). In the hippocampus, CRH neurons were found to be positive for PV, CR and CCK but not for calbindin (CB) or SOM (Gunn et al., 2019). In subregions of the extended amygdala encompassing the central amygdala (CeA), the lateral part of the interstitial nucleus of the posterior limb of the anterior commissure (IPACL) and the bed nucleus of the stria terminalis (BNST), CRH neurons again express a diverse and region-specific set of GABAergic markers including protein kinase C δ (PKCδ), SOM, neurokinin B (NKB), neurotensin (NTS) or CB (Sanford et al., 2017; Dedic et al., 2018b; Chang et al., 2022; Soden et al., 2022). Cortical and hippocampal CRH neurons possess typical features of interneurons. The extended amygdala, however, harbors a large fraction of CRH neurons representing GABAergic long-range projection neurons which co-express calcium/calmodulin-dependent protein kinase 2α (CAMK2A) and innervate midbrain structures, such as the ventral tegmental area and the substantia nigra (Dedic et al., 2018b; Chang et al., 2022; Soden et al., 2022). The heterogeneity of neuronal CRH populations suggests a unique role of these neurons in the regulation of responses to salient stimuli in different brain regions.

Accordingly, the CRH system has been shown to bidirectionally modulate anxiety- and stress-related behaviors in dependence of its localization and prior stress experience (Refojo et al., 2011; Lemos et al., 2012; Dedic et al., 2018b).

As a neuropeptide, CRH is sorted into large dense core vesicles and immediately transported to be stored at its release sites, making reliable detection of CRH^+ soma somewhat difficult. Moreover, it is of note that even with the most efficient antiserum raised against CRH more than 4 decades ago in the Vale lab (Bloom et al., 1982), the accessibility of CRH by immunohistochemistry is largely unsatisfying (Itoi et al., 2014). Hence, extensive efforts have been undertaken in the past years to gain genetic access to CRH^+ cells by developing respective reporter and SSR mouse lines (Table 1). Different strategies have been applied, ranging from classic transgenic approaches using small promoter fragments to large bacterial artificial chromosome (BAC)-based constructs and knock-in approaches. The first transgenic β-galactosidase reporter mice, carrying the *lacZ* construct flanked by 8.7 kb of *Crh* promoter region, already revealed difficulties in fully recapitulating the endogenous CRH expression pattern (Keegan et al., 1994). This has been further corroborated by some of the subsequently generated transgenic reporter or Cre driver lines revealing limitations in their use because of ectopic expression and/or failure of expression (Alon et al., 2009; Martin et al., 2010; Sarkar et al., 2011; Chen et al., 2015; Korecki et al., 2019). These observations underscore the utter importance to extensively characterize SSR mouse models to validate spatial and temporal expression patterns as a prerequisite for a meaningful interpretation of studies using these GEMMs (Heffner et al., 2012; Luo et al., 2020). In this regard, knock-in strategies, also in the case of CRH, have proven their superiority as reflected by reliable and reproducible reporter and Cre expression (Taniguchi et al., 2011; Itoi et al., 2014; Krashes et al., 2014; Kono et al., 2017). Accordingly, *CRH-Cre* knock-in mice have been widely applied to explore the physiology of CRH neurons in the central nervous system (Krashes et al., 2014; Marcinkiewcz et al., 2016; Fadok et al., 2017; Sanford et al., 2017; Dedic et al., 2018b; Wang et al., 2021; Chang et al., 2022).

The *Flp-FRT* system was initially introduced to remove selection markers from *Cre-loxP*-dependent conditional alleles (Rodríguez et al., 2000) but with the concerted improvement of its recombination efficiency (Buchholz et al., 1998; Raymond and Soriano, 2007) the *Flp-FRT* system has developed into a powerful alternative SSR which, in combination with the *Cre-loxP* system, allows for parallel, intersectional or subtractive approaches. Only recently, a first *CRH-FlpO* mouse line was established, thus expanding the CRH system-related tool box (Salimando et al., 2020) and providing alternative access to CRH neurons, which is highly demanded considering their enormous diversity. However, a systematic characterization of this novel mouse line has not been reported so far which to some extent limits its immediate use. In particular, considering repeated accounts on the diversity of reporter expression conveyed by previously established *CRH-Cre* lines demands a comprehensive assessment of the recombination pattern in this novel *CRH-FlpO* mouse line (Chen et al., 2015; Dedic et al., 2018a). Here, we characterized *CRH-FlpO* mice and directly compared their recombination properties

throughout the brain with a well-established *CRH-Cre* mouse line as a reference (Taniguchi et al., 2011) using 9 different reporter mouse models. We focused our evaluation of SSR-activated reporter gene expression patterns on brain regions well-known to possess CRH^{+} neurons involved in the neuroendocrine and behavioral stress response. Our analysis revealed similarities but also discrepancies between *CRH-FlpO* and *CRH-Cre* mice that have direct implications for the use of SSRs driven by the *Crh* locus.

2 Materials and Methods

2.1 Animals

All animal experiments were conducted with the approval of and in accordance with the Guide of the Care and Use of Laboratory Animals of the Government of Upper Bavaria, Germany. Mice were group housed under standard lab conditions (22 ± 1°C, 55 ± 5% humidity) and maintained under a 12 h light-dark cycle with food and water ad libitum. All experiments were conducted with adult male or female mice (age: 2-5 months). For each mouse line 3 - 7 animals were analyzed of which representative images are included in the figures.

The following transgenic mouse lines were used in this study: *CRH-Cre* (*Crh*$^{tm1(cre)Zjh}$, Jackson Laboratory stock no. 012704) (Taniguchi et al., 2011), *CRH-FlpO* (*Crh*$^{tm1.1(flpo)Bsab}$, Jackson Laboratory stock no. 031559; **Supplementary Data,** provided by Bernado Sabatini and Caiying Guo) (Salimando et al., 2020), *CRH-Venus* (*Crh*$^{tm1.1Ksak}$, RIKEN BRC stock no. BRC09893) (Kono et al., 2017), *Ai9* (*Gt(ROSA)26Sor*$^{tm9(CAG-tdTomato)Hze}$, Jackson Laboratory stock no. 007909) (Madisen et al., 2010), *Ai65* (*Gt(ROSA)26Sor*$^{tm65.1(CAG-tdTomato)Hze}$, Jackson Laboratory stock no. 021875) (Madisen et al., 2015) and *CAG-LSL-FlpO* (*Gt(ROSA)26Sor*$^{tm5(CAG-flpo)Zjh}$, Jackson Laboratory stock no. 028584) (He et al., 2016). A pure Flp reporter line was generated by breeding the intersectional *Ai65* reporter to a *Deleter-Cre* line removing the *loxP*-flanked transcriptional terminator. This novel mouse line, reporting only Flp recombinase activity, was designated as *Ai65F*. In this study, the following double and triple transgenic lines were generated by cross-breeding of single transgenic lines: *CRH-Cre::Ai9*, *CRH-FlpO::Ai65F*, *CRH-Venus::CRH-Cre::Ai9*, *CRH-Venus::CRH-FlpO::Ai65F, CRH-Cre::CRH-FlpO::Ai65*, CRH-Cre::CRH-FlpO::Ai9, *CRH-Cre::CAG-LSL-FlpO::Ai65* and *CRH-Cre::CAG-LSL-FlpO::Ai9*. All transgenic alleles involving the *Rosa26* locus were heterozygous. Detailed breeding schemes, primer sequences and protocols for genotyping are available upon request.

2.2 Preparation of brain sections

Vibratome sections: Mice were sacrificed by an overdose of isoflurane and transcardially perfused with 20 ml 0.1 M PBS (4 °C) supplemented with heparin and subsequently with 20 ml of 4% paraformaldehyde (PFA) in 0.1 M PBS (4 °C). After recovery, brains were post-fixed overnight in 4% PFA at 4 °C and coronal 50 µm sections were prepared using a vibratome (Microm HM 650 V, Thermo-Fisher Scientific). *Cryosections*: Perfused and dissected brains were post-fixed in 4% PFA for 6 h. After 48 h in 30% sucrose in 0.1 M PBS at 4 °C, brains were snap frozen on dry ice and 40 µm sections were prepared using a cryostat (Microm, Walldorf, Germany). All sections were stored at -20 °C in cryopreservation solution (25% glycerol, 25% ethylene glycol, 50% 0.1M PBS, pH 7.4) until further use.

2.3 Immunohistochemistry

Vibratome sections were blocked with 10% normal goat serum (NGS) and 0.15% Triton in PBS for 30 min at RT and then washed in 0.1 M PBS for 3 × 5 min. Subsequently, sections were incubated with anti-GFP primary antibody (chicken polyclonal antibody; 1:500; abcam) diluted in 0.15% NGS and 0.15% Triton in PBS overnight at 4 °C. After another washing step, sections were incubated with an Alexa Fluor 488 secondary antibody (goat anti-chicken IgG; 1:250; Invitrogen) while shaking for 2 h at RT. Following 3 more washing steps, sections were mounted on glass slides (epredia) with Fluoromount-G (SouthernBiotech).

2.4 *In situ* hybridization (ISH)

Freshly dissected brains were snap frozen on dry ice and stored at -80 °C until further use. Brains were sectioned coronally at 20 µm using a cryostat. Sections were mounted onto SuperFrost slides and kept at -80 °C until further use. ISH was performed as previously described (Dedic et al., 2018b). The following FlpO-specific riboprobe was used: bp 311-641 of MH493814.

2.5 Acute restraint stress

To test the capacity of the *CRH-FlpO* mouse line to induce reporter gene expression in CRH^+ cells following stress exposure, *CRH-FlpO::Ai65F* mice were exposed to acute restraint stress. On the day of the experiment, animals were placed for 15 min in a 50-ml conical tube with the bottom removed. Animals were sacrificed one week later and brains were used for the assessment stress-induced expression of tdTomato.

2.6 Image acquisition

Vibratome sections and cryosections were imaged using a slidescanner or confocal microscope. *Slidescanner*: Overviews of whole brain sections and region-specific scans were performed with an Olympus VS120 Slide Scanner. Image capturing and initial processing was conducted with the Olympus VS Software. Briefly, overview images of the whole slide were acquired in the batch scanning mode. Subsequently, region-specific scans were taken with the 20×, whole sections images with the 10× objective. The scan region was adjusted to the size of the region. Exposure time and focus were set to automated mode. Sections were acquired with the C3 (TdTomato) channel or the FITC (GFP) channel. *Confocal microscopy*: For higher resolution, confocal images of regions of interest were acquired with a Zeiss Axioplan2 fluorescence microscope using Axio Vision 4.5 software. Fluorescently labeled cells were excited at 488 nm (GFP Alexa-488) and 559 nm (Td-tomato, Alexa-594), respectively, using a 20× objective. After acquisition in virtual slide (.VSI file) or Carl Zeiss (.CZI) format, images were extracted and saved as Tagged Image File Format (.tiff) for further processing. Images were analyzed using Fiji (http://rsweb.nih.gov/ij/) and Inkscape (version 1.2.2.).

3 Results

3.1 FlpO expression pattern in CRH-FlpO mice recapitulates endogenous CRH expression

CRH-FlpO mice were generated by targeted insertion of a FlpO expression cassette into the murine *Crh* locus immediately downstream of the stop codon. FlpO expression driven by the *Crh* locus is conveyed by an internal ribosomal entry site (IRES). As a selection marker, a self-excising neomycin cassette driven by the testis-specific angiotensin converting enzyme promotor (tACE) was used, which removed itself in the male germline leaving a single *loxP2272* site behind (**Figure 1A; Supplementary Data**). To validate FlpO expression, we used heterozygous *CRH-FlpO* mice and performed an *in situ* hybridization (ISH) against *FlpO*. The spatial pattern of *FlpO* mRNA expression fully recapitulated the expression of endogenous *Crh* as indicated by the detection of distinct signals in all regions of salient CRH expression including the piriform cortex (Pir), IPACL, BNST, CeA, and PVN. The expression of *FlpO* appeared generally weaker, as *CRH-FlpO* mice were only heterozygous (**Figure 1B**).

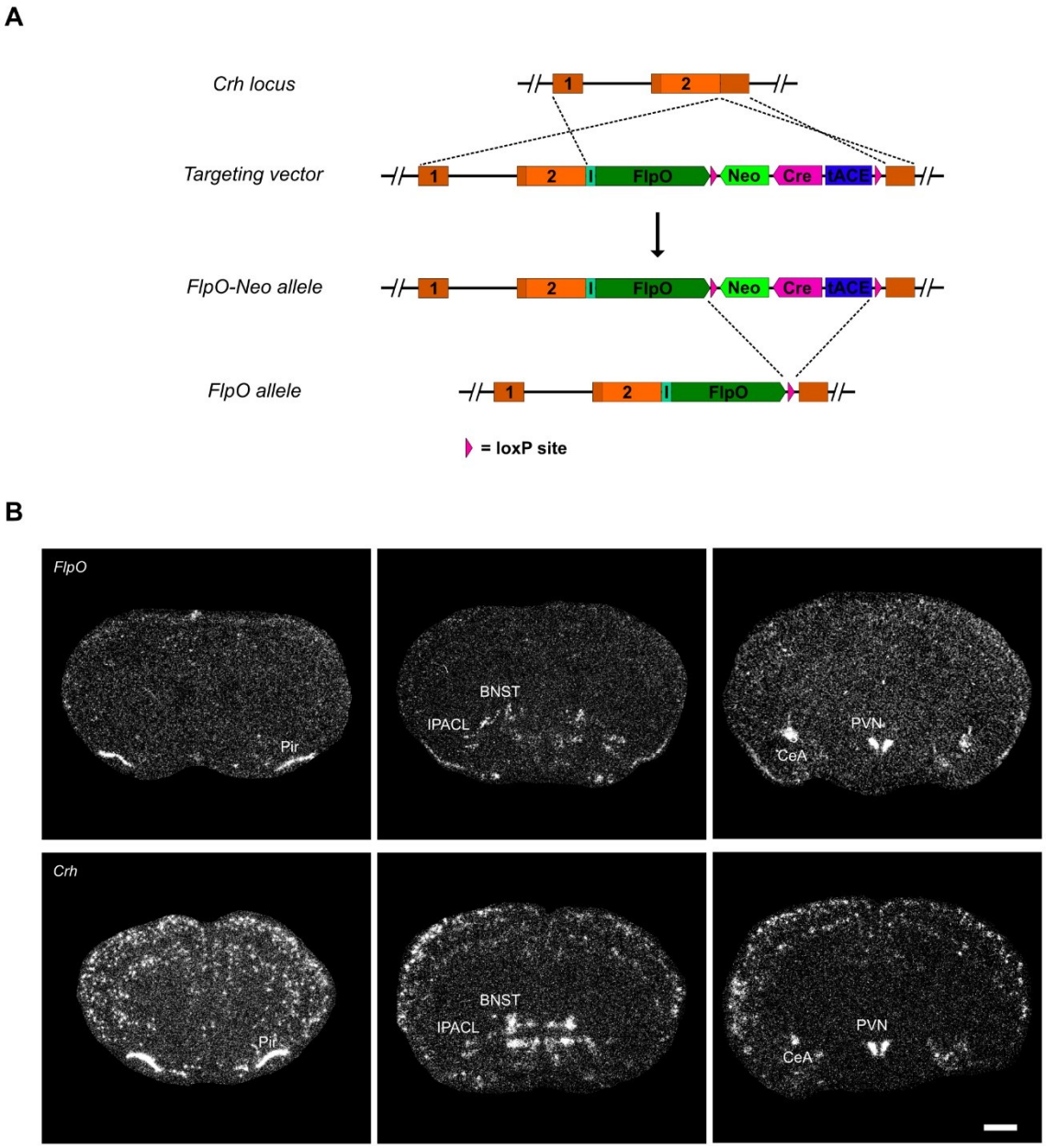

Figure 1

FlpO expression pattern in *CRH-FlpO* mice recapitulates endogenous CRH expression. **(A)** Scheme illustrating the generation of *CRH-FlpO* mice by homologous recombination-mediated gene targeting. **(B)** *In situ* hybridization (ISH) on coronal brain sections of heterozygous ($Crh^{+/FlpO}$) (n = 3) and wild-type ($Crh^{+/+}$) *CRH-FlpO* (n = 3) mice using *FlpO*- and *Crh*-specific riboprobes showing comparable expression patterns, e.g., the in piriform cortex (Pir), lateral part of the interstitial nucleus of the anterior commissure (IPACL), bed nucleus of the stria terminalis (BNST), central amygdala (CeA) and paraventricular nucleus of the hypothalamus (PVN). I, internal ribosomal entry site; Neo, neomycine resistance gene. Scale bar, 1000 µm.

3.2 Comparison of FlpO- and Cre-activated reporter gene expression

To compare the pattern and efficiency of FlpO- and Cre-mediated recombination driven by the *Crh* locus, we bred *CRH-FlpO* and *CRH-Cre* mice to appropriate reporter lines (**Figure 2A, B**). The reporter alleles in *Ai65F* and *Ai9* mice are ideally suited for direct comparison of FlpO and Cre activity, as both are based on the *Rosa26* locus harboring an identical *CAG* promotor-driven tdTomato expression unit, which is preceded by an *FRT*- and a *loxP*-flanked transcriptional terminator (STOP), respectively (**Figure 2A, B**). Similarly, the *Crh* alleles harboring either FlpO or Cre recombinase were designed in the same way, i.e., the recombinase was integrated immediately downstream of the *Crh* STOP codon and is driven by an IRES.

The tdTomato expression pattern was analyzed throughout the brain of *CRH-FlpO::Ai65F* and *CRH-Cre::Ai9* mice. In both mouse lines, tdTomato-positive neurons were detectable in all brain regions which have previously been reported to endogenously express CRH (Kono et al., 2017; Wang et al., 2021), including the olfactory bulb (OB), cortex (CTX), IPACL, BNST, PVN, CeA, Barrington's nucleus (BAR) and inferior olivary nucleus (IO) (**Figure 2C**). Moreover, characteristic tdTomato-labeled CRH^+ fibers were visible in the anterior commissure (ac) and the inferior cerebellar peduncle (icp), the latter representing climbing fibers originating in the IO and innervating the cerebellum (Ezra-Nevo et al., 2018). In addition, prominent tdTomato-labeled terminals were detectable in the ME and substantia nigra (SN), sites well-known for their massive CRH afferents (Chang et al., 2022). Taken together, our results indicate that the *CRH-FlpO* mice are able to promote site-specific recombination at endogenous CRH expression sites comparable with *CRH-Cre* mice. However, imaging with identical exposure times revealed an overall lower fluorescence intensity detectable throughout brain sections of *CRH-FlpO::Ai65F* compared to *CRH-Cre::Ai9* mice (**Figure 2C**). This discrepancy in intensity likely originates from a reduced number of tdTomato-labeled soma and fibers present in *CRH-FlpO::Ai65F* mice, an observation which necessitated closer inspection.

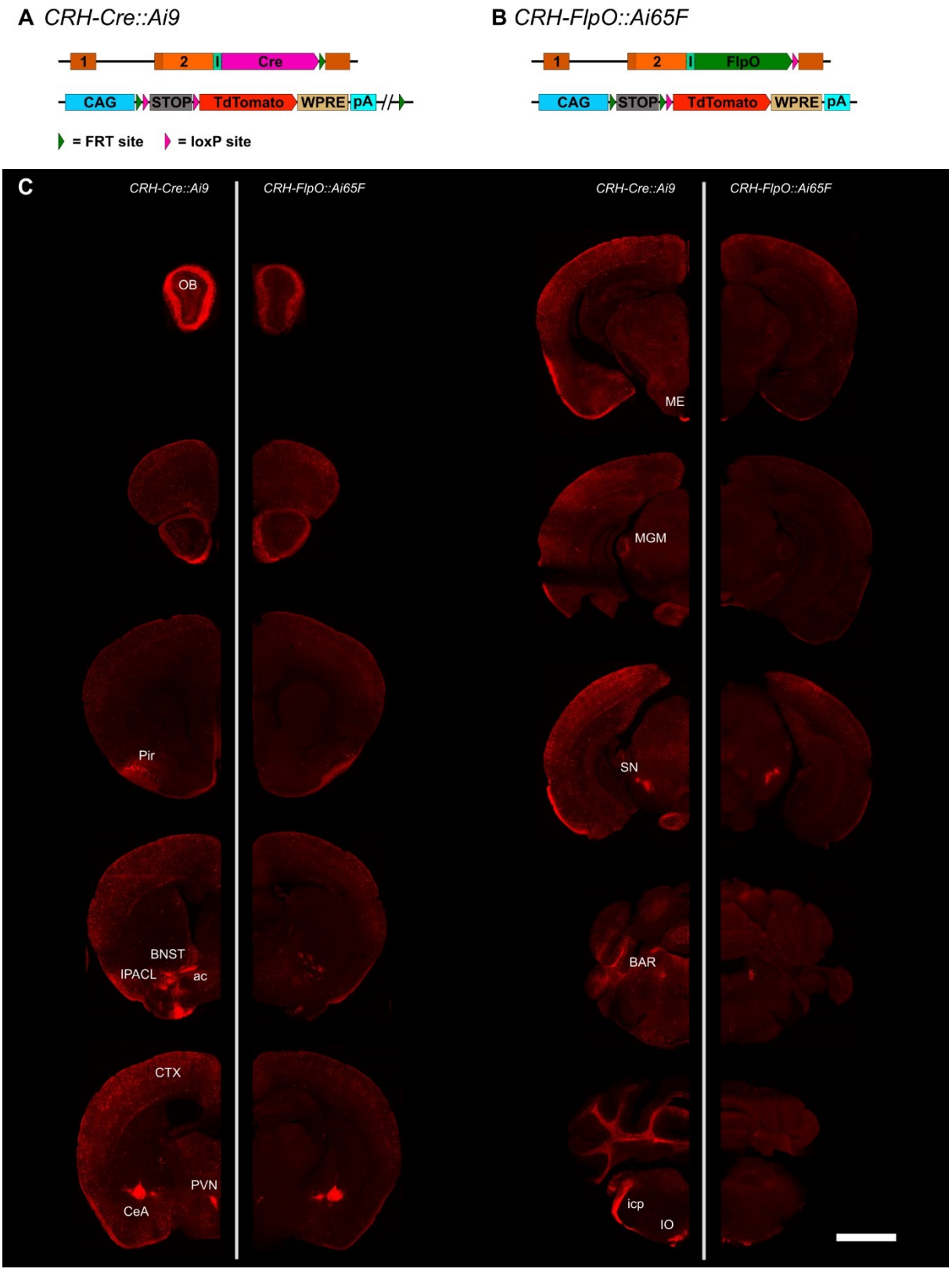

Figure 2

Comparison of the distribution of tdTomato$^+$ cells and fibers in the brain of *CRH-Cre::Ai9* and *CRH-FlpO::Ai65F* mice. **(A-B)** Schematic illustration combining photomicrographs of *CRH-Cre::Ai9* (left, n = 5) and *CRH-FlpO::Ai65F* (right, n = 4) reporter mice. **(C)** Distribution of tdTomato$^+$ cells and fibers in *CRH-Cre::Ai9* and *CRH-FlpO::Ai65F* mice. ac, anterior commissure; BAR, Barrington's nucleus; BNST, bed nucleus of the stria

terminalis; CeA, central amygdala; I, internal ribosomal entry site; icp, inferior cerebellar peduncle; IO, inferior olivary nucleus; IPACL, lateral part of the interstitial nucleus of the anterior commissure; ME, median eminence; MGM, medial division of the medial geniculate; OB, olfactory bulb; Pir, piriform cortex; PVN, paraventricular nucleus of the hypothalamus; SN, substantia nigra. WRPE, woodchuck hepatitis virus posttranscriptional regulatory element. Scale bar, 1000 μm.

3.3 FlpO-dependent recombination is inferior to Cre-mediated recombination.

To interrogate the discrepancy in tdTomato expression between *CRH-FlpO::Ai65F* and *CRH-Cre::Ai9* mice in more detail, we focused our analysis on CRH-expressing brain structures involved in the neuroendocrine (HPA axis: PVN, ME) and behavioral (extended amygdala: CeA, IPACL, BNST) stress response as well as on the CTX, because of its homogeneous and scattered distribution of CRH^+ neurons. First, we tested the degree of overlapping Cre and FlpO expression, comparing the occurrence of $tdTomato^+$ cells in the intersectional reporter mouse line *CRH-Cre::CRH-FlpO::Ai65* with *CRH-Cre::Ai9* mice (**Figure 3A**). In all analyzed structures, *CRH-Cre::CRH-FlpO::Ai65* mice showed a markedly reduced number of $tdTomato^+$ cells compared to *CRH-Cre::Ai9* mice. Instead, the number of $tdTomato^+$ cells was comparable to *CRH-FlpO::Ai65F* mice, suggesting that the FlpO-mediated recombination in CRH^+ cells was less efficient compared to Cre-mediated recombination driven by the *Crh* locus (**Figure 3B**).

To rule out the possibility that differences in the genetic composition in which the tdTomato reporter is embedded in *Ai9* vs *Ai65F* mice was causal for the differential reporting, we used the subtractive capacity of the *Ai9* reporter line. This reporter line still contains the neomycin selection marker and a downstream *FRT* site, which makes the tdTomato expression cassette vulnerable to deletion via Flp recombinase, resulting in a loss of tdTomato expression in cells previously activated by Cre-mediated recombination (**Figure 3C**). However, the analysis of the PVN, ME, IPACL, BNST, CeA and CTX in *CRH-Cre::CRH-FlpO::Ai9* mice did not reveal any substantial reduction in tdTomato expression but instead showed similar numbers of tdTomato expressing cells as detected in *CRH-Cre::Ai9* mice (**Figure 3D**).

Taken together, these data confirm a high degree of co-expression of Cre and FlpO driven from the *Crh* locus but also provide evidence that the Cre recombinase is more efficiently activating reporter gene expression compared to the FlpO recombinase.

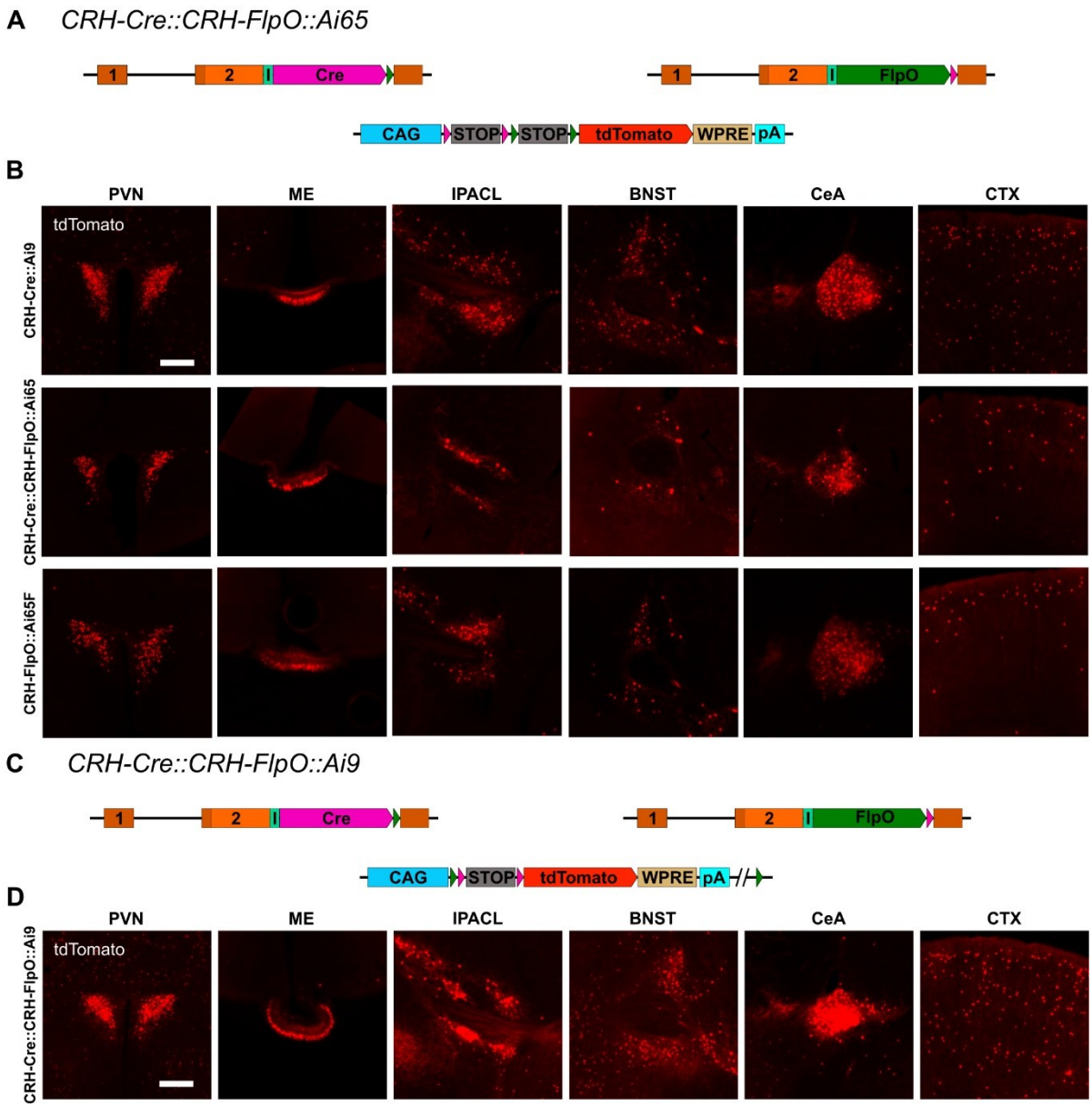

Figure 3

Reporter mice reveal diverging FlpO- and Cre-mediated recombination efficiency. **(A)** Schematic illustration of *CRH-Cre::CRH-FlpO::Ai65 reporter* mice. **(B)** Comparison of the distribution of tdTomato$^+$ cells and fibers in regions of interest in *CRH-Cre::Ai9* (n = 5), *CRH-Cre::CRH-FlpO::Ai65* (n = 4) and *CRH-FlpO::Ai65F* (n = 4) mice. **(C)** Schematic illustration of *CRH-Cre::CRH-FlpO::Ai9* reporter mice. **(D)** Distribution of tdTomato$^+$ cells and fibers in regions of interest in *CRH-Cre::CRH-FlpO::Ai9* mice (n = 6). BNST, bed nucleus of the stria terminalis; CeA, central amygdala; I, internal ribosomal entry site; CTX, cortex; IPACL, lateral part of the interstitial nucleus of the anterior commissure; ME, median eminence; pA, BGH polyA signal; PVN, paraventricular nucleus of the hypothalamus; WRPE, woodchuck hepatitis virus posttranscriptional regulatory element. Scale bars, 200 µm.

3.4 Discrepancies between direct and indirect reporting of CRH expression

The recombination efficiency is determined by intrinsic properties of the respective SSR itself and by environmental conditions, e.g., the accessibility of recognition sites within the chromatin structure. Another important aspect is the expression, which needs to reach a certain threshold to allow site-specific recombination. To evaluate the influence of the expression level, we used *CRH-Venus* reporter mice in which the fluorescent protein Venus was integrated at the *Crh* start codon. This direct reporter allele readily reports CRH expression and is at the same time a CRH knockout allele (**Figure 4A**), whereas *CRH-Cre::Ai9* and *CRH-FlpO::Ai65F* mice serve as indirect reporters enabling the identification of CRH^+ cells which are labeled by accumulating and enduring tdTomato expression subsequent to CRH expression. Generally, the CRH expression level is rather low and does not allow reliable detection of Venus expression without antibody staining (**Figure 4B**). We generated *CRH-Venus::CRH-Cre::Ai9* and *CRH-Venus::CRH-FlpO::Ai65F* mice to directly compare CRH-Venus expression with Cre/FlpO-induced tdTomato expression, i.e., direct versus indirect reporting. Detailed analysis revealed a largely congruent expression in all regions of interest in both mouse lines (**Figure 4C, D**), i.e., a significant proportion of $tdTomato^+$ cells showed co-expression of Venus. The distribution of $Venus^+$ cells in both mouse lines shows a high degree of concordance indicating similar levels of CRH expression. Thus, the differences observed in $tdTomato^+$ cells cannot be attributed to general variations in CRH expression in the two mouse lines. Moreover, we observed in *CRH-Venus::CRH-Cre::Ai9* mice an excess of $tdTomato^+$ cells compared to Venus expressing cells (**Supplementary Figure S1**). The detection of $tdTomato^+/Venus^-$ cells suggests that either i) Cre caused ectopic CRH reporting by tdTomato, ii) CRH expression remained below a certain threshold, preventing reliable visualization by antibody staining or iii) CRH expression occurred only transiently during development but had ceased in adulthood. To evaluate the influence of the Venus expression level on the number of reported neurons, we bred *CRH-Venus* mice to homozygosity, which resulted in a significantly enhanced Venus signal and an increased number of $Venus^+$ cells in all regions of interest. This result indicated that $tdTomato^+/Venus^-$ neurons were not a consequence of ectopic Cre expression but rather reflected their low level of CRH expression. Accordingly, the Venus levels of these cells were too low to be detected by antibody staining, whereas the similarly low amount of Cre recombinase was sufficient to activate tdTomato expression (**Figure 4E**). Of note, a small proportion of $Venus^+$ cells did not express tdTomato, which additionally suggests some limitations of *CAG* promoter-based reporters located in the *Rosa26* locus (**Figure 4C, Supplementary Figure S1**). *CRH-Venus::CRH-FlpO::Ai65F* mice generally displayed less $tdTomato^+/Venus^+$ cells. However, no clear correlation between the detected Venus expression level and expression of tdTomato was observed (**Figure 4D**).

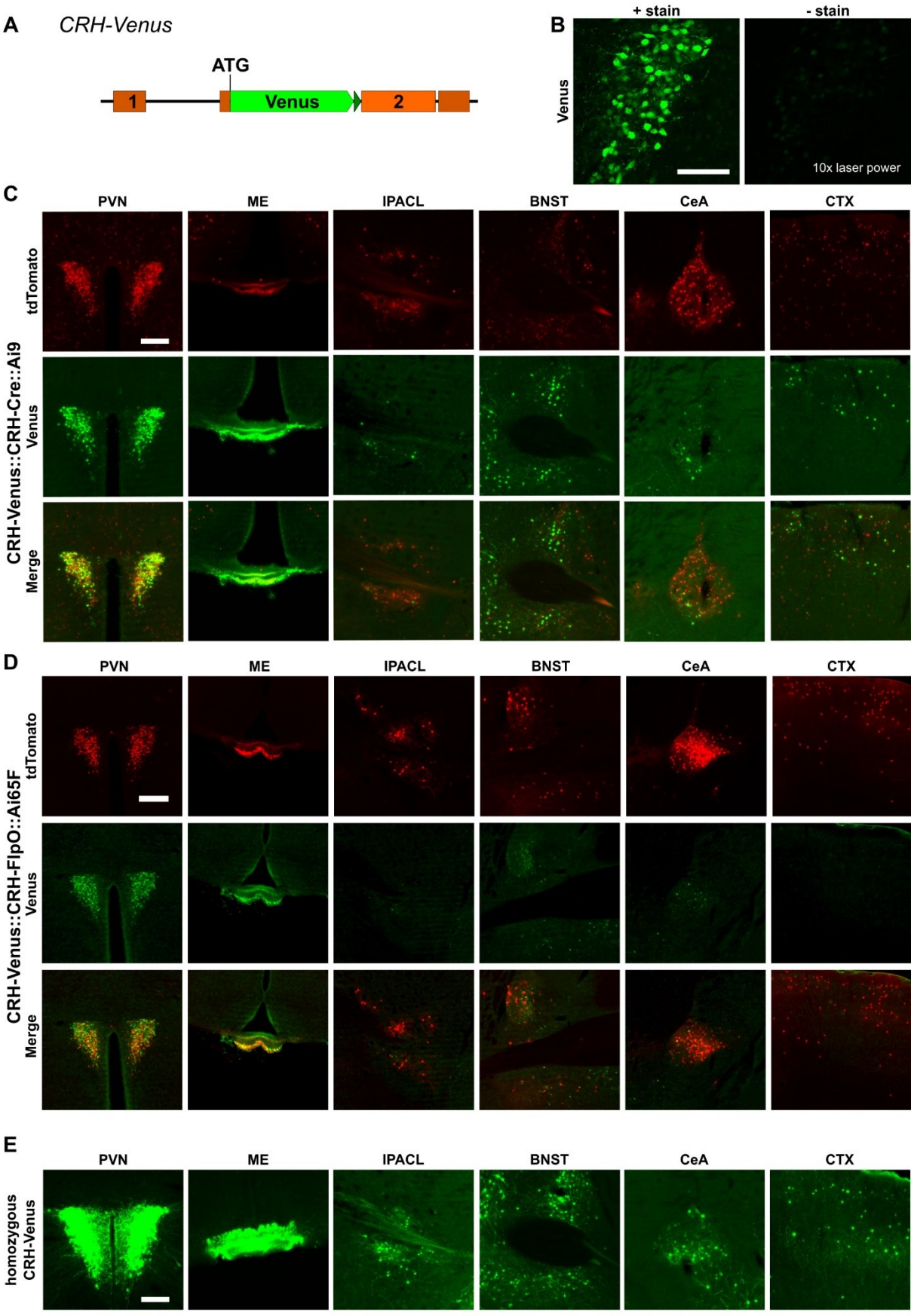
A
CRH-Venus
ATG
1
Venus
2
B
+ stain
- stain
Venus
10x laser power
C
PVN
ME
IPACL
BNST
CeA
CTX
CRH-Venus::CRH-Cre::Ai9
tdTomato
Venus
Merge
D
PVN
ME
IPACL
BNST
CeA
CTX
CRH-Venus::CRH-FlpO::Ai65F
tdTomato
Venus
Merge
E
PVN
ME
IPACL
BNST
CeA
CTX
homozygous
CRH-Venus

Figure 4

Cre recombinase possesses high recombination efficiency, even at low expression levels. **(A)** Schematic illustration of *CRH-Venus* reporter mice. **(B)** Visualization of Venus$^+$ cells with or without GFP antibody staining. Scale bar, 100 µm. **(C)** Comparison of the distribution of tdTomato$^+$ and Venus$^+$ cells and fibers in regions of interest in *CRH-Venus::CRH-Cre::Ai9* mice (n = 3). Scale bar, 200 µm. **(D)** Comparison of the distribution of tdTomato$^+$ and Venus$^+$ cells and fibers in regions of interest in *CRH-Venus::CRH-FlpO::Ai65F* mice (n = 6). Scale bar, 200 µm. **(E)** Distribution of Venus$^+$ cells and fibers in regions of interest in homozygous *CRH-Venus* mice (n = 3). Scale bar, 200 µm. BNST, bed nucleus of the stria terminalis; CeA, central amygdala; CTX, cortex; IPACL, lateral part of the interstitial nucleus of the anterior commissure; ME, median eminence; PVN, paraventricular nucleus of the hypothalamus.

3.5 FlpO recombination efficacy in CRH cells depends on the FlpO expression level

The previous results revealed that the strength of the *Crh* promoter differs strongly between neurons, even in the same region of interest. Therefore, *CAG-LSL-FlpO* mice were used to functionally validate the impact of the expression level on FlpO recombination efficiency. Since the recombination efficiency of a specific recombinase is dependent on its nuclear availability, it is also influenced by its expression level and therefore by the strength of its driving promoter. *CAG-LSL-FlpO* mice allow to convert any Cre activity into FlpO activity, which is then driven by the strong *CAG* promoter. Accordingly, *CRH-Cre::CAG-LSL-FlpO::Ai65* mice express high levels of FlpO in all CRH$^+$ cells previously expressing Cre (**Figure 5A**). Careful analysis of brain regions of interest revealed a considerable increase of tdTomato-expressing CRH neurons throughout the brain resembling the pattern and extent of expression previously observed in *CRH-Ai9* mice (**Figure 5C**). These findings provide strong evidence for a direct correlation of FlpO recombination efficacy with its expression level in CRH$^+$ neurons. Along those lines, and in contrast to *CRH-Cre::CRH-FlpO::Ai9* mice, *CRH-Cre::CAG-LSL-FlpO::Ai9* mice (**Figure 5D**) showed a substantial reduction of tdTomato-expressing CRH$^+$ cells, which was most prominent in the PVN, ME and CeA (**Figure 5C**). Along these lines, homozygous mice expressing *FlpO* from both *Crh* alleles, showed a considerable increase in tdTomato$^+$ cells compared heterozygous CRH-FlpO mice. This result directly proves that the level of FlpO expression determines the efficiency of FlpO recombination in CRH$^+$ cells.

Taken together, our results demonstrate that the *FlpO-FRT* system possesses a considerably lower sensitivity compared to the *Cre-loxP* system. Nevertheless, the attenuated sensitivity can be compensated by a higher expression level allowing the *FlpO-FRT* system to reach an efficacy which is comparable to the *Cre-loxP* system.

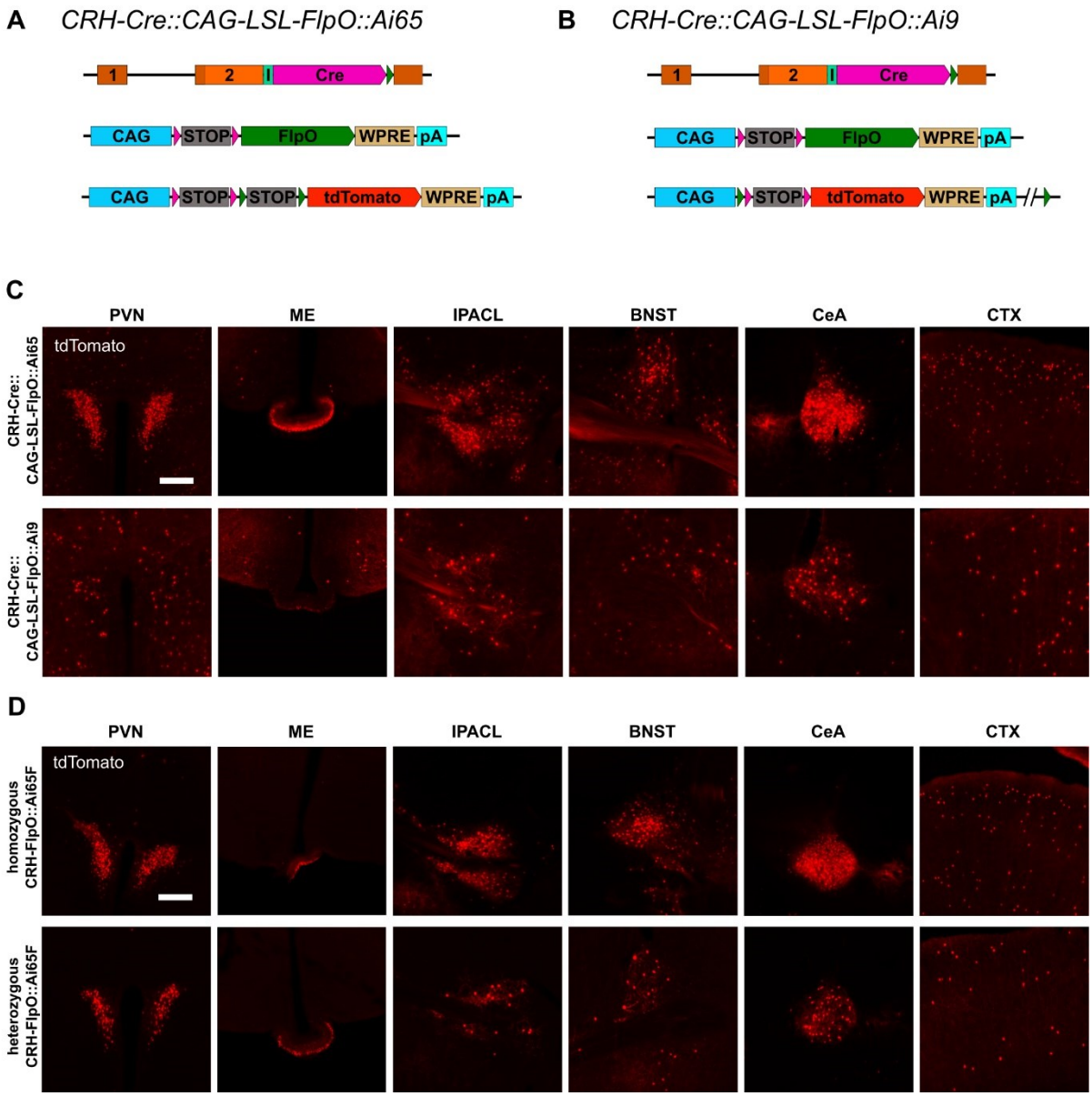

Figure 5

FlpO recombination efficiency depends on strength of driving promoter. **(A-B)** Schematic illustration of *CRH-Cre::CAG-LSL-FlpO::Ai65* and *CRH-Cre::CAG-LSL-FlpO::Ai9* reporter mice. **(C)** Distribution of tdTomato$^+$ cells and fibers in regions of interest in *CRH-Cre::CAG-LSL-FlpO::Ai65* (n = 3) and *CRH-Cre::CAG-LSL-FlpO::Ai9* (n = 7) mice. **(D)** Distribution of tdTomato$^+$ cells and fibers in regions of interest in homozygous *CRH-FlpO::Ai65F* mice (n = 4) and heterozygous *CRH-FlpO::Ai65F* mice (n = 4). BNST, bed nucleus of the stria terminalis; CeA, central amygdala; CTX, cortex; I, internal ribosomal entry site; IPACL, lateral part of the interstitial nucleus of the anterior commissure; ME, median eminence; pA, BGH polyA signal; PVN, paraventricular nucleus of the hypothalamus. Scale bar, 200 µm.

3.6 *CRH-FlpO* mice allow the visualization of stress-induced CRH expression

While previous studies have demonstrated the faithful reproduction of endogenous CRH expression when combining *CRH-Cre* mice (Taniguchi et al., 2011) with Cre-dependent reporters, such as *CRH-Cre::Ai9*, *CRH-Cre::Ai14* and *CRH-Cre::Ai32* (Chen et al., 2015; Dedic et al., 2018b; Wang et al., 2021; Chang et al., 2022), Walker *et al.* (2019) reported that there were no significant changes in the number of tdTomato-expressing neurons in *CRH-Cre::Ai14* mice after exposure to stress (Walker et al., 2019). In order to interrogate the suitability of the *CRH-FlpO*-based reporting system for evaluating the response to stress, we exposed *CRH-FlpO::Ai65F* mice to acute restraint stress. Analysis of brain sections revealed a considerable increase in tdTomato-expressing CRH neurons in the investigated brain region which was most prominent in the PVN of stressed compared to unstressed *CRH-FlpO::Ai65F* mice (**Figure 6A**). These results indicate an upregulation of CRH and concomitant FlpO expression in CRH^+ neurons following acute stress suggesting that the *CRH-FlpO*-based reporter mouse model provides a more dynamic range of recombination that overcomes the reported limitations of the *CRH-Cre* line (Walker et al., 2019).

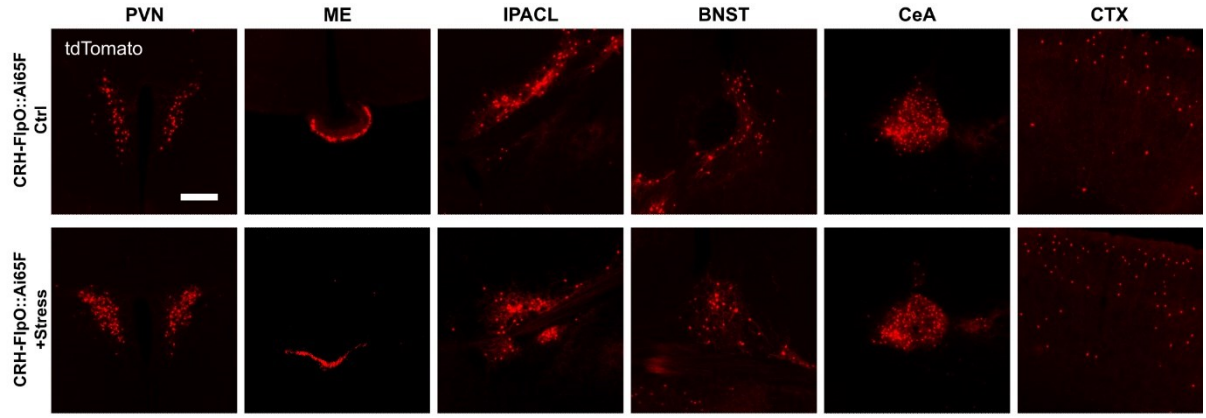

Figure 6

FlpO recombination efficiency is enhanced by acute restraint stress. Comparison of distribution of $tdTomato^+$ cells and fibers in regions of interest in stressed and unstressed *CRH-FlpO::Ai65F* mice (n = 4). BNST, bed nucleus of the stria terminalis; CeA, central amygdala; CTX, cortex; I, internal ribosomal entry site; IPACL, lateral part of the interstitial nucleus of the anterior commissure; ME, median eminence; pA, BGH polyA signal; PVN, paraventricular nucleus of the hypothalamus. Scale bar, 200 µm.

4 Discussion

CRH$^+$ neurons are widely distributed throughout the brain and possess a high diversity with regards to their identity and physiology. The limited accessibility of CRH neurons by antibody-based approaches and particularly the quest to disentangle CRH neuron function has raised increasing interest in CRH-specific SSR and reporter mouse lines. While reliable CRH-specific Cre mouse lines have been available for some time (Taniguchi et al., 2011), only recently, the development of a novel *CRH-FlpO* line (Salimando et al., 2020) has opened up additional opportunities to address the CRH system with increasing precision. To meaningfully apply CRH-specific SSR mouse lines, it is utterly important to understand their capacity to recapitulate endogenous CRH expression. In this study, we therefore compared the recently developed *CRH-FlpO* line with endogenous CRH expression and a well-established and widely used *CRH-Cre* line (Taniguchi et al., 2011). We demonstrated that the overall reporting pattern of *CRH-FlpO* mice is very similar to *CRH-Cre* mice. The efficiency of FlpO, however, is strongly correlated with its expression level in the analyzed population of CRH$^+$ neurons.

The comparison of *FlpO* expression with endogenous *Crh* expression on mRNA level and the evaluation of tdTomato induction in *CRH-FlpO::Ai65F* compared to *CRH-Cre::Ai9* mice both confirmed that the FlpO expression and recombination pattern strongly align with that of endogenous *Crh*. These results corroborate the high potential of the chosen knock-in strategy to reliably convey properties of the endogenous *Crh* locus to an integrated transgene.

Nevertheless, the overall intensity of FlpO-activated tdTomato fluorescence appeared somewhat decreased in *CRH-FlpO::Ai65F* compared to *CRH-Cre::Ai9* mice, raising the question whether these discrepancies were caused by differences in their reporting capacity in general. The in-depth analysis of CRH-expressing nuclei revealed that, indeed, the number of tdTomato$^+$ labeled cells and fibers were lower in FlpO- than in Cre-dependent reporter animals, strengthening the hypothesis of a differential reporting capacity. Although *CRH-Cre::Ai9* and *CRH-FlpO::Ai65* both utilize tdTomato as a reporter in combination with the *CAG* promoter followed by an identical floxed STOP cassette, the genetic composition in which the tdTomato reporter is embedded differs slightly between the *Ai9* and *Ai65F* lines (Madisen et al., 2010; Madisen et al., 2015). Thus, we wondered whether the *Ai65F* reporter, rather than the FlpO recombinase itself, was responsible for the observed differences. Unexpectedly, the intersectional reporter mice *CRH-Cre::CRH-FlpO::Ai65* and *CRH-Cre::CRH-FlpO::Ai9* revealed that FlpO was neither able to report all CRH$^+$ cells in the *Ai65*-based model nor did it deplete tdTomato from Cre-activated cells in the *Ai9*-based model. These results imply that not the used *Ai65F* reporter line but FlpO recombination efficiency itself could be the limiting factor. To rule out that the higher cell numbers were not caused by ectopic Cre activity in *CRH-Cre* mice, the *CRH-Venus* mouse line as a direct reporter of CRH expression was used to compare tdTomato and Venus expression in the same individual. It is worth noting that Cre-mediated recombination, resulting in cumulative tdTomato expression, effectively reflects the cellular history of *Crh* gene transcription over the time. In contrast, the Venus$^+$ knock-in allele reports a snapshot of the current protein content above a certain detection threshold, providing a

glimpse into the present state rather than the developmental timeline. Despite the differences between the direct and indirect reporting systems and the distinct characteristics of the two applied fluorescent proteins, such as their disparate fluorescent protein lifetimes (Sarkar et al., 2009; Drobizhev et al., 2011), the comparable number of Venus$^+$ cells observed in the analyzed brain regions of *CRH-Venus::CRH-Cre::Ai9* and *CRH-Venus::CRH-FlpO::Ai65F* mice suggests that there is no variation in CRH expression between the two mouse lines. Accordingly, this indicates that the disparity of tdTomato$^+$ cells in *CRH-Cre::Ai9* and *CRH-FlpO::Ai65F* mice may be attributed to the inherent properties of these two recombinases. Indirect reporting via Cre recombinase-mediated activation of tdTomato showed a high degree of co-localization with Venus expression. Interestingly, also a substantial number of tdTomato$^+$/Venus$^-$ cells were detectable, which left open the possibility that tdTomato expression in Venus$^-$ neurons represent ectopic or legacy expression due to transient activation of CRH and, thus, Cre expression, e.g., during development or in response to experienced stressors, which would not be detected by the Venus reporter. In this regard, homozygous *CRH-Venus* mice were instructive, as we were able to visualize an increased number of Venus$^+$ cells in all analyzed brain regions compared to heterozygous *CRH-Venus* mice. This observation suggests that more cells reached the detection threshold, supporting the notion that CRH neurons possess a broad spectrum of expression levels, even within the same brain region. This result additionally confirms that Cre-mediated reporter activation is substantially more sensitive than the detection of Venus via antibody staining, as the tdTomato is driven by the strong and ubiquitously active *CAG* promoter. Seemingly, a few molecules of Cre are sufficient to activate tdTomato expression. Although a compensatory upregulation of CRH, caused by the de facto knockout of CRH in homozygous CRH-Venus mice, may also have contributed to the higher number of Venus$^+$ neurons, the differences in intensity still confirm a broad diversity of CRH expression levels in respective neurons. In contrast to the PVN, CRH expression in the CeA has been reported to be positively regulated by corticosterone (Makino et al., 1994). Consequentially, CRH inactivation, resulting in low corticosterone levels, should lead to a decreased Venus expression in the CeA. Of note, in our experiments we observed a general increase of Venus expression in all regions analyzed, including the CeA. This observation indicates that homozygosity of the reporter is potentially overriding the hypothesized downregulation of CRH by the low corticosterone levels entailed by the CRH knockout.

These results suggest that, if FlpO-mediated recombination, and therefore reporter efficacy, depends on the expression level of the driving promoter, an enhanced expression should be able to elevate the number of reported cells. Indeed, the combination of FlpO with the *CAG* promoter, a strong synthetic promoter integrated in the *Rosa26* locus, did not only increase reporting efficacy in the *CRH-Cre::CAG-LSL-FlpO::Ai65* model to a level comparable to *CRH-Cre::Ai9* mice but was also able to vastly decrease the reporting in the *CRH-Cre::CAG-LSL-FlpO::Ai9* model. These results also demonstrate that the larger distance between the *FRT* sites flanking the tdTomato cassette in the *Ai9* line (3.9 kb) is not limiting FlpO recombination activity in general (Coppoolse et al., 2005; Liu et al., 2013). Ultimately, homozygous *CRH-FlpO::Ai65F* mice, expressing FlpO from both *Crh* alleles, confirmed that the level

of FlpO expression is directly correlated with its recombination efficiency. Along these lines, while *CRH-Cre* females show 100% germline recombination when combined with a floxed allele, the respective frequency observed in *CRH-FlpO* females is also significantly lower.

Thermo-instability of yeast-derived Flp-related recombinases has been shown to decrease their recombination efficiency in mammalian cells (Buchholz et al., 1996). Despite previous optimization efforts (Buchholz et al., 1998; Raymond and Soriano, 2007) our results clearly demonstrate a persistent difference in recombination efficiency between Cre and FlpO, which particularly matters in low gene expression conditions. Whether this discrepancy is related to differences in protein thermo-stability or the intrinsic reaction rate of Cre and FlpO, remains to be investigated. To what extent other recombinases, such as Dre, can keep up with Cre recombinase efficiency, requires further examination (Anastassiadis et al., 2009; Karimova et al., 2018). The utilized IRES might further aggravate the situation, as IRES-dependent gene expression of the second gene in a bicistronic construct is up to 10-fold lower than cap-dependent expression of the first gene (Mizuguchi et al., 2000; Martin et al., 2006). Today, 2A-related self-cleaving peptides are used to overcome the drawbacks of IRES (Liu et al., 2017). However, 2A peptides leave a couple of amino acids to the N-terminally located protein. This would not be compatible with CRH maturation which involves proteolytic processing by prohormone convertases at predetermined recognition sites which will be disturbed by remnants of 2A peptides (Hook et al., 2008). In fact, this poses a general difficulty for the expression of neuropeptides using multicistronic expression vectors.

Mouse models targeting the CRH system, particularly those employing Cre-dependent reporters, are widely utilized to study the neurobiology of stress and related circuits. On the one hand, the robust efficacy of Cre recombinase provides a reliable tool for investigating the spatial distribution and connectivity of CRH neurons throughout the brain. On the other hand, the high efficacy of Cre recombination seemingly labels almost all cells which have the potential to express CRH in the course of their lifetime. Consequently, the recruitment of new stress-induced tdTomato$^+$ cells in *CRH-Cre::Ai9* cells is very limited (Walker et al., 2019). Our results demonstrate that this particular limitation of *CRH-Cre*-based models can be overcome by using *CRH-FlpO* mice. Following exposure to acute stress, we observed an increased number of tdTomato$^+$ cells in *CRH-FlpO::Ai65F* mice. Thus, *de novo* tdTomato expression can serve as a proxy for stress-responsive neurons characterized by the upregulation of the stress peptide CRH. These results highlight the utility of *CRH-FlpO* mice as a valuable tool for functional analysis of the CRH system under both physiological and pathological conditions.

In conclusion, we show a difference in the recombination efficiency of Cre and FlpO in CRH$^+$ neurons and demonstrate that the expression level of FlpO contributes to discrepancies in reporter gene activation observed between *CRH-Cre* and *CRH-FlpO* mice. These results have strong implications for future experiments using the investigated mouse lines but also for SSR-based approaches in general. i) When using and comparing FlpO- and Cre-based reporter systems, the strength of the driving promoter has to be taken into account. ii) In intersectional approaches, the number of reported co-expressing cells is

limited by the efficacy of the FlpO. iii) In approaches involving knockout or overexpression of a specific target gene, the efficacy is highly dependent on the used SSR. These results are essential to interpret and reconcile divergent scientific discoveries which will ultimately advance our comprehension of the physiological role of CRH in the central nervous system.

Conflict of Interest

The authors declare no competing interests.

Author Contributions

C.Z., C.R. and Y.D. designed and performed all experiments, analyzed and interpreted data, drafted figures and wrote the manuscript. J.Z. performed a subset of experiments and reviewed the manuscript. K.S. and K.I. provided materials, edited the manuscript and contributed scientific advice. J.M.D. designed the project, supervised all experiments and analyses, edited the manuscript and provided scientific advice, guidance and support. All authors approved the submitted manuscript.

Funding

The project was supported by the Max Planck Society (J.M.D.) and the Federal Ministry of Education and Research (FKZ 01KU1901, J.M.D.). J.Z. and Y.D. received funding from the Chinese Scholarship Council. C.R. received funding from the International Max Planck Research School for Translational Psychiatry and the Gunter Sachs Donation.

Acknowledgements

The authors thank Stefanie Unkmeir and Sabrina Bauer of the scientific core unit Genetically Engineered Mouse Models for genotyping support; Elfi Fesl for proofreading and editing of the manuscript. We thank Minsuk Huyn, Caiying Guo and Bernado Sabatini for sharing details on the generation of *CRH-FlpO* mice.

References

Alon T, Zhou L, Perez CA, Garfield AS, Friedman JM, Heisler LK (2009) Transgenic mice expressing green fluorescent protein under the control of the corticotropin-releasing hormone promoter. Endocrinology 150:5626-5632.

Anastassiadis K, Fu J, Patsch C, Hu S, Weidlich S, Duerschke K, Buchholz F, Edenhofer F, Stewart AF (2009) Dre recombinase, like Cre, is a highly efficient site-specific recombinase in E. coli, mammalian cells and mice. Dis Model Mech 2:508-515.

Arias A, Manubens-Gil L, Dierssen M (2022) Fluorescent transgenic mouse models for whole-brain imaging in health and disease. Front Mol Neurosci 15:958222.

Bloom FE, Battenberg ELF, Rivier J, Vale W (1982) Corticotropin releasing factor (CRF): immunoreactive neurones and fibers in rat hypothalamus. Regulatory Peptides 4:43-48.

Buchholz F, Angrand PO, Stewart AF (1998) Improved properties of FLP recombinase evolved by cycling mutagenesis. Nat Biotechnol 16:657-662.

Buchholz F, Ringrose L, Angrand PO, Rossi F, Stewart AF (1996) Different thermostabilities of FLP and Cre recombinases: implications for applied site-specific recombination. Nucleic Acids Res 24:4256-4262.

Chang S, Fermani F, Lao CL, Huang L, Jakovcevski M, Di Giaimo R, Gagliardi M, Menegaz D, Hennrich AA, Ziller M, Eder M, Klein R, Cai N, Deussing JM (2022) Tripartite extended amygdala-basal ganglia CRH circuit drives locomotor activation and avoidance behavior. Sci Adv 8:eabo1023.

Chen Y, Molet J, Gunn BG, Ressler K, Baram TZ (2015) Diversity of Reporter Expression Patterns in Transgenic Mouse Lines Targeting Corticotropin-Releasing Hormone-Expressing Neurons. Endocrinology 156:4769-4780.

Coppoolse ER, de Vroomen MJ, van Gennip F, Hersmus BJ, van Haaren MJ (2005) Size does matter: cre-mediated somatic deletion efficiency depends on the distance between the target lox-sites. Plant Mol Biol 58:687-698.

Dabrowska J, Hazra R, Guo JD, Dewitt S, Rainnie DG (2013) Central CRF neurons are not created equal: phenotypic differences in CRF-containing neurons of the rat paraventricular hypothalamus and the bed nucleus of the stria terminalis. Front Neurosci 7:156.

Dedic N, Chen A, Deussing JM (2018a) The CRF Family of Neuropeptides and their Receptors - Mediators of the Central Stress Response. Curr Mol Pharmacol 11:4-31.

Dedic N, Kuhne C, Gomes KS, Hartmann J, Ressler KJ, Schmidt MV, Deussing JM (2019) Deletion of CRH From GABAergic Forebrain Neurons Promotes Stress Resilience and Dampens Stress-Induced Changes in Neuronal Activity. Front Neurosci 13:986.

Dedic N et al. (2018b) Chronic CRH depletion from GABAergic, long-range projection neurons in the extended amygdala reduces dopamine release and increases anxiety. Nat Neurosci 21:803-807.

Deussing JM (2013) Targeted mutagenesis tools for modelling psychiatric disorders. Cell Tissue Res 354:9-25.

Drobizhev M, Makarov NS, Tillo SE, Hughes TE, Rebane A (2011) Two-photon absorption properties of fluorescent proteins. Nat Methods 8:393-399.

Ezra-Nevo G, Volk N, Ramot A, Kuehne C, Tsoory M, Deussing J, Chen A (2018) Inferior olive CRF plays a role in motor performance under challenging conditions. Transl Psychiatry 8:107.

Fadok JP, Krabbe S, Markovic M, Courtin J, Xu C, Massi L, Botta P, Bylund K, Muller C, Kovacevic A, Tovote P, Luthi A (2017) A competitive inhibitory circuit for selection of active and passive fear responses. Nature 542:96-100.

Gunn BG, Sanchez GA, Lynch G, Baram TZ, Chen Y (2019) Hyper-diversity of CRH interneurons in mouse hippocampus. Brain Struct Funct 224:583-598.

He M, Tucciarone J, Lee S, Nigro MJ, Kim Y, Levine JM, Kelly SM, Krugikov I, Wu P, Chen Y, Gong L, Hou Y, Osten P, Rudy B, Huang ZJ (2016) Strategies and Tools for Combinatorial Targeting of GABAergic Neurons in Mouse Cerebral Cortex. Neuron 91:1228-1243.

Heffner CS, Herbert Pratt C, Babiuk RP, Sharma Y, Rockwood SF, Donahue LR, Eppig JT, Murray SA (2012) Supporting conditional mouse mutagenesis with a comprehensive cre characterization resource. Nat Commun 3:1218.

Hook V, Funkelstein L, Lu D, Bark S, Wegrzyn J, Hwang SR (2008) Proteases for processing proneuropeptides into peptide neurotransmitters and hormones. Annu Rev Pharmacol Toxicol 48:393-423.

Itoi K, Talukder AH, Fuse T, Kaneko T, Ozawa R, Sato T, Sugaya T, Uchida K, Yamazaki M, Abe M, Natsume R, Sakimura K (2014) Visualization of corticotropin-releasing factor neurons by fluorescent proteins in the mouse brain and characterization of labeled neurons in the paraventricular nucleus of the hypothalamus. Endocrinology 155:4054-4060.

Karimova M, Baker O, Camgoz A, Naumann R, Buchholz F, Anastassiadis K (2018) A single reporter mouse line for Vika, Flp, Dre, and Cre-recombination. Sci Rep 8:14453.

Keegan CE, Herman JP, Karolyi IJ, O'Shea KS, Camper SA, Seasholtz AF (1994) Differential expression of corticotropin-releasing hormone in developing mouse embryos and adult brain. Endocrinology 134:2547-2555.

Kono J, Konno K, Talukder AH, Fuse T, Abe M, Uchida K, Horio S, Sakimura K, Watanabe M, Itoi K (2017) Distribution of corticotropin-releasing factor neurons in the mouse brain: a study using corticotropin-releasing factor-modified yellow fluorescent protein knock-in mouse. Brain Struct Funct 222:1705-1732.

Korecki AJ, Hickmott JW, Lam SL, Dreolini L, Mathelier A, Baker O, Kuehne C, Bonaguro RJ, Smith J, Tan CV, Zhou M, Goldowitz D, Deussing JM, Stewart AF, Wasserman WW, Holt

RA, Simpson EM (2019) Twenty-Seven Tamoxifen-Inducible iCre-Driver Mouse Strains for Eye and Brain, Including Seventeen Carrying a New Inducible-First Constitutive-Ready Allele. Genetics 211:1155-1177.

Krashes MJ, Shah BP, Madara JC, Olson DP, Strochlic DE, Garfield AS, Vong L, Pei H, Watabe-Uchida M, Uchida N, Liberles SD, Lowell BB (2014) An excitatory paraventricular nucleus to AgRP neuron circuit that drives hunger. Nature 507:238-242.

Kubota Y, Shigematsu N, Karube F, Sekigawa A, Kato S, Yamaguchi N, Hirai Y, Morishima M, Kawaguchi Y (2011) Selective coexpression of multiple chemical markers defines discrete populations of neocortical GABAergic neurons. Cereb Cortex 21:1803-1817.

Lemos JC, Wanat MJ, Smith JS, Reyes BA, Hollon NG, Van Bockstaele EJ, Chavkin C, Phillips PE (2012) Severe stress switches CRF action in the nucleus accumbens from appetitive to aversive. Nature 490:402-406.

Liu J, Willet SG, Bankaitis ED, Xu Y, Wright CV, Gu G (2013) Non-parallel recombination limits Cre-LoxP-based reporters as precise indicators of conditional genetic manipulation. Genesis 51:436-442.

Liu Z, Chen O, Wall JBJ, Zheng M, Zhou Y, Wang L, Vaseghi HR, Qian L, Liu J (2017) Systematic comparison of 2A peptides for cloning multi-genes in a polycistronic vector. Sci Rep 7:2193.

Luo L, Callaway EM, Svoboda K (2018) Genetic Dissection of Neural Circuits: A Decade of Progress. Neuron 98:256-281.

Luo L et al. (2020) Optimizing Nervous System-Specific Gene Targeting with Cre Driver Lines: Prevalence of Germline Recombination and Influencing Factors. Neuron 106:37-65 e35.

Madisen L, Zwingman TA, Sunkin SM, Oh SW, Zariwala HA, Gu H, Ng LL, Palmiter RD, Hawrylycz MJ, Jones AR, Lein ES, Zeng H (2010) A robust and high-throughput Cre reporting and characterization system for the whole mouse brain. Nat Neurosci 13:133-140.

Madisen L et al. (2015) Transgenic mice for intersectional targeting of neural sensors and effectors with high specificity and performance. Neuron 85:942-958.

Makino S, Gold PW, Schulkin J (1994) Corticosterone effects on corticotropin-releasing hormone mRNA in the central nucleus of the amygdala and the parvocellular region of the paraventricular nucleus of the hypothalamus. Brain Res 640:105-112.

Marcinkiewcz CA, Mazzone CM, D'Agostino G, Halladay LR, Hardaway JA, DiBerto JF, Navarro M, Burnham N, Cristiano C, Dorrier CE, Tipton GJ, Ramakrishnan C, Kozicz T, Deisseroth K, Thiele TE, McElligott ZA, Holmes A, Heisler LK, Kash TL (2016) Serotonin engages an anxiety and fear-promoting circuit in the extended amygdala. Nature 537:97-101.

Martin EI, Ressler KJ, Jasnow AM, Dabrowska J, Hazra R, Rainnie DG, Nemeroff CB, Owens MJ (2010) A novel transgenic mouse for gene-targeting within cells that express corticotropin-releasing factor. Biol Psychiatry 67:1212-1216.

Martin P, Albagli O, Poggi MC, Boulukos KE, Pognonec P (2006) Development of a new bicistronic retroviral vector with strong IRES activity. BMC Biotechnol 6:4.

Mizuguchi H, Xu Z, Ishii-Watabe A, Uchida E, Hayakawa T (2000) IRES-dependent second gene expression is significantly lower than cap-dependent first gene expression in a bicistronic vector. Mol Ther 1:376-382.

Peng J, Long B, Yuan J, Peng X, Ni H, Li X, Gong H, Luo Q, Li A (2017) A Quantitative Analysis of the Distribution of CRH Neurons in Whole Mouse Brain. Front Neuroanat 11:63.

Raymond CS, Soriano P (2007) High-efficiency FLP and PhiC31 site-specific recombination in mammalian cells. PLoS One 2:e162.

Refojo D, Schweizer M, Kuehne C, Ehrenberg S, Thoeringer C, Vogl AM, Dedic N, Schumacher M, von Wolff G, Avrabos C, Touma C, Engblom D, Schutz G, Nave KA, Eder M, Wotjak CT, Sillaber I, Holsboer F, Wurst W, Deussing JM (2011) Glutamatergic and dopaminergic neurons mediate anxiogenic and anxiolytic effects of CRHR1. Science 333:1903-1907.

Rodríguez CI, Buchholz F, Galloway J, Sequerra R, Kasper J, Ayala R, Stewart AF, Dymecki SM (2000) High-efficiency deleter mice show that FLPe is an alternative to Cre-loxP. Nat Genet 25:139-140.

Romanov RA et al. (2017) Molecular interrogation of hypothalamic organization reveals distinct dopamine neuronal subtypes. Nat Neurosci 20:176-188.

Salimando GJ, Hyun M, Boyt KM, Winder DG (2020) BNST GluN2D-Containing NMDA Receptors Influence Anxiety- and Depressive-like Behaviors and ModulateCell-Specific Excitatory/Inhibitory Synaptic Balance. J Neurosci 40:3949-3968.

Sanford CA, Soden ME, Baird MA, Miller SM, Schulkin J, Palmiter RD, Clark M, Zweifel LS (2017) A Central Amygdala CRF Circuit Facilitates Learning about Weak Threats. Neuron 93:164-178.

Sarkar J, Wakefield S, MacKenzie G, Moss SJ, Maguire J (2011) Neurosteroidogenesis is required for the physiological response to stress: role of neurosteroid-sensitive GABAA receptors. J Neurosci 31:18198-18210.

Sarkar P, Koushik SV, Vogel SS, Gryczynski I, Gryczynski Z (2009) Photophysical properties of Cerulean and Venus fluorescent proteins. J Biomed Opt 14:034047.

Soden ME, Yee JX, Cuevas B, Rastani A, Elum J, Zweifel LS (2022) Distinct Encoding of Reward and Aversion by Peptidergic BNST Inputs to the VTA. Front Neural Circuits 16:918839.

Taniguchi H, He M, Wu P, Kim S, Paik R, Sugino K, Kvitsiani D, Fu Y, Lu J, Lin Y, Miyoshi G, Shima Y, Fishell G, Nelson SB, Huang ZJ (2011) A resource of Cre driver lines for genetic targeting of GABAergic neurons in cerebral cortex. Neuron 71:995-1013.

Ulrich-Lai YM, Herman JP (2009) Neural regulation of endocrine and autonomic stress responses. Nat Rev Neurosci 10:397-409.

Walker LC, Cornish LC, Lawrence AJ, Campbell EJ (2019) The effect of acute or repeated stress on the corticotropin releasing factor system in the CRH-IRES-Cre mouse: A validation study. Neuropharmacology 154:96-106.

Wang Y, Hu P, Shan Q, Huang C, Huang Z, Chen P, Li A, Gong H, Zhou JN (2021) Single-cell morphological characterization of CRH neurons throughout the whole mouse brain. BMC Biol 19:47.

Tables

Table 1. Summary of CRH-related Cre/Flp-driver and reporter mouse lines

Mouse lines*	MGI ID	Description	Reference
CRH-Cre lines			
CRFp3.0Cre	MGI:4457114	Transgenic - random insertion in mouse genome	(Martin et al., 2010)
CRH-Cre(KN282)	MGI:4366795	BAC transgenic - random insertion in mouse genome	(Sarkar et al., 2011)
CRH-ires-Cre	MGI:4452089	Knock-in - in the endogenous *Crh* locus	(Taniguchi et al., 2011)
Crh-IRES-Cre	MGI:5559540	Knock-in - in the endogenous *Crh* locus	(Krashes et al., 2014)
CRF-iCre	MGI:5707348	Knock-in - in the endogenous *Crh* locus	(Itoi et al., 2014)
CRH-icreERT2	MGI:5568222	BAC transgenic - insertion in the *Hprt* locus	(Korecki et al., 2019)
CRH-Flp line			
Crh-IRES-FlpO	MGI:6116854	Knock-in - in the endogenous *Crh* locus	(Salimando et al., 2020)
CRH reporter lines			
8.7 CRH β-gal	n/a	Transgenic - random insertion in mouse genome	(Keegan et al., 1994)
CRH-GFP	MGI:5586654	BAC transgenic - random insertion in mouse genome	(Alon et al., 2009)
CRF-Venus	MGI:5707346	Knock-in - in the endogenous *Crh* locus	(Itoi et al., 2014)
CRF-VenusΔNeo	MGI:6144041	Knock-in - in the endogenous *Crh* locus	(Kono et al., 2017)

*Names of mouse lines adhere to the nomenclature used in the indicated references. CRH/CRF: corticotropin releasing hormone/factor. MGI: Mouse Genome Informatics. n/a: not available.

3 Discussion

3.1 Short summary of main results

3.1.1 Brain injury-induced expression of neuropeptide CRH in oligodendrocyte progenitor cells influences early oligodendroglial differentiation

In this study we identified a new neuropeptide system in the OL lineage, connecting CRH and CRHR1 with the modulation of regenerative processes following injury. We were able to show that CRH expression and the likely release of CRH precedes OPC proliferation, identifying it as one of the earliest reactions towards injury described so far. By using different CRH and CRHR1 reporters, KO and OE mouse models we demonstrated that CRH-expressing OPCs target CRHR1-expressing OPCs and astrocytes, thereby stalling early differentiation processes of the whole OLC population. Our study highlights the potential role that neuropeptides, either released from glia or neurons can take in the process of oligodendrogenesis.

3.1.2 Differential CRH expression level determines efficiency of Cre- and Flp-dependent recombination

In this study we investigated the differential reporting properties of *CRH-Cre* and *CRH-FlpO* mouse models, to better understand their capacity to report CRH expression. In both models, the spatial expression pattern replicated that of CRH itself, with *CRH-Cre* reporting a higher number of cells. By using 9 different mouse models we demonstrated, that FlpO recombination efficiency and consequential reporting capacity is highly dependent on the strength and current activation state of the driving promoter. In case of *CRH-FlpO,* recombination efficiency was increased by an acute stressor, like restrained stress, which led to an increase in CRH reported cells in the analysed brain regions. These results highlight the need for in-depth characterization and a detailed assessment of new site-specific recombinase mouse lines, before use. In sum, the presented results were not only essential for the interpretation of our own data, but can contribute to the reasonable interpretation of experiments performed by the scientific community, using Cre and FlpO-harbouring mouse lines.

3.2 CRH expression in OPCs

The identification of CRH-expressing cells around an injury site in the CRH reporter mouse model *CRH-Cre::Ai9* was an intriguing finding that called for further investigation. In contrast to other neuropeptides like dynorphin A (Faden et al. 1985; Przewłocki et al. 1988; Yakovlev and Faden 1994), CRH upregulation following CNS injury had not been described, so far. Following identification of these cells as OPCs by anti-NG2 staining, their identity and CRH-expressing nature was confirmed using different approaches, like intersectional mouse models visualizing CRH-NG2 co-expression by FlpO- and Cre-dependent tdTomato expression, direct anti-CRH staining and DISH against *Crh* and *Pdgfrα* mRNA. The identification of CRH^+ cells as OPCs was especially surprising because due to the genetic structure of the *Crh* gene locus with its neuron restrictive element RE-1/NRSE, its expression was thought to be exclusive to neurons (Schoenherr and Anderson 1995). Although, interaction between RE-1/NRSE and the RE-1 silencing transcription factor (REST) leads to the silencing of the gene locus, its' expression can also be enhanced by it (Seth and Majzoub 2001b). REST is also expressed in OPCs and has been shown to be upregulated during differentiation processes. Here it was thought to prevent neuronal gene expression, because implementation of a dysfunctional REST led to impaired oligodendrogenesis and more OLs with neuronal morphology (Dewald, Rodriguez, and Levine 2011). Whether CRH expression in OPCs is due to a failed RE-1/NRSE-mediated silencing or an enhancement by REST, future research has to show. Interestingly, CRH^+ OPCs were not found in the murine brain under non-injury conditions, wherefore CRH expression had to be triggered by acute injury. Because OPCs are known to react to injuries in different ways, CRH^+ OPCs were investigated concerning their population dynamics, reaction towards the injury site as well as CRH expression kinetics.

3.3 Identification and population dynamics

A well described reaction of OPCs upon injury is their strong proliferative response (Simon, Gotz, and Dimou 2011). The population dynamics of CRH^+ OPCs, with their steep increase between 1 and 7 days, their subsequent decrease and presence at relatively steady numbers up to 4 months post injury was comparable to what had been described in the literature (Dimou et al. 2008). By spatiotemporal analysis of the injury site, CRH-expressing OPCs were shown to appear within the first 300 µm around the wound centre followed by an increase in their total number, reaching up to 15% of the total OLC population. Subsequent to a progressive inward movement towards the injury core, the total number of cells was reduced again. As already mentioned above, the steep increase was caused by their appearance as well as their inward movement, but also by their strong proliferation, as 100% of cells were $Ki67^+$ at 2 dpi. Therefore, CRH-expressing OPCs show a behaviour similar to the whole population of OPCs as revealed in a very detailed *in vivo* 2-photon imaging study analysing the time-dependent reaction of cortical OPCs following stab wound injury (von Streitberg et al. 2021). Here, the inward movement as well as proliferation were found to be the main drivers of increased OPC numbers upon damage. Also,

the time course of migration and proliferation seems to be comparable between their study and our results. Although their general behaviour seems to be similar, CRH-expressing OPCs have a significantly higher tendency to proliferate. In their study, a maximum of 40 % in the whole population proliferated, compared to 100 % in CRH^+ OPCs. Therefore, CRH expression either is a reaction that is triggered by the same or a comparable stimulus that later on leads to proliferation or CRH-expressing OPCs resemble a subpopulation of cells with an exceptionally high capacity to proliferate. Obviously, the observed differences in proliferation could also be caused by the different injury models and the region, that was analysed. WM and GM OPCs have already been shown to differ in their properties under physiological conditions (Dimou et al. 2008), thus their reaction to injury might also differ. Whether this regional heterogeneity is caused by intrinsic differences or depends on the environment, remains not fully understood.

3.4 Maturation into OLs

As mentioned above, CRH-expressing OLCs reduce their number following 7 dpi. This decrease in cell number could be explained by the current model of OPC differentiation into mature OLs following demyelination or injury, as described in the introduction. In brief, a high differentiation rate results in a high number of premyelinating OLs and thus to a higher number of cells that do not find a stable connection to the surrounding axons. Subsequently, this leads to their death because of the limited access to nutrients (Hughes et al. 2018; Hughes and Stockton 2021). Indeed, the high maturation rate of CRH-expressing OPCs, of approximately 80%, supports this idea. Additionally, it has to be mentioned, that previous experiments analysing acute injury in the cortex showed that cortical OPCs differentiate at a lower rate of around 30% (Dimou et al. 2008). This difference to our results might be explained by the fact that the injury in our study was performed in the midbrain, a region which is very rich in myelinated fibre tracts and possesses a high number of OLs, more comparable to pure WM (Tripathi et al. 2017). As WM OPCs have a higher tendency to differentiate under non-injury conditions, the higher maturation rate of CRH^+ OPCs following injury could also be caused by region-specific properties, independent of CRH expression (Dimou et al. 2008). Although the population dynamics of CRH-expressing OLCs are comparable with non-CRH-expressing OLCs, their stronger long-term decrease in total number is characteristic only for the CRH^+ population. This observation might also be explained by their high differentiation rate, but no further data was gathered to analyse these potential differences in more detail. All the above described properties like appearance, subsequent proliferation and migration as well as maturation were confirmed on a single cell level by *in vivo* 2-Photon imaging. Furthermore, we were able to confirm that CRH-expressing OPCs mature in a stepwise manner, typical for OL generation (de Faria et al. 2021). The generated premyelinating OLs, which were identified by their morphology, high motility of filopodia and formation of lamellipodia, were also shown to disappear. Likely this disappearance was caused by their degeneration, because an outward movement that would lead to the appearance of CRH^+ OLCs at distant regions from an injury site, was never observed. Still, a day-by-

day tracking of CRH$^+$ premyelinating OLs is necessary to confirm this hypothesis. In sum, the CRH-expressing OPC population shows the hallmarks of OPCs' injury reaction, including migration, proliferation and maturation, but differs in its long-term development, potentially caused by its high maturation rate.

3.5 Expression kinetics and sequential cellular response

CRH expression was shown to start within the first 12 h following injury infliction and therefore precedes any other transcriptional change by OPCs towards acute injury described so far. An in-depth literature analysis additionally showed that in a very recent study analysing transcriptional changes between 15 min and 42 days post spinal cord injury, CRH-upregulation was detected at 1 dpi, so exactly within the time window described in our study (Li et al. 2022). These results further validate and strengthen our finding. Because most studies concentrate on a time scale of days following injury, in many analysis OPC-connected changes within the first 24 hpi are not well described and OPC reactions are mainly analysed concerning morphological changes like polarization and hypertrophy and their increase in cell numbers by proliferation (von Streitberg et al. 2021).

As implicated by the early start of its expression, injury-induced CRH upregulation within OPCs seemed to precede proliferation, which is usually initiated around 2 dpi. As *CRH-Venus* mice harbour a YFP, that is not destabilized (Li et al. 1998), its degradation within the cell can take more than 24 h (He et al. 2019). Although this prolongs the reporting of CRH expression within this model, it enables the short-term tracking of cells after they expressed CRH. When performing Ki67 staining, co-localization of Venus and Ki67 was not observed before 36 hpi and also later, remained a rare event. Additionally, Venus$^+$ doublets, supposedly caused by proliferation, were only visible starting at 36 hpi, confirming the Ki67 result. Still, in *CRH-Cre::Ai9* mice 100% of tdTomato$^+$ cells were also Ki67$^+$ at 48 hpi. Although this finding might be counter intuitive, it follows the logic of the used reporter models. Because in Cre-driven reporting, the level of Cre recombinase needs to be high enough, to delete the STOP cassette upstream of tdTomato. Only then, tdTomato expression is driven by the strong synthetic CAG promoter. Therefore, cells that are tdTomato$^+$ around 2 dpi must be the earliest CRH-expressing cells already observed at 12 hpi in the *CRH-Venus* model and probably do not express CRH anymore. Whether CRH expression in CRH$^+$ OPCs is a prerequisite for proliferation was not analysed in more detail. Because the initiation of proliferation upon injury is only poorly understood, this question should be addressed in future experiments. Although, it has to be mentioned that CRHR1 KO experiments did not show any difference in the proliferative properties of the OLC population, wherefore, a direct involvement of CRH or its receptor is unlikely. Concerning the expression strength, it is noteworthy that in our *CRH-FlpO* validation paper *CRH-Venus* mice were clearly shown to report CRH-expressing cells depending on the strength of their endogenous CRH expression. The fact that CRH-expressing OPCs surrounding the injury site in *CRH-Venus* mice were found to be visible even without any anti-GFP staining and, therefore, drastically brighter than the majority of CRH-expressing neurons, implies a

superior expression level (Zhao et al. 2023). This high expression level is also shown by direct anti-CRH staining. As already mentioned above, CRH-peptide was identified by anti-CRH staining within PDGFRα$^+$ cells surrounding the injury site, confirming CRH expression in OPCs. This result was further validated by CRH$^+$ vesicles in Venus$^+$ cells in *CRH-Venus* mice. The analysis of these CRH$^+$ OPCs showed that the whole cell was filled with CRH$^+$ vesicles, contributing to the notion that CRH expression and potential release upon injury is rather strong. With an approximated diameter between 250 and 600 nm (data not shown) their size was comparable to neuropeptide releasing vesicles, namely LDCVs, in other cell types (Merighi 2018). Whether these vesicles also display other properties of LDCVs like the name giving "dense core", future studies, including super resolution microscopy and electron microscopy, have to show (van den Pol 2012). Still the identification of potential secretory vesicles in these reporter-expressing cells raised the question for potential target structures. Further, it necessitates an in-depth analysis of the secretory properties of OPCs in general.

3.6 Identification of CRHR1-expressing cells surrounding the injury site

In recent years, OPCs have been attributed with an immune modulatory function. They were shown to respond to pro inflammatory cytokines like IFNγ by antigen presentation (Kirby et al. 2019) and influence microglial activation by targeting TGFβR2 via TGFβ2 secretion (Zhang et al. 2019). Therefore, the analysis of possible target receptors on other cell types, surrounding the injury site was necessary. CRH is known to bind two different GPCRs, CRHR1 and CRHR2. Centrally, CRHR1 is the predominant CRHR and CRH's high affinity receptor. We identified CRHR1 in OPCs as well as astrocytes, both surrounding the injury site, but also under uninjured conditions. In contrast to earlier studies, showing CRHR1 expression also in microglia (Stevens et al. 2003), we did not find any CRHR1$^+$/IBA1$^+$ cells. The analysis of different openly accessible sequencing repositories confirmed the expression of CRHR1 by OLCs and astrocytes (Zhang et al. 2014; Zeisel et al. 2015; Brown et al. 2016; Zeisel et al. 2018; Falcao et al. 2019). Although, one has to mention that CRHR1 expression was found to be very low in all studies. This is in line with data from our own lab, showing that CRHR1 expression in single cell sequencing is only detected at very low levels even when the analysis is concentrated on CRHR1$^+$ cells derived from a CRHR1-reporter mouse model (Chang et al. 2022). Because both CRHR1-expressing glial populations were identified in a Cre-dependent mouse model, the question, whether their reporting resembled an ongoing adult receptor expression or represented a legacy expression caused by transient developmental upregulation, needed to be answered. Therefore, adult expression was tested using two approaches: Identification of CRHR1-expressing cells i) in the reporter line R1-GFP, a model harbouring a GFP knock-in inside the *Crhr1* locus, therefore, enabling visualisation of endogenous expression and ii) by using different Cre-dependent AAV models. Adult receptor expression in OPCs was confirmed in R1-GFP and via AAV reporting and in astrocytes by AAV mediated reporting, only. Thus, two main questions arose: i) Whether CRH and CRHR1-expressing

OPCs represent the same or two distinct populations of cells and ii) whether CRHR1-expressing OPCs and astrocytes had a functional influence on post-injury processes.

3.6.1 CRHR1$^+$ subpopulation of OLCs: Characterization and functional relevance

First, the question whether the CRH/CRHR1 system in OPCs resembles an autocrine or paracrine system was addressed. The analysis of *CRHR1-Cre::CRH-FlpO::Ai65* mice, a mouse model in which only CRH/CRHR1 co-expressing cells express the reporter tdTomato, showed that co-expressing cells were present. Still, the number of cells around the injury site was smaller compared to the number of CRH-expressing cells found in close proximity of the injury in the *CRH-Cre::Ai9* mouse model. Two explanations were imaginable: i) A reduced reporting capacity of CRH in combination with FlpO, leading to an overall reduced reporting in the Ai65 model, as shown in the *CRH-FlpO* reporter study (Zhao et al. 2023) or ii) a minor overlap of two distinct populations of OPCs expressing either CRH or CRHR1, respectively. Therefore, a quadrupole reporter line was generated in which CRH expression was reported by FlpO-dependent tdTomato expression and CRHR1 expression by Cre-dependent Sun1-GFP labelling of cells. Thereby, all three potential populations could be visualized. It turned out that, CRH/CRHR1 co-expressing cells resembled only a small minority of cells (≈5 %), identifying CRH and CRHR1-expressing OPCs as two separate populations. The separation of these two subpopulations necessitated an in-depth analysis of CRHR1-expressing OLCs. Their quantification under non-injured conditions at different ages showed that their numbers increased on an absolute level, but also in relation to the whole population of OLCs present at these stages. Because the number of OPCs is tightly regulated within the murine brain (Hughes et al. 2013), this elevation could only be caused by an increase in the total number of mature OLs. This hypothesis is further supported by the fact, that the increase in the total number of CRHR1-expressing OLCs was far greater than that observed for CRHR1$^+$ OPCs. Although oligodendrogenesis has been shown to happen mainly in an early developmental time window, it is indeed a life-long process (Tripathi et al. 2017; de Faria et al. 2021). Therefore, CRHR1-expressing OLCs seemingly contribute to this adult oligodendrogenesis more than other OPC subpopulations. Additionally, CRHR1-expressing OLCs also co-localized with GPR17. The subpopulation of GPR17$^+$ OPCs is a clearly identified and deeply characterized OPC subset, which makes up ≈14 % of all OPCs and has been connected to maturation processes during development (Chen et al. 2009) but also following injury and other pathophysiological conditions (Vigano et al. 2016; Bonfanti et al. 2020; Miralles et al. 2023). Their maturation rate under non-injured conditions was shown to be rather low and their cell numbers to be stable over long periods of time (Vigano et al. 2016; Miralles et al. 2023). Therefore, the fact that CRHR1$^+$ cells, apparently a population with a high maturation rate under non-injured conditions, and GPR17$^+$ cells with their low maturation rate, show a population overlap, raises important questions. i) Do CRHR1-expressing OPCs resemble a subpopulation as was shown for GPR17$^+$ OPCs? ii) Is CRHR1 constantly expressed in the OLC population or only transiently

during certain stages along their differentiation? iii) Does the GPR17-expressing fraction of the CRHR1$^+$ OPCs contribute to the increase in CRHR1$^+$ OLCs?

For future experiments, one mouse model related issue has to be addressed. Due to the wide expression of CRHR1 throughout the brain, targeting it with transgenic mouse models is a challenging endeavour. To visualize single cells, neuronal expression has to be reduced by complementing a *CRHR1-Cre::Ai9* model, in which tdTomato is flanked by FRT sites, with a *Tau-LSL-FlpO*. This leads to the repression of tdTomato expression in all Tau-expressing cells by the FlpO-dependent excision of tdTomato. Tau is mainly expressed in neurons, but can also be found in mature OLs. As we have shown, FlpO-dependent recombination is influenced by the strength of the driving promoter, wherefore, depletion of reporting in OLs might be only slightly reduced. Still, to not underestimate the amount of CRHR1$^+$ OLCs, the quantification should be validated within a different reporter model like *CRHR1-INTACT* in which only the nuclear membrane of CRHR1-expressing cells is visible, wherefore, a clear identification of single cells, even without decreased reporting, is possible.

3.6.2 Functional effects of CRH/CRHR1 modulation on OPCs

To better understand the actual role of CRH expression by OPCs and its potential effect on CRHR1-expressing OLCs, different gain- (GOF) and loss-of-function (LOF) experiments were performed, including CRH injection, global and OPC-specific CRH OE, OPC-specific CRH KO as well as OPC-specific and global CRHR1 KO. GOF experiments showed no influence on the OPC nor on the OL population surrounding the injury site. Apparently, the further increase of CRH, above the already present level caused by the released from OPCs and neurons upon injury and the resulting increase in CRH/CRHR1 signalling does not influence OLC processes. LOF experiments, on the other hand, showed a significant decrease in OPCs and a non-significant increase of CC1$^+$ OLs at 7 dpi. Seemingly, OLC behaviour is unchanged as long as CRH/CRHR1 signalling is present, independent of an increased amount, but is altered only when signalling is reduced. Interestingly, in OPC-specific CRHR1 KO animals this result was not replicated, implying that also other CRHR1-expressing cells in the area influence OPCs' behaviour following injury. However, the reason for the decreased number of OPCs in close proximity of the injury site could have had two reasons: i) Alterations in the proliferative response of the OPC population or ii) a higher differentiation rate. Labelling proliferating OPCs by BrdU and subsequently comparing the number of newly generated OLs in global CRHR1 KO vs WT animals revealed that an increased differentiation of OPCs into OLs was the cause. Further, the total number of OLs within the first 150 µm around the injury site was found to be increased by an extend, that could not only be explained by the number of BrdU$^+$ OLs. Therefore, direct differentiation, without prior proliferation probably contributed to the observed differences in the population of newly generated OLs. Of course, also an increased survival of OLs following injury could be the cause for the higher number of OL in CRHR1 KO animals. Because of the consistent observation of a reduced number of OPCs surrounding the injury site in OPC-specific CRH and global CRHR1 KO, this explanation loses its

plausibility, though. If an increased OL survival would be the cause, this could only influence the OPC population by a differential proliferative response. This difference is not visible in the BrdU experiment, wherefore, OL survival is probably not a contributing factor. The increased number of $BrdU^+$ but also $BrdU^-$ $CC1^+$ cells did not persist and the overall number of mature OLs at 6 weeks post injury was equal between the genotypes. Therefore, rather than long-term OL generation, the speed of differentiation following injury seems to be influenced by the CRH/CRHR1 system.

To fully understand the potential function of the CRHR1 in OLCs, one has to look at the complete picture, which includes results gathered from the modulation studies, but also from the quantification of $CRHR1^+$ OLCs under non-injury conditions. CRHR1 signalling acts as a stalling mechanism for OPC differentiation following injury. Still, CRHR1-expressing OPCs have a higher maturation rate compared to other OPCs under non-injury conditions. Although this seems contradictory, it is not. OPC differentiation is, as commonly known, influenced by many different factors including neuronal activity, hormonal function and the interaction with other cell types or the ECM (see Introduction, (Hughes and Stockton 2021)). Therefore, CRHR1 cannot be the only determining factor in the differentiation of CRHR1-expressing OPCs. The higher maturation rate of $CRHR1^+$ OPCs might necessitate a stalling mechanism that prevents premature differentiation only under certain conditions, e.g., following injury. This would also explain why under non-injury conditions CRHR1 KO animals did not show a difference in the number of newly generated OLs nor in the total number of mature OLs. The total amount of newly generated OLs is unchanged because only the speed of early differentiation processes was increased.

Although CRH-expressing OPCs are not present under non-injury conditions, the functional relevance of this system under non-injury conditions has to be seen in the light of i) the unphysiological holding conditions, ii) potential other sources of CRH, like neurons connected to stress-related behaviour and ii) our limited insight into the downstream signalling pathways of CRHR1 within OLCs and its potential contribution to OL maturation under non-injury conditions. As compared to GPR17, which apparently only modulates OPC differentiation following acute injury, CRHR1 might have a context-dependent effect on the expressing cell. In case of non-injured animals, the KO leads to no change in the number of mature OLs, but following injury the lack of CRHR1 leads to an increased number of newly formed OLs. Therefore, CRHR1 signalling seems to represent an inhibitory drive, that transiently slows maturation down when activated by CRH, without influencing the total number of mature OLs. Interestingly, a comparable phenomenon was reported in one of the earlier studies of GPR17 and its role in oligodendrogenesis (Chen et al. 2009). Here, the global KO of GPR17 led to an increased speed of oligodendrogenesis, without effecting the overall number of OLs. Furthermore, neuropeptides like galanin and dynorphin A have already been connected to the process of oligodendrogenesis. Due to their wide-spread expression throughout the brain and their, compared to neurotransmitters, long-lasting release mechanisms, neuropeptides are ideally suited to influence changes in CNS myelination.

3.6.3 CRHR1-expressing astrocytes: an additional factor

As already discussed above, the CRH/CRHR1 system seems to influence OPC differentiation following injury. While global CRHR1 inactivation and OPC-specific CRH KO are able to induce changes in the OLC population, the OPC-specific CRHR1 KO is not. Therefore, the observed differences might be influenced by CRHR1-expressing astrocytes, also identified around the injury site. The fact that astrocytes can influence OPC differentiation and oligodendrogenesis by different factors has long been acknowledged (see introduction). Therefore, astrocytic changes were also analysed in the previously described GOF and LOF experiments. CRH injection led to an increased GFAP expression in astrocytes surrounding the injury site. Although CRHR1-expressing astrocytes only resemble a minority of all astrocytes present, these changes were shown to have a global influence on the astrocytic population. This effect was mediated by CRHR1, as its KO depleted the CRH-induced GFAP upregulation. Furthermore, not only GFAP but also vimentin expression was influenced by the astrocytic CRHR1. Thus, rather than influencing only GFAP, CRHR1-dependent signalling in astrocytes apparently has an effect on astrocyte activation, in general. How the signal is transmitted from the minority of CRHR1-expressing astrocytes to the whole population remains unclear. Fast communication between astrocytes via gap junctions has been proposed in the past (Stephan, Eitelmann, and Zhou 2021). This form of communication does not necessitate the relatively long transmission by release of a diffusible factor within the extracellular space and would explain the fast transmission from one $CRHR1^+$ astrocytes to the surrounding cells within a short time window following CRH-release from OPCs. Besides, it remains unclear, whether CRHR1-expressing astrocytes resemble a distinct subpopulation with other specific characteristics. Because the astrocyte population has been shown to be rather diverse (Tsai et al. 2012; Hasel et al. 2021), this is a question that needs to be addressed in future experiments.

Parameters associated with enhanced wound healing like increased vascular recovery and neuronal survival were not changed following CRH injection. Apparently, rather than having a long-term effect, CRH seems to influence the speed of GFAP upregulation. Changes in neuronal survival, a factor also influenced by the amount of astrogliosis, was only changed in CRHR1 KO animals. In combination with the result that the OLC population also displays changes only under conditions of reduced CRH/CRHR1 signalling shows, that a further increase or antedating of CRH's action by its direct injection does not affect the healing process. It only causes a premature GFAP upregulation in astrocytes, which is attenuated by 7 dpi. Thus, the presence of CRH above a certain threshold seems to be essential, while a further increase is not as influential. As already described in the introduction, CRHR1 inhibition led to a downregulation of GFAP, IBA1 an TNFα following global cerebral ischemia (de la Tremblaye et al. 2017b). Although no functional connection with CRHR1-expressing astrocytes is put forward, they might have been involved. Future experiments have to show whether astrocytes display other, e.g., transcriptional changes, when modulating the CRH/CRHR1 system by up or downregulation and

whether they release substances like PDGFA, known to mediate astrocytic influence on OLC behaviour (Pringle et al. 1989; Richardson et al. 1988).

3.7 Expression strength as determining factor of FlpO recombination efficiency and its influence on CRH-related scientific questions

Because of the limited accessibility of the CRH/CRHR1 system by antibody-based approaches, the study of the CRH/CRHR1 system in OPCs and astrocytes had to rely on a plethora of different reporter mouse models. Although *CRH-Cre* reporter lines have been widely used and extensively validated concerning their expression pattern in the murine brain (Taniguchi et al. 2011; Chen et al. 2015), the singular use of one recombinase sets limitations in the analysis of this system. First of all, by using only one recombinase, specific subpopulations, like the CRH-expressing OPCs, cannot be specifically visualized. Therefore, the development of a *CRH-FlpO* mouse line by Salimando and colleagues opened up new opportunities for the analysis of the CRH/CRHR1 system (Salimando et al. 2020). Although early experiments, using the *CRH-FlpO::Ai65F* or the intersectional *NG2-Cre::CRH-FlpO::Ai65* line showed that CRH expression in OPCs can be reported with these systems, the number of reported cells was found to be smaller compared to the *CRH-Cre::Ai9* model. This, in addition to the observation that reporting of neuronal CRH expression using *CRH-FlpO::Ai65F* was reduced, compared to *CRH-Cre::Ai9* raised the need for a more detailed analysis of the *CRH-FlpO* line to identify the cause of differential reporting and to reasonably evaluate future results. Although following recombination of an identical STOP cassette reporting by tdTomato is driven by a CAG promoter in both lines, the genetic composition in which the tdTomato is incorporated differs slightly (Madisen et al. 2015; Madisen et al. 2010). The very detailed analysis of 9 different CRH reporter mouse lines, led to the conclusion that the reduced reporting was not caused by these differences but by FlpO-associated properties. We were able to show that CRH reporting in *CRH-FlpO* mice recapitulates the expression pattern in *CRH-Cre* models, but is inferior in its capacity to report CRH expression, due to a reduced recombination efficiency. Additionally, reporting could be increased, e.g., by applying an acute stress model, wherefore, expression strength of the driving promoter is the main determinant of FlpO-dependent recombination. These results also have direct implications for the study concerning the CRH/CRHR1 system in OPCs. First of all, the number of cells reported in *CRH-Cre::Ai9* mice following injury represent the best approximation of the CRH-expressing population of OPCs in this area. Reduced cell numbers, visible in intersectional approaches harbouring *NG2-CreERT2* and *CRH-FlpO* are not only limited in their reporting capacity by the tamoxifen inducible CreERT2, usually having a recombination efficiency between 60 and 80% (Zhu et al. 2011), but also by the FlpO-connected impairment. Therefore, *NG2-CreERT2::CRH-FlpO::Ai65* mice could be used for a validation of CRH-NG2 co-expression upon injury, but not for any quantification of this specific population. Further testing is necessary to validate, whether this inefficient CRH-reporting is compensated for in homozygous FlpO mice. In sum, we are

certain that general rules can be deduced from this characterization study that apply to any given scientific question that necessitates the singular or combinatorial use of recombinases: i) When comparing *Cre* and *FlpO* driven reporting the strength of the driving promoter has to be taken into account, ii) when using trans sectional approaches to label specific subpopulation the efficacy of reporting is determined by the recombination efficiency of *FlpO* and iii) when using *FlpO* for OE or KO of a certain marker a deep validation of its efficacy in the specific population is necessary. Furthermore, data gathered from *FlpO* experiments cannot directly be compared to those using *Cre*, without prior characterization.

3.8 Conclusion and outlook

In this thesis we present a novel neuropeptide system, consisting of CRH and its receptor CRHR1 in OLCs and astrocytes influencing regenerative processes following acute brain injury. The thorough confirmation and characterization of the neuropeptide CRH as well as its receptor CRHR1 distinguishes this study from previous ones concerning neuropeptide expression in OPCs in which the validation of peptide expression but also of the receptors was not performed as intensely. We further show, that early CRH release from OPCs targets CRHR1-expressing OPCs and astrocytes stalling premature differentiation of OPCs. Although the functional role of this stalling mechanism remains elusive, the gathered results have to be seen in the light of previously published work on neuropeptides and GPCRs and their influence on OLCs, namely dynorphin A, galanin and GPR17. These have already been shown to modulate OPC differentiation. Therefore, this study represents the next step in understanding neuropeptides' role in CNS function and recovery, especially in the context of glia-glia communication and its influence on OL generation. Still, many open questions remain that necessitate further experiments.

To better understand the endogenous differences between CRH-expressing versus non-expressing OPCs and their long-term reaction following injury, a label retaining experiment in *CRH-Cre::Ai9* mice has to be performed. This enables the assessment and comparison of their proliferative capacity and their oligodendrogenic potential. Although, one needs to mention that direct differentiation without prior proliferation could only be assessed in the CRH-expressing population in this experimental setup. Another important question is whether CRH expression necessarily precedes proliferation or can also stand by itself. To answer this question, other triggers have to be identified first because BBB breakdown usually leads to a strong proliferative response.

Also, CRHR1-expressing OPCs and the population of OLs derived from them need further investigation. Therefore, the function of CRHR1-expressing OPCs following injury but also under non-injury conditions needs to be deeply analysed. On the one hand, a long-term label retaining experiment has to be performed in *CRHR1-Cre::INTACT* mice, either confirming or neglecting the hypothesis of their high oligodendrogenic potential under physiological conditions. In this context, the influence of CRH on CRHR1-expressing OPCs should also be tested, by searching for conditions in which this

oligodendrogenic potential is changed, e.g., during chronic stress, associated with increased CRH release and expression from and in neurons. Additionally, a detailed analysis of the reaction of CRHR1-expressing OPCs following injury is mandatory. Ideally, this analysis would be complemented by the assessment of the effect of CRH/CRHR1 signalling downregulation on these processes. Because of the genetic design of the currently used mouse models for CRH or CRHR1 KO an analysis of the CRHR1-expressing cells while CRH or CRHR1 is knocked out, is impossible. Pharmacological targeting of CRHR1 would be the solution. Although CRHR1 inhibitors are available, their application has proven to be difficult and mostly did not lead to the desired performance in previous experiments.

The most important question, however, is why CRH expression in OPCs and the proposed stalling of OL generation is necessary following injury and whether there are other conditions that trigger this mechanism. Obviously, murine housing conditions are rather artificial, without essential stimuli like exposure to predators, life-long social stress or immune stimulation by infection. Therefore, it is hard to estimate, whether wild mice do express and release CRH from OPCs on a regular basis. It seems necessary to test as many different stimuli as possible. Thus, different animal models of diseases with and without clear involvement of OLCs should be tested. This includes but is not limited to the MS models cuprizone and EAE, ALS models, Alzheimer's disease models, peripheral infection as well as different models inducing elevated stress, e.g., chronic social defeat or acute restraint stress. In these, not only the appearance of CRH-expressing OPCs, but also the effect of CRH/CRHR1 system modulation should be analysed. Like other neuropeptides, e.g., dynorphin A or galanin, CRH could play a vital role in the condition-dependent modulation of oligodendrogenesis under physiological but also pathophysiological conditions, thus resembling a potential target for future treatment.

4 References

Abd El-Aleem, S. A., and B. M. Morales-Aza. 2019. 'In Situ Hybridisation Study of Neuronal Neuropeptides Expression in Models of Mandibular Denervation with or without Inflammation: Injury Dependant Neuropeptide Plasticity', *J Cytol Histol*, 9.

Adjan, V. V., K. F. Hauser, G. Bakalkin, T. Yakovleva, A. Gharibyan, S. W. Scheff, and P. E. Knapp. 2007. 'Caspase-3 activity is reduced after spinal cord injury in mice lacking dynorphin: differential effects on glia and neurons', *Neuroscience*, 148: 724-36.

Aggarwal, S., N. Snaidero, G. Pahler, S. Frey, P. Sanchez, M. Zweckstetter, A. Janshoff, A. Schneider, M. T. Weil, I. A. Schaap, D. Gorlich, and M. Simons. 2013. 'Myelin membrane assembly is driven by a phase transition of myelin basic proteins into a cohesive protein meshwork', *PLoS Biol*, 11: e1001577.

Agnati, L. F., K. Fuxe, M. Zoli, I. Ozini, G. Toffano, and F. Ferraguti. 1986. 'A correlation analysis of the regional distribution of central enkephalin and beta-endorphin immunoreactive terminals and of opiate receptors in adult and old male rats. Evidence for the existence of two main types of communication in the central nervous system: the volume transmission and the wiring transmission', *Acta Physiol Scand*, 128: 201-7.

Aguilera, G., and Y. Liu. 2012. 'The molecular physiology of CRH neurons', *Front Neuroendocrinol*, 33: 67-84.

Allen, N. J., and C. Eroglu. 2017. 'Cell Biology of Astrocyte-Synapse Interactions', *Neuron*, 96: 697-708.

Almazan, G., P. Honegger, and J. M. Matthieu. 1985. 'Triiodothyronine stimulation of oligodendroglial differentiation and myelination. A developmental study', *Dev Neurosci*, 7: 45-54.

Alon, T., L. Zhou, C. A. Perez, A. S. Garfield, J. M. Friedman, and L. K. Heisler. 2009. 'Transgenic mice expressing green fluorescent protein under the control of the corticotropin-releasing hormone promoter', *Endocrinology*, 150: 5626-32.

Anderson, C. M., and M. Nedergaard. 2003. 'Astrocyte-mediated control of cerebral microcirculation', *Trends Neurosci*, 26: 340-4; author reply 44-5.

Andriezen, W. L. 1893. 'The Neuroglia Elements in the Human Brain', *Br Med J*, 2: 227-30.

Angelini, J., D. Marangon, S. Raffaele, D. Lecca, and M. P. Abbracchio. 2021. 'The Distribution of GPR17-Expressing Cells Correlates with White Matter Inflammation Status in Brain Tissues of Multiple Sclerosis Patients', *Int J Mol Sci*, 22.

Apletalina, Ekaterina, Jon Appel, Nazarius S. Lamango, Richard A. Houghten, and Iris Lindberg. 1998. 'Identification of Inhibitors of Prohormone Convertases 1 and 2 Using a Peptide Combinatorial Library*', *Journal of Biological Chemistry*, 273: 26589-95.

Asrican, B., J. Wooten, Y. D. Li, L. Quintanilla, F. Zhang, C. Wander, H. Bao, C. Y. Yeh, Y. J. Luo, R. Olsen, S. A. Lim, J. Hu, P. Jin, and J. Song. 2020. 'Neuropeptides Modulate Local Astrocytes to Regulate Adult Hippocampal Neural Stem Cells', *Neuron*, 108: 349-66.e6.

Bachiller, Sara, Itzia Jiménez-Ferrer, Agnes Paulus, Yiyi Yang, Maria Swanberg, Tomas Deierborg, and Antonio Boza-Serrano. 2018. 'Microglia in Neurological Diseases: A Road Map to Brain-Disease Dependent-Inflammatory Response', *Frontiers in Cellular Neuroscience*, 12.

Back, S. A., T. M. Tuohy, H. Chen, N. Wallingford, A. Craig, J. Struve, N. L. Luo, F. Banine, Y. Liu, A. Chang, B. D. Trapp, B. F. Bebo, Jr., M. S. Rao, and L. S. Sherman. 2005. 'Hyaluronan accumulates in demyelinated lesions and inhibits oligodendrocyte progenitor maturation', *Nat Med*, 11: 966-72.

Baigent, S. M., and P. J. Lowry. 2000. 'mRNA expression profiles for corticotrophin-releasing factor (CRF), urocortin, CRF receptors and CRF-binding protein in peripheral rat tissues', *J Mol Endocrinol*, 25: 43-52.

Banik, N. L., and M. E. Smith. 1977. 'Protein determinants of myelination in different regions of developing rat central nervous system', *Biochem J*, 162: 247-55.

Bardehle, Sophia, Martin Krüger, Felix Buggenthin, Julia Schwausch, Jovica Ninkovic, Hans Clevers, Hugo J. Snippert, Fabian J. Theis, Melanie Meyer-Luehmann, Ingo Bechmann, Leda Dimou, and

Magdalena Götz. 2013. 'Live imaging of astrocyte responses to acute injury reveals selective juxtavascular proliferation', *Nature Neuroscience*, 16: 580-86.
Barres, A, MA Lazar, and MC Raff. 1994. 'A novel role for thyroid hormone, glucocorticoids and retinoic acid in timing oligodendrocyte development', *Development*, 120: 1097-108.
Barres, B. A., I. K. Hart, H. S. R. Coles, J. F. Burne, J. T. Voyyodic, W. D. Richardson, and M. C. Raff. 1992. 'Cell-Death and Control of Cell-Survival in the Oligodendrocyte Lineage', *Cell*, 70: 31-46.
Barres, B. A., and M. C. Raff. 1994. 'Control of Oligodendrocyte Number in the Developing Rat Optic-Nerve', *Neuron*, 12: 935-42.
Beiter, R. M., C. Rivet-Noor, A. R. Merchak, R. Bai, D. M. Johanson, E. Slogar, K. Sol-Church, C. C. Overall, and A. Gaultier. 2022. 'Evidence for oligodendrocyte progenitor cell heterogeneity in the adult mouse brain', *Scientific Reports*, 12.
Bergles, D. E., and W. D. Richardson. 2016. 'Oligodendrocyte Development and Plasticity', *Cold Spring Harbor Perspectives in Biology*, 8.
Bergles, Dwight E., J. David B. Roberts, Peter Somogyi, and Craig E. Jahr. 2000. 'Glutamatergic synapses on oligodendrocyte precursor cells in the hippocampus', *Nature*, 405: 187-91.
Birey, F., M. Kloc, M. Chavali, I. Hussein, M. Wilson, D. J. Christoffel, T. Chen, M. A. Frohman, J. K. Robinson, S. J. Russo, A. Maffei, and A. Aguirre. 2015. 'Genetic and Stress-Induced Loss of NG2 Glia Triggers Emergence of Depressive-like Behaviors through Reduced Secretion of FGF2', *Neuron*, 88: 941-56.
Bloom, F. E., E. L. Battenberg, J. Rivier, and W. Vale. 1982. 'Corticotropin releasing factor (CRF): immunoreactive neurones and fibers in rat hypothalamus', *Regul Pept*, 4: 43-8.
Bohus, B., and D. De Wied. 1966. 'Inhibitory and facilitatory effect of two related peptides on extinction of avoidance behavior', *Science*, 153: 318-20.
Bondy, C. A., H. Gainer, and J. T. Russell. 1987. 'Effects of Stimulus Frequency and Potassium Channel Blockade on the Secretion of Vasopressin and Oxytocin from the Neurohypophysis', *Neuroendocrinology*, 46: 258-67.
Bonetto, G., D. Belin, and R. T. Karadottir. 2021. 'Myelin: A gatekeeper of activity-dependent circuit plasticity?', *Science*, 374: eaba6905.
Bonfanti, E., T. Bonifacino, S. Raffaele, M. Milanese, E. Morgante, G. Bonanno, M. P. Abbracchio, and M. Fumagalli. 2020. 'Abnormal Upregulation of GPR17 Receptor Contributes to Oligodendrocyte Dysfunction in SOD1 G93A Mice', *Int J Mol Sci*, 21.
Bonfanti, E., P. Gelosa, M. Fumagalli, L. Dimou, F. Vigano, E. Tremoli, M. Cimino, L. Sironi, and M. P. Abbracchio. 2017. 'The role of oligodendrocyte precursor cells expressing the GPR17 receptor in brain remodeling after stroke', *Cell Death Dis*, 8: e2871.
Broach, J. R., V. R. Guarascio, and M. Jayaram. 1982. 'Recombination within the yeast plasmid 2mu circle is site-specific', *Cell*, 29: 227-34.
Brown, T. I., V. A. Carr, K. F. LaRocque, S. E. Favila, A. M. Gordon, B. Bowles, J. N. Bailenson, and A. D. Wagner. 2016. 'Oligodendrocyte heterogeneity in the mouse juvenile and adult central nervous system', *Science*, 352: 1323-26.
Bunge, M. B., R. P. Bunge, and G. D. Pappas. 1962. 'Electron microscopic demonstration of connections between glia and myelin sheaths in the developing mammalian central nervous system', *J Cell Biol*, 12: 448-53.
Bunnemann, B., K. Fuxe, R. Metzger, B. Bjelke, and D. Ganten. 1992. 'The Semiquantitative Distribution and Cellular-Localization of Angiotensinogen Messenger-Rna in the Rat-Brain', *Journal of Chemical Neuroanatomy*, 5: 245-62.
Burbach, J. P. H. 2011. 'What Are Neuropeptides?', *Neuropeptides: Methods and Protocols*, 789: 1-36.
Burcin Duan, Sahbaz, and Iyison Necla Birgul. 2018. 'Neuropeptides as Ligands for GPCRs.' in Saravanan Chandraleka and Biswas Bhaskar (eds.), *Ligand* (IntechOpen: Rijeka).
Butt, A. M., A. Duncan, and M. Berry. 1994. 'Astrocyte associations with nodes of Ranvier: ultrastructural analysis of HRP-filled astrocytes in the mouse optic nerve', *J Neurocytol*, 23: 486-99.

Buzas, B. 2002. 'Regulation of nociceptin/orphanin FQ gene expression in astrocytes by ceramide', *Neuroreport*, 13: 1707-10.

Cai, J., Y. C. Qi, X. M. Hu, M. Tan, Z. J. Liu, J. S. Zhang, Q. Li, M. Sander, and M. Qiu. 2005. 'Generation of oligodendrocyte precursor cells from mouse dorsal spinal cord independent of Nkx6 regulation and Shh signaling', *Neuron*, 45: 41-53.

Calza, L., L. Giardino, M. Pozza, A. Micera, and L. Aloe. 1997. 'Time-course changes of nerve growth factor, corticotropin-releasing hormone, and nitric oxide synthase isoforms and their possible role in the development of inflammatory response in experimental allergic encephalomyelitis', *Proceedings of the National Academy of Sciences of the United States of America*, 94: 3368-73.

Cao, J., N. Papadopoulou, D. Kempuraj, W. S. Boucher, K. Sugimoto, C. L. Cetrulo, and T. C. Theoharides. 2005. 'Human mast cells express corticotropin-releasing hormone (CRH) receptors and CRH leads to selective secretion of vascular endothelial growth factor', *J Immunol*, 174: 7665-75.

Chang, Simon, Federica Fermani, Chu-Lan Lao, Lianyun Huang, Mira Jakovcevski, Rossella Di Giaimo, Miriam Gagliardi, Danusa Menegaz, Alexander Adrian Hennrich, Michael Ziller, Matthias Eder, Rüdiger Klein, Na Cai, and Jan M. Deussing. 2022. 'Tripartite extended amygdala - basal ganglia CRH circuit drives arousal and avoidance behaviour', *bioRxiv*: 2022.03.15.484057.

Chen, Y., J. Molet, B. G. Gunn, K. Ressler, and T. Z. Baram. 2015. 'Diversity of Reporter Expression Patterns in Transgenic Mouse Lines Targeting Corticotropin-Releasing Hormone-Expressing Neurons', *Endocrinology*, 156: 4769-80.

Chen, Y., H. Wu, S. Wang, H. Koito, J. Li, F. Ye, J. Hoang, S. S. Escobar, A. Gow, H. A. Arnett, B. D. Trapp, N. J. Karandikar, J. Hsieh, and Q. R. Lu. 2009. 'The oligodendrocyte-specific G protein-coupled receptor GPR17 is a cell-intrinsic timer of myelination', *Nat Neurosci*, 12: 1398-406.

Chittajallu, R., A. Aguirre, and V. Gallo. 2004. 'NG2-positive cells in the mouse white and grey matter display distinct physiological properties', *Journal of Physiology-London*, 561: 109-22.

Choi, D. I., S. K. Park, H. S. Kim, M. O. Seo, S. J. Kim, J. S. Kim, M. H. Won, and T. C. Kang. 2001. 'Expression of corticotropin releasing factor, but not its binding protein, in CA1 pyramidal cells of gerbil hippocampus following transient ischemia', *Brain Res*, 899: 255-9.

Cohen, Steven R., and Michael Guarnieri. 1976. 'Immunochemical measurement of myelin basic protein in developing rat brain: An index of myelin synthesis', *Developmental Biology*, 49: 294-99.

Colonna, M., and O. Butovsky. 2017. 'Microglia Function in the Central Nervous System During Health and Neurodegeneration', *Annu Rev Immunol*, 35: 441-68.

Crawford, A. H., R. B. Tripathi, W. D. Richardson, and R. J. M. Franklin. 2016. 'Developmental Origin of Oligodendrocyte Lineage Cells Determines Response to Demyelination and Susceptibility to Age-Associated Functional Decline', *Cell Reports*, 15: 761-73.

Cristobal, C. D., and H. K. Lee. 2022. 'Development of myelinating glia: An overview', *Glia*, 70: 2237-59.

Cummings, S., R. Elde, J. Ells, and A. Lindall. 1983. 'Corticotropin-releasing factor immunoreactivity is widely distributed within the central nervous system of the rat: an immunohistochemical study', *J Neurosci*, 3: 1355-68.

Cursano, S., C. R. Battaglia, C. Urrutia-Ruiz, S. Grabrucker, M. Schon, J. Bockmann, S. Braumuller, P. Radermacher, F. Roselli, M. Huber-Lang, and T. M. Boeckers. 2021. 'A CRHR1 antagonist prevents synaptic loss and memory deficits in a trauma-induced delirium-like syndrome', *Mol Psychiatry*, 26: 3778-94.

Dave, J. R., L. E. Eiden, and R. L. Eskay. 1985. 'Corticotropin-releasing factor binding to peripheral tissue and activation of the adenylate cyclase-adenosine 3',5'-monophosphate system', *Endocrinology*, 116: 2152-9.

Dawson, M. R., A. Polito, J. M. Levine, and R. Reynolds. 2003. 'NG2-expressing glial progenitor cells: an abundant and widespread population of cycling cells in the adult rat CNS', *Mol Cell Neurosci*, 24: 476-88.

de Faria, O., H. Pivonkova, B. Varga, S. Timmler, K. A. Evans, and R. T. Karadottir. 2021. 'Periods of synchronized myelin changes shape brain function and plasticity', *Nature Neuroscience*, 24: 1508-21.

de la Tremblaye, P. B., S. M. Benoit, S. Schock, and H. Plamondon. 2017a. 'CRHR1 exacerbates the glial inflammatory response and alters BDNF/TrkB/pCREB signaling in a rat model of global cerebral ischemia: implications for neuroprotection and cognitive recovery', *Progress in Neuro-Psychopharmacology & Biological Psychiatry*, 79: 234-48.

———. 2017b. 'CRHR1 exacerbates the glial inflammatory response and alters BDNF/TrkB/pCREB signaling in a rat model of global cerebral ischemia: implications for neuroprotection and cognitive recovery', *Prog Neuropsychopharmacol Biol Psychiatry*, 79: 234-48.

De Wied, D. 1971. 'Long term effect of vasopressin on the maintenance of a conditioned avoidance response in rats', *Nature*, 232: 58-60.

Dedic, N., C. Kuhne, M. Jakovcevski, J. Hartmann, A. J. Genewsky, K. S. Gomes, E. Anderzhanova, M. L. Pohlmann, S. Chang, A. Kolarz, A. M. Vogl, J. Dine, M. W. Metzger, B. Schmid, R. C. Almada, K. J. Ressler, C. T. Wotjak, V. Grinevich, A. Chen, M. V. Schmidt, W. Wurst, D. Refojo, and J. M. Deussing. 2018. 'Chronic CRH depletion from GABAergic, long-range projection neurons in the extended amygdala reduces dopamine release and increases anxiety', *Nature Neuroscience*, 21: 803-+.

Del Rio-Hortega, P. 2012. 'Studies on neuroglia: Glia with very few processes (oligodendroglia) by PÃ-o del RÃ-o-Hortega. 1921', *Clinical Neuropathology*, 31: 440-59.

del Rio-Hortega, P., J. R. Iglesias-Rozas, and M. Garrosa. 2012. 'Studies on neuroglia Glia with very few processes (oligodendroglia) by Pio del Rio-Hortega', *Clinical Neuropathology*, 31: 440-59.

DeLaney, K., A. R. Buchberger, L. Atkinson, S. Gründer, A. Mousley, and L. Li. 2018. 'New techniques, applications and perspectives in neuropeptide research', *J Exp Biol*, 221.

Deussing, J. M. 2013. 'Targeted mutagenesis tools for modelling psychiatric disorders', *Cell Tissue Res*, 354: 9-25.

Dewald, L. E., J. P. Rodriguez, and J. M. Levine. 2011. 'The RE1 binding protein REST regulates oligodendrocyte differentiation', *J Neurosci*, 31: 3470-83.

Dimou, L., and V. Gallo. 2015. 'NG2-glia and their functions in the central nervous system', *Glia*, 63: 1429-51.

Dimou, L., and M. Gotz. 2014. 'Glial cells as progenitors and stem cells: new roles in the healthy and diseased brain', *Physiol Rev*, 94: 709-37.

Dimou, L., C. Simon, F. Kirchhoff, H. Takebayashi, and M. Gotz. 2008. 'Progeny of Olig2-expressing progenitors in the gray and white matter of the adult mouse cerebral cortex', *J Neurosci*, 28: 10434-42.

Donaldson, C. J., S. W. Sutton, M. H. Perrin, A. Z. Corrigan, K. A. Lewis, J. E. Rivier, J. M. Vaughan, and W. W. Vale. 1996. 'Cloning and characterization of human urocortin', *Endocrinology*, 137: 2167-70.

Dreifuss, J. J., I. Kalnins, J. S. Kelly, and K. B. Ruf. 1971. 'Action Potentials and Release of Neurohypophysial Hormones in-Vitro', *Journal of Physiology-London*, 215: 805-&.

Du, C., Y. Duan, W. Wei, Y. Cai, H. Chai, J. Lv, X. Du, J. Zhu, and X. Xie. 2016. 'Kappa opioid receptor activation alleviates experimental autoimmune encephalomyelitis and promotes oligodendrocyte-mediated remyelination', *Nat Commun*, 7: 11120.

Dutta, Dipankar J., Dong Ho Woo, Philip R. Lee, Sinisa Pajevic, Olena Bukalo, William C. Huffman, Hiroaki Wake, Peter J. Basser, Shahriar SheikhBahaei, Vanja Lazarevic, Jeffrey C. Smith, and R. Douglas Fields. 2018. 'Regulation of myelin structure and conduction velocity by perinodal astrocytes', *Proceedings of the National Academy of Sciences*, 115: 11832-37.

Dymecki, S. M., and J. C. Kim. 2007. 'Molecular neuroanatomy's "Three Gs": a primer', *Neuron*, 54: 17-34.

Eschenroeder, A. C., A. A. Vestal-Laborde, E. S. Sanchez, S. E. Robinson, and C. Sato-Bigbee. 2012. 'Oligodendrocyte responses to buprenorphine uncover novel and opposing roles of μ-opioid- and nociceptin/orphanin FQ receptors in cell development: implications for drug addiction treatment during pregnancy', *Glia*, 60: 125-36.

Eugenín-von Bernhardi, J., and L. Dimou. 2016. 'NG2-glia, More Than Progenitor Cells', *Adv Exp Med Biol*, 949: 27-45.

Eugenin von Bernhardi, J., and L. Dimou. 2022. 'Oligodendrogenesis is a key process for cognitive performance improvement induced by voluntary physical activity', *Glia*, 70: 1052-67.

Faden, A. I., C. J. Molineaux, J. G. Rosenberger, T. P. Jacobs, and B. M. Cox. 1985. 'Endogenous opioid immunoreactivity in rat spinal cord following traumatic injury', *Ann Neurol*, 17: 386-90.

Falcao, A. M., D. van Bruggen, S. Marques, M. Meijer, S. Jakel, E. Agirre, S. Samudyata, E. M. Floriddia, D. Vanichkina, C. Ffrench-Constant, A. Williams, A. O. Guerreiro-Cacais, and G. Castelo-Branco. 2019. 'Disease-specific oligodendrocyte lineage cells arise in Multiple Sclerosis', *Glia*, 67: E79-E79.

Fard, M. K., F. van der Meer, P. Sanchez, L. Cantuti-Castelvetri, S. Mandad, S. Jakel, E. F. Fornasiero, S. Schmitt, M. Ehrlich, L. Starost, T. Kuhlmann, C. Sergiou, V. Schultz, C. Wrzos, W. Bruck, H. Urlaub, L. Dimou, C. Stadelmann, and M. Simons. 2017. 'BCAS1 expression defines a population of early myelinating oligodendrocytes in multiple sclerosis lesions', *Science Translational Medicine*, 9.

Faulkner, J. R., J. E. Herrmann, M. J. Woo, K. E. Tansey, N. B. Doan, and M. V. Sofroniew. 2004. 'Reactive astrocytes protect tissue and preserve function after spinal cord injury', *Journal of Neuroscience*, 24: 2143-55.

Feltri, M. L., M. R. Weaver, S. Belin, and Y. Poitelon. 2021. 'The Hippo pathway: Horizons for innovative treatments of peripheral nerve diseases', *J Peripher Nerv Syst*, 26: 4-16.

Filbin, Marie T. 2003. 'Myelin-associated inhibitors of axonal regeneration in the adult mammalian CNS', *Nature Reviews Neuroscience*, 4: 703-13.

Filosa, J. A., A. D. Bonev, and M. T. Nelson. 2004. 'Calcium dynamics in cortical astrocytes and arterioles during neurovascular coupling', *Circ Res*, 95: e73-81.

Flechsig Of Leipsic, Paul. 1901. 'DEVELOPMENTAL (MYELOGENETIC) LOCALISATION OF THE CEREBRAL CORTEX IN THE HUMAN SUBJECT', *The Lancet*, 158: 1027-30.

Flechsig, Paul. 1927. *Meine Myelogenetische Hirnlehre* (Springer Berlin, Heidelberg).

Foster, A. Y., H. Bujalka, and B. Emery. 2019. 'Axoglial interactions in myelin plasticity: Evaluating the relationship between neuronal activity and oligodendrocyte dynamics', *Glia*, 67: 2038-49.

Friede, R. L. 1972. 'Control of myelin formation by axon caliber (with a model of the control mechanism)', *Journal of Comparative Neurology*, 144: 233-52.

Fu, C., Z. Yin, D. Yu, and Z. Yang. 2013. 'Substance P and calcitonin gene-related peptide expression in dorsal root ganglia in sciatic nerve injury rats', *Neural Regen Res*, 8: 3124-30.

Fumagalli, M., E. Bonfanti, S. Daniele, E. Zappelli, D. Lecca, C. Martini, M. L. Trincavelli, and M. P. Abbracchio. 2015. 'The Ubiquitin Ligase Mdm2 Controls Oligodendrocyte Maturation by Intertwining mTOR with G Protein-Coupled Receptor Kinase 2 in the Regulation of GPR17 Receptor Desensitization', *Glia*, 63: 2327-39.

Fuzesi, T., N. Daviu, J. I. W. Cusulin, R. P. Bonin, and J. S. Bains. 2016. 'Hypothalamic CRH neurons orchestrate complex behaviours after stress', *Nature Communications*, 7.

Gaillard, R. C. 1994. 'Neuroendocrine-immune system interactions The immune-hypothalamo-pituitary-adrenal axis', *Trends Endocrinol Metab*, 5: 303-9.

Gainer, H., S. A. Wolfe, A. L. Obaid, and B. M. Salzberg. 1986. 'Action-Potentials and Frequency-Dependent Secretion in the Mouse Neurohypophysis', *Neuroendocrinology*, 43: 557-63.

García-Mateo, N., R. Pascua-Maestro, A. Pérez-Castellanos, C. Lillo, D. Sanchez, and M. D. Ganfornina. 2018. 'Myelin extracellular leaflet compaction requires apolipoprotein D membrane management to optimize lysosomal-dependent recycling and glycocalyx removal', *Glia*, 66: 670-87.

Gautier, H. O. B., K. A. Evans, K. Volbracht, R. James, S. Sitnikov, I. Lundgaard, F. James, C. Lao-Peregrin, R. Reynolds, R. J. M. Franklin, and R. T. Karadottir. 2015. 'Neuronal activity regulates remyelination via glutamate signalling to oligodendrocyte progenitors', *Nature Communications*, 6.

Gibbs, Marie E., Dana Hutchinson, and Leif Hertz. 2008. 'Astrocytic involvement in learning and memory consolidation', *Neuroscience & Biobehavioral Reviews*, 32: 927-44.

Gibson, E. M., D. Purger, C. W. Mount, A. K. Goldstein, G. L. Lin, L. S. Wood, I. Inema, S. E. Miller, G. Bieri, J. B. Zuchero, B. A. Barres, P. J. Woo, H. Vogel, and M. Monje. 2014. 'Neuronal Activity Promotes Oligodendrogenesis and Adaptive Myelination in the Mammalian Brain', *Science*, 344: 487-+.

Ginhoux, Florent, Melanie Greter, Marylene Leboeuf, Sayan Nandi, Peter See, Solen Gokhan, Mark F. Mehler, Simon J. Conway, Lai Guan Ng, E. Richard Stanley, Igor M. Samokhvalov, and Miriam Merad. 2010. 'Fate Mapping Analysis Reveals That Adult Microglia Derive from Primitive Macrophages', *Science*, 330: 841-45.

Grady, Eileen, Stephan Böhm, Karen McConalogue, Adella Garland, John Ansel, John Olerud, and Nigel Bunnett. 1997. 'Mechanisms Attenuating Cellular Responses to Neuropeptides: Extracellular Degradation of Ligands and Desensitization of Receptors', *Journal of Investigative Dermatology Symposium Proceedings*, 2: 69-75.

Gresle, M. M., H. Butzkueven, V. M. Perreau, A. Jonas, J. Xiao, S. Thiem, F. E. Holmes, W. Doherty, P. Y. Soo, M. D. Binder, R. Akkermann, V. G. Jokubaitis, H. S. Cate, M. P. Marriott, A. L. Gundlach, D. Wynick, and T. J. Kilpatrick. 2015. 'Galanin is an autocrine myelin and oligodendrocyte trophic signal induced by leukemia inhibitory factor', *Glia*, 63: 1005-20.

Harle, G., S. Kaminski, D. Dubayle, J. P. Frippiat, and A. Ropars. 2018. 'Murine splenic B cells express corticotropin-releasing hormone receptor 2 that affect their viability during a stress response', *Sci Rep*, 8: 143.

Hasel, P., I. V. L. Rose, J. S. Sadick, R. D. Kim, and S. A. Liddelow. 2021. 'Neuroinflammatory astrocyte subtypes in the mouse brain', *Nat Neurosci*, 24: 1475-87.

Hashimoto, H., W. Jiang, T. Yoshimura, K. H. Moon, J. Bok, and K. Ikenaka. 2018. 'Strong sonic hedgehog signaling in the mouse ventral spinal cord is not required for oligodendrocyte precursor cell (OPC) generation but is necessary for correct timing of its generation', *Neurochem Int*, 119: 178-83.

Hauger, R. L., D. E. Grigoriadis, M. F. Dallman, P. M. Plotsky, W. W. Vale, and F. M. Dautzenberg. 2003. 'International Union of Pharmacology. XXXVI. Current status of the nomenclature for receptors for corticotropin-releasing factor and their ligands', *Pharmacol Rev*, 55: 21-6.

Hawkins, B. T., and T. P. Davis. 2005. 'The blood-brain barrier/neurovascular unit in health and disease', *Pharmacol Rev*, 57: 173-85.

Hayakawa, K., L. D. Pham, A. T. Som, B. J. Lee, S. Guo, E. H. Lo, and K. Arai. 2011. 'Vascular endothelial growth factor regulates the migration of oligodendrocyte precursor cells', *J Neurosci*, 31: 10666-70.

He, L., R. Binari, J. Huang, J. Falo-Sanjuan, and N. Perrimon. 2019. 'In vivo study of gene expression with an enhanced dual-color fluorescent transcriptional timer', *Elife*, 8.

Heinrichs, S. C., and G. F. Koob. 2004. 'Corticotropin-releasing factor in brain: A role in activation, arousal, and affect regulation', *Journal of Pharmacology and Experimental Therapeutics*, 311: 427-40.

Hillhouse, E. W., and D. K. Grammatopoulos. 2006. 'The molecular mechanisms underlying the regulation of the biological activity of corticotropin-releasing hormone receptors: implications for physiology and pathophysiology', *Endocr Rev*, 27: 260-86.

Hiratsuka, D., E. Kurganov, E. Furube, M. Morita, and S. Miyata. 2019. 'VEGF- and PDGF-dependent proliferation of oligodendrocyte progenitor cells in the medulla oblongata after LPC-induced focal demyelination', *J Neuroimmunol*, 332: 176-86.

Hoess, R. H., M. Ziese, and N. Sternberg. 1982. 'P1 site-specific recombination: nucleotide sequence of the recombining sites', *Proc Natl Acad Sci U S A*, 79: 3398-402.

Hökfelt, Tomas, Christian Broberger, Zhi-Qing David Xu, Valeriy Sergeyev, Ruud Ubink, and Margarita Diez. 2000. 'Neuropeptides — an overview', *Neuropharmacology*, 39: 1337-56.

Hökfelt, Tomas, Olle Johansson, Åke Ljungdahl, Jan M. Lundberg, and Marianne Schultzberg. 1980. 'Peptidergic neurones', *Nature*, 284: 515-21.

Hong, J., J. M. Kirkland, J. Acheta, L. N. Marziali, B. Beck, H. Jeanette, U. Bhatia, G. Davis, J. Herron, C. Roue, C. Abi-Ghanem, M. L. Feltri, K. L. Zuloaga, M. E. Bechler, Y. Poitelon, and S. Belin. 2023. 'YAP and TAZ regulate remyelination in the central nervous system', *Glia*.

Hortega, P Río. 1918. 'Noticia de un nuevo y fácil método para la coloración de la neuroglia y el tejido conjuntivo', *Trab Lab Invest Biol Univ Madrid*, 15: 367-78.

Hughes, E. G., S. H. Kang, M. Fukaya, and D. E. Bergles. 2013. 'Oligodendrocyte progenitors balance growth with self-repulsion to achieve homeostasis in the adult brain', *Nature Neuroscience*, 16: 668-+.

Hughes, E. G., J. L. Orthmann-Murphy, A. J. Langseth, and D. E. Bergles. 2018. 'Myelin remodeling through experience-dependent oligodendrogenesis in the adult somatosensory cortex', *Nature Neuroscience*, 21: 696-+.

Hughes, Ethan G., and Michael E. Stockton. 2021. 'Premyelinating Oligodendrocytes: Mechanisms Underlying Cell Survival and Integration', *Frontiers in Cell and Developmental Biology*, 9.

Huntemer-Silveira, A., N. Patil, M. A. Brickner, and A. M. Parr. 2021. 'Strategies for Oligodendrocyte and Myelin Repair in Traumatic CNS Injury', *Frontiers in Cellular Neuroscience*, 14.

Hur, Y. S., K. D. Kim, S. H. Paek, and S. H. Yoo. 2010. 'Evidence for the existence of secretory granule (dense-core vesicle)-based inositol 1,4,5-trisphosphate-dependent Ca2+ signaling system in astrocytes', *PLoS One*, 5: e11973.

Itoi, K., N. Horiba, F. Tozawa, Y. Sakai, K. Sakai, K. Abe, H. Demura, and T. Suda. 1996. 'Major role of 3',5'-cyclic adenosine monophosphate-dependent protein kinase A pathway in corticotropin-releasing factor gene expression in the rat hypothalamus in vivo', *Endocrinology*, 137: 2389-96.

Itoi, K., A. H. Talukder, T. Fuse, T. Kaneko, R. Ozawa, T. Sato, T. Sugaya, K. Uchida, M. Yamazaki, M. Abe, R. Natsume, and K. Sakimura. 2014. 'Visualization of Corticotropin-Releasing Factor Neurons by Fluorescent Proteins in the Mouse Brain and Characterization of Labeled Neurons in the Paraventricular Nucleus of the Hypothalamus', *Endocrinology*, 155: 4054-60.

Jackson, M. B., A. Konnerth, and G. J. Augustine. 1991. 'Action-Potential Broadening and Frequency-Dependent Facilitation of Calcium Signals in Pituitary Nerve-Terminals', *Proceedings of the National Academy of Sciences of the United States of America*, 88: 380-84.

Jacobson, S. 1963. 'Sequence of Myelinization in the Brain of the Albino Rat. A. Cerebral Cortex, Thalamus and Related Structures', *Journal of Comparative Neurology*, 121: 5-29.

Jakel, S., and L. Dimou. 2017. 'Glial Cells and Their Function in the Adult Brain: A Journey through the History of Their Ablation', *Frontiers in Cellular Neuroscience*, 11.

Jan, L. Y., and Y. N. Jan. 1982. 'Peptidergic Transmission in Sympathetic-Ganglia of the Frog', *Journal of Physiology-London*, 327: 219-&.

Jiang, H. S., Y. Z. Wang, X. Liang, X. F. Xing, X. Z. Xu, and C. F. Zhou. 2018. 'Toll-Like Receptor 4 Knockdown Attenuates Brain Damage and Neuroinflammation After Traumatic Brain Injury via Inhibiting Neuronal Autophagy and Astrocyte Activation', *Cellular and Molecular Neurobiology*, 38: 1009-19.

Kamen, Y., H. Pivonkova, K. A. Evans, and R. T. Karadottir. 2022. 'A Matter of State: Diversity in Oligodendrocyte Lineage Cells', *Neuroscientist*, 28: 144-62.

Karadottir, R., P. Cavelier, L. H. Bergersen, and D. Attwell. 2005. 'NMDA receptors are expressed in oligodendrocytes and activated in ischaemia', *Nature*, 438: 1162-66.

Kawai, K., T. Itoh, A. Itoh, M. Horiuchi, K. Wakayama, P. Bannerman, J. Y. Garbern, D. Pleasure, and T. Lindsten. 2009. 'Maintaince of the relative proportion of oligodendrocytes to axons even in the absence of BAX and BAK', *European Journal of Neuroscience*, 30: 2030-41.

Keegan, Catherine E., I. Jill Karolyi, Lauren T. Knapp, Francis J. Bourbonais, Sally A. Camper, and Audrey F. Seasholtz. 1994. 'Expression of Corticotropin-Releasing Hormone Transgenes in Neurons of Adult and Developing Mice', *Molecular and Cellular Neuroscience*, 5: 505-14.

Kempuraj, D., N. G. Papadopoulou, M. Lytinas, M. Huang, K. Kandere-Grzybowska, B. Madhappan, W. Boucher, S. Christodoulou, A. Athanassiou, and T. C. Theoharides. 2004. 'Corticotropin-

releasing hormone and its structurally related urocortin are synthesized and secreted by human mast cells', *Endocrinology*, 145: 43-8.

Kessaris, N., M. Fogarty, P. Iannarelli, M. Grist, M. Wegner, and W. D. Richardson. 2006. 'Competing waves of oligodendrocytes in the forebrain and postnatal elimination of an embryonic lineage', *Nature Neuroscience*, 9: 173-79.

Khan, A. M., T. A. Ponzio, G. Sanchez-Watts, B. G. Stanley, G. I. Hatton, and A. G. Watts. 2007. 'Catecholaminergic control of mitogen-activated protein kinase signaling in paraventricular neuroendocrine neurons in vivo and in vitro: a proposed role during glycemic challenges', *J Neurosci*, 27: 7344-60.

Kirby, L., and G. Castelo-Branco. 2021. 'Crossing boundaries: Interplay between the immune system and oligodendrocyte lineage cells', *Seminars in Cell & Developmental Biology*, 116: 45-52.

Kirby, L., J. Jin, J. G. Cardona, M. D. Smith, K. A. Martin, J. Y. Wang, H. Strasburger, L. Herbst, M. Alexis, J. Karnell, T. Davidson, R. Dutta, J. Goverman, D. Bergles, and P. A. Calabresi. 2019. 'Oligodendrocyte precursor cells present antigen and are cytotoxic targets in inflammatory demyelination', *Nature Communications*, 10.

Knapp, P. E., V. V. Adjan, and K. F. Hauser. 2009. 'Cell-specific loss of kappa-opioid receptors in oligodendrocytes of the dysmyelinating jimpy mouse', *Neuroscience Letters*, 451: 114-8.

Koelliker, Albert. 1889. *Handbuch der Gewebelehre des Menschen*.

Kol, Adi, Adar Adamsky, Maya Groysman, Tirzah Kreisel, Michael London, and Inbal Goshen. 2020. 'Astrocytes contribute to remote memory formation by modulating hippocampal–cortical communication during learning', *Nature Neuroscience*, 23: 1229-39.

Kono, J., K. Konno, A. H. Talukder, T. Fuse, M. Abe, K. Uchida, S. Horio, K. Sakimura, M. Watanabe, and K. Itoi. 2017. 'Distribution of corticotropin-releasing factor neurons in the mouse brain: a study using corticotropin-releasing factor-modified yellow fluorescent protein knock-in mouse', *Brain Structure & Function*, 222: 1705-32.

Kovacs, K. J., and P. E. Sawchenko. 1996. 'Regulation of stress-induced transcriptional changes in the hypothalamic neurosecretory neurons', *J Mol Neurosci*, 7: 125-33.

Krzan, M., M. Stenovec, M. Kreft, T. Pangrsic, S. Grilc, P. G. Haydon, and R. Zorec. 2003. 'Calcium-dependent exocytosis of atrial natriuretic peptide from astrocytes', *J Neurosci*, 23: 1580-3.

Kuboyama, K., N. Tanga, R. Suzuki, A. Fujikawa, and M. Noda. 2017. 'Protamine neutralizes chondroitin sulfate proteoglycan-mediated inhibition of oligodendrocyte differentiation', *PLoS One*, 12: e0189164.

Lam, Mable, Koji Takeo, Rafael G. Almeida, Madeline H. Cooper, Kathryn Wu, Manasi Iyer, Husniye Kantarci, and J. Bradley Zuchero. 2022. 'CNS myelination requires VAMP2/3-mediated membrane expansion in oligodendrocytes', *Nature Communications*, 13: 5583.

Lang, T., I. Wacker, J. Steyer, C. Kaether, I. Wunderlich, T. Soldati, H. H. Gerdes, and W. Almers. 1997. 'Ca2+-triggered peptide secretion neurotechnique in single cells imaged with green fluorescent protein and evanescent-wave microscopy', *Neuron*, 18: 857-63.

Larhammar, D. 2009. 'Neuropeptides Phylogeny and Evolution.' in Larry R. Squire (ed.), *Encyclopedia of Neuroscience* (Academic Press: Oxford).

Le Bras, B., M. J. Barallobre, J. Homman-Lidiye, A. Ny, S. Wyns, T. Tammela, P. Haiko, M. J. Karkkainen, L. Yuan, M. P. Muriel, E. Chatzopoulou, A. Breant, B. Zalc, P. Carmeliet, K. Alitalo, A. Eichmann, and J. L. Thomas. 2006. 'VEGF-C is a trophic factor for neural progenitors in the vertebrate embryonic brain', *Nature Neuroscience*, 9: 340-48.

Lee, Hong-Gyun, Michael A. Wheeler, and Francisco J. Quintana. 2022. 'Function and therapeutic value of astrocytes in neurological diseases', *Nature Reviews Drug Discovery*, 21: 339-58.

Lee, J. Y., and S. Petratos. 2016. 'Thyroid Hormone Signaling in Oligodendrocytes: from Extracellular Transport to Intracellular Signal', *Mol Neurobiol*, 53: 6568-83.

Lee, S., M. K. Leach, S. A. Redmond, S. Y. Chong, S. H. Mellon, S. J. Tuck, Z. Q. Feng, J. M. Corey, and J. R. Chan. 2012. 'A culture system to study oligodendrocyte myelination processes using engineered nanofibers', *Nature Methods*, 9: 917-22.

Lewcock, J. W., K. Schlepckow, G. Di Paolo, S. Tahirovic, K. M. Monroe, and C. Haass. 2020. 'Emerging Microglia Biology Defines Novel Therapeutic Approaches for Alzheimer's Disease', *Neuron*, 108: 801-21.

Li, C., Z. Wu, L. Zhou, J. Shao, X. Hu, W. Xu, Y. Ren, X. Zhu, W. Ge, K. Zhang, J. Liu, R. Huang, J. Yu, D. Luo, X. Yang, W. Zhu, R. Zhu, C. Zheng, Y. E. Sun, and L. Cheng. 2022. 'Temporal and spatial cellular and molecular pathological alterations with single-cell resolution in the adult spinal cord after injury', *Signal Transduct Target Ther*, 7: 65.

Li, Xianqiang, Xiaoning Zhao, Yu Fang, Xin Jiang, Tommy Duong, Connie Fan, Chiao-Chain Huang, and Steven R. Kain. 1998. 'Generation of Destabilized Green Fluorescent Protein as a Transcription Reporter *', *Journal of Biological Chemistry*, 273: 34970-75.

Lin, S. C., and D. E. Bergles. 2004. 'Synaptic signaling between GABAergic interneurons and oligodendrocyte precursor cells in the hippocampus', *Nat Neurosci*, 7: 24-32.

Liu, Y., H. S. Knobloch, V. Grinevich, and G. Aguilera. 2011. 'Stress induces parallel changes in corticotrophin-releasing hormone (CRH) Transcription and nuclear translocation of transducer of regulated cAMP response element-binding activity 2 in hypothalamic CRH neurones', *J Neuroendocrinol*, 23: 216-23.

Loane, D. J., and A. Kumar. 2016. 'Microglia in the TBI brain: The good, the bad, and the dysregulated', *Exp Neurol*, 275 Pt 3: 316-27.

Loddick, S. A., A. V. Turnbull, and N. J. Rothwell. 1998. 'Cerebral interleukin-6 is neuroprotective during permanent focal cerebral ischemia in the rat', *J Cereb Blood Flow Metab*, 18: 176-9.

Long, K. L. P., J. M. Breton, M. K. Barraza, O. S. Perloff, and D. Kaufer. 2021a. 'Hormonal Regulation of Oligodendrogenesis I: Effects across the Lifespan', *Biomolecules*, 11.

Long, Kimberly L. P., Jocelyn M. Breton, Matthew K. Barraza, Olga S. Perloff, and Daniela Kaufer. 2021b. 'Hormonal Regulation of Oligodendrogenesis I: Effects across the Lifespan', *Biomolecules*, 11: 283.

Low, K. G., R. G. Allen, and M. H. Melner. 1992. 'Differential regulation of proenkephalin expression in astrocytes by cytokines', *Endocrinology*, 131: 1908-14.

Lowry, C. A., and F. L. Moore. 2006. 'Regulation of behavioral responses by corticotropin-releasing factor', *General and Comparative Endocrinology*, 146: 19-27.

Ludwig, M., and G. Leng. 2006. 'Dendritic peptide release and peptide-dependent behaviours', *Nature Reviews Neuroscience*, 7: 126-36.

Ludwig, M., and J. Stern. 2015. 'Multiple signalling modalities mediated by dendritic exocytosis of oxytocin and vasopressin', *Philos Trans R Soc Lond B Biol Sci*, 370.

Lundgaard, I., A. Luzhynskaya, J. H. Stockley, Z. Wang, K. A. Evans, M. Swire, K. Volbracht, H. O. B. Gautier, R. J. M. Franklin, C. Ffrench-Constant, D. Attwell, and R. T. Karadottir. 2013. 'Neuregulin and BDNF Induce a Switch to NMDA Receptor-Dependent Myelination by Oligodendrocytes', *Plos Biology*, 11.

Lundgaard, I., M. J. Osório, B. T. Kress, S. Sanggaard, and M. Nedergaard. 2014. 'White matter astrocytes in health and disease', *Neuroscience*, 276: 161-73.

Lyons, M. K., R. E. Anderson, and F. B. Meyer. 1991. 'Corticotropin releasing factor antagonist reduces ischemic hippocampal neuronal injury', *Brain Res*, 545: 339-42.

Lyubetska, H., L. Zhang, J. Kong, and M. Vrontakis. 2015. 'An elevated level of circulating galanin promotes developmental expression of myelin basic protein in the mouse brain', *Neuroscience*, 284: 581-89.

Mackay, K. B., H. Bozigian, D. E. Grigoriadis, S. A. Loddick, G. Verge, and A. C. Foster. 2001. 'Neuroprotective effects of the CRF1 antagonist R121920 after permanent focal ischemia in the rat', *J Cereb Blood Flow Metab*, 21: 1208-14.

Madisen, L., T. A. Zwingman, S. M. Sunkin, S. W. Oh, H. A. Zariwala, H. Gu, L. L. Ng, R. D. Palmiter, M. J. Hawrylycz, A. R. Jones, E. S. Lein, and H. K. Zeng. 2010. 'A robust and high-throughput Cre reporting and characterization system for the whole mouse brain', *Nature Neuroscience*, 13: 133-U311.

Madisen, Linda, Aleena R Garner, Daisuke Shimaoka, Amy S Chuong, Nathan C Klapoetke, Lu Li, Alexander van der Bourg, Yusuke Niino, Ladan Egolf, Claudio Monetti, Hong Gu, Maya Mills, Adrian Cheng, Bosiljka Tasic, Thuc Nghi Nguyen, Susan M Sunkin, Andrea Benucci, Andras Nagy, Atsushi Miyawaki, Fritjof Helmchen, Ruth M Empson, Thomas Knöpfel, Edward S Boyden, R. Clay Reid, Matteo Carandini, and Hongkui Zeng. 2015. 'Transgenic Mice for Intersectional Targeting of Neural Sensors and Effectors with High Specificity and Performance', *Neuron*, 85: 942-58.

Malkoski, S. P., and R. I. Dorin. 1999. 'Composite glucocorticoid regulation at a functionally defined negative glucocorticoid response element of the human corticotropin-releasing hormone gene', *Mol Endocrinol*, 13: 1629-44.

Mark F. Bear, Barry W. Connors. 2009. 'Neurowissenschaften', 3.

Martin, E. I., K. J. Ressler, A. M. Jasnow, J. Dabrowska, R. Hazra, D. G. Rainnie, C. B. Nemeroff, and M. J. Owens. 2010. 'A novel transgenic mouse for gene-targeting within cells that express corticotropin-releasing factor', *Biol Psychiatry*, 67: 1212-6.

Martins, J. M., W. A. Banks, and A. J. Kastin. 1997. 'Transport of CRH from mouse brain directly affects peripheral production of beta-endorphin by the spleen', *Am J Physiol*, 273: E1083-9.

Mattugini, N., R. Bocchi, V. Scheuss, G. L. Russo, O. Torper, C. L. Lao, and M. Götz. 2019. 'Inducing Different Neuronal Subtypes from Astrocytes in the Injured Mouse Cerebral Cortex', *Neuron*, 103: 1086-95.e5.

McCall, J. G., R. Al-Hasani, E. R. Siuda, D. Y. Hong, A. J. Norris, C. P. Ford, and M. R. Bruchas. 2015. 'CRH Engagement of the Locus Coeruleus Noradrenergic System Mediates Stress-Induced Anxiety', *Neuron*, 87: 605-20.

McKerracher, L., and K. M. Rosen. 2015. 'MAG, myelin and overcoming growth inhibition in the CNS', *Front Mol Neurosci*, 8: 51.

Mei, F., S. R. Mayoral, H. Nobuta, F. Wang, C. Desponts, D. S. Lorrain, L. Xiao, A. J. Green, D. Rowitch, J. Whistler, and J. R. Chan. 2016. 'Identification of the Kappa-Opioid Receptor as a Therapeutic Target for Oligodendrocyte Remyelination', *J Neurosci*, 36: 7925-35.

Mens, W. B., A. Witter, and T. B. van Wimersma Greidanus. 1983. 'Penetration of neurohypophyseal hormones from plasma into cerebrospinal fluid (CSF): half-times of disappearance of these neuropeptides from CSF', *Brain Res*, 262: 143-9.

Merighi, A. 2018. 'Costorage of High Molecular Weight Neurotransmitters in Large Dense Core Vesicles of Mammalian Neurons', *Frontiers in Cellular Neuroscience*, 12.

Michalski, John-Paul, and Rashmi Kothary. 2015. 'Oligodendrocytes in a Nutshell', *Frontiers in Cellular Neuroscience*, 9.

Miralles, A. J., N. Unger, N. Kannaiyan, M. J. Rossner, and L. Dimou. 2023. 'Analysis of the GPR17 receptor in NG2-glia under physiological conditions unravels a new subset of oligodendrocyte progenitor cells with distinct functions', *Glia*, 71: 1536-52.

Molina-Gonzalez, Irene, Rebecca K. Holloway, Zoeb Jiwaji, Owen Dando, Sarah A. Kent, Katie Emelianova, Amy F. Lloyd, Lindsey H. Forbes, Ayisha Mahmood, Thomas Skripuletz, Viktoria Gudi, James A. Febery, Jeffrey A. Johnson, Jill H. Fowler, Tanja Kuhlmann, Anna Williams, Siddharthan Chandran, Martin Stangel, Andrew J. M. Howden, Giles E. Hardingham, and Veronique E. Miron. 2023. 'Astrocyte-oligodendrocyte interaction regulates central nervous system regeneration', *Nature Communications*, 14: 3372.

Monje, M. 2015. 'Neuronal activity promotes oligodendrogenesis and adaptive myelination in the mammalian brain', *Glia*, 63: E17-E18.

Mount, Christopher W, and Michelle Monje. 2017. 'Wrapped to adapt: experience-dependent myelination', *Neuron*, 95: 743-56.

Mousa, S. A., C. P. Bopaiah, C. Stein, and M. Schafer. 2003. 'Involvement of corticotropin-releasing hormone receptor subtypes 1 and 2 in peripheral opioid-mediated inhibition of inflammatory pain', *Pain*, 106: 297-307.

Muschol, M., and B. M. Salzberg. 2000. 'Dependence of transient and residual calcium dynamics on action-potential patterning during neuropeptide secretion', *Journal of Neuroscience*, 20: 6773-80.

Nave, K. A., and H. B. Werner. 2014. 'Myelination of the Nervous System: Mechanisms and Functions', *Annual Review of Cell and Developmental Biology, Vol 30*, 30: 503-+.

Neil A. Campbell, Jane B. Reece. 2009. 'Biologie', 8: 1190-205.

Nimmerjahn, Axel, Frank Kirchhoff, and Fritjof Helmchen. 2005. 'Resting Microglial Cells Are Highly Dynamic Surveillants of Brain Parenchyma in Vivo', *Science*, 308: 1314-18.

NINDS, National Institute of Neurological Disorders and Stroke. 2023. 'Traumatic Brain Injury (TBI)', Accessed October 6, 2023. https://www.ninds.nih.gov/health-information/disorders/traumatic-brain-injury-tbi.

Nishiyama, A., M. Komitova, R. Suzuki, and X. Zhu. 2009. 'Polydendrocytes (NG2 cells): multifunctional cells with lineage plasticity', *Nature Reviews Neuroscience*, 10: 9-22.

Nishiyama, A., X. H. Lin, N. Giese, C. H. Heldin, and W. B. Stallcup. 1996a. 'Co-localization of NG2 proteoglycan and PDGF alpha-receptor on O2A progenitor cells in the developing rat brain', *Journal of Neuroscience Research*, 43: 299-314.

———. 1996b. 'Interaction between NG2 proteoglycan and PDGF alpha-receptor on O2A progenitor cells is required for optimal response to PDGF', *Journal of Neuroscience Research*, 43: 315-30.

Niu, J., H. H. Tsai, K. K. Hoi, N. Huang, G. Yu, K. Kim, S. E. Baranzini, L. Xiao, J. R. Chan, and S. P. J. Fancy. 2019. 'Aberrant oligodendroglial-vascular interactions disrupt the blood-brain barrier, triggering CNS inflammation', *Nat Neurosci*, 22: 709-18.

Orentas, D. M., J. E. Hayes, K. L. Dyer, and R. H. Miller. 1999. 'Sonic hedgehog signaling is required during the appearance of spinal cord oligodendrocyte precursors', *Development*, 126: 2419-29.

Orthmann-Murphy, J. L., A. D. Enriquez, C. K. Abrams, and S. S. Scherer. 2007. 'Loss-of-function GJA12/Connexin47 mutations cause Pelizaeus-Merzbacher-like disease', *Mol Cell Neurosci*, 34: 629-41.

Osso, L., K. Rankin, and J. Chan. 2021. 'Experience-dependent myelination following stress is mediated by the neuropeptide dynorphin', *Glia*, 69: E401-E01.

Pan, H., D. Clary, and P. D. Sadowski. 1991. 'Identification of the DNA-binding domain of the FLP recombinase', *J Biol Chem*, 266: 11347-54.

Paolicelli, Rosa C., Giulia Bolasco, Francesca Pagani, Laura Maggi, Maria Scianni, Patrizia Panzanelli, Maurizio Giustetto, Tiago Alves Ferreira, Eva Guiducci, Laura Dumas, Davide Ragozzino, and Cornelius T. Gross. 2011. 'Synaptic Pruning by Microglia Is Necessary for Normal Brain Development', *Science*, 333: 1456-58.

Parolisi, Roberta, and Enrica Boda. 2018. 'NG2 Glia: Novel Roles beyond Re-/Myelination', *Neuroglia*, 1: 151-75.

Penfield, W. 1924. 'Oligodendroglia and its relation to classical neuroglia', *Brain*, 47: 430-52.

Peng, Wanling, Xiaotong Liu, Guofen Ma, Zhaofa Wu, Ziyue Wang, Xiang Fei, Meiling Qin, Lizhao Wang, Yulong Li, Siyu Zhang, and Min Xu. 2023. 'Adenosine-independent regulation of the sleep–wake cycle by astrocyte activity', *Cell Discovery*, 9: 16.

Perrin, M. H., and W. W. Vale. 1999. 'Corticotropin releasing factor receptors and their ligand family', *Ann N Y Acad Sci*, 885: 312-28.

Peters, A. 2004. 'A fourth type of neuroglial cell in the adult central nervous system', *J Neurocytol*, 33: 345-57.

Pfeiffer, F. 2022. 'Reciprocal Interactions between Oligodendrocyte Precursor Cells and the Neurovascular Unit in Health and Disease', *Cells*, 11.

Pfeiffer, F., A. Sherafat, and A. Nishiyama. 2021. 'The Impact of Fixation on the Detection of Oligodendrocyte Precursor Cell Morphology and Vascular Associations', *Cells*, 10.

Pringle, N., E. J. Collarini, M. J. Mosley, C. H. Heldin, B. Westermark, and W. D. Richardson. 1989. 'PDGF A chain homodimers drive proliferation of bipotential (O-2A) glial progenitor cells in the developing rat optic nerve', *EMBO J*, 8: 1049-56.

Przewłocki, R., I. Haarmann, K. Nikolarakis, A. Herz, and V. Höllt. 1988. 'Prodynorphin gene expression in spinal cord is enhanced after traumatic injury in the rat', *Brain Res*, 464: 37-41.

Raff, M. C., R. H. Miller, and M. Noble. 1983. 'A glial progenitor cell that develops in vitro into an astrocyte or an oligodendrocyte depending on culture medium', *Nature*, 303: 390-6.

Raff, Martin C., Barbara A. Barres, Julia F. Burne, Harriet S. Coles, Yasuki Ishizaki, and Michael D. Jacobson. 1993. 'Programmed Cell Death and the Control of Cell Survival: Lessons from the Nervous System', *Science*, 262: 695-700.

Rassouli, O., G. Liapakis, and M. Venihaki. 2018. 'Role of Central and Peripheral CRH in Skin', *Curr Mol Pharmacol*, 11: 72-80.

Rassouli, Olga, George Liapakis, Iakovos Lazaridis, George Sakellaris, Kostas Gkountelias, Achille Gravanis, Andrew N. Margioris, Katia P. Karalis, and Maria Venihaki. 2011. 'A Novel Role of Peripheral Corticotropin-Releasing Hormone (CRH) on Dermal Fibroblasts', *PLoS One*, 6: e21654.

Refojo, D., M. Schweizer, C. Kuehne, S. Ehrenberg, C. Thoeringer, A. M. Vogl, N. Dedic, M. Schumacher, G. von Wolff, C. Avrabos, C. Touma, D. Engblom, G. Schutz, K. A. Nave, M. Eder, C. T. Wotjak, I. Sillaber, F. Holsboer, W. Wurst, and J. M. Deussing. 2011. 'Glutamatergic and Dopaminergic Neurons Mediate Anxiogenic and Anxiolytic Effects of CRHR1', *Science*, 333: 1903-07.

Reiter, C. R., and E. R. Bongarzone. 2020. 'The Role of Vesicle Trafficking and Release in Oligodendrocyte Biology', *Neurochem Res*, 45: 620-29.

Richardson, W. D., N. Pringle, M. J. Mosley, B. Westermark, and M. Dubois-Dalcq. 1988. 'A role for platelet-derived growth factor in normal gliogenesis in the central nervous system', *Cell*, 53: 309-19.

Ries, Clemens. 2018. 'Identification and Characterization of CRH system Components in Glial Cells', Master thesis, Technische Universität München.

Ries, Clemens, and Jan M. Deussing. 2020. 'Corticotropin-Releasing Hormone System.' in Stefan Offermanns and Walter Rosenthal (eds.), *Encyclopedia of Molecular Pharmacology* (Springer International Publishing: Cham).

Rio-Hortega, PioDel. 1939. 'THE MICROGLIA', *The Lancet*, 233: 1023-26.

Rivers, Leanne E., Kaylene M. Young, Matteo Rizzi, Françoise Jamen, Konstantina Psachoulia, Anna Wade, Nicoletta Kessaris, and William D. Richardson. 2008. 'PDGFRA/NG2 glia generate myelinating oligodendrocytes and piriform projection neurons in adult mice', *Nature Neuroscience*, 11: 1392-401.

Robel, S., B. Berninger, and M. Gotz. 2011. 'The stem cell potential of glia: lessons from reactive gliosis', *Nat Rev Neurosci*, 12: 88-104.

Rodríguez, C. I., F. Buchholz, J. Galloway, R. Sequerra, J. Kasper, R. Ayala, A. F. Stewart, and S. M. Dymecki. 2000. 'High-efficiency deleter mice show that FLPe is an alternative to Cre-loxP', *Nature Genetics*, 25: 139-40.

Rosenbaum, D. M., S. G. F. Rasmussen, and B. K. Kobilka. 2009. 'The structure and function of G-protein-coupled receptors', *Nature*, 459: 356-63.

Salimando, G. J., M. Hyun, K. M. Boyt, and D. G. Winder. 2020. 'BNST GluN2D-Containing NMDA Receptors Influence Anxiety- and Depressive-like Behaviors and Modulate Cell-Specific Excitatory/Inhibitory Synaptic Balance', *Journal of Neuroscience*, 40: 3949-68.

Sanchez, E. S., J. W. Bigbee, W. Fobbs, S. E. Robinson, and C. Sato-Bigbee. 2008. 'Opioid addiction and pregnancy: perinatal exposure to buprenorphine affects myelination in the developing brain', *Glia*, 56: 1017-27.

Sanford, C. A., M. E. Soden, M. A. Baird, S. M. Miller, J. Schulkin, R. D. Palmiter, M. Clark, and L. S. Zweifel. 2017. 'A Central Amygdala CRF Circuit Facilitates Learning about Weak Threats', *Neuron*, 93: 164-78.

Sarkar, Jhimly, Seth Wakefield, Georgina MacKenzie, Stephen J. Moss, and Jamie Maguire. 2011. 'Neurosteroidogenesis Is Required for the Physiological Response to Stress: Role of Neurosteroid-Sensitive GABA_A Receptors', *The Journal of Neuroscience*, 31: 18198-210.

Sauer, B., and N. Henderson. 1988. 'Site-specific DNA recombination in mammalian cells by the Cre recombinase of bacteriophage P1', *Proc Natl Acad Sci U S A*, 85: 5166-70.

Schafer, D. P., E. K. Lehrman, and B. Stevens. 2013. 'The "quad-partite" synapse: microglia-synapse interactions in the developing and mature CNS', *Glia*, 61: 24-36.

Schoenherr, C. J., and D. J. Anderson. 1995. 'The neuron-restrictive silencer factor (NRSF): a coordinate repressor of multiple neuron-specific genes', *Science*, 267: 1360-3.

Seasholtz, A. F., R. C. Thompson, and J. O. Douglass. 1988. 'Identification of a cyclic adenosine monophosphate-responsive element in the rat corticotropin-releasing hormone gene', *Mol Endocrinol*, 2: 1311-9.

Seo, J. H., T. Maki, M. Maeda, N. Miyamoto, A. C. Liang, K. Hayakawa, L. D. Pham, F. Suwa, A. Taguchi, T. Matsuyama, M. Ihara, K. W. Kim, E. H. Lo, and K. Arai. 2014. 'Oligodendrocyte precursor cells support blood-brain barrier integrity via TGF-beta signaling', *PLoS One*, 9: e103174.

Seth, K. A., and J. A. Majzoub. 2001a. 'Repressor element silencing transcription factor/neuron-restrictive silencing factor (REST/NRSF) can act as an enhancer as well as a repressor of corticotropin-releasing hormone gene transcription', *J Biol Chem*, 276: 13917-23.

Seth, Kim A., and Joseph A. Majzoub. 2001b. 'Repressor Element Silencing Transcription Factor/Neuron-restrictive Silencing Factor (REST/NRSF) Can Act as an Enhancer as Well as a Repressor of Corticotropin-releasing Hormone Gene Transcription*', *Journal of Biological Chemistry*, 276: 13917-23.

Shen, P. J., J. A. Larm, and A. L. Gundlach. 2003. 'Expression and plasticity of galanin systems in cortical neurons, oligodendrocyte progenitors and proliferative zones in normal brain and after spreading depression', *European Journal of Neuroscience*, 18: 1362-76.

Shen, Pei-Juan, Chong-Gang Yuan, Ji Ma, Shuang Cheng, May Yao, Ann M. Turnley, and Andrew L. Gundlach. 2005. 'Galanin in neuro(glio)genesis: expression of galanin and receptors by progenitor cells in vivo and in vitro and effects of galanin on neurosphere proliferation', *Neuropeptides*, 39: 201-05.

Shinoda, H., A. M. Marini, C. Cosi, and J. P. Schwartz. 1989. 'Brain region and gene specificity of neuropeptide gene expression in cultured astrocytes', *Science*, 245: 415-7.

Shinoda, H., A. M. Marini, and J. P. Schwartz. 1992. 'Developmental Expression of the Proenkephalin and Prosomatostatin Genes in Cultured Cortical and Cerebellar Astrocytes', *Developmental Brain Research*, 67: 205-10.

Sieburth, D., Q. Ch'ng, M. Dybbs, M. Tavazoie, S. Kennedy, D. Wang, D. Dupuy, J. F. Rual, D. E. Hill, M. Vidal, G. Ruvkun, and J. M. Kaplan. 2005. 'Systematic analysis of genes required for synapse structure and function', *Nature*, 436: 510-17.

Sieburth, D., J. M. Madison, and J. M. Kaplan. 2007. 'PKC-1 regulates secretion of neuropeptides', *Nature Neuroscience*, 10: 49-57.

Silberstein, F. C., R. De Simone, G. Levi, and F. Aloisi. 1996. 'Cytokine-regulated expression of platelet-derived growth factor gene and protein in cultured human astrocytes', *Journal of Neurochemistry*, 66: 1409-17.

Simon, C., M. Gotz, and L. Dimou. 2011. 'Progenitors in the adult cerebral cortex: cell cycle properties and regulation by physiological stimuli and injury', *Glia*, 59: 869-81.

Singh, V. K., and H. H. Fudenberg. 1988. 'Binding of [125I]corticotropin releasing factor to blood immunocytes and its reduction in Alzheimer's disease', *Immunol Lett*, 18: 5-8.

Sloane, J. A., C. Batt, Y. Ma, Z. M. Harris, B. Trapp, and T. Vartanian. 2010. 'Hyaluronan blocks oligodendrocyte progenitor maturation and remyelination through TLR2', *Proceedings of the National Academy of Sciences*, 107: 11555-60.

Slominski, A., J. Wortsman, A. Pisarchik, B. Zbytek, E. A. Linton, J. E. Mazurkiewicz, and E. T. Wei. 2001. 'Cutaneous expression of corticotropin-releasing hormone (CRH), urocortin, and CRH receptors', *FASEB J*, 15: 1678-93.

Snaidero, N., W. Mobus, T. Czopka, L. H. P. Hekking, C. Mathisen, D. Verkleij, S. Goebbels, J. Edgar, D. Merkler, D. A. Lyons, K. A. Nave, and M. Simons. 2014. 'Myelin Membrane Wrapping of CNS Axons by PI(3,4,5) P3-Dependent Polarized Growth at the Inner Tongue', *Cell*, 156: 277-90.

Snaidero, N., C. Velte, M. Myllykoski, A. Raasakka, A. Ignatev, H. B. Werner, M. S. Erwig, W. Möbius, P. Kursula, K. A. Nave, and M. Simons. 2017. 'Antagonistic Functions of MBP and CNP Establish Cytosolic Channels in CNS Myelin', *Cell Reports*, 18: 314-23.

Spiess, J., J. Villarreal, and W. Vale. 1981. 'Isolation and sequence analysis of a somatostatin-like polypeptide from ovine hypothalamus', *Biochemistry*, 20: 1982-8.

Stephan, J., S. Eitelmann, and M. Zhou. 2021. 'Approaches to Study Gap Junctional Coupling', *Front Cell Neurosci*, 15: 640406.

Sternberg, N., and D. Hamilton. 1981. 'Bacteriophage P1 site-specific recombination. I. Recombination between loxP sites', *J Mol Biol*, 150: 467-86.

Stevens, S. L., T. E. Shaw, E. Dykhuizen, N. S. Lessov, J. K. Hill, W. Wurst, and M. P. Stenzel-Poore. 2003. 'Reduced cerebral injury in CRH-R1 deficient mice after focal ischemia: a potential link to microglia and atrocytes that express CRH-R1', *J Cereb Blood Flow Metab*, 23: 1151-9.

Strijbos, P. J., J. K. Relton, and N. J. Rothwell. 1994. 'Corticotrophin-releasing factor antagonist inhibits neuronal damage induced by focal cerebral ischaemia or activation of NMDA receptors in the rat brain', *Brain Res*, 656: 405-8.

Sun, L. O., S. B. Mulinyawe, H. Y. Collins, A. Ibrahim, Q. Y. Li, D. J. Simon, M. Tessier-Lavigne, and B. Barres. 2018. 'Spatiotemporal Control of CNS Myelination by Oligodendrocyte Programmed Cell Death through the TFEB-PUMA Axis', *Cell*, 175: 1811-+.

Swanson, L. W., P. E. Sawchenko, J. Rivier, and W. W. Vale. 1983. 'Organization of ovine corticotropin-releasing factor immunoreactive cells and fibers in the rat brain: an immunohistochemical study', *Neuroendocrinology*, 36: 165-86.

Tagen, M., L. Stiles, D. Kalogeromitros, S. Gregoriou, D. Kempuraj, M. Makris, J. Donelan, M. Vasiadi, N. G. Staurianeas, and T. C. Theoharides. 2007. 'Skin corticotropin-releasing hormone receptor expression in psoriasis', *J Invest Dermatol*, 127: 1789-91.

Taniguchi, H., M. He, P. Wu, S. Kim, R. Paik, K. Sugino, D. Kvitsiani, Y. Fu, J. T. Lu, Y. Lin, G. Miyoshi, Y. Shima, G. Fishell, S. B. Nelson, and Z. J. Huang. 2011. 'A Resource of Cre Driver Lines for Genetic Targeting of GABAergic Neurons in Cerebral Cortex (vol 71, pg 995, 2011)', *Neuron*, 72: 1091-91.

Taveggia, C., G. Zanazzi, A. Petrylak, H. Yano, J. Rosenbluth, S. Einheber, X. R. Xu, R. M. Esper, J. A. Loeb, P. Shrager, M. V. Chao, D. L. Falls, L. Role, and J. L. Salzer. 2005. 'Neuregulin-1 type III determines the ensheathment fate of axons', *Neuron*, 47: 681-94.

Tawfik, B., J. S. Martins, S. Houy, C. Imig, P. S. Pinheiro, S. M. Wojcik, N. Brose, B. H. Cooper, and J. B. Sorensen. 2021. 'Synaptotagmin-7 places dense-core vesicles at the cell membrane to promote Munc13-2-and Ca2+-dependent priming', *Elife*, 10.

Tekki-Kessaris, N., R. Woodruff, A. C. Hall, W. Gaffield, S. Kimura, C. D. Stiles, D. H. Rowitch, and W. D. Richardson. 2001. 'Hedgehog-dependent oligodendrocyte lineage specification in the telencephalon', *Development*, 128: 2545-54.

Theoharides, T. C., L. K. Singh, W. Boucher, X. Pang, R. Letourneau, E. Webster, and G. Chrousos. 1998. 'Corticotropin-releasing hormone induces skin mast cell degranulation and increased vascular permeability, a possible explanation for its proinflammatory effects', *Endocrinology*, 139: 403-13.

Thureson-Klein, A. K., and R. L. Klein. 1990. 'Exocytosis from neuronal large dense-cored vesicles', *Int Rev Cytol*, 121: 67-126.

Tognatta, Reshmi, Molly T. Karl, Sharyl L. Fyffe-Maricich, Anastas Popratiloff, Eric D. Garrison, Jessica K. Schenck, Mohammad Abu-Rub, and Robert H. Miller. 2020. 'Astrocytes Are Required for Oligodendrocyte Survival and Maintenance of Myelin Compaction and Integrity', *Frontiers in Cellular Neuroscience*, 14.

Tooze, S. A., G. J. Martens, and W. B. Huttner. 2001. 'Secretory granule biogenesis: rafting to the SNARE', *Trends Cell Biol*, 11: 116-22.

Trapp, Bruce D., Akiko Nishiyama, David Cheng, and Wendy Macklin. 1997. 'Differentiation and Death of Premyelinating Oligodendrocytes in Developing Rodent Brain', *Journal of Cell Biology*, 137: 459-68.

Tripathi, R. B., L. E. Clarke, V. Burzomato, N. Kessaris, P. N. Anderson, D. Attwell, and W. D. Richardson. 2011. 'Dorsally and ventrally derived oligodendrocytes have similar electrical properties but myelinate preferred tracts', *J Neurosci*, 31: 6809-19.

Tripathi, R. B., M. Jackiewicz, I. A. McKenzie, E. Kougioumtzidou, M. Grist, and W. D. Richardson. 2017. 'Remarkable Stability of Myelinating Oligodendrocytes in Mice', *Cell Reports*, 21: 316-23.

Tsai, H. H., H. L. Li, L. C. Fuentealba, A. V. Molofsky, R. Taveira-Marques, H. L. Zhuang, A. Tenney, A. T. Murnen, S. P. J. Fancy, F. Merkle, N. Kessaris, A. Alvarez-Buylla, W. D. Richardson, and D. H. Rowitch. 2012. 'Regional Astrocyte Allocation Regulates CNS Synaptogenesis and Repair', *Science*, 337: 358-62.

Tsuboi, Takashi, Harvey T. McMahon, and Guy A. Rutter. 2004. 'Mechanisms of Dense Core Vesicle Recapture following “Kiss and Run” (“Cavicapture”) Exocytosis in Insulin-secreting Cells *', *Journal of Biological Chemistry*, 279: 47115-24.

Ubink, R., L. Calza, and T. Hökfelt. 2003. ''Neuro'-peptides in glia: focus on NPY and galanin', *Trends Neurosci*, 26: 604-9.

Ubink, R., N. Halasz, X. Zhang, A. Dagerlind, and T. Hökfelt. 1994. 'Neuropeptide tyrosine is expressed in ensheathing cells around the olfactory nerves in the rat olfactory bulb', *Neuroscience*, 60: 709-26.

Vamvakopoulos, N. C., and G. P. Chrousos. 1993. 'Evidence of direct estrogenic regulation of human corticotropin-releasing hormone gene expression. Potential implications for the sexual dimophism of the stress response and immune/inflammatory reaction', *J Clin Invest*, 92: 1896-902.

van den Pol, A. N. 2012. 'Neuropeptide transmission in brain circuits', *Neuron*, 76: 98-115.

Vana, A. C., N. C. Flint, N. E. Harwood, T. Q. Le, M. Fruttiger, and R. C. Armstrong. 2007. 'Platelet-derived growth factor promotes repair of chronically demyelinated white matter', *J Neuropathol Exp Neurol*, 66: 975-88.

Vardjan, N., V. Parpura, A. Verkhratsky, and R. Zorec. 2019. 'Gliocrine System: Astroglia as Secretory Cells of the CNS', *Adv Exp Med Biol*, 1175: 93-115.

Verkhratsky, A., V. Parpura, B. Li, and C. Scuderi. 2021. 'Astrocytes: The Housekeepers and Guardians of the CNS', *Adv Neurobiol*, 26: 21-53.

Vigano, F., and L. Dimou. 2016. 'The heterogeneous nature of NG2-glia', *Brain Res*, 1638: 129-37.

Vigano, F., S. Schneider, M. Cimino, E. Bonfanti, P. Gelosa, L. Sironi, M. P. Abbracchio, and L. Dimou. 2016. 'GPR17 expressing NG2-Glia: Oligodendrocyte progenitors serving as a reserve pool after injury', *Glia*, 64: 287-99.

Vilijn, M. H., P. J. J. Vaysse, R. S. Zukin, and J. A. Kessler. 1988. 'Expression of Preproenkephalin Messenger-Rna by Cultured Astrocytes and Neurons', *Proceedings of the National Academy of Sciences of the United States of America*, 85: 6551-55.

Virchow, Rudolf. 1846. 'Über das granulierte Ansehen der Wandungen der Gerhirnventrikel', *Allg Z Psychiatr*, 3: 242.

von Muecke-Heim, I. A., C. Ries, L. Urbina, and J. M. Deussing. 2021. 'P2X7R antagonists in chronic stress-based depression models: a review', *Eur Arch Psychiatry Clin Neurosci*, 271: 1343-58.

von Streitberg, A., S. Jakel, J. Eugenin von Bernhardi, C. Straube, F. Buggenthin, C. Marr, and L. Dimou. 2021. 'NG2-Glia Transiently Overcome Their Homeostatic Network and Contribute to Wound Closure After Brain Injury', *Front Cell Dev Biol*, 9: 662056.

Voyvodic, J. T. 1989. 'Target size regulates calibre and myelination of sympathetic axons', *Nature*, 342: 430-3.

Wagner, L., R. Wolf, U. Zeitschel, S. Rossner, A. Petersen, B. R. Leavitt, F. Kastner, M. Rothermundt, U. T. Gartner, D. Gundel, D. Schlenzig, N. Frerker, J. Schade, S. Manhart, J. U. Rahfeld, H. U. Demuth, and S. von Horsten. 2015. 'Proteolytic degradation of neuropeptide Y (NPY) from head to toe: Identification of novel NPY-cleaving peptidases and potential drug interactions in CNS and Periphery', *Journal of Neurochemistry*, 135: 1019-37.

Wake, Hiroaki, Philip R. Lee, and R. Douglas Fields. 2011. 'Control of Local Protein Synthesis and Initial Events in Myelination by Action Potentials', *Science*, 333: 1647-51.

Wang, W., P. Ji, and K. E. Dow. 2003. 'Corticotropin-releasing hormone induces proliferation and TNF-alpha release in cultured rat microglia via MAP kinase signalling pathways', *J Neurochem*, 84: 189-95.

Waters, R. P., M. Rivalan, D. A. Bangasser, J. M. Deussing, M. Ising, S. K. Wood, F. Holsboer, and C. H. Summers. 2015. 'Evidence for the role of corticotropin-releasing factor in major depressive disorder', *Neurosci Biobehav Rev*, 58: 63-78.

Webster, E. L., G. Battaglia, and E. B. De Souza. 1989. 'Functional corticotropin-releasing factor (CRF) receptors in mouse spleen: evidence from adenylate cyclase studies', *Peptides*, 10: 395-401.

Webster, E. L., D. E. Tracey, M. A. Jutila, S. A. Wolfe, Jr., and E. B. De Souza. 1990. 'Corticotropin-releasing factor receptors in mouse spleen: identification of receptor-bearing cells as resident macrophages', *Endocrinology*, 127: 440-52.

Weinberg, M. S., M. Girotti, and R. L. Spencer. 2007. 'Restraint-induced fra-2 and c-fos expression in the rat forebrain: relationship to stress duration', *Neuroscience*, 150: 478-86.

Wiemelt, A. P., M. Lehtinen, and F. A. McMorris. 2001. 'Agonists calcitonin, corticotropin-releasing hormone, and vasoactive intestinal peptide, but not prostaglandins or beta-adrenergic agonists, elevate cyclic adenosine monophosphate levels in oligodendroglial cells', *Journal of Neuroscience Research*, 65: 165-72.

Wilkins, A., S. Chandran, and A. Compston. 2001. 'A role for oligodendrocyte-derived IGF-1 in trophic support of cortical neurons', *Glia*, 36: 48-57.

Wilkins, A., H. Majed, R. Layfield, A. Compston, and S. Chandran. 2003. 'Oligodendrocytes promote neuronal survival and axonal length by distinct intracellular mechanisms: a novel role for oligodendrocyte-derived glial cell line-derived neurotrophic factor', *J Neurosci*, 23: 4967-74.

Wong, M. L., S. A. Loddick, P. B. Bongiorno, P. W. Gold, N. J. Rothwell, and J. Licinio. 1995. 'Focal cerebral ischemia induces CRH mRNA in rat cerebral cortex and amygdala', *Neuroreport*, 6: 1785-8.

Wraith, D. C., R. Pope, H. Butzkueven, H. Holder, P. Vanderplank, P. Lowrey, M. J. Day, A. L. Gundlach, T. J. Kilpatrick, N. Scolding, and D. Wynick. 2009. 'A role for galanin in human and experimental inflammatory demyelination', *Proc Natl Acad Sci U S A*, 106: 15466-71.

Xiao, L., D. Ohayon, I. A. McKenzie, A. Sinclair-Wilson, J. L. Wright, A. D. Fudge, B. Emery, H. Li, and W. D. Richardson. 2016. 'Rapid production of new oligodendrocytes is required in the earliest stages of motor-skill learning', *Nat Neurosci*, 19: 1210-17.

Xin, Wendy, and Jonah R. Chan. 2020. 'Myelin plasticity: sculpting circuits in learning and memory', *Nature Reviews Neuroscience*, 21: 682-94.

y Cajal, Ramón. 1913. 'Contribución al conocimiento de la neuroglia del cerebro humano', *Trab. Lab. Invest. Biol.*, 11: 255.

Yakovlev, A. G., and A. I. Faden. 1994. 'Sequential expression of c-fos protooncogene, TNF-alpha, and dynorphin genes in spinal cord following experimental traumatic injury', *Mol Chem Neuropathol*, 23: 179-90.

Yuan, H., S. Xu, Y. Wang, H. Xu, C. Wang, Q. Zhu, R. K. Yang, X. Chen, P. C. Yang, and X. Shi. 2010. 'Corticotrophin-releasing hormone (CRH) facilitates axon outgrowth', *Spinal Cord*, 48: 850-56.

Yuen, T. J., J. C. Silbereis, A. Griveau, S. M. Chang, R. Daneman, S. P. J. Fancy, H. Zahed, E. Maltepe, and D. H. Rowitch. 2014. 'Oligodendrocyte-encoded HIF function couples postnatal myelination and white matter angiogenesis', *Cell*, 158: 383-96.

Zeisel, A., H. Hochgerner, P. Lonnerberg, A. Johnsson, F. Memic, J. van der Zwan, M. Haring, E. Braun, L. E. Borm, G. La Manno, S. Codeluppi, A. Furlan, K. Lee, N. Skene, K. D. Harris, J. Hjerling-Leffler, E. Arenas, P. Ernfors, U. Marklund, and S. Linnarsson. 2018. 'Molecular Architecture of the Mouse Nervous System', *Cell*, 174: 999-+.

Zeisel, A., A. B. Munoz-Manchado, S. Codeluppi, P. Lonnerberg, G. La Manno, A. Jureus, S. Marques, H. Munguba, L. Q. He, C. Betsholtz, C. Rolny, G. Castelo-Branco, J. Hjerling-Leffler, and S.

Linnarsson. 2015. 'Cell types in the mouse cortex and hippocampus revealed by single-cell RNA-seq', *Science*, 347: 1138-42.

Zhang, Lin, Wu Yu, Ingo Schroedter, Jiming Kong, and Maria Vrontakis. 2012. 'Galanin Transgenic Mice with Elevated Circulating Galanin Levels Alleviate Demyelination in a Cuprizone-Induced MS Mouse Model', *PLoS One*, 7: e33901.

Zhang, S. Z., Q. Q. Wang, Q. Q. Yang, H. Y. Gu, Y. Q. Yin, Y. D. Li, J. C. Hou, R. Chen, Q. Q. Sun, Y. F. Sun, G. Hu, and J. W. Zhou. 2019. 'NG2 glia regulate brain innate immunity via TGF-beta2/TGFBR2 axis', *BMC Med*, 17: 204.

Zhang, Y., K. N. Chen, S. A. Sloan, M. L. Bennett, A. R. Scholze, S. O'Keeffe, H. P. Phatnani, P. Guarnieri, C. Caneda, N. Ruderisch, S. Y. Deng, S. A. Liddelow, C. L. Zhang, R. Daneman, T. Maniatis, B. A. Barres, and J. Q. Wu. 2014. 'An RNA-Sequencing Transcriptome and Splicing Database of Glia, Neurons, and Vascular Cells of the Cerebral Cortex', *Journal of Neuroscience*, 34: 11929-47.

Zhao, C., C. Ries, Y. Du, J. Zhang, K. Sakimura, K. Itoi, and J. M. Deussing. 2023. 'Differential CRH expression level determines efficiency of Cre- and Flp-dependent recombination', *Front Neurosci*, 17: 1163462.

Zhu, X., R. A. Hill, D. Dietrich, M. Komitova, R. Suzuki, and A. Nishiyama. 2011. 'Age-dependent fate and lineage restriction of single NG2 cells', *Development*, 138: 745-53.

Appendix

List of publications

1. **Ries C.**, Deussing J.M. (2020) Corticotropin-Releasing Hormone System. In: Offermanns S., Rosenthal W. (eds) Encyclopedia of Molecular Pharmacology. Springer, Cham. https://doi.org/10.1007/978-3-030-21573-6_10040-1
2. Zhao, C.*, **C. Ries***, Y. Du*, J. Zhang, K. Sakimura, K. Itoi, and J. M. Deussing. 2023. 'Differential CRH expression level determines efficiency of Cre- and Flp-dependent recombination', Front Neurosci, 17: 1163462.
   * authors contributed equally
3. von Muecke-Heim IA, **Ries C**, Urbina L, Deussing JM. P2X7R antagonists in chronic stress-based depression models: a review. Eur Arch Psychiatry Clin Neurosci. 2021 Oct;271(7):1343-1358. doi: 10.1007/s00406-021-01306-3. Epub 2021 Jul 19. PMID: 34279714; PMCID: PMC8429152.
4. von Mücke-Heim I-A, Martin J, Uhr M, **Ries C** and Deussing JM (2023) The human P2X7 receptor alters microglial morphology and cytokine secretion following immunomodulation. Front. Pharmacol. 14:1148190. doi: 10.3389/fphar.2023.1148190
5. von Mücke-Heim IA, Urbina-Treviño L, Bordes J, **Ries C**, Schmidt MV, Deussing JM. Introducing a depression-like syndrome for translational neuropsychiatry: a plea for taxonomical validity and improved comparability between humans and mice. Mol Psychiatry. 2022 Sep 14. doi: 10.1038/s41380-022-01762-w. Epub ahead of print. PMID: 36104436.

Acknowledgement

First of all, my deepest gratitude goes to PD Dr. Jan Deussing for his unconditional support, encouragement and mentorship throughout the years. Thank you for giving me the freedom to develop the project in the directions I wanted and for showing me, that the first impression can be misleading. Additionally, I want to thank you for all the discussions on the way, about science but also about other things. I am sure the HSV and the BVB will reach their goals, eventually!

A special thanks also goes to Professor Dr. Leda Dimou. You were invaluable for me along the way and supported me far beyond your duties as a TAC member! Even during the most stressful times you offered help and guidance which I will always be thankful for.

Of course, I also want to thank my other TAC members Professor Dr. Silvia Cappello and PD Dr. Carsten Wotjak for their constant support and scientific advice during my PhD. Your critical view and encouragement made a real difference. I would also like to thank the examination board for the effort to evaluate my thesis, including PD Dr. Jan Deussing, Professor Dr. Silvia Cappello, PD Dr. Mathias Schmidt and Professor Dr. Klaus-Armin Nave.

Also, I would like to thank all the colleagues that I had the pleasure to work with and who shared the difficulties of the PhD life: Julia Richter, Dr. Paromita Sen, Dr. Simon Chang, Dr. Srivaishnavi Loganathan, Dr. Lidia Urbina-Trevino, Laura Sotillos-Elliot, Du Ying, Dr. Zhao Chen, Dr. Iven von Mücke-Heim, Zhang Jingwei and Tang Hao. Although we went through troublesome times together, it was a pleasure getting to know and work with all of you. A special thanks goes to Dr. Iven von Mücke-Heim. Not only an outstanding colleague, but also a friend. Countless hours of discussions, complaints and jokes made my life easier, even if I couldn't always show it. Thank you!
I also want to thank my former master student Julia von Poblotzki. It was a real pleasure working with you. Not only because you are a great young scientist, but also because of your energetic and kind nature. Not to forget the many train rides and the well-enjoyed lunch-time.

My gratitude also goes to all collaborators for their willingness to help. To Antonio Miralles Infante for performing GPR17 stainings and subsequent quantification in *CRHR1-INTACT* mice, but also for many fun zoom-meetings! To Dr. Alessio Attardo and Dr. Alessandro Ulivi, who helped me with setting up and performing the 2-Photon microscope experiments. To Zhao Chen, Du Ying and Zhang Jingwei for working on the characterization of the *CRH-FlpO* mouse line. Also, to Dr. Kenji Sakimura and Dr. Keichii Itoi for sharing their *CRH-Venus* mouse line with us. Although the data was not included in the thesis, a special thanks to Dr. Wiebke Möbius and Torben Ruhwedel for performing electron microscopy experiments! Also, to Dr. Michael Czisch, Dr. Tibor Stark and Dr. Benoit Boulat for NMR measurements and analysis, although, also this dataset, was not included in the thesis.

Additionally, I want to thank our technicians Stefanie Unkmeir and Sabrina Bauer for all the help with genotyping and Rainer Stoffel for his major support in the cuprizone experiments! And, of course, Andrea Parl for all the assistance in the lab but also for just being there and chatting about this and that. Life in the lab is a lot more fun, when you are around!
I also want to thank all animal caretakers, who helped with the maintenance of the animals but also all other staff of the institute, without whom we would not be able to work properly.

My gratitude also goes to the Graduate School of Systemic Neuroscience (GSN) and the International Max Planck Research School for Translational Psychiatry (IMPRS-TP) for their administrative and financial support, bringing me together with other junior and senior scientists and enabling me to acquire my PhD.

Am meisten danken möchte ich allerdings meiner Familie.
Zu allererst meiner Frau und meinen beiden Kindern. Ihr drei seid ein Geschenk und ich bin unendlich dankbar, dass ihr bei mir seid und stolz, dass wir diesen anspruchsvollen Lebensabschnitt gemeinsam gemeistert haben. Es war wahrlich nicht immer einfach, aber ihr habt mir auch in den schwierigsten Phasen Halt geboten. Danke!

Und meiner Schwester. Ich bin froh eine große Schwester wie dich zu haben und dankbar für dein großes Vertrauen in mich und meine Fähigkeiten.

Und natürlich meinen Eltern. Ihr seid der Grund warum ich hier bin. Danke, dass ihr mich meinen eigenen Weg habt finden lassen, ohne mich allein zu lassen, mich und uns unterstützt wo es nur geht und mir immer zur Seite steht! Dafür werde ich ewig dankbar sein.

Author Contributions

Manuscript 1: "*Brain injury-induced expression of neuropeptide CRH in oligodendrocyte progenitor cells influences early oligodendroglial differentiation*"

Clemens Ries[*], Antonio Miralles Infante, Julia von Poblotzki, Alessandro Ulivi, Iven-Alex von Mücke-Heim, Simon Chang, Kenji Sakimura, Keiichi Itoi, Alessio Attardo, Leda Dimou, Jan M. Deussing[*]

C.R. designed, led and performed all experiments, analyzed and interpreted data and wrote the manuscript. T.M.I. performed GPR17 staining and analysis, provided scientific input and subedited the manuscript. J.P. performed the quantification of CRHR1-expressing astrocytes after reporter virus injection, analyzed data and subedited the manuscript. A. U. helped with cannula implantations for *in vivo* imaging, gave scientific expertise, helped with image acquisition at the 2-photon setup and subedited the manuscript. S. C. aided methodological and scientific expertise. I.M.H. aided methodological expertise in cranial window implantation, provided scientific input and subedited the manuscript. K.S. and K.I. created and provided the CRH-Venus mouse line and reviewed the manuscript. A.A. provided scientific input concerning 2-photon imaging, reviewed and subedited the manuscript. L.D. provided constant scientific input, helped with planning label retaining experiments, reviewed and subedited the manuscript. J. M. D. provided essential scientific advice and support, supervised all experiments and analysis, reviewed and edited the manuscript.

_____	_____
Clemens Ries	PD Dr. Jan Deussing

Manuscript 2: "*Differential CRH expression level determines efficiency of Cre- and Flp-dependent recombination*"

Chen Zhao[1†], **Clemens Ries[1†]**, Ying Du[1†], Jingwei Zhang[1], Kenji Sakimura[2], Keiichi Itoi[3], Jan M. Deussing[1*]

CZ, CR, and YD designed and performed all experiments, analyzed and interpreted data, drafted figures, and wrote the manuscript. JZ performed a subset of experiments and reviewed the manuscript. KS and KI provided materials, edited the manuscript and contributed scientific advice. JD designed the project, supervised all experiments and analyses, edited the manuscript, and provided scientific advice, guidance and support. All authors contributed to the article and approved the submitted version.

My contribution to this publication in detail:
For this publication, I sacrificed, cut and mounted *CRH-FlpO::CRH-Cre::Ai65* animals. I imaged the analyzed regions in all mouse lines and drafted all figures, but Fig. 6. Additionally, I was critically involved in the interpretation of data. Besides, I drafted the discussion and subedited the manuscript.

_____	_____
Clemens Ries	PD Dr. Jan Deussing
_____	_____
Zhao Chen	Du Ying